



Università degli Studi di Firenze

DOTTORATO DI RICERCA IN
INGEGNERIA CIVILE E AMBIENTALE

CICLO XXV

COORDINATORE Prof. Ing. La Torre Francesca

Wave energy harvesting in the Mediterranean Sea

Settore Scientifico Disciplinare ICAR/02

Dottoranda

Dott. Ing. Vannucchi Valentina

Tutore

Prof. Ing. Aminti Pier Luigi

Tutori scientifici

Prof. Ing. Cappiotti Lorenzo

Prof. Ing. Falcão António

Anni 2010/2012

To my husband Gianfranco
and my parents

ACKNOWLEDGEMENTS

I wish to thank Prof. Eng. Pier Luigi Aminti and Prof. Eng. Lorenzo Cappiotti, for their support to my research and for the precious advices and assistance that they gave me.

Part of this study has been conducted at the Institute of Mechanical Engineering (IDMEC) of the Instituto Superior Técnico (IST) in Lisbon. I'm very grateful to had the opportunity to work in such a stimulant place.

Special thanks to Prof. Eng. António Falcão, for his help, his continuous advices and for the remote assistance, and to Prof. Eng. Luis Gato for his help in providing the data required for the numerical simulations.

Many thanks to Lorenzo and Gianfranco that supported me also during the thesis writing!

CONTENTS

ACKNOWLEDGEMENTS.....	iii
CONTENTS.....	v
LIST OF TABLES.....	ix
LIST OF FIGURES.....	xiii
SOMMARIO.....	xxi
SUMMARY.....	xxiii
CHAPTER 1 INTRODUCTION.....	1
1.1 World energy market.....	1
1.2 Motivations and objectives.....	5
1.3 Outline of the thesis.....	7
CHAPTER 2 CURRENT STATUS OF WAVE ENERGY CONVERTERS TECHNOLOGIES.....	9
2.1 Description of the TRL approach.....	9
2.1.1 Validation model.....	10
2.1.2 Design model.....	12
2.1.3 Process model.....	13
2.1.4 Prototype device.....	16

2.1.5	Demonstration device.....	18
2.2	Methodology for the WECs site selection.....	19
2.2.1	Preliminary assessment.....	20
2.2.1.1	Gathering information.....	20
2.2.1.2	Resource assessment.....	24
2.2.2	Geographical analysis.....	28
2.2.3	Summarizing table.....	29
2.3	WECs classification.....	30
2.3.1	Location.....	30
2.3.2	Type.....	30
2.3.3	Operating principle	31
2.3.4	Power take off.....	32
2.4	Existing technologies	34
CHAPTER 3 OFFSHORE WAVE ENERGY CHARACTERIZATION		39
3.1	Linear surface wave theory.....	39
3.1.1	Regular waves.....	39
3.1.2	Random waves.....	45
3.2	Previous findings for the Mediterranean Sea.....	52
3.3	Offshore characterization.....	57
3.3.1	Methodology.....	57
3.3.2	Results	59
3.3.2.1	Mediterranean Sea.....	59
3.3.2.2	North-Western Mediterranean Sea.....	63
3.3.3	Comparison PREVIMER model with other data	68
3.3.3.1	Gorgona Buoy	68
3.3.3.2	WorldWaves data	72

3.3.3.3	Med Sea model.....	77
3.3.3.4	RON wave buoy measurements data	78
CHAPTER 4	NEARSHORE WAVE ENERGY CHARACTERIZATION.....	85
4.1	Description of the numerical model used.....	85
4.1.1	Model equations.....	86
4.1.2	Model output.....	89
4.2	Nearshore characterization.....	91
4.2.1	Methodology	92
4.2.2	Results	96
4.3	Non-technical barriers.....	119
4.3.1	Methodology	120
4.3.2	Results	121
4.3.2.1	Tuscany area.....	122
4.3.2.2	Liguria area	124
4.3.2.3	Sardinia area	124
CHAPTER 5	HYDRODYNAMICS OF WAVE ENERGY ABSORPTION BY A FLOATING DEVICE.....	127
5.1	Governing equations	127
5.1.1	Single Body.....	128
5.1.1.1	Linear system in regular waves: frequency domain analysis.....	129
5.1.1.2	JONSWAP spectrum formulation.....	132
5.1.1.3	Linear system in irregular waves: frequency domain analysis	133
5.1.2	Spar-Buoy OWC.....	134
5.1.2.1	Linear system in regular waves: frequency domain analysis.....	135
5.1.2.2	Linear system in irregular waves: frequency domain analysis	139
5.2.	Numerical simulation for devices optimization	140

5.2.1	Single Body.....	140
5.2.1.1	Northern Tuscany area.....	141
5.2.1.2	Central Tuscany area.....	144
5.2.1.3	Liguria area.....	147
5.2.1.4	Sardinia area.....	150
5.2.2	Spar-Buoy OWC.....	153
5.2.2.1	Northern Tuscany area.....	156
5.2.2.2	Central Tuscany area.....	158
5.2.2.3	Liguria area.....	160
5.2.2.4	Sardinia area.....	163
CHAPTER 6	CONCLUSIONS.....	165
APPENDIX A:	WEC DATA SHEET	171
APPENDIX B:	OFFSHORE CHARACTERIZATION.....	225
APPENDIX C:	NEARSHORE CHARACTERIZATION.....	247
APPENDIX D:	NEARSHORE PROPAGATION.....	285
APPENDIX E:	WEC OPTIMIZATION.....	355
REFERENCES	393

LIST OF TABLES

Table 2.1. Site selection characteristic	29
Table 2.2 List of the analyzed devices	34
Table 2.3 Characterization by type of the devices	36
Table 2.4 Characterization by country of the devices	37
Table 3.1. Mean monthly and yearly wave power at RON buoys [12].....	56
Table 3.2 Maximum values of the monthly mean power and their location	60
Table 3.3 Maximum values of the monthly mean power and its location	64
Table 3.4.Monthly and yearly mean wave power of the Gorgona Buoy and NW Med Sea PREVIMER model.....	71
Table 3.5.Monthly and yearly mean wave power of the (44° E, 9.5° N) point and PREVIMER model.....	73
Table 3.6.Monthly and yearly mean wave power of the (43.5° E , 9.5° N) point and PREVIMER model.....	73
Table 3.7.Monthly and yearly mean wave power of the (43.5° E, 10° N) point and PREVIMER model.....	74
Table 3.8.Monthly and yearly mean wave power of the (43° E, 10° N) point and PREVIMER model.....	74
Table 3.9.Monthly and yearly mean wave power of the (42.5° E, 10.5° N) point and PREVIMER model.....	75
Table 3.10.Monthly and yearly mean wave power of the (42° E, 11° N) point and PREVIMER model.....	75

Table 3.11. Monthly and yearly mean wave power of the (42° E, 11.5° N) point and PREVIMER model.....	76
Table 3.12. Yearly mean wave power in 20 points Liberti & al. [11] model and PREVIMER model.....	77
Table 3.13. Yearly mean wave power in the 15 RON buoy: Vicinanza&al. [12] and PREVIMER values	78
Table 4.1. Coordinates and yearly mean wave power values at the offshore boundary points	95
Table 4.2. Sea state values	96
Table 4.3. Value, location, water depth of the maximum yearly mean wave power nearshore and area above the threshold selected. All the wave power values of the years 2010 and 2011 were used to compute the “yearly mean wave power”	104
Table 4.4. Northern Tuscany – location and yearly mean wave power values of the extracted points	106
Table 4.5. Northern Tuscany - scatter diagraph (%) of H_{m0} and T_e at the point 9.....	107
Table 4.6. Northern Tuscany - scatter diagraph (%) of H_{m0} and T_e at the point 19	108
Table 4.7. Central Tuscany – location and yearly mean wave power values of the extracted points.....	109
Table 4.8. Central Tuscany - scatter diagraph (%) of H_{m0} and T_e at the point 3	110
Table 4.9. Central Tuscany - scatter diagraph (%) of H_{m0} and T_e at the point 9	111
Table 4.10. Liguria – location and yearly mean wave power values of the extracted points	112
Table 4.11. Liguria - scatter diagraph (%) of H_{m0} and T_e at the point 7	113
Table 4.12. Liguria - scatter diagraph (%) of H_{m0} and T_e at the point 17	114
Table 4.13. Liguria - scatter diagraph (%) of H_{m0} and T_e at the point 19	115
Table 4.14. Sardinia – location and yearly mean wave power values of the extracted points	116
Table 4.15. Sardinia - scatter diagraph (%) of H_{m0} and T_e in the point 1	117
Table 4.16. Sardinia - scatter diagraph (%) of H_{m0} and T_e at the point 9.....	118
Table 4.17. Range cable costs [58]	119
Table 4.18. Pelamis cable laying costs [58]	120
Table 4.19. Area, population [63] and population density of the selected Region	122
Table 5.1. Shape parameters for the JONSWAP spectrum	133

Table 5.2. Optimized values for the point 9 Northern Tuscany	142
Table 5.3. Optimized values for the point 19 Northern Tuscany	143
Table 5.4. Optimized values for the point 3 Central Tuscany	144
Table 5.5. Optimized values for the point 9 Central Tuscany	145
Table 5.6. Optimized values for the point 7 Liguria	147
Table 5.7. Optimized values for the point 17 Liguria	148
Table 5.8. Optimized values for the point 19 Liguria	149
Table 5.9. Optimized values for the point 1 Sardinia.....	151
Table 5.10. Optimized values for the point 9 Sardinia.....	152
Table 5.11. Analyzed Spar-Buoy OWC geometries [72].....	154
Table 5.12. $L_{c,ann}^*$ values on varying of chamber height.....	156
Table 5.13. Optimized values for the point 19 Northern Tuscany	157
Table 5.14 Optimized values for the point 9 Central Tuscany	159
Table 5.15. Optimized values for the point 17 Liguria	160
Table 5.16. Optimized values for the point 19 Liguria	161
Table 5.17. Optimized values for the point 9 Sardinia.....	163

LIST OF FIGURES

Figure 1.1. World energy demand 1980 - 2035 [1]	1
Figure 1.2. Renewable Energy Share of Global Final Energy Consumption, 2010 [2].....	2
Figure 1.3. World total primary energy supply from 1971 to 2009 by fuel (Mtoe) [3].....	3
Figure 1.4. 1973 and 2009 fuel shares (other includes geothermal, solar, wind, heat, etc.) [3]	3
Figure 1.5. Wave energy global map [6]	4
Figure 2.1. WEC develop protocol [17]	10
Figure 2.2. Diagram showing the main activities contained in the methodology [19]	20
Figure 2.3. The power table for a given Pelamis configuration [27]	26
Figure 2.4. Illustration of a yearly distribution of wave power output [26]	26
Figure 2.5. Scatter diagram for Arch Point location and plot of the lines that represent the constant significant steepness and the incident wave power [28]	27
Figure 2.6. Sixteen-sector power-weighted wave rose plot. [29]	27
Figure 2.7. Sixteen-sector power-weighted wave rose plot.	31
Figure 2.8. Operating principle: a) OWC, b) OTD, c1) OB floating rotation, c2) OB submerged rotation [33].....	32
Figure 2.9. A schematic of a linear electrical generator based on a permanent magnet generator [31]	33
Figure 3.1. The linearised basic equations and boundary conditions in terms of the velocity potential [37].....	41
Figure 3.2. The definition of wave height and wave period in a time record of the surface elevation	45

Figure 3.3. The random-phase/amplitude model [37].....	47
Figure 3.4. The characteristics of the waves for three different widths of the spectrum[37]	48
Figure 3.5. The directional energy distribution at a given frequency and its directional width σ_0 [37].....	51
Figure 3.6. WERATLAS - Wave power rose in the Mediterranean Sea [8]	53
Figure 3.7. Annual global gross theoretical wave power for all WorldWaves grid points worldwide [9].....	54
Figure 3.8. Mean yearly wave power in the Mediterranean Sea, based on WWA [43].....	54
Figure 3.9. Mean wave power in the Mediterranean Sea, based on MEDATLAS [44]	55
Figure 3.10. Mean wave power in the Mediterranean Sea, based on [11]	55
Figure 3.11. RON buoys locations [12].....	57
Figure 3.12. Maximum values of the monthly mean power	59
Figure 3.13. Location map of sea sites characterized by the maximum monthly mean power	61
Figure 3.14. Spatial distribution of the mean power for May 2011 [kW/m].....	61
Figure 3.15. Spatial distribution of the mean power for January 2012 [kW/m]	61
Figure 3.16. Spatial distribution of the mean power for the year 2010 [kW/m]	62
Figure 3.17. Coefficient of variation distribution for the year 2010	62
Figure 3.18. Spatial distribution of the mean power for the year 2011 [kW/m]	62
Figure 3.19. Coefficient of variation distribution for the year 2011	63
Figure 3.20. Maximum values of the monthly mean power	63
Figure 3.21. Location map of sea sites characterized by the maximum monthly mean power	65
Figure 3.22. Spatial distribution of the mean power for May 2011 [kW/m].....	65
Figure 3.23. Spatial distribution of the mean power for December 2011 [kW/m]	66
Figure 3.24. Spatial distribution of the mean power for the year 2010 [kW/m]	66
Figure 3.25. Coefficient of variation distribution for the year 2010	67
Figure 3.26. Spatial distribution of the mean power for the year 2011 [kW/m]	67
Figure 3.27. Coefficient of variation distribution for the year 2011	68
Figure 3.28. Gorgona buoy location.....	69
Figure 3.29. Relation between Gorgona buoy and NW Med Sea PREVIMER model.....	69
Figure 3.30. Wave rose: a) Gorgona buoy, b) NW Med Sea PREVIMER model.....	70

Figure 3.31. Gorgona Buoy: relation between peak period and mean period.....	70
Figure 3.32. Monthly mean wave power of the Gorgona Buoy and NW Med Sea PREVIMER model.....	71
Figure 3.33. Monthly and yearly mean power of the Gorgona Buoy and NW Med Sea PREVIMER model.....	71
Figure 3.34. WorldWaves data points location.....	72
Figure 3.35. Monthly and yearly mean power of the (44° E, 9.5° N) point and PREVIMER model.....	73
Figure 3.36. Monthly and yearly mean power of the (43.5° E , 9.5° N) point and PREVIMER model.....	73
Figure 3.37. Monthly and yearly mean power of the (43.5° E, 10° N) point and PREVIMER model.....	74
Figure 3.38. Monthly and yearly mean power of the (43° E, 10° N) point and PREVIMER model.....	74
Figure 3.39. Monthly and yearly mean power of the (42.5° E, 10.5° N) point and PREVIMER model.....	75
Figure 3.40. Monthly and yearly mean power of the (42° E, 11° N) point and PREVIMER model.....	75
Figure 3.41. Monthly and yearly mean power of the (42° E, 11.5° N) point and PREVIMER model.....	76
Figure 3.42. Yearly mean power in 20 points Liberti & al. [11] model and PREVIMER model.....	77
Figure 3.43. Monthly and yearly mean power in the Alghero Buoy	79
Figure 3.44. Monthly and yearly mean power in the Ancona Buoy.....	79
Figure 3.45. Monthly and yearly mean power in the Cagliari Buoy	79
Figure 3.46. Monthly and yearly mean power in the Capo Comino Buoy.....	80
Figure 3.47. Monthly and yearly mean power in the Capo Gallo Buoy	80
Figure 3.48. Monthly and yearly mean power in the Capo Linaro Buoy	80
Figure 3.49. Monthly and yearly mean power in the Catania Buoy	81
Figure 3.50. Monthly and yearly mean power in the Cetraro Buoy	81
Figure 3.51. Monthly and yearly mean power in the Crotone Buoy	81
Figure 3.52. Monthly and yearly mean power in the La Spezia Buoy.....	82
Figure 3.53. Monthly and yearly mean power in the Mazara del Vallo Buoy.....	82

Figure 3.54. Monthly and yearly mean power in the Monopoli Buoy.....	82
Figure 3.55. Monthly and yearly mean power in the Ortona Buoy	83
Figure 3.56. Monthly and yearly mean power in the Ponza Buoy	83
Figure 3.57. Monthly and yearly mean power in the Punta della Maestra Buoy.....	83
Figure 4.1. Sites selected location.....	91
Figure 4.2. Northern Tuscany: a) mesh and boundaries, b) bathymetry.....	93
Figure 4.3. Central Tuscany: a) mesh and boundaries, b) bathymetry.....	93
Figure 4.4. Liguria: a) mesh and boundaries, b) bathymetry.....	94
Figure 4.5. Sardinia: a) mesh and boundaries, b) bathymetry	94
Figure 4.6. Power map of Tuscany for the event 5th of January 2012 hour 18.00: a) Northern, b) Central	96
Figure 4.7. Power map of Liguria for the event 5th of January 2012 hour 18.00.....	97
Figure 4.8. Power map of Sardinia for the event 5th of January 2012 hour 18.00.....	97
Figure 4.9. Meloria shoals details of the event of 5 January 2012 at 18.00: a) power map, b) significant wave height map, c) energetic period map, d) peak period map.....	98
Figure 4.10. Northern Tuscany 2010: a) yearly mean wave power, b) yearly mean wave power normalized.....	99
Figure 4.11. Northern Tuscany 2011: a) yearly mean wave power, b) yearly mean wave power normalized by using the maximum wave power within the model spatial domain ..	99
Figure 4.12. Central Tuscany 2010: a) yearly mean wave power, b) yearly mean wave power normalized by using the maximum wave power within the model spatial domain.....	100
Figure 4.13. Central Tuscany 2011: a) yearly mean wave power, b) yearly mean wave power normalized by using the maximum wave power within the model spatial domain.....	100
Figure 4.14. Northern Tuscany detailed yearly mean wave power map: a) 2010, b) 2011 ..	101
Figure 4.15. Liguria 2010: a) yearly mean wave power, b) yearly mean wave power normalized.....	101
Figure 4.16. Liguria 2011: a) yearly mean wave power, b) yearly mean wave power normalized by using the maximum wave power within the model spatial domain.....	102
Figure 4.17. Liguria detailed yearly mean wave power map: a) 2010, b) 2011	102
Figure 4.18. Sardinia 2010: a) yearly mean wave power, b) yearly mean wave power normalized.....	103
Figure 4.19. Sardinia 2011: a) yearly mean wave power, b) yearly mean wave power normalized.....	103

Figure 4.20. Sardinia detailed yearly mean wave power map: a) 2010, b) 2011	104
Figure 4.21. Wave power values trend in December 2010 in the 20 points extracted in the Northern Tuscany : a) on 15m water depth, b) on 50m water depth.....	105
Figure 4.22. Northern Tuscany - location and wave roses of the extracted points	106
Figure 4.23. Northern Tuscany – Annual energy at the point 9.....	107
Figure 4.24. Northern Tuscany – Annual energy at the point 19.....	108
Figure 4.25. Central Tuscany - location and wave roses of the extracted points.....	109
Figure 4.26. Central Tuscany – Annual energy at the point 3.....	110
Figure 4.27. Central Tuscany – Annual energy at the point 9.....	111
Figure 4.28. Liguria - location and wave roses of the extracted points	112
Figure 4.29. Liguria – Annual energy at the point 7	113
Figure 4.30. Liguria – Annual Energy at the point 17	114
Figure 4.31. Liguria – Annual energy at the point 19.....	115
Figure 4.32. Sardinia - location and wave roses of the extracted points	116
Figure 4.33. Sardinia – Annual energy at the point 1	117
Figure 4.34. Sardinia – Annual energy at the point 9	118
Figure 4.35. Perimeter of Pelagos Sanctuary [65]	121
Figure 4.36. Navigation routes [64].....	122
Figure 4.37. Tuscany area: analysis of the non-technical barriers.....	123
Figure 4.38. Liguria area: analysis of the non-technical barriers.....	124
Figure 4.39. Sardinia area: analysis of the non-technical barriers	125
Figure 5.1. Degrees of freedom of a rigid body [66].....	127
Figure 5.2. Schematic representation of a single body oscillating in heave.....	128
Figure 5.3. The shapes of the PM spectrum and the JONSWAP spectrum [37].....	132
Figure 5.4. Spar-Buoy OWC cross section view [72]	135
Figure 5.5. Point 9 – Regular waves for each optimization criterion: a) $X_o/ampl$, b) P/P_{max}	142
Figure 5.6. Point 9 – Irregular waves for each optimization criterion: a) P_{irr}/H_s^2 , b) P_{irr}/P_{maxirr}	142
Figure 5.7. Point 19 – results of $F_1 \alpha=0$ normalized to the maximum value	143
Figure 5.8. Point 19 – Regular waves for each optimization criterion: a) $X_o/ampl$, b) P/P_{max}	143

Figure 5.9. Point 19 – Irregular waves for each optimization criterion: a) P_{irr}/H_s^2 , b) P_{irr}/P_{maxirr}	144
Figure 5.10. Point 3 – Regular waves for each optimization criterion: a) $X_o/ampl$, b) P/P_{max}	145
Figure 5.11. Point 3 – Irregular waves for each optimization criterion: a) P_{irr}/H_s^2 , b) P_{irr}/P_{maxirr}	145
Figure 5.12. Point 9 – results of F_1 $\alpha=0.5$ normalized to the maximum value.....	146
Figure 5.13. Point 9 – Regular waves for each optimization criterion: a) $X_o/ampl$, b) P/P_{max}	146
Figure 5.14. Point 9 – Irregular waves for each optimization criterion: a) P_{irr}/H_s^2 , b) P_{irr}/P_{maxirr}	146
Figure 5.15. Point 7 – Regular waves for each optimization criterion: a) $X_o/ampl$, b) P/P_{max}	147
Figure 5.16. Point 7 – Irregular waves for each optimization criterion: a) P_{irr}/H_s^2 , b) P_{irr}/P_{maxirr}	148
Figure 5.17. Point 17 – Regular waves for each optimization criterion: a) $X_o/ampl$, b) P/P_{max}	148
Figure 5.18. Point 17 – Irregular waves for each optimization criterion: a) P_{irr}/H_s^2 , b) P_{irr}/P_{maxirr}	149
Figure 5.19. Point 17 – results of F_2 normalized to the maximum value.....	149
Figure 5.20. Point 19 – Regular waves for each optimization criterion: a) $X_o/ampl$, b) P/P_{max}	150
Figure 5.21. Point 19 – Irregular waves for each optimization criterion: a) P_{irr}/H_s^2 , b) P_{irr}/P_{maxirr}	150
Figure 5.22. Point 1 – Regular waves for each optimization criterion: a) $X_o/ampl$, b) P/P_{max}	151
Figure 5.23. Point 1 – Irregular waves for each optimization criterion: a) P_{irr}/H_s^2 , b) P_{irr}/P_{maxirr}	151
Figure 5.24. Point 9 – results of F_3 normalized to the maximum value.....	152
Figure 5.25. Point 9 – Regular waves for each optimization criterion: a) $X_o/ampl$, b) P/P_{max}	152
Figure 5.26. Point 9 – Irregular waves for each optimization criterion: a) P_{irr}/H_s^2 , b) P_{irr}/P_{maxirr}	153

Figure 5.27. Efficiency curve	155
Figure 5.28. The influence of the chamber height on the performance of the optimized devices	156
Figure 5.29. Point 19 – results of $F_1 \alpha=0$ normalized to the maximum value (geometry N)	157
Figure 5.30. Point 19 – Regular waves for each optimization criterion: a) X/ampl and Y/ampl, b) Lc,reg.....	158
Figure 5.31. Point 19 – Irregular waves for each optimization criterion: a) Pt/Hs ² , b) Lc,irr	158
Figure 5.32. Point 9 – results of $F_1 \alpha=0.25$ normalized to the maximum value (geometry N)	159
Figure 5.33. Point 9 – Regular waves for each optimization criterion: a) X/ampl and Y/ampl, b) Lc,reg.....	159
Figure 5.34. Point 9 – Irregular waves for each optimization criterion: a) Pt/Hs ² , b) Lc,irr	160
Figure 5.35. Point 17 – results of $F_1 \alpha=0.5$ normalized to the maximum value (geometry B)	161
Figure 5.36. Point 19 – results of $F_1 \alpha=0.75$ normalized to the maximum value (geometry B).....	162
Figure 5.37. Regular waves for each optimization criterion: a) X/ampl and Y/ampl, b) Lc,reg.....	162
Figure 5.38. Irregular waves for each optimization criterion: a) Pt/Hs ² , b) Lc,irr.....	162
Figure 5.39. Point 9 – results of F_2 normalized to the maximum value (geometry E)	164
Figure 5.40. Point 9 – Regular waves for each optimization criterion: a) X/ampl and Y/ampl, b) Lc,reg.....	164
Figure 5.41. Point 9 – Irregular waves for each optimization criterion: a) Pt/Hs ² , b) Lc,irr	164

SOMMARIO

Gli obiettivi principali di questa tesi sono la caratterizzazione sottocosta della potenza ricavata dal moto ondoso in aree italiane non ancora studiate o poco studiate e l'ottimizzazione di dispositivi per la conversione dell'energia disponibile dal moto ondoso (WEC - Wave Energy Converters), nei due punti maggiormente energetici di ciascuna area. I dispositivi studiati sono un corpo oscillante (il caso di studio più semplice) fissato al fondale marino per mezzo di un sistema di conversione di energia e di un dispositivo galleggiante a colonna d'acqua oscillante chiamato Spar Buoy OWC e studiato presso l'Istituto di Ingegneria Meccanica (IDMEC) dell'Istituto Superiore Tecnico (IST) di Lisbona. La caratterizzazione sottocosta è stata ottenuta mediante simulazioni numeriche effettuate con il MIKE21- Spectral Wave, un modello spettrale di onda che permette la simulazione di fenomeni come l'interazione non lineare onda-onda, la dissipazione dovuta all'attrito con il fondale, la dissipazione indotta dal frangimento delle onde, la rifrazione e lo shoaling dovuti alla variazione della profondità. Come condizioni al contorno in mare aperto sono stati utilizzati i valori di altezza d'onda, periodo di picco, direzione media e fattore di diffusione estratti dal modello PREVIMER MENOR-4000M. Le aree analizzate sono: la Toscana Settentrionale (La Spezia - Livorno), la Toscana Centrale (Livorno - Piombino), la Liguria Occidentale (Ventimiglia - Imperia), la Sardegna Nord-Occidentale (Stintino - Alghero). Per i due climi d'onda corrispondenti ai punti maggiormente energetici di ciascuna area sono stati ottimizzati i due dispositivi studiati (corpo oscillante ancorato al fondale e Spar Buoy OWC) in base alla geometria e al sistema di conversione dell'energia. L'ottimizzazione è stata effettuata massimizzando delle funzioni obiettivo che tenessero conto del costo, dell'efficienza e delle prestazioni del dispositivo.

SUMMARY

The main purposes of this thesis are the nearshore wave energy characterization in Italian areas not yet analysed or little analysed and the optimization, in the two locations with the highest wave power of each area, of devices for the Wave Energy Conversion (WEC). The analysed devices were a single floating body linked to the seabed by means of a Power Take Off (PTO) mechanism (the simplest case of study) and of the Spar Buoy Oscillating Water Column (OWC), an axisymmetric floating OWC that was studied at Institute of Mechanical Engineering (IDMEC) of the Instituto Superior Técnico (IST) in Lisbon. The nearshore characterization is computed with numerical simulations that were carried out by the MIKE21-Spectral Wave, a spectral wind-wave model based on unstructured mesh that allows the simulation of the phenomena as non-linear wave-wave interaction, dissipation due to white-capping, dissipation due to bottom friction, dissipation due to depth-induced wave breaking, refraction and shoaling due to depth variations. As offshore boundary conditions the values of wave height, peak period, average direction and spreading factor, of the points extracted by the MENOR-4000M PREVIMER model on a depth of 100 m, were used. This methodology is applied to four selected areas: the North of the Tuscany coast (La Spezia – Livorno), the centre of the Tuscany coast (Livorno – Piombino), the Western part of Liguria coast (Ventimiglia – Imperia) and the North-West of the Sardinia coast (Stintino – Alghero). The device optimization was performed for the geometry and for the PTO system in local wave climates selected for each area. The optimization procedure followed different criteria that consisted in maximizing objective functions, in order to consider the cost, particularly useful in the fully commercial stage, the efficiency and the performance of the devices.

CHAPTER 1

INTRODUCTION

1.1. World energy market

The global energy demand is expected to increase by 33% between 2010 and 2035, with China, India and the Middle East accounting for 60 % of the increase [1], due to faster rates of growth of economy activities, industrial production, population and urbanisation (Figure 1.1).

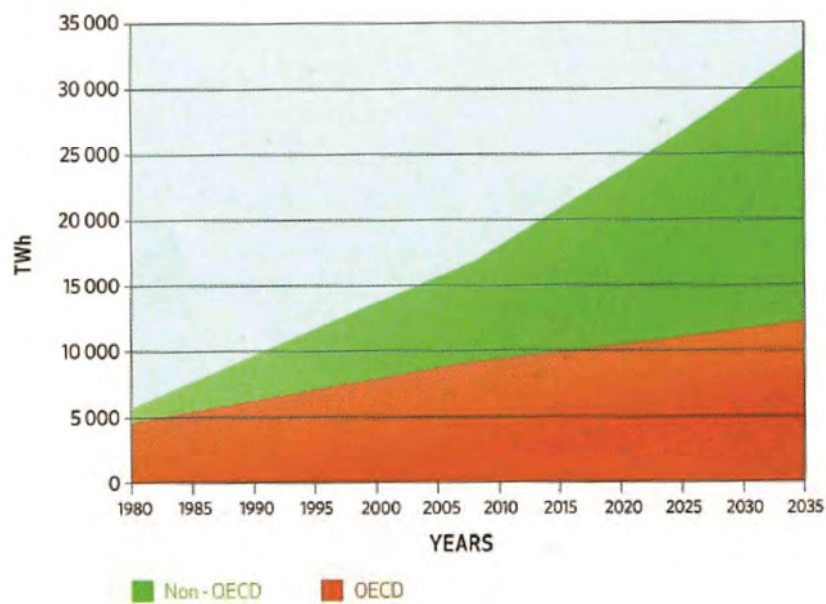


Figure 1.1. World energy demand 1980 - 2035 [1]

The renewable energy, that consists of energy produced and/or derived from sources that can be renewed indefinitely (such as sun, wind, rain, tides and geothermal heat) or sustainably produced (such as biomass), in 2010 supplied an estimated 16.7 % of global final energy consumption [2]. Of this total, modern renewable energy, counting hydropower, wind, solar, geothermal, biofuels and modern biomass, accounted for an estimated 8.2 %, while the other 8.5 % come from the traditional biomass, which is used primarily for cooking and heating in rural areas of developing countries (Figure 1.2). During 2011, the modern renewables continued to grow strongly in all end-use sectors: power, heating, cooling and transport. In the power sector, renewables accounted for almost half of the estimated 208 GW of electric capacity added globally during 2011. By the end of 2011, total renewable power capacity worldwide exceeded 1360 GW, up 8% over 2010. The renewables comprised more than 25% of total global power-generating capacity (estimated at 5360 GW in 2011) and supplied an estimated 20.3% of global electricity and the non-hydropower renewables exceeded 390 GW, a 24% capacity increase over 2010.

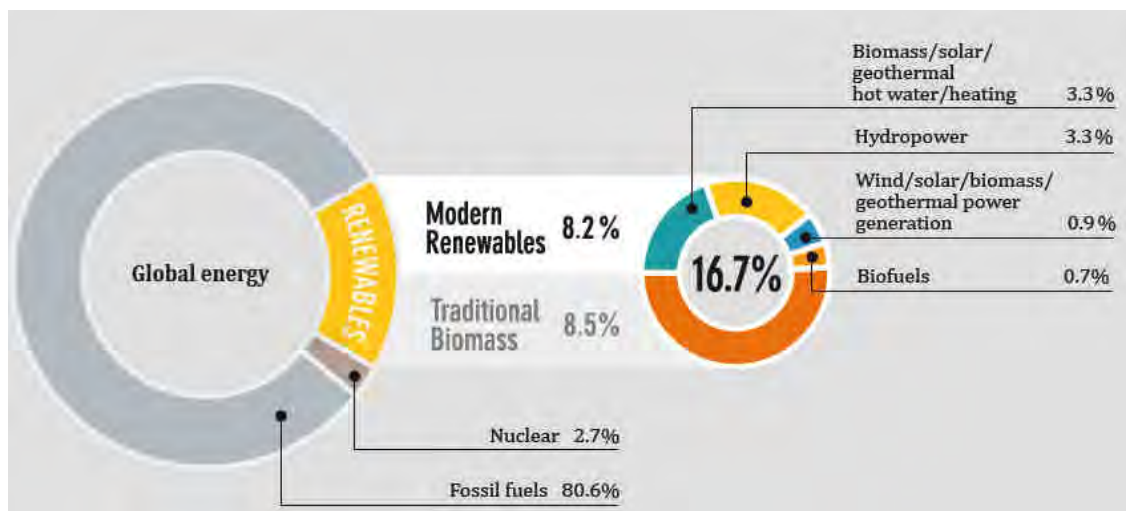


Figure 1.2. Renewable Energy Share of Global Final Energy Consumption, 2010 [2]

Despite the growth in low-carbon sources of energy, the fossil fuels (oil, coal and natural gas) remain dominant in the global energy mix (Figure 1.3 and Figure 1.4), supported by subsidies that amounted to \$523 billion in 2011, up almost 30% on 2010 and six times more than subsidies to renewables. The cost of fossil-fuel subsidies has been driven up by higher oil prices; they remain most prevalent in the Middle East and North Africa, where momentum towards their reform appears to have been lost [4].

An increasing amount of attention is being paid to energy production from renewable energy source and low-carbon technologies due to anthropic effects on climate change,

increasing oil prices, energy security, industrial competitiveness, local economic development and other environmental impacts such as urban air pollution.

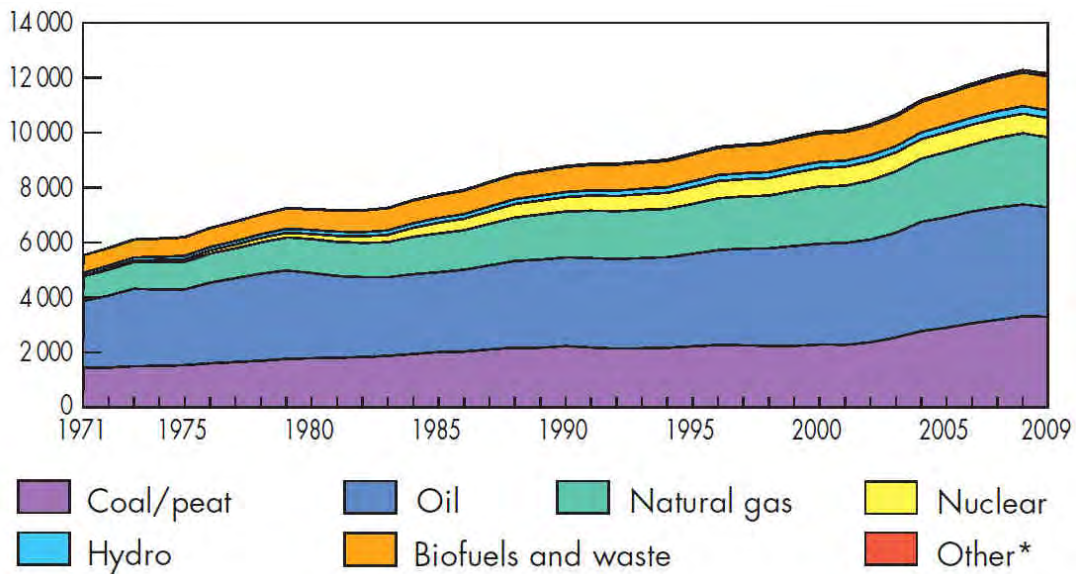


Figure 1.3. World total primary energy supply from 1971 to 2009 by fuel (Mtoe) [3]

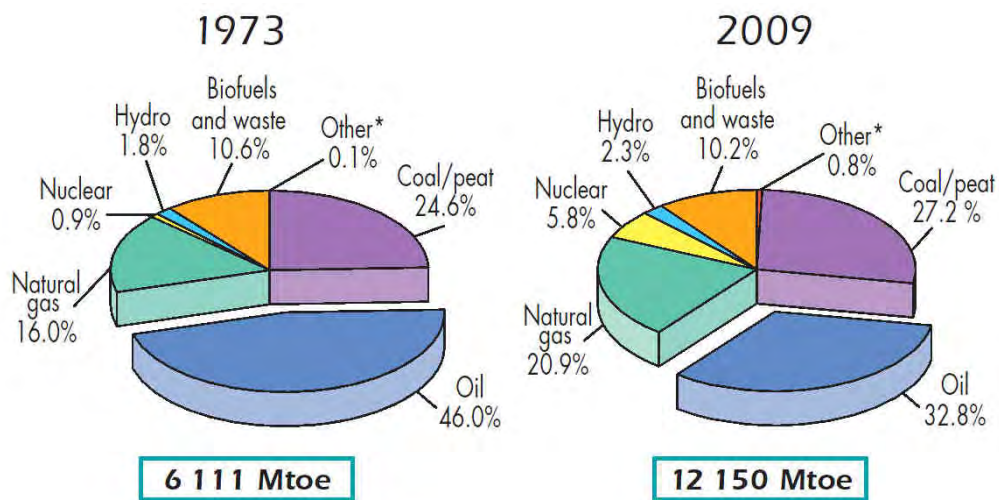


Figure 1.4. 1973 and 2009 fuel shares (other includes geothermal, solar, wind, heat, etc.) [3]

The Ocean energy is the least mature of the renewable energy technologies, but interest is growing in a wide range of possible technologies. Ocean energy technologies for generating electricity include wave, tidal (barrages and turbines), and ocean thermal energy conversion (OTEC) systems [5].

The tidal dynamics can be used to produce energy in two different manners: the first one uses local tidal currents while the second uses the rise and fall of the sea level. The kinetic energy present in tidal currents can be transformed into electrical energy by

concepts similar to those used in wind turbine, using horizontal or vertical axis turbines located at the surface, submerged or fixed to the seafloor. Tidal energy results from the rotation of the Earth within the gravitational fields of the Moon and the Sun. The potential energy obtained by the difference in height of the tide, can be converted in energy through floating or fixed devices in estuaries or oceans.

The OTEC is obtained from the temperature difference between water at the surface, heated by the effect of solar radiation, and the colder water in the depths of the ocean.

The waves are created by the action of wind passing over the surface of the ocean. The wave heights, and then their energy, are larger at higher latitudes between the 40° and 60° for both hemispheres (North and South), where the trade winds blow across large stretches of open ocean and transfer power to the sea swells. The coastal areas such as Western Europe, North America, South America, South Africa, Australia and New Zealand are characterized by high energy resources and therefore with favorable geographical conditions for the implementation of wave energy devices (Figure 1.5).

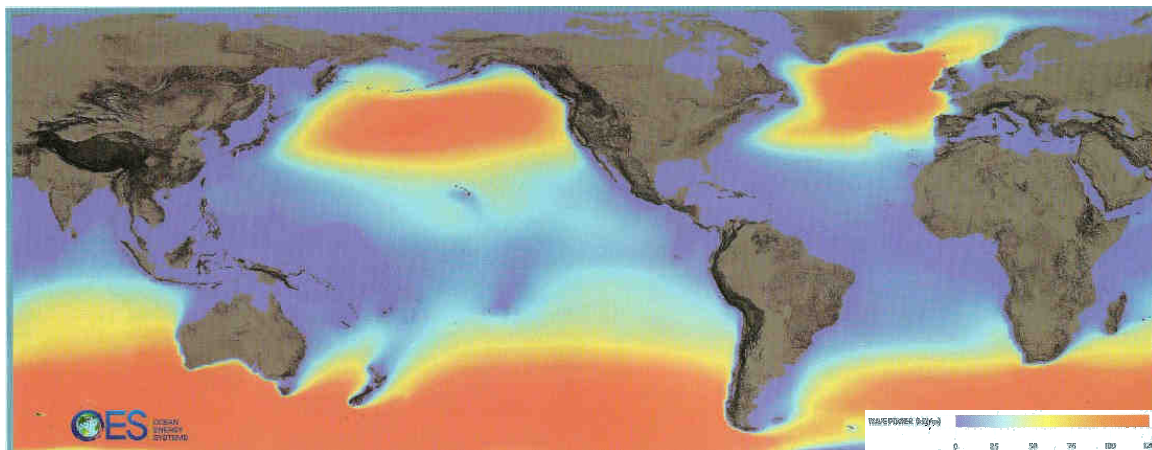


Figure 1.5. Wave energy global map [6]

In 2003, the World Energy Council estimated a value of available power greater than 2 TW for energy production. From the different ocean energy resources, wave energy is the largest and is not completely explored. The solutions for transforming wave energy contained in the Oceans and Seas (WEC – wave energy converters), into useful energy are not recent.

The first worldwide patent for the conversion of this energy into mechanical energy was published in 1799, Paris (France) by Girard (father and son). In Europe intensive research and development studies about the wave energy conversion began, however, after the dramatic increase of the oil prices in 1973; in fact at the end of 1973 there were 340

registered patents. More than 200 years after the registration of the first patent for a system for converting wave energy, there are currently more than 1000 patents regarding techniques for exploiting this form of energy.

Different European countries with exploitable wave power resources considered wave energy as a possible source of power supply and introduced support measures and related programs for wave energy. Several research programs with government and private support started thenceforth, mainly in the United Kingdom, Portugal, Ireland, Norway, Sweden and Denmark, aiming at developing industrially exploitable wave power conversion technologies in the medium and long term.

In the last 25 years wave energy has gone through a cyclic process of phases of enthusiasm, disappointment and reconsideration. However, the persistent efforts in R&D, and the experience accumulated during the past years, have constantly improved the performance of wave power techniques and have led today to bring wave energy closer to commercial exploitation than ever before. Different schemes have proven their applicability on a large scale, under hard operational conditions, and a number of commercial plants are currently being built in Europe, Australia, Israel and elsewhere. Other devices are in the final stage of their R&D phase with certain prospects for successful implementation. Nevertheless, extensive R&D work is continuously required, at both fundamental and application level, in order to improve steadily the performance of the particular technologies and to establish their competitiveness in the global energy market [7].

1.2. Motivations and objectives

In recent years several authors presented wave energy atlas of the Mediterranean Sea relied on wave measurements obtained from buoys, satellite and output from hindcast model. A first attempt to assess the offshore European wave energy resource using very accurate data was made through the European Wave Energy Atlas – WERATLAS, the adopted methodology established the basis for further development of other atlas at a regional scale [8]. Other atlas are the World Wave Atlas (WWA) that can be used for the geographical presentation of wave and wind statistics worldwide [9] and the most recent wind and wave atlas for the Mediterranean Sea area, the MEDATLAS [10]. The most

recent studies on the assessment of the wave energy availability on the Med Sea were done by Liberti et al. [11] and Vicinanza et al. [12].

The offshore characterization performed in this thesis contributes to the present knowledge with a additional contribution on the basis of a new data set focused on the last three years. It was computed for all the Mediterranean Sea and in detail, with a higher accuracy, for the North-Western Mediterranean Sea, with the wave data, provided by IFREMER (arising from numerical simulation of the model PREVIMER. The analyzed data-set covers a period of 2 years and 10 months, from 17 June 2009 for Mediterranean Sea model, and from 2 July 2009 for the NW Mediterranean Sea, to 31 March 2012.

Although the offshore wave energy potential was known from this offshore characterization or from the existing atlas, the processes affecting waves as they propagate towards the near-shore can modify the wave energy potential, leading to reductions or, sometime, local enhancements due to focusing mechanisms. To quantify these processes, and thus select the most energetic locations, a numerical simulation was used to propagate the power time series from deep water into the nearshore area of the selected test sites. The numerical simulations were carried out by the MIKE21-Spectral Wave, a spectral wind-wave model based on unstructured mesh that allows the simulation of the phenomena as non-linear wave-wave interaction, dissipation due to white-capping, dissipation due to bottom friction, dissipation due to depth-induced wave breaking, refraction and shoaling due to depth variations. This methodology was applied to four selected areas in Italy: the North of the Tuscany coast (La Spezia – Livorno), the central of the Tuscany coast (Livorno – Piombino), the Western part of Liguria coast (Ventimiglia – Imperia) and the North-West of the Sardinia coast (Stintino – Alghero). Another important analysis performed to select possible wave energy farm installation was the extraction of the local values of the yearly mean wave power in 36 different points (10 for Northern Tuscany and Liguria, 8 for Central Tuscany and Sardinia) equally spaced in the computational model or located in areas of interest, on 15 m and 50 m water depths. The two points of each site with the highest wave power values, one on 15 m water depth and the other on 50 m water depth, were analysed in order to estimate the “non-technical” barriers (as the environmental, logistical and social constraints) present in those areas and to optimize the “single body” and the Spar Buoy OWC devices in these hot-spots. The optimization was performed according to different criteria.

1.3. Outline of the thesis

The purposes of the present work are the nearshore wave energy characterization in areas not yet analysed in detail and the optimization, in two different locations of each area, of a single floating body linked to the seabed by means of a Power Take Off (PTO) mechanism (the simplest case of study) and of the Spar Buoy Oscillating Water Column (OWC), an axisymmetric floating OWC that researchers studied at Institute of Mechanical Engineering (IDMEC) of the Instituto Superior Técnico (IST) in Lisbon.

A list of the steps to follow (TRL approach) in order to develop a Wave Energy Converters (WECs) from the idea to the commercialization, the constraints to evaluate when choosing a suitable installation site and the classification of the WECs are presented in Chapter 2. This chapter describes the theoretical basis considerations used in the description of the devices that passed the phase 3 of the TRL approach and in the analysis of the “non-technical” barriers present in the selected areas in Chapter 4.

The linear theory of wave motion from which is obtained the formula of wave power in deep water used to estimate the offshore wave energy availability from the dataset of the PREVIMER models, is exposed in Chapter 3. The reliability of the data extracted from the PREVIMER models were compared with the real measurements of the Gorgona buoy, that was installed in 2008 off the Livorno coast. Moreover, the results of the monthly and yearly mean wave power were compared with those available in the literature.

In Chapter 4 the results of the propagation in the chosen nearshore areas are summarized, highlighting the focus of energy and their possible suitability for the installation of the studied devices.

The optimization of the devices regarding a single floating body and Spar Buoy OWC at these sites, performed according to different criteria (as cost and efficiency), is described in Chapter 5.

Chapter 7 presents conclusions about the results of the offshore and nearshore characterizations, of the optimization of the devices in the different selected locations and discussion for possible future developments.

CHAPTER 2

CURRENT STATUS OF WAVE ENERGY CONVERTERS TECHNOLOGIES

2.1. Description of the TRL approach

While substantial knowledge has been gained about the requirements for extracting energy from ocean waves, at the current stage of technical advancement, the development of wave energy devices still requires to employ a cautious and measured methodology. Commercial scale wave energy can only become a reality following full scale testing of wave energy converters at sea and it is essential that the correct engineering procedures are used leading up to the first sea trial. The most efficient and effective way to achieve this result is to proceed according to the development programme step by step. The principle behind this is to sequence design development so that the required knowledge is obtained at different phases to facilitate safe transmission along a course of increasing technical complexity and investment requirements. This structured program is proposed by HMRC[13] and recently by OES-IA [14].

These phases are: i) validation model, ii) design model, iii) process model, iv) prototype device and finally v) demonstration full-scale device. In all of these steps there are requirements for testing the physical models: an outline of the Protocol is given in Figure 2.1. In the past, many device developers took research results from small scales and jumped

directly to the large scale field devices: all of the devices that missed these intermediate steps failed [17].

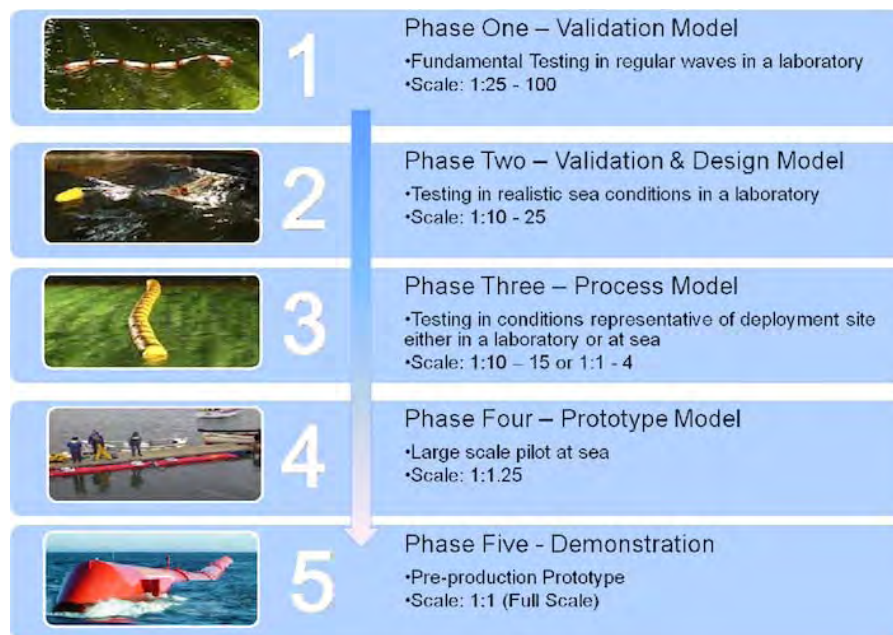


Figure 2.1.WEC develop protocol [17]

2.1.1. VALIDATION MODEL

This first phase aims to understand the overall dimension, configurations, dynamic, response characteristics and preliminary power production so it is suggested to operate with small model (1:25-100 scale) in order to modify the configurations quickly. The main purpose of this phase is therefore to unfold the idea and look more deeply into the possibilities of optimisation of the device.

Facilities

There are three types of wave tanks that can be taken into account for testing programmes and each one can prove useful for different applications.

One is the flume, which is a long narrow tank with a single wave generating paddle at one end and a downstream energy absorbing system at the other one. It is preferable if the wave generator has an active reflected wave absorption system to prevent wave build up and interfere. In the flume it is possible to produce both regular and irregular waves, but always uni-directional.

The towing tank is usually longer than flume. The additional feature is a powered mobile carriage that can travel up and down the tank to tow models through the water as required, but this is rarely useful during wave testing since devices are moored, or fixed.

The basin might be the most useful type of tank: this allows the wave approach direction variety, the short crested waves generation and the full mooring configurations accommodation, but the model handling can be more difficult than in flume.

Methodology

Firstly it is necessary to verify the concept and take care to minimise scale and laboratory effects, such as sharp corners that introduce excessive hydrodynamic damping. This is particularly important because the viscosity is a parameter poorly represented by Froude similitude. If the device is a complex structure, like, for example, a multi-hulled, initially the components can be evaluated separately. The number of degrees of freedom of the body(s) may also initially be limited. The response characteristics are the principal criteria investigated, including any interactions or interference between the independent bodies. Data should be in a form that can validate and/or calibrate any numerical models being produced in parallel with the physical modelling. A useful introduction in the early stage is the measurement of the hydrodynamic coefficients, in particular viscous damping, added mass, radiated wave damping, forces on the static bodies, (diffractions forces) etc. All the primary design variables should be evaluated and the results are principally used for comparative purposes rather than to produce absolute values; during the tests it is important to change only one parameter to identify its contribution to the power absorption. These tests are conducted in single frequency, regular wave fields of small to moderate amplitude (steepness) to remain in the linear regime, with a basic model power take-off (PTO) mechanism.

Secondly, the model performance and response can be excited by irregular waves to ascertain initial power absorption characteristics in real seaways. The range of options for the model configuration and PTO damping settings can be specified from the former trial results. Seaways should adequately cover a conventional bi-variate scatter diagram from the selected sea area. A strategic selection of the summary sea state statistics is made based on occurrence, extremes and resource turning options; the offshore engineering recommendation, which can be adopted for wave energy studies, is about 20 independent sea states. In these tests the classic spectra can be used (e.g. Pierson-Moskowitz,

Bretschneider, JONSWAP) and Holmes [3] recommends that the duration of an energy capture trial corresponds to at least of 20-30 minutes at prototype scale.

Finally, before passing to the full design feasibility, detailed measurements on an enhanced model and optimisation procedures should be conducted.

2.1.2. DESIGN MODEL

Following a satisfactory conclusion of the first phase, the additional data, such as wave forces, mooring loads and phase relationships, should also have been considered in the initial results analysis, together with any device specific measurements. In this way the overall layout of the WEC can be established and a naval architects office or an engineering consultancy can confirm the construction feasibility and establish the fabrication/manufacturing costs. Care in this process is required because unfortunately it is very easy to envisage and model components that will not be practical to produce. A systems engineering approach is essential.

Facilities

Because of the size of the model and since an important component of phase 2 testing of a buoyant WEC is the mooring, most trials must be conducted in 3-D basins. However, there are certain exceptions and specialist works can utilise other types of facilities.

In the large flume or towing tank the bottom standing, fixed or tension leg moored units can have limited testing. Waves will be uni-directional but for point absorber type WEC this will not be a significant problem. If a model represents a section of a terminator type device the trials can become fully 2-D. Towing tanks might be particularly useful for active control trials on attenuator type devices which are relatively long to their width.

Methodology

This phase requires a new or modified model at typical scale 1:10-25 with extended measurement array and a larger set of physical parameters to be measured with a more realistic PTO. The model tests are led in extreme wave conditions in order to provide the extreme motions and loads exerted on the hull, PTO, mooring lines, anchors and foundations for fixed or gravity structures and they should ensure safe station keeping, seaworthiness, survivability and validating failure modes of a device. The duration may be a typical storm length of 3 h at full-scale and some trials will be conducted for 50-100 year storms [15].

An accurately representative power take-off simulation is essential in this phase of the test programme and a numerical modelling is particularly important with regard to PTO control and strategies. The PTO should also be tested in order to simulate the worst case failure scenarios.

Furthermore, different wave approach directions should be tested to validate mooring system and anchorage requirements: a series of different wave crest approach angles to evaluate this variable should be conducted. This may be achieved in modern facilities by changing the angle the wavefront leaves the generation paddles. If this is not possible the mooring can be rotated as required. This section should even be included in axisymmetric point absorbers since the mooring influence is not non-directional. So it is important the mooring layout, which is based on load–displacement curves for several directions of motion, additional extreme wave approach angles, failure mode test when one or more mooring lines have be disconnected to simulate the line breaking. The line may be lost before a wave attack when the model is stationary or dynamically when waves are present.

In conclusion, by the end of this phase, the device specification should be defined sufficiently to allow a full design feasibility study to be undertaken.

2.1.3. PROCESS MODEL

This phase represents the change from a laboratory test tank where the conditions are controllable to a natural site where conditions have to be accepted as they occur. Device scale must advance to allow actual components to be incorporated, especially regarding the power take-off and mooring and so a scale should be selected between 1:3-15, which means that either a large-scale hydraulic test facility or a benign outdoor site can be utilised.

The process model is introduced to reduce both the technical and financial risk that would be required if the device development went straight from the laboratory scale model to a full size prototype deployed at an exposed ocean location which historically has not proven successful [14].

Tests in this phase provide the final opportunity to quickly, reasonably easily and relatively inexpensively learn about the inevitable problems still associated with a device, its operation and deployment techniques. The specific aims of large scale model tests at benign sea sides are: investigation of not well scaled physical properties, implication of a realistic/actual PTO and generating system, qualification of future environmental factors

(marine growth, corrosion, windage and current drag), validation of the electrical supply quality.

Facilities

Two specific and distinct approaches can be taken to completing this phase of the development. There are advantages and disadvantages for both. The two different options are:

- a) an internal large-scale test facility;
- b) an external benign sea trial site.

The main advantage of the large scale tank (flume or basin) approach is that the facility is fully controllable both in terms of the actual sea states produced and the exact repeatability of conditions for test comparisons. The primary disadvantages are the high cost of hiring such facilities and the upper limit on the size scale of the model that can be accommodated. The scale model is between 1:10-15 and the two objectives are: validate or calibrate, the smaller scale results, and introduce advanced trials not trustworthy at the smaller scale.

The benign sea side is a wave active but partially protected location such as a fresh water lake or a sheltered bay offering sufficient water depth and easy land access. The wave climate is probably the most important factor when selecting a large scale test site. Correctly scaled wave conditions relative to the final site are an important aspect to consider for the outdoor location and may reduce safe testing of the device to specific seasons of the year. The sea states must be scaled proportionally to represent the full ocean conditions that the prototype will actually encounter. This involves adjusting both the height, that scales linearly, and the period, that is a square root term, so there are not many ocean sites that satisfy both these requirements. If the proposed wave park location is in a lower energy area, such as the North Sea and the Mediterranean Sea, the ratios may be closer to 1:2 and 1:4 so the device would be scaled to half the proposed prototype. A primary list of requirements for a benign test site could be summarized as follows:

- a) acceptable wave climate;
- b) sufficient wave depth;
- c) low tidal elevation range and currents;
- d) adjacent harbour for service and personnel transport vessels;

- e) tugs or similar vessels capable of handling the device;
- f) sheltered port with lifting facilities;
- g) local heavy engineering infrastructure;
- h) on shore data acquisition station;
- i) attitude / acceptance (by national and local inhabitants);
- j) convenient travel hub;
- k) modern communication links.

The advantages of using external deployment sites are that there is usually only a moderate hire fee, if any, and the model scale can be larger. The principal disadvantage is that there is no control on the input conditions so the test programmes must be well structured to achieve repeated trials and cover the extensive set of different excitation forces required. One approach is to extend the testing period, which could be perfectly acceptable depending on the cost of monitoring the device once it is on station.

Methodology

This will be the first time all the required components, from primary converter to electrical generators and power electronics, will be assembled, albeit at reduced scale. This means that design teams can experience and develop both technical and managerial skills to bring these tasks together. It can be noted from past experience that if this step is neglected, usually there is a high price to pay later [14].

The main difference between systems trials and the previous two phases is that the wave conditions are no longer controllable, selectable or supplied on demand and for this the test schedule must be robust and capable of accommodating sea states when they occur.

Due to the high cost of submarine cables and strict connection requirements to a national electricity supply network, the level of power output may not justify grid connection.

It is also essential that all parts of the PTO system are verified prior to deployment at sea with extended bench testing.

2.1.4. PROTOTYPE DEVICE

In this phase, the device is built at scale 1:1-2 and tested in the sea. Here the device must progress from a pre-production to a pre-commercial machine. The device to be tested at this level would be at, or close to, full size but still a solo machine. Essentially during this stage, testing should verify the overall design to individual component suitability, through to electrical production and quality of supply. The main objectives are [16]:

- a) demonstration of system integrity and viability of technology;
- b) to seek for aspects that had not been identified during the previous project phases and to gain experience;
- c) establish controllability;
- d) gain operational experience;
- e) calibration of analytical/numerical model from data from prototype at sea;
- f) early indication of availability of systems considering degradation mechanisms and maintenance routines;
- g) establish power conversion capabilities.

Facilities

The tests can be performed in a sea trial test centre or in an ad hoc test station.

The principle requirements of a test centre [14] are:

- a) correct met-ocean conditions (wave climate, water depth, low current, no ice etc) for both types of sites; electrical grid connection and sub-station;
- b) adjacent wave monitoring equipment (more than one sensor);
- c) convenient connection mooring berths;
- d) on-shore data receiving facility with internet connections;
- e) local launch, recovery & facilitating harbour with service vessels;
- f) suitable travel and communication infrastructure;
- g) experienced engineering yards with mobile operating capability;
- h) agreed simplified licensing and consenting regime;
- i) agreed procedures for environmental monitoring;

- j) agreeable berth leasing charges, personnel fees, equipment hire, etc.

The ad hoc test station, besides possessing most of the criteria listed above, must offer an electricity grid passing close to the submarine cable landfall or use a grid emulator alongside and for a solo device this will probably be a low voltage distribution network connection. The licensing, permissions, environmental impact assessments and engagement with local stakeholder groups must be possessed before the installation of the cable and the device.

A local site with low to moderate wave conditions where the WEC behaviour can be safely experienced by the operators should be considered to establish emergency control strategies, and when sufficient experience and operational results have been obtained, the WEC can be deployed in a more exposed energetic open ocean site.

Methodology

In the initial tests the grid connection is not essential and so the deployment site can be selected to facilitate extensive testing rather the electrical distribution network. Anyway, towards the end of the tests, the device should be connected to test the quality of supply to the electrical grid. The deployment site can be a test centre, which should offer easier grid connection that includes performance monitoring instrumentation, or an ad hoc site. It should be highlighted that the location for testing a single device and of the wave energy farm in test phase 5 would then not be identical and the device may be moved afterwards.

During these sea trial programmes, the environmental impact issues should begin to be addressed, and, if phase 3 studies have not furnished sufficiently detailed generic recommendations for array interactions, some specific tests should be conducted in the preparation for the next phase activities.

2.1.5 DEMONSTRATION DEVICE

When a device successfully completes the rigorous technical sea trials outlined in the previous phases, the pre-production converter should have evolved into a pre-commercial machine ready for economic demonstration in phase 5 [18]. The purpose of this phase is to test small groups of wave energy devices that, if successful, can be expanded into a full electricity generating station. During this phase the power electronics controlling the output and the physical influence of one machine on another will be determined.

The principal objectives of this full scale device are [14]:

- a) verify the multi-device park configuration interactions;
- b) validate power conditioning equipment associated with array output aggregation;
- c) subsea cable installation, interconnectors and substation construction;
- d) quantification and qualification of power supply quality to the grid;
- e) investigate electrical control interaction;
- f) precise proof of economic feasibility;
- g) establish component lifecycle, maintenance and service operations;
- h) consenting, licensing, permits, certification, insurance health & safety aspects;
- i) multiple device/wave park environmental impact assessment;
- j) marine growth & corrosion monitoring;
- k) de-risked business plan;
- l) early engagement with stakeholders;
- m) navigational risk assessment.

Economic analysts suggest that ocean energy parks will only become commercially viable when large arrays of devices (50-100MW) are deployed [14]. However, the purpose of this phase 5 is to start testing a small group of WECs that, if successful, will be developed into fully commercial electricity generating stations.

Environmental effects on the machines must also be carefully monitored, especially marine growth and corrosion issues and the influence of this on power production.

Facilities

There is only one site dedicated to pre-commercial sea trials for small array testing, the Wavehub in Cornwall, England, which should be operational in 2012-13 [14]. However, at the moment, there are other test centres available with high capacity subsea cables and a robust grid connection, such as the Spanish BIMEP, the Portuguese's Pilot Zone and the Irish WEC.

The submarine cable and the landfall grid connection distinguish this phase from the previous. A dedicated substation will be required to facilitate grid connection of the device array. The grid operators will impose strict quality control measures on the electricity supplied, so this will need to be monitored and managed effectively. Cable landfall planning

applications and permissions, including Environmental Impact Assessment (EIA), will of course be required.

Methodology

The array interactions studied in the previous phases, are now confirmed at full scale in the uncontrolled conditions found in the open sea. The multiple device physical interactions and the multiple electricity source aggregation must be considered. It is important to establish if either, or both, of these effects produce a result that is greater than the individual parts, or at worst, no less.

Besides it should be considered the use of mechanical inertial storage, hydraulic accumulators and the electrical storage in combination with power electronic converters, in order to smooth the irregular supply from a single WEC, due to the irregular input flux.

Finally the failure rates and breakdown, the impact of the devices on the environment and of the environment on the devices should be carefully monitored.

2.2. Methodology for the WECs site selection

The selection of the location, for the deployment of a wave energy pilot plan with the aim of energy production or for the field laboratory where it is possible to test the device, is a technical, economic and strategic problem that the developer has to address. In order to provide an estimate of the available energy resource over a particular area, a wave resource characterization and a site assessment are necessary. A methodology for site selection (Figure 2.2), developed by the Waveplam project [19], consists of two phases: the first is where information is gathered and a preliminary assessment of the suitability is undertaken and the second, where all the information is integrated into a relevant geographic analysis tool for the decision making.

This procedure does not cover the planning and site selection phases of onshore devices nor breakwater or near shore coastal structure-mounted devices because they are extremely dependent on the construction of the structures; the planning process is necessarily triggered by the construction of the breakwater, and the factors that affect the site selection are limited to the location of the port facility.

Before this it is necessary to identify the general area of interest and to define the characteristics and requirements of the project, like, for example, the overall power and type of wave energy devices expected to be installed (see paragraph 2.3).

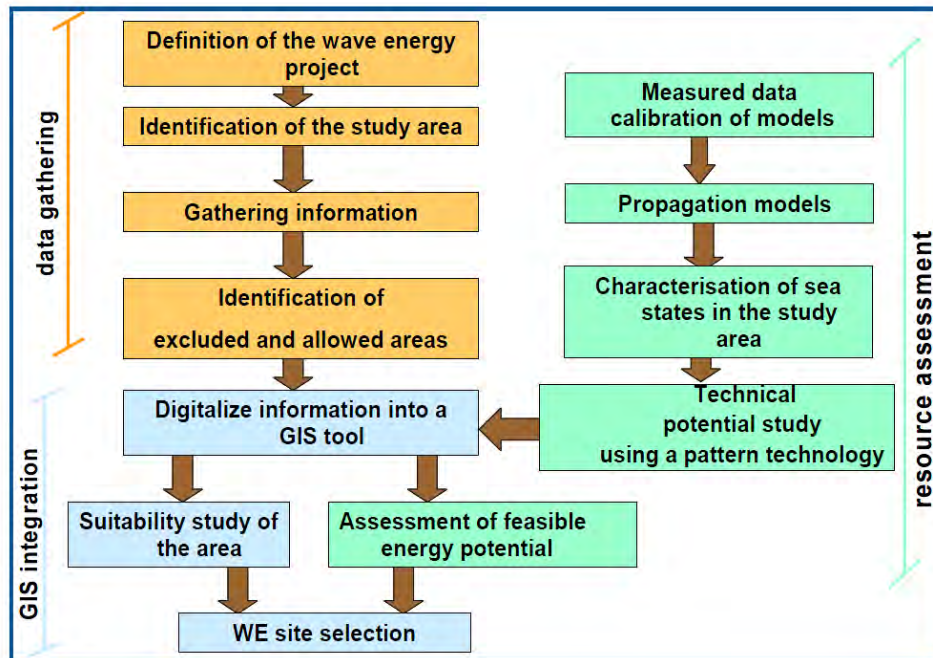


Figure 2.2. Diagram showing the main activities contained in the methodology [19]

2.2.1 PRELIMINARY ASSESSMENT

2.2.1.1. *Gathering information*

Initially it is important to gather information about:

- energy resource,
- bathymetry and seabed,
- electric grid,
- infrastructure and supply,
- environmental and planning issues,
- environment characterisation,
- interference with other uses.

Energy resource

The first parameter that needs to be assessed is what level of power resource is available in the area. A small resource does not necessarily mean that the site is unsuitable, since

wave parks, and especially certain wave energy devices, can be scaled to meet the power requirements [20]. For assessing the wave power resource of a specific location, wave climate needs to be known. In the open ocean wave conditions do not change significantly within distances of the order of few hundreds of kilometres in large ocean basins or some tenths of kilometres in smaller basins. As waves travel towards the coast through waters of decreasing depth, they are changed due to the effect of the seabed which causes energy concentration in some areas and rarefaction in others due to refraction and diffraction phenomena. Energy dissipation occurs due to bottom friction and percolation and mainly by wave breaking. Such shallow water phenomena start to occur when the water depth becomes smaller than half of the wavelength, however, most relevant modifications occur for $h < 20\text{m}$. Other important sources of resource spatial variability is shelter by the coastline and neighbouring islands and, in the shoreline, diffraction caused indented coastlines [21].

There are several ways to obtain statistic wave data: remotely sensed data (satellites), in-situ measurements (buoys) and data obtained from numerical models. For this analysis it is recommended a minimum of 10 years data (measured or derived from numerical models) for understanding the seasonal and inter-annual variance of the resource and identifying some constraints on resource harvesting [22]. To characterize the nearshore and shoreline resource, shallow water wave propagation models taking as input offshore wave conditions provided by wind-wave models or by buoy data are used.

Moreover local wave measurements are necessary for the power plant design. For these measurements the most widely used sensor type is the wave surface following buoy. This may either be a pitch-roll buoy which measures the elevation and the slope of the surface, or a particle following buoy which measures the elevation and the orbital motions at the surface. Another type of fixed instrument is the Acoustic Doppler Current Profiler. These have been in use for wave measurement for a comparatively short time, but may offer advantages in shallower water (depth $\sim 10\text{m}$). They are usually bottom-mounted and work by transmitting pulses of acoustic energy upwards towards the surface. The acoustic energy is scattered by particles in the water and some of this is received by the instrument. If the water is moving the backscattered signal is Doppler shifted, allowing calculation of the along-beam velocity. They typically use three mutually inclined beams and also a vertical central beam which is essentially an upward looking echo sounder. The acoustic return is range-gated so that a profile of current measurements through depth is obtained. The directional information is derived from the velocity measurements from the near-surface

range-gates which form a horizontal array of vector measurements. A remote sensing (i.e. non-contact) system which should be considered for near shore test sites (range \sim a few km) is X-band radar, which can provide high-resolution directional spectra when used in conjunction with an additional instrument to provide absolute scaling. The system provides directional spectra averaged over an area of order half square kilometre of sea. For very shallow water the use of an array of pressure sensors should be considered [23].

Bathymetry and seabed

An accurate knowledge of the bathymetry allows a good understanding of the processes and the wave field in the area, and, also, allows knowing the distance from the shore at which the required depth is reached and, therefore, the length of the submarine cables that influences greatly the cost of the project. Shoreline/nearshore devices should be located at sites where the depth is less than one quarter of the wavelength of the principal component and the bathymetry is regular. They also should not be located in areas where boulders are found to avoid wave energy dissipation by breaking. Offshore devices should be located in 50 – 80 m water depth, where the wave conditions are similar to deep water, except if shelter by the coastline and/or neighbouring islands occurs [21]. The berths for floating WECs would usually be on compliant moorings or possibly taut moorings in depths of order one half of the wavelength of the principal wave component. The depth should ideally be constant over the test area but in any case there should be an absence of bathymetric features which could lead to small-scale wave focusing or defocusing effects and the currents should be spatially uniform and of order 2 m/s maximum [23].

For bottom standing OWCs, seabed coverage by sand or gravel may pose problems because it may partially fill the pneumatic chamber. Regarding offshore devices, the nature of the seabed and the morphology will also have influence on installation methods. Very irregular and rocky seabed will not be an advantage and may obstruct the installation of elements such as the moorings of the buoyant devices and the submarine cable. In fact burying the cable can be a simple operation on sandy or on unconsolidated sediments, using techniques such as ploughing and jetting, or become a more complex and costly process on hard rocky bottoms, where a trench needs to be opened.

Electrical grid

A wave energy park must be next to an electrical grid because the aim is to supply the produced power to the grid. So it is necessary obtaining technical information about the existence of distribution lines, substations, connection points, voltage and supply capacity

in the interest area. Moreover the proximity of the electric grid allows that the production point is at a short distance from the consumption point.

Infrastructure and supply

The wave energy park or installation will need a series of services as maintenance operations and monitoring, and so the proximity to infrastructure and supply is indispensable. A good-sized harbour will be necessary for the installation and good servicing of the facilities, due to this constant need for vessels that carry out deployment, maintenance and/or decommissioning works. Also the existence of local industries that can manufacture and supply some of the elements is useful. These would involve facilities and skills as shipyards, monitoring equipment, ROVs, divers, maintenance boats for in-situ works, maintenance in harbour, installation-decommissioning activity, qualified staff for these operations [19].

Environmental impact

Impacts on flora and fauna are larger during construction and decommissioning phases than during operation and so a characterization of these is required for the planning of wave energy power plants. For shore-based plants the most likely potential impacts are noise and visual intrusion but if shoreline/neashore power plants are integrated or connected to breakwater or other coastal structure, no environmental impact is added by these plants. However there are numerous uncertainties regarding the environmental impacts and so it is essential to carry out a detailed analysis of all the relevant legislation that is in place in the interest area, to ensure that there are no incompatibilities with those plans and the projected activity, and, thus, carry out the relative Environmental Impact Assessment (EIA).

Environment characterisation

Knowledge of the environment characterisation (coastal morphology, climatic conditions, seismicity and volcanology) of an area is essential for the planning of the installation works. The coastal morphology can condition the works of cable lying in the transition zone between the sea and the land because there are different installation work types depending on cliffs, beaches, rivers or deltas. For example the shorelines with cliffs are not appropriate for the landing of the submarine electrical cables.

The climatic conditions as wind regimes, tidal range and currents, temperature are additional conditions that will influence the installation and seeing that the useful life of

these kinds of project is typically 25 years, the extreme event records and the return period data should be gathered [20].

Interference with other uses

Finally it is important to analyse the interference with other uses that are present in the interest area and impose limitation to the project development. These activities are:

- a) oil and gas extraction;
- b) aquaculture: incompatible also because the presence of a fish farm could prevent the installation of cables or other structures;
- c) military activities: these areas should be avoided in the search for placing wave energy devices due to temporary firing periods [24];
- d) other marine renewables;
- e) sand and gravel extraction and dredging: incompatible for the presence of moorings and elements on the seabed;
- f) navigation routes: busy maritime traffic lines should be mapped and interference with them avoided;
- g) submarine telecom/ electric cables, pipelines, sewage pipes: they should be carefully mapped and avoided and so, for security reasons, a 500 m buffer around the cables was set as non-usable [24];
- h) fisheries;
- i) submarine archaeology;
- j) sports and leisure use of the coast;
- k) landscape and seascape as public heritage: three areas are restricted for the protection and maintenance of biodiversity.

2.2.1.2. Resource assessment

When the gathering information has been completed, a detailed resource assessment needs to be undertaken. One way of estimating wave resource is with the use of numerical models that can predict the wave height and energy that can reach a particular coast stretch. This evaluation is obtained by the propagation of the offshore data to coast, considering the bottom friction and the reflection and refraction phenomena. Before the propagation, the offshore data need to be calibrated and validated with real measurements data from a

wave buoy, and parameters such as RMS errors, scatter index etc. should be calculated to quantify the model performance.

Knowledge of the temporal variation of the wave resource at a prospective site for a wave power development is crucial to the long-term viability of the project. In general, sites with lower variability will prove more attractive to developers. Devices are designed for optimum performance in sea states with specific characteristics, and although many can be tuned to respond to changing sea states, the rate of tuning will reduce the efficiency of energy generation. Additionally, the issue of device survivability will lead to a preference for sites which only experience infrequent extreme storm conditions. Therefore sites with a more moderate but consistent resource will often be preferable to sites with a notionally more energetic, but less reliable, resource.

The term ‘temporal variation’ can refer to [22]:

a) Long-term assessments are performed to identify the annual average power level in a specific site and to investigate its inter-annual and seasonal variations. A minimum of ten years of data is recommended for such a study. The level of resource over this period and the seasonal variations and inter-annual trends should be summarised and identified with scatter diagrams, a wave time series data, that include the frequency of occurrence of different combinations of sea states, described by intervals of significant wave height, H_{m0} , and energy period, T_e [25]. When the WEC power output is considered, it is also important to refer to the power matrix (Figure 2.3) that gives the expected power output (in kW) for a particular combination of H_{m0} and period (typically T_e).

b) Medium-term assessments: knowledge of how the available power varies over the course of a year will enable predictions of annual power output (Figure 2.4), and hence economic viability of a site, to be made. Although seasonal variations are inevitable, with lower energy expected during summer months, too large a degree of monthly or seasonal variation will reduce the viability of projects if sufficient power output levels cannot be maintained year round. Scatter diagrams shall be produced to summarise the annual wave resource and seasonal diagrams (Figure 2.5) corresponding to winter (December, January, February), spring (March, April, May), summer (June, July, August) and autumn (September, October, November) may additionally be presented.

c) Short-term assessments, e.g. daily or weekly variations. This will be important to help define the power that will be provided into any grid for matching and will support the producer in achieving a better price for production.

		Power period (T_{pow} , s)																
		5.0	5.5	6.0	6.5	7.0	7.5	8.0	8.5	9.0	9.5	10.0	10.5	11.0	11.5	12.0	12.5	13.0
Significant wave height (H_{sig} , m)	0.5	idle	idle	idle	idle	idle	idle	idle	idle	idle	idle	idle	idle	idle	idle	idle	idle	idle
	1.0	idle	22	29	34	37	38	38	37	35	32	29	26	23	21	idle	idle	idle
	1.5	32	50	65	76	83	86	86	83	78	72	65	59	53	47	42	37	33
	2.0	57	88	115	136	148	153	152	147	138	127	116	104	93	83	74	66	59
	2.5	89	138	180	212	231	238	238	230	216	199	181	163	146	130	116	103	92
	3.0	129	198	260	305	332	340	332	315	292	266	240	219	210	188	167	149	132
	3.5	-	270	354	415	438	440	424	404	377	362	326	292	260	230	215	202	180
	4.0	-	-	462	502	540	546	530	499	475	429	384	366	339	301	267	237	213
	4.5	-	-	544	635	642	648	628	590	562	528	473	432	382	356	338	300	266
	5.0	-	-	-	739	726	731	707	687	670	607	557	521	472	417	369	348	328
	5.5	-	-	-	750	750	750	750	750	737	667	658	586	530	496	446	395	355
	6.0	-	-	-	-	750	750	750	750	750	750	711	633	619	558	512	470	415
	6.5	-	-	-	-	750	750	750	750	750	750	750	743	658	621	579	512	481
	7.0	-	-	-	-	-	750	750	750	750	750	750	750	750	676	613	584	525
	7.5	-	-	-	-	-	-	750	750	750	750	750	750	750	750	686	622	593
	8.0	-	-	-	-	-	-	-	750	750	750	750	750	750	750	750	690	625

Figure 2.3. The power table for a given Pelamis configuration [27]

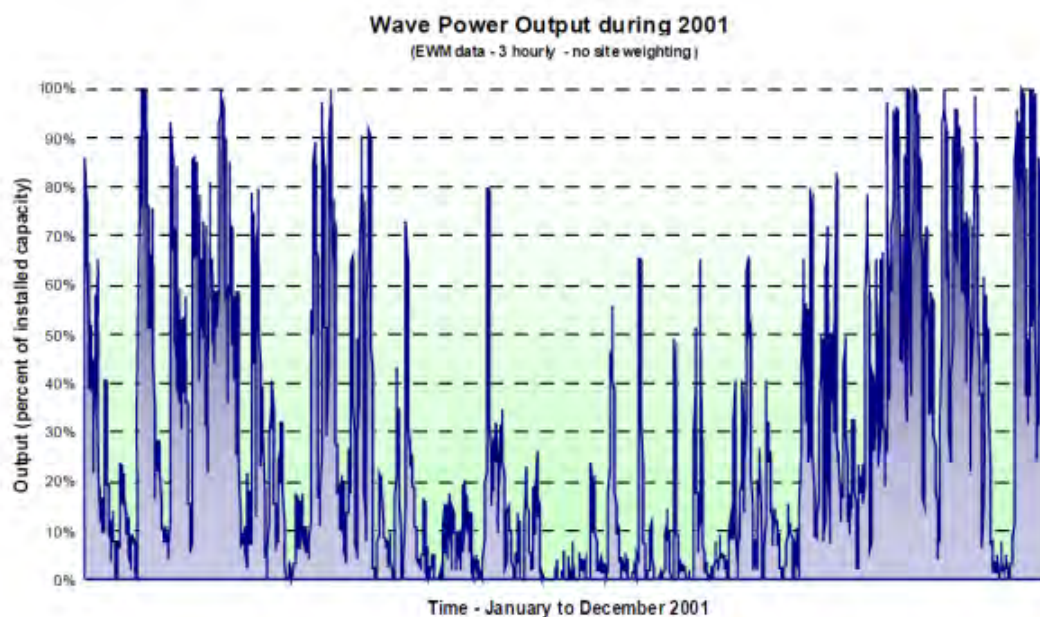


Figure 2.4. Illustration of a yearly distribution of wave power output [26]

d) Time series variations, e.g. the variation of sea surface elevation over the length of an individual record, usually of the order 20 minutes to one hour.

For the resource assessment it can be useful also do an all-year power-weighted wave rose [29]. This plot has a form of histogram and is based on the power-weighted mean wave direction that is contained within each sea-record. The individual power-weighted mean wave direction values, in Figure 2.6, from the set of sea records for the year are binned into sixteen bins, each of which represents one of the 22.5 degree sectors. The area

of each drawn sector in the plot is then made proportional to the number of entries assigned to it.

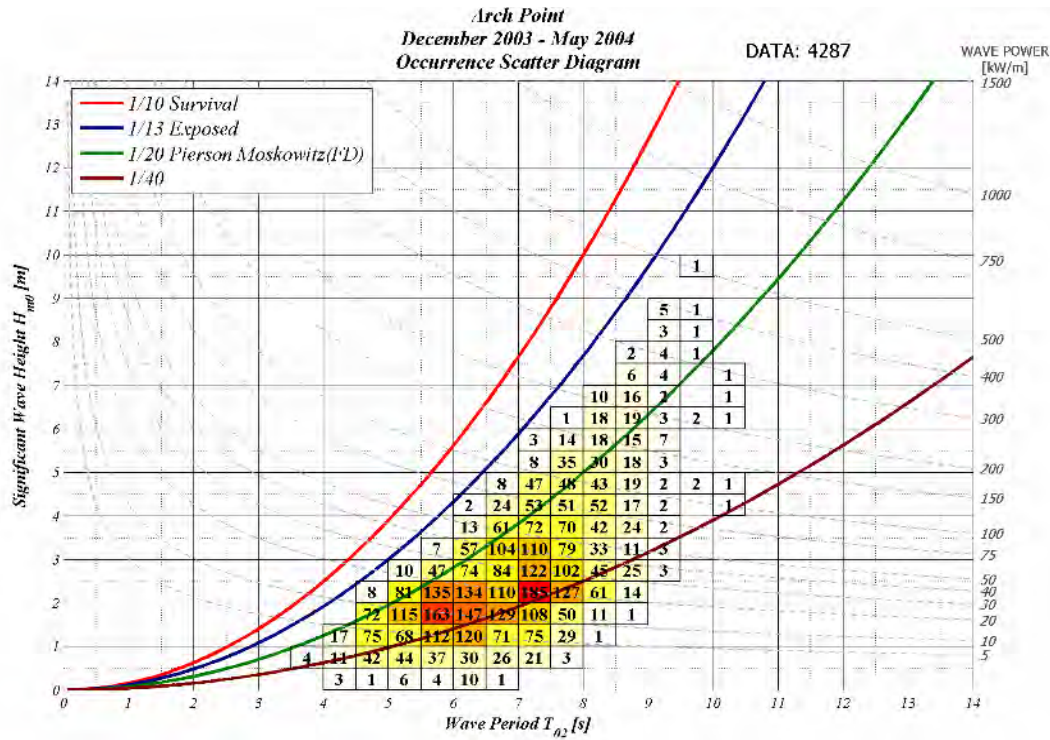


Figure 2.5. Scatter diagram for Arch Point location and plot of the lines that represent the constant significant steepness and the incident wave power [28]

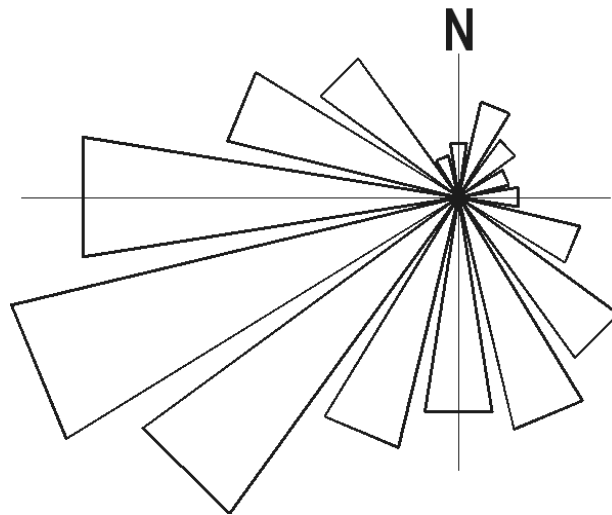


Figure 2.6. Sixteen-sector power-weighted wave rose plot. [29]

Finally the assessment of the 10, 25 and 50 year return period H_{m0} is not mandatory, but is recommended at the early stage of a project where a wide geographical area may be under consideration and the 90% and 95% confidence intervals shall be reported [22]. These values are necessary for the structural engineering design.

2.2.2 GEOGRAPHICAL ANALYSIS

Geo-spatial multi-criteria analysis is a suitable technique to take into account, at an early stage of the design process, a wide variety of environmental and administrative factors (water depth, distance to shore, distance to the electric grid in land, geology, environmental impact) and assign corresponding weights, which returns numerical results (called sometimes Suitability Index) and, consequently, suitability chart for each location. The value of the Suitability Index in each point is the result of multiplying the values of all the layers that are present at that point. This value can be given in a percentage, 0-100% format, in 0 (where are present an excluding factor) to 1 numbers or in any other suitable way. Identifying the best location to implement a wave energy farm can be specifically treated as a geo-spatial problem. Geographic information system (GIS) is specially designed to solve this type of problems and is able to integrate, process, represent and analyse geographically referenced data. It allows quick visualisation of conflicts of use and interactions, analysis of alternatives, and it makes it easy to change, if needed, position, shape, orientation, size and other parameters of the elements of the wave farm, to fit in better areas and enables observation of how the conflicts change with these modifications.

For the purpose of the addressed problem, GIS provides the framework in performing geo-spatial analysis based on overlay and map algebra functionality aiming at a multi-criteria analysis of several conditioning factors.

As for the criteria analysis selection the authors consider different options. Nobre et al. (2007) use two factor types: restrictions and weighted factors. Restrictions (e.g. existing underwater cables, marine protected areas, military exercise areas) are used to define exclusion areas, meaning that their areas of coverage are eliminated from the analysis process; weighted factors (e.g. ocean depth, bottom type, distance to ports, distance to shoreline and to power grid, wave climate characterized by significant wave height, period and power) are evaluated for their impact on the system implementation and weighted according to their relevance.

Instead in the Waveplam protocol [19] three factors are picked out, divided into exclusive and limiting: technical, environmental and socioeconomic factors. The technical factors are those that affect the installation from a technical point of view, conditions that can make the installation non-viable because of technical impossibility or because of too high costs. The wave energy flux, the type of seabed, the access to ports and anchoring zones, the maritime routes, the submarine cables and pipelines, the marine military areas,

the Oil&Gas extraction, the sand and gravel extraction and dredging, the distance to a sizeable harbour could be included in these factors. The environmental factors consider the environmental restrictions put by the legislation on a particular area and on resources contained in it. Both coastal and maritime areas are usually subject to spatial planning regulations and plans by the competent authorities that are necessary to know. The socioeconomic factors do not represent technical non viabilities, but they are factors that can hinder the installation because they are related to government policies, primarily, and then to public perception and impact on local lifestyle. In these factors can be included the fishing activity, the economic exploitation of other resources (shellfish, algae, ...), submarine archaeology, swimming, surfing and beach leisure.

2.2.3 SUMMARIZING TABLE

Finally it is useful to summarize all the information necessary for the site selection for a pilot plant finalized to the energy production or for a field laboratory for device testing (Table 2.1).

Table 2.1. Site selection characteristic

Characteristic	Pilot Plant → Energy production	Field laboratory → Test
energy resource	×	×
current and tidal value	× ¹	× ¹
bathymetry	×	×
seabed	×	× ¹
electrical grid	×	-
Infrastructure (harbours, shipyards...)	×	×
supply	×	×
environmental protected areas	×	×
environment characterisation	×	×
technical factor	×	×
socioeconomic factor	×	×

¹ It is important only for the mooring system.

2.3. WECs classification

At present a large number of Wave Energy Converters (WECs) have been proposed with a wide variety of wave technologies [30], depending on the different ways in which energy can be captured (or power take off), the water depth and the location, the type of the device and the operating principle.

2.3.1 LOCATION

Three types of WECs can be listed: a) *onshore*, b) *nearshore*, c) *offshore*.

The *onshore* (also called first generation) devices are located completely onshore and therefore they are easy to maintain and are less likely to be damaged in extreme conditions. One disadvantage is the lower wave power, but this can be partially compensated by natural energy concentrated locations [31].

The *nearshore* (also called second generation) devices are defined as devices that are in relatively shallow water. These WECs are often connected to the seabed, they capture wave energy in the nearshore and convert it into electricity in an onshore facility.

The *offshore* (also called third generation) devices are located in deep water and don't have any onshore facility. The last two categories are characterised by a larger amount of available wave energy but at the same time the device construction, maintenance and energy transport is more difficult.

2.3.2 TYPE

Despite the large variation in designs and concepts, WECs can be classified into three predominant types (Figure 2.7): a) *attenuator*, b) *point absorber*, c) *terminator*.

The *attenuator* is a floating device aligned with the incident wave direction with their breadth much smaller than their length.

The *point absorber* is a device that has small dimensions relatively to the incident wavelength, then the wave direction is not important for these devices. It is able to capture energy from a wave front larger than the physical dimension of the absorber. It can be a

floating structure that heave up and down on the surface of the water or submerged below the surface relying on a pressure differential.

The *terminator* devices have their principal axis parallel to the wave front (perpendicular to the predominant wave direction) and physically intercept waves [31].

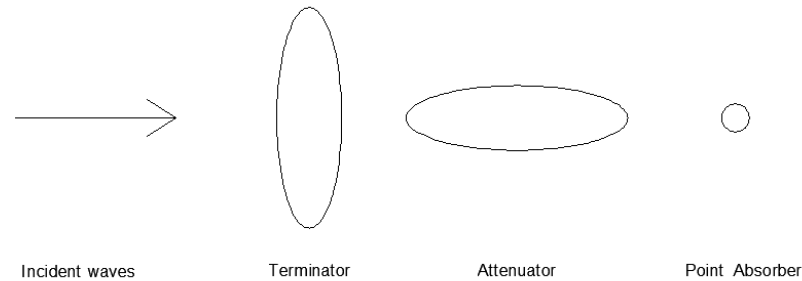


Figure 2.7. Sixteen-sector power-weighted wave rose plot.

2.3.3 OPERATING PRINCIPLE

The energy extraction methods or operating principles can be categorised into three main groups: a) *oscillating water column (OWC)*, b) *overtopping device (OTD)*, c) *oscillating body (OB)*. In the *OWC* the waves cause the water column to rise and fall, which alternately compress and depressurise an air column. This trapped air is allowed to flow to and from the atmosphere through a Wells turbine, which usually has the ability to rotate regardless of the direction of the airflow. The rotation of the turbine is used to generate electricity (Figure 2.8a).

The *OTD* device relies on the physical capture of water from waves that is held in a reservoir above the sea level, before being returned to the sea through low-head Kaplan turbines which generates power. Collectors may be present to concentrate the wave energy (Figure 2.8b).

In the *OB* the oscillatory motion of body parts of a device relative to each other's, or of one body part relative to a fixed reference, is activated by the wave motion. Typically the energy is extracted by using hydraulic systems to compress oil, which is then used to drive a generator [32]. The *OB* devices can be categorised in sub-groups describing the energy extraction by the device position (floating or submerged) and by the principle motion (heave or roll). The *OB* submerged heave can also be called *submerged pressure differential* and is typically located nearshore. The motion of the waves causes the sea level to rise and fall above the device, inducing a pressure differential, that can pump fluid through a system to

generate electricity. The OB submerged roll can also called *oscillating wave surge converter* (Figure 2.8c2). In these devices the arm oscillates as a pendulum mounted on a pivot joint in response to the movement of water in the waves [33].

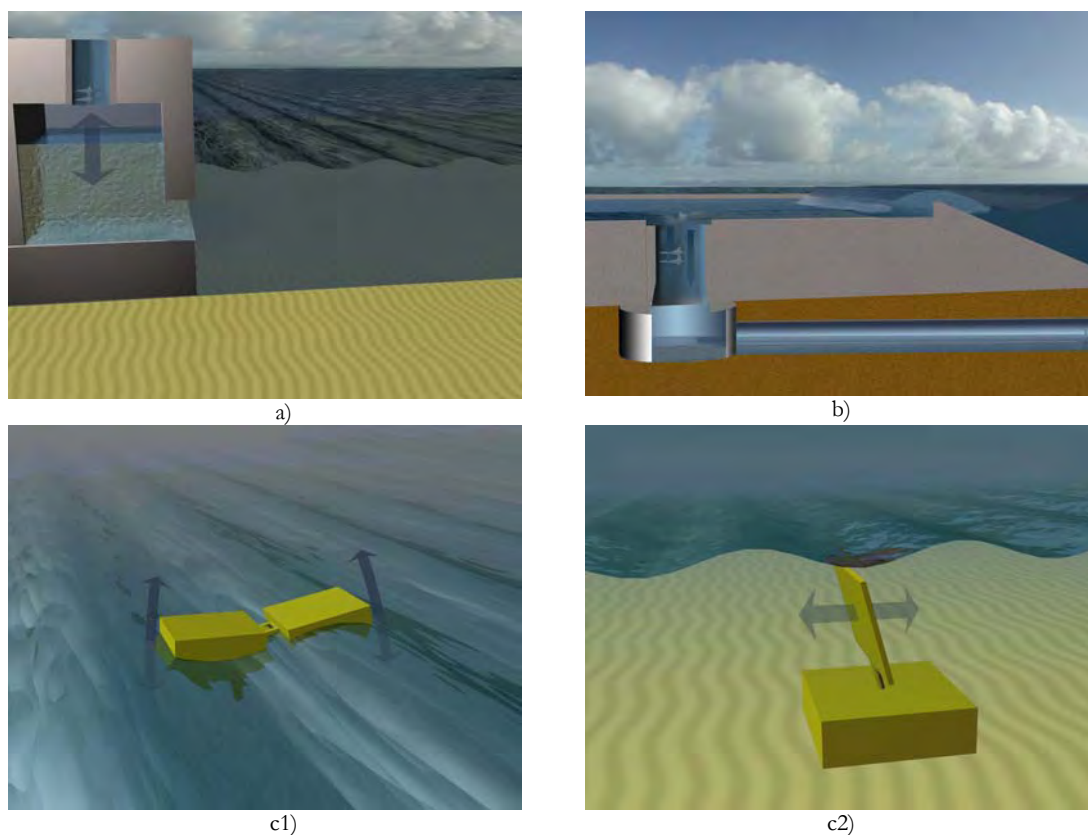


Figure 2.8. Operating principle: a) OWC, b) OTD, c1) OB floating rotation, c2) OB submerged rotation [33]

2.3.4 POWER TAKE OFF

The power take-off (PTO) is the mechanism by which the energy is transferred between the waves and the WEC, and subsequently or directly into useful form [34]. The PTO varies from device to device, but, generally, it can be classified into: a) *water turbine*, b) *air turbine*, c) *hydraulic motor/generator*, d) *linear generator*.

The most popular *air turbine* design is the Wells turbine, because of its ability to rotate in the same direction, irrespective of airflow direction [31]. This turbine has been the most commonly adopted solution to the air-to-electricity energy conversion problem in the OWC devices [35], despite inherent disadvantages in comparison with conventional turbines: lower efficiency, poorer starting and higher noise level [36].

Hydraulic turbines as in conventional mini-hydroelectric low-head plants (axial-flow reaction turbines) are used to convert the head (typically 3-4 m at full size) created between

the reservoir of an overtopping device (OTD) and the mean sea level into electricity. High-head (typically tens to hundreds of meters) impulse turbines (mostly of Pelton type) are adopted in some oscillating bodies, as alternatives to hydraulic motors, with the advantage of using non-pollutant water (rather than oil). These low and high-head hydraulic turbines may reach efficiency peaks up to 0.9 [30].

Another method of converting the low-speed oscillating motion of the primary WEC interface is to use a *hydraulic motor/generator*. Waves apply large forces at slow speeds and hydraulic systems are suited to absorbing energy under this regime. Moreover, it is a simple matter to achieve short-term energy storage, necessary to achieve the smooth electricity production required for a marketable machine, with the use of cheap and available high-pressure gas accumulators [34].

A *linear generator* offers the possibility of directly converting mechanical energy into electrical energy, without intermediate steps between the primary interface and the electrical machine. The basic concept of a linear generator (Figure 2.9) is to have a translator (what would be the rotor in a rotary machine) on which magnets are mounted with alternating polarity directly coupled to a heaving buoy, with the stator containing windings, mounted in a relatively stationary structure (connected to a drag plate, a large inertia, or fixed to the sea bed). As the heaving buoy oscillates, an electric current will be induced in the stator [31].

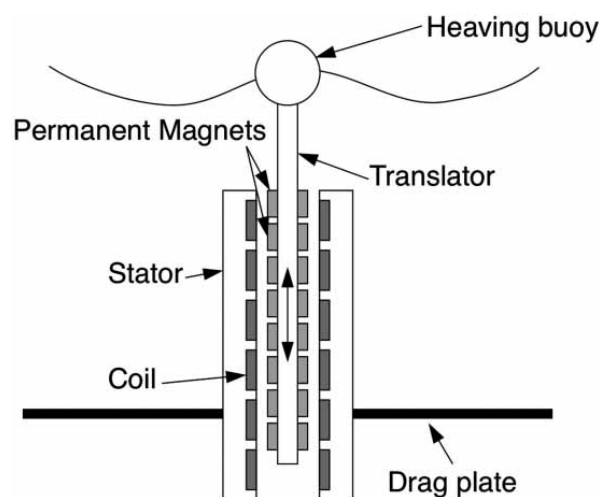


Figure 2.9. A schematic of a linear electrical generator based on a permanent magnet generator [31]

2.4. Existing technologies

There is a large number of concepts for wave energy conversion in different stage of development, in fact over 1000 wave energy conversion techniques are patented in Japan, North America and Europe [7].

In order to establish which were the most advanced technologies, only the devices that passed the phase 3 of the TRL approach were analyzed (see Paragraph 2.1).

A summary sheet (see Appendix A) was made for each of the selected devices, containing information about the company, the technology specification (classification, position, nominal power, PTO, power transmission system), the development phase, the costs or the prices, the impacts.

In the Table 2.2 all the analyzed devices are summarized, with the information of the reached phase, the country where they were invented, and the type or classification. The devices MRC, Manchester Bobber, Searev and bioWAVE were included because they planned to reach soon the phase 3.

It was considered important to divide by type the devices (OB, OWC, OTD and point absorber), in order to understand which were the most tested and the most advanced in the state of development. Thus, as it is possible to see from Table 2.3, it results that the devices in phase 5 are a OB (Pelamis) and a OWC (Mutriku), but the most analyzed typology is the point absorber (23 against 12 OB, 10 OWC, 3 OTD).

Table 2.2 List of the analyzed devices

<i>WEC name</i>	<i>Phase</i>	<i>Country</i>	<i>Type</i>
Wavestar	4	Denmark	Multi point absorber
Waveroller	4	Finland	OB - submerged
Oyster	4	UK	OB - submerged
Pelamis	5	UK	Attenuator – OB
Direct drive linear generator	4	Sweden	Point absorber
Wavebob	3	Ireland	Point absorber
OE-buoy	3	Ireland	OWC - floating
Wave dragon	3	Denmark	Overtopping - floating
L10 Buoy	3	USA	Point absorber
Power Buoy	4	USA	Point absorber
WaveEL-Buoy (IPS)	3	Sweden	Point absorber
FO3/BOLT	4	Norway	Multi point absorber/point absorber
SSG	3	Norway	Overtopping - in breakwater

<i>SEAREV</i>	2	<i>France</i>	<i>Point absorber</i>
GreenWAVE/BlueWAVE	4	Australia	OWC
Mutriku	5	Spain	OWC - in breakwater
Ceto	4	Australia	Point absorber – submerged
<i>MRC</i>	2/3	<i>UK</i>	<i>Multiple resonant chamber OWC</i>
Waveberg	3	USA	OB - floating
Waveplane	4	Denmark	Overtopping - floating
WET En Gen	3	Canada	Point absorber
Dexa	3	Denmark	OB
Mighty Whale	4	Japan	OWC - floating
Pico	4	Portugal	OWC
Limpet	4	UK	OWC
AWS	4	UK	Point absorber
Oceantec	3	Spain	OB
DECM	3	UK	Point absorber
SEADOG Pump	3	USA	Point absorber
Poseidon	3/4	Denamrk	OB - floating
Sperbuoy	3	UK	OWC – floating buoy
REWEC	3	Italy	OWC - in breakwater
Danish Wave Power (DWP)	3	Denmark	Point absorber
AquaBuOY	3	Canada	Point absorber
<i>bioWAVE</i>	2	<i>Australia</i>	<i>OB - submerged</i>
Searaser	3	UK	Point absorber
<i>Manchester bobber</i>	2/3	<i>UK</i>	<i>Point absorber</i>
Waverotor	3	Netherlands	Point absorber
R38/R115	4	Italy	OB
WEST	3	USA	Point absorber
Nautilus	3	Russia	OWC - floating
BRANDL GENERATOR	3	Germany	Point absorber
MAWEC	3	Denmark	Multi OWC - floating
PROTEAN ECP	3	Australia	Point absorber
RME	3	USA	OB
LOPF	3	USA	Point absorber
SDE	3	Israel	OB in breakwater
W2Power	3	Norway	OB - floating

Table 2.3 Characterization by type of the devices

<i>Phase</i>	<i>Point absorber</i>	<i>OB</i>	<i>OWC</i>	<i>OTD</i>
5		Pelamis	Mutriku	
4	Wavestar Direct drive linear generator Power Buoy FO3/BOLT Ceto AWS	Waveroller Oyster R38/R115	GreenWAVE/BlueWAVE Mighty Whale Pico Limpet	Waveplane
3	Wavebob L10 Buoy WaveEL-Buoy (IPS) WET En Gen SEADOG Pump DECM Danish Wave Power (DWP) AquaBuOY Searaser Waverotor WEST BRANDL GENERATOR PROTEAN ECP LOPF	Waveberg Dexa Oceantec Poseidon RME SDE W2Power	OE-buoy Sperbuoy REWEC Nautilus MAWEC	Wave dragon SSG
2	<i>SEAREV</i> <i>MRC</i> <i>Manchester bobber</i>	<i>bioWAVE</i>		

In order to highlight the countries that are more engaged in the wave energy, all the analyzed devices were subdivided by country.

The Table 2.4 shows that UK (9 WECs), USA (7 WECs) and Denmark (7 WECs) are the most involved in the wave energy technology.

Table 2.4 Characterization by country of the devices

	<i>Phase 5</i>	<i>Phase 4</i>	<i>Phase 3</i>	<i>Phase 2</i>
<i>UK</i>	Pelamis	Oyster Limpet AWS	DECM Sperbuoy Searaser	MRC <i>Manchester bobber</i>
<i>USA</i>		Power Buoy	L10 Buoy Waveberg SEADOG Pump WEST RME LOPF	
<i>Denmark</i>		Wavestar Waveplane	Poseidon Wave dragon Dexa DWP MAWEC	
<i>Ireland</i>			Wavebob OE-buoy	
<i>Australia</i>		Green/BlueWAVE Ceto	PROTEAN ECP	<i>bioWAVE</i>
<i>Italy</i>		R38/R115	REWEC	
<i>Norway</i>		FO3/BOLT	SSG W2Power	
<i>Canada</i>			WET En Gen AquaBuOY	
<i>Finland</i>		Waveroller		
<i>France</i>				<i>SEAREV</i>
<i>Germany</i>			BRANDL GENERATOR	
<i>Israel</i>			SDE	
<i>Japan</i>		Mighty Whale		
<i>Netherlands</i>			Waverotor	
<i>Portugal</i>		PICO		
<i>Russia</i>			Nautilus	
<i>Spain</i>	Mutriku		Oceantec	
<i>Sweden</i>		Direct drive linear generator	WaveEL-Buoy (IPS)	

CHAPTER 3

OFFSHORE WAVE ENERGY CHARACTERIZATION

3.1 Linear surface wave theory

The main assumption of this chapter is that random waves can be modelled as sum of a large number of independent regular waves, that can be described with the linear theory for surface gravity waves [37].

3.1.1 REGULAR WAVES

The small-amplitude wave theory, implying that the waves amplitudes are small compared to wave length and water depth, is known as the Airy wave theory. Others assumed hypotheses are that the water is an ideal fluid (i.e. constant density and zero viscosity) and the water motion is irrotational [37].

The mass balance equation, known as continuity equation (3.1) and the linearized momentum balance equation in eq. (3.2) are the basis for the linear wave theory.

$$\frac{\partial u_x}{\partial x} + \frac{\partial u_y}{\partial y} + \frac{\partial u_z}{\partial z} = 0 \quad (3.1)$$

$$\begin{cases} \frac{\partial u_x}{\partial t} = -\frac{1}{\rho} \frac{\partial p}{\partial x} \\ \frac{\partial u_y}{\partial t} = -\frac{1}{\rho} \frac{\partial p}{\partial y} \\ \frac{\partial u_z}{\partial t} = -\frac{1}{\rho} \frac{\partial p}{\partial z} - g \end{cases} \quad (3.2)$$

where u_x , u_y , u_z are the water particle velocities, ρ ($\approx 1025 \text{ kg/m}^3$ for sea water) the mass density, p the pressure and g the gravity.

The equations (3.1) and (3.2) are solved for specific boundary conditions that are of kinematic nature, related to the motions of the water particles, and of dynamic nature, related to the forces acting on the water particles.

The kinematic boundary condition, at the water surface, is that the particles may not leave the surface and then the water particle velocity normal to the surface is equal to the speed of the surface in that direction. At the bottom the condition is that the particles may not penetrate the bottom and then the bottom is impermeable. In the linearised approach and in presence of a horizontal bottom, the expressions of these boundary conditions are given by (3.3)

$$\begin{cases} u_z = \frac{\partial \eta}{\partial t} & \text{at } z = 0 \\ u_z = 0 & \text{at } z = -d \end{cases} \quad (3.3)$$

where z is located in the still-water level and d is the water depth, see Figure 3.1.

The dynamic boundary condition requires that the pressure distribution is uniform along the wave form [38] and the expression, assuming the surface tension is zero, is

$$p = 0 \quad \text{at } z = 0 \quad (3.4)$$

In order to find analytical solutions for the eqs. (3.1) - (3.4) it is necessary to employ the velocity potential function $\phi = \phi(x, y, z, t)$, which is defined as a function the spatial derivatives of which are equal to the water particles velocities:

$$u_x = \frac{\partial \phi}{\partial x}, \quad u_y = \frac{\partial \phi}{\partial y}, \quad u_z = \frac{\partial \phi}{\partial z} \quad (3.5)$$

Replacing the eq. (3.5) in the eq. (3.1) it yields the *Laplace equation* (3.6)

$$\frac{\partial^2 \phi}{\partial x^2} + \frac{\partial^2 \phi}{\partial y^2} + \frac{\partial^2 \phi}{\partial z^2} = 0 \quad (3.6)$$

Replacing the eq. (3.5) in the eq. (3.3) it yields the kinematic boundary conditions in term of the velocity potential function

$$\begin{cases} \frac{\partial \phi}{\partial z} = \frac{\partial \eta}{\partial t} & \text{at } z = 0 \\ \frac{\partial \phi}{\partial z} = 0 & \text{at } z = -d \end{cases} \quad (3.7)$$

Replacing the eq. (3.5) in the eq. (3.2) and adding a term gz in the first two equations (3.2), it yields the *linearised Bernoulli equation* for unsteady flow (3.8)

$$\frac{\partial \phi}{\partial t} + \frac{p}{\rho} + gz = 0 \quad (3.8)$$

Replacing the eq. (3.4) in the Bernoulli equation (3.8), it yields the dynamic boundary condition in term of the velocity potential function (see Figure 3.1)

$$\frac{\partial \phi}{\partial t} + g\eta = 0 \quad \text{at } z = 0 \quad (3.9)$$

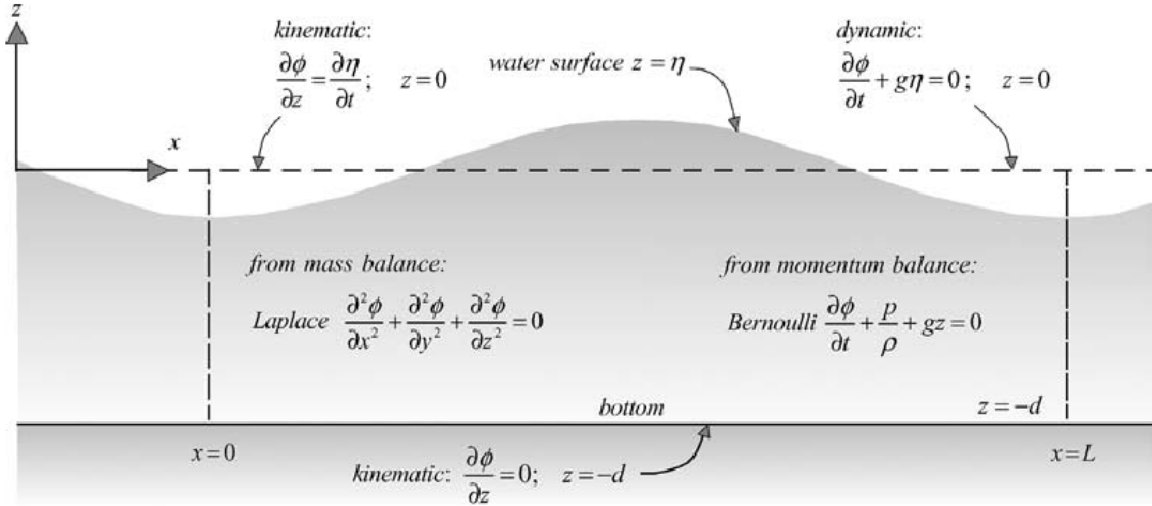


Figure 3.1. The linearised basic equations and boundary conditions in terms of the velocity potential [37]

The lateral boundary conditions, if the waves are propagating in one direction (i.e. x -direction), are two-dimensional and then “no-flow” conditions are appropriate for the velocities in the y -direction. For waves that are periodic in space and time, these conditions are expressed as periodicity conditions [38]

$$\begin{cases} \phi(x, t) = \phi(x + L, t) \\ \phi(x, t) = \phi(x, t + T) \end{cases} \quad (3.10)$$

where L is the wave length and T the wave period.

The Laplace equation (3.6), the lateral periodicity, the kinematic bottom boundary condition and the dynamic free surface boundary condition are used in order to obtain solutions for the velocity potential. One of the analytical solutions is a long-crested harmonic wave propagating in the positive x -direction

$$\eta(t) = a \sin(\omega t - kx) \quad (3.11)$$

with the following velocity potential function

$$\phi = \hat{\phi} \cos(\omega t - kx) \quad \text{with} \quad \hat{\phi} = \frac{\omega a}{k} \frac{\cosh[k(d+z)]}{\sinh(kd)} \quad (3.12)$$

where $a = H/2$ is the amplitude (H is the wave height), $\omega = 2\pi/T$ is the radian frequency, $k = 2\pi/L$ is the wave number.

The particle velocities are obtained from the velocity potential in eq. (3.12), just by using the definition of ϕ in eq. (3.5)

$$\begin{cases} u_x = \hat{u}_x \sin(\omega t - kx) & \text{with} \quad \hat{u}_x = \omega a \frac{\cosh[k(d+z)]}{\sinh(kd)} \\ u_z = \hat{u}_z \cos(\omega t - kx) & \text{with} \quad \hat{u}_z = \omega a \frac{\sinh[k(d+z)]}{\sinh(kd)} \end{cases} \quad (3.13)$$

The kinematic free surface boundary condition (3.3) is used, in combination with the solution for the harmonic surface profile (3.11) and for the velocity potential (3.12), in order to obtain the relationship between the radian frequency ω and wave number k , called *dispersion relationship*.

$$\omega^2 = gk \tanh(kd) \quad \text{or} \quad L = \frac{gT^2}{2\pi} \tanh\left(\frac{2\pi d}{L}\right) \quad (3.14)$$

In deep water ($\tanh(kd) \rightarrow 1$ for $kd \rightarrow \infty$) the eq. (3.14) becomes

$$\omega = \sqrt{gk_0} \quad \text{or} \quad L_0 = gT^2 / (2\pi) \approx 1.56T^2 \quad (3.15)$$

In shallow water ($\tanh(kd) \rightarrow kd$ for $kd \rightarrow 0$) the eq. (3.14) becomes

$$\omega = k\sqrt{gd} \quad \text{or} \quad L = T\sqrt{gd} \quad (3.16)$$

The wave speed, or celerity, c , is given by

$$c = \frac{\omega}{k} = \frac{L}{T} = \frac{g}{\omega} \tanh(kd) = \sqrt{\frac{g}{k} \tanh(kd)} \quad (3.17)$$

In deep water the eq. (3.17) becomes

$$c_0 = \sqrt{\frac{g}{k_0}} = \frac{g}{2\pi} T \approx 1.56T \quad (3.18)$$

In shallow water the eq. (3.17) becomes

$$c_{\text{shallow}} = \sqrt{gd} \quad (3.19)$$

The velocity of a wave group, or the velocity of the energy transmission, is given by

$$c_{\text{group}} = c_g = nc \quad (3.20)$$

where c is the celerity of the wave and n , obtained by eq. (3.14), is

$$n = \frac{1}{2} \left(1 + \frac{2kd}{\sinh(2kd)} \right) \quad (3.21)$$

Since $0 \leq kd \leq \infty$ and therefore $0 \leq 2kd / \sinh(2kd) \leq 1$, the eq. (3.21) varies between $n = 1/2$ in deep water and $n = 1$ in shallow water. This implies that the speed of the individual waves is always higher than the wave group velocity: $c \geq c_g$.

The total pressure expression is obtained replacing the eq. (3.12) in the Bernoulli equation (3.8):

$$p = -\rho gz + \rho ga \frac{\cosh[k(d+z)]}{\cosh(kd)} \sin(\omega t - kx) \quad z < 0 \quad (3.22)$$

where ρgz is the hydrostatic pressure (independent of the presence of the wave) and the second term on the right-hand side represents the wave-induced pressure, denoted as p_{wave}

$$p_{\text{wave}} = \hat{p}_{\text{wave}} \sin(\omega t - kx) \quad \text{with} \quad \hat{p}_{\text{wave}} = \rho ga \frac{\cosh[k(d+z)]}{\cosh(kd)} \quad (3.23)$$

The total energy contained in a wave is given by the sum of the potential energy, resulting from the displacement of the free surface, and the kinetic energy, due to the fact that the water particles throughout the fluid are moving [38].

The potential energy averaged over one wave length for a wave of height H is given by

$$E_{\text{potential}} = \frac{\rho g}{L} \int_x^{x+L} \left[\frac{1}{2} (d^2 + 2\eta d + \eta^2) \right] - \rho g \frac{d^2}{2} = \frac{1}{16} \rho g H^2 \quad \left[\frac{\text{J}}{\text{m}^2} \right] \quad (3.24)$$

where the term $\rho g \frac{d^2}{2}$ represents the potential energy with no waves present.

The kinetic energy per unit surface area, integrated over depth and averaged over a wave length, is given by

$$E_{\text{kinetic}} = \frac{1}{L} \int_x^{x+L} \int_{-d}^{\eta} \rho \frac{u_x^2 + u_z^2}{2} dz dx = \frac{1}{16} \rho g H^2 \quad \left[\frac{\text{J}}{\text{m}^2} \right] \quad (3.25)$$

The total average energy per unit surface area of the wave is given by

$$E = E_{\text{potential}} + E_{\text{kinetic}} = \frac{1}{16} \rho g H^2 + \frac{1}{16} \rho g H^2 = \frac{1}{8} \rho g H^2 \quad \left[\frac{\text{J}}{\text{m}^2} \right] \quad (3.26)$$

Small-amplitude water waves do not transmit mass as they propagate across a fluid, but they do transmit energy. The rate at which the energy is transferred is called the energy flux, and for the linear theory it is the rate at which work is being done by wave-induced pressure p_{wave} (3.23) in the direction of wave propagation.

Thus the flux of energy per unit crest length, averaged over a wave period, is given by

$$P_{\text{energy}} = \frac{1}{T} \int_t^{t+T} \int_{-d}^0 p_{\text{wave}} u_x dz = \left(\frac{1}{2} \rho g a^2 \right) \frac{1}{2} \left(1 + \frac{2kd}{\sinh(2kd)} \right) \frac{\omega}{k} \quad \left[\frac{\text{W}}{\text{m}} \right] \quad (3.27)$$

Replacing in the eq. (3.27) the eqs. (3.17), (3.20), (3.21), (3.26) it yields

$$P_{\text{energy}} = E \cdot n \cdot c = E \cdot c_g \quad \left[\text{W} / \text{m} \right] \quad (3.28)$$

The direction of the energy transport is normal to the wave crest because the water particles move in that direction [37].

3.1.2 RANDOM WAVES

The sea surface is composed of a large variety of waves moving in different directions and with different frequencies, phases and amplitudes. For an adequate description of the sea surface, then, a large number of waves must be superimposed to be realistic [38].

The short-term description of the sea waves requires statistical stationary. In a stationary record the wave condition can be characterized with average wave parameters, such as the significant wave height, the significant wave period [37] and a given frequency distribution of energy in terms of the so called "variance density spectrum" or "frequency spectrum".

In terms of time-domain short-term wave analysis, the significant wave height is defined as the mean of the highest one-third of wave in the wave record (Figure 3.2):

$$H_s = H_{1/3} = \frac{1}{N/3} \sum_{j=1}^{N/3} H_j \quad (3.29)$$

where j is the rank number of the wave, based on the wave height (i.e. $j=1$ is the highest wave, $j=2$ the second-highest wave, etc.).

The significant wave period is defined as the mean period of the highest one-third of waves (Figure 3.2):

$$T_s = T_{1/3} = \frac{1}{N/3} \sum_{j=1}^{N/3} T_{0,j} \quad (3.30)$$

where j is the rank number of the wave, based on the wave height.

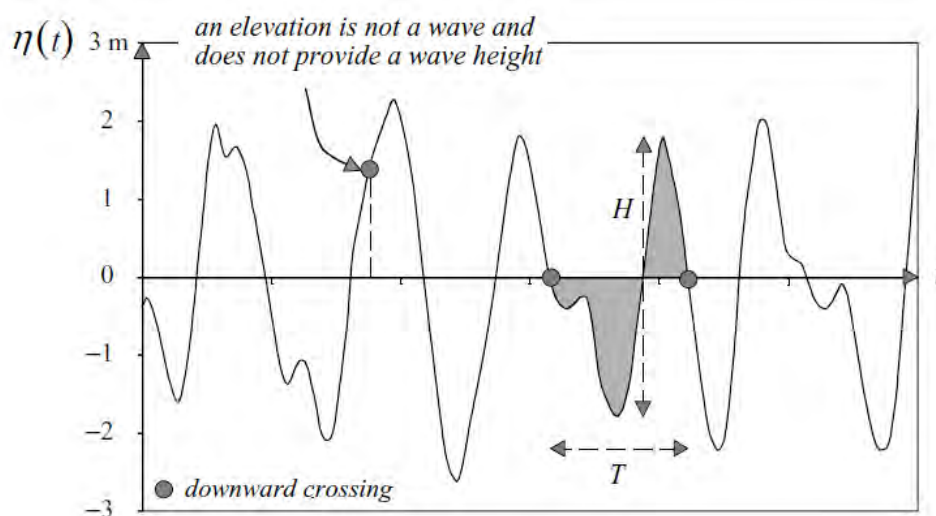


Figure 3.2. The definition of wave height and wave period in a time record of the surface elevation (the wave is defined with downward zero-crossings) [37]

A more complete description of the wave condition is obtained with the spectral technique, by approximating the time record of the surface elevation as the sum of a large number of statistically independent harmonic waves components. In this concept, called the random-phase/amplitude model, each harmonic wave has a constant amplitude and a random phase (3.31)

$$\eta(t) = \sum_{i=1}^N a_i \sin(2\pi f_i t + \alpha_i) \quad (3.31)$$

where N is a large number of frequencies, $f_i = i/D$ is the frequency, D the wave record duration, a the amplitude and α the phase.

Using trigonometric identities the eq. (3.31) may also be written as

$$\eta(t) = \sum_{i=1}^N [A_i \cos(2\pi f_i t) + B_i \sin(2\pi f_i t)] \quad (3.32)$$

with amplitude a_i and phase α_i :

$$a_i = \sqrt{A_i^2 + B_i^2} \quad \text{and} \quad \tan \alpha_i = -\frac{B_i}{A_i} \quad (3.33)$$

The amplitudes A_i and B_i can be determined from the record with Fourier integrals

$$\begin{cases} A_i = \frac{2}{D} \int_D \eta(t) \cos(2\pi f_i t) & \text{for } f_i = 1/D \\ B_i = \frac{2}{D} \int_D \eta(t) \sin(2\pi f_i t) & \text{for } f_i = 1/D \end{cases} \quad (3.34)$$

The analysis of wave records proves that these phases and amplitudes are random variables, so they can be fully characterized with their respective probability density functions. In the random-phase/amplitude model (Figure 3.3), at each frequency f_i the phase is uniformly distributed

$$p(\alpha_i) = \frac{1}{2\pi} \quad \text{for } 0 < \alpha_i \leq 2\pi \quad (3.35)$$

and the amplitude follows a Rayleigh distribution

$$p(a_i) = \frac{\pi a_i}{2 \mu_i^2} \exp\left(-\frac{\pi a_i^2}{4 \mu_i^2}\right) \quad \text{for } a_i \geq 0 \quad (3.36)$$

where $\mu_i = E\{a_i\}$ is the expected value of the amplitude.

The variance of the surface elevation $\eta(t)$ is the average of the squared surface elevation and for a harmonic wave with amplitude a , the time-averaging variance is

$$\overline{\eta^2} = \frac{1}{2} a^2 \quad (3.37)$$

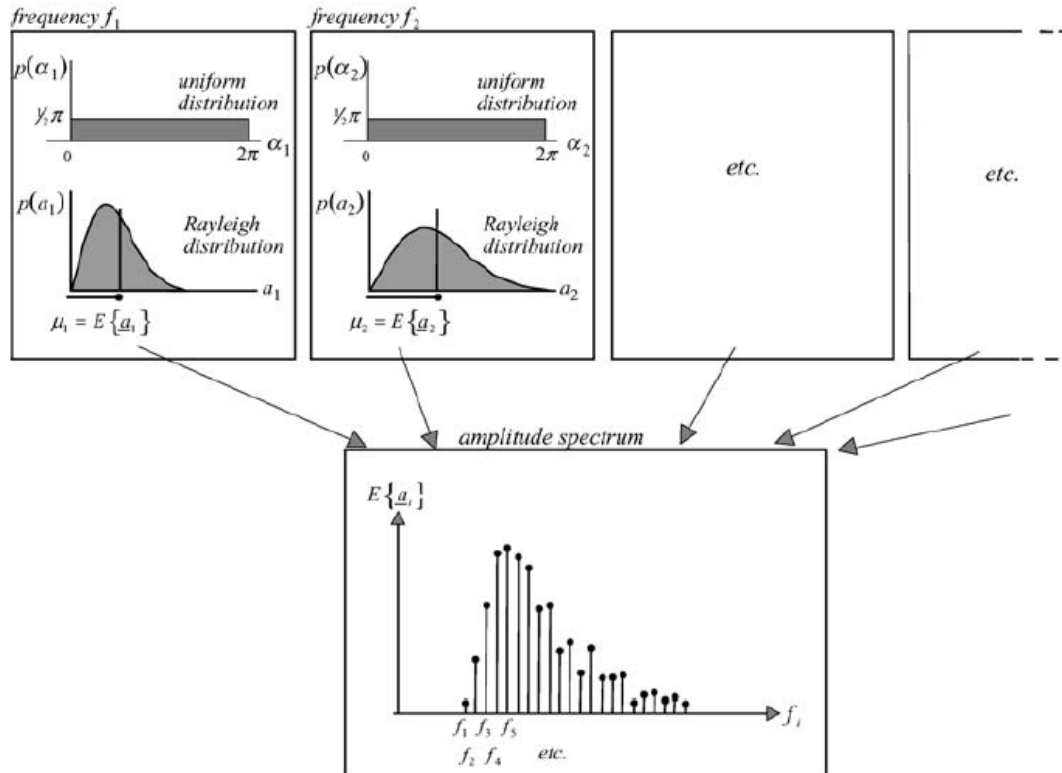


Figure 3.3. The random-phase/amplitude model [37]

Comparing the eq. (3.37) with eq. (3.26) it is possible to see that the wave energy is proportional to the variance. Moreover an important statistical propriety of the variance is that the variance of the sum is the sum of the variances and so

$$\text{variance} = \overline{\eta^2} = E\{\eta^2\} = \sum_{i=1}^N E\left\{\frac{1}{2} a_i^2\right\} \quad (3.38)$$

For these reasons the variance spectrum is considered instead of the amplitude spectrum. The variance density spectrum is given by

$$E(f_i) = \frac{1}{\Delta f_i} E\left\{\frac{1}{2} a_i^2\right\} \quad (3.39)$$

where Δf_i is the interval between the frequencies. The spectrum in eq. (3.39), defined for all frequencies, varies discontinuously from one frequency band to the next. A continuous version is obtained by having $\Delta f_i \rightarrow 0$

$$E(f_i) = \lim_{\Delta f_i \rightarrow 0} \frac{1}{\Delta f_i} E \left\{ \frac{1}{2} a_i^2 \right\} \quad (3.40)$$

For a continuous spectrum the total variance is given by

$$\text{total variance} = \overline{\eta^2} = \int_0^{\infty} E(f) df \quad (3.41)$$

The variance density spectrum $E(f)$ shows how the variance of the sea-surface elevation is distributed over the frequencies, so this kind of spectrum is also called *frequency spectrum*. The overall appearance of the waves can be inferred from the shape of the spectrum: the narrower the spectrum, the more regular the waves are (Figure 3.1). The narrowest spectrum is the spectrum of one harmonic wave with only one frequency, that consists of a delta function at that frequency. Distributing the variance over a slightly wider frequency band gives a slowly modulating harmonic wave and over a wider frequency band gives a rather chaotic wave field (irregular waves).

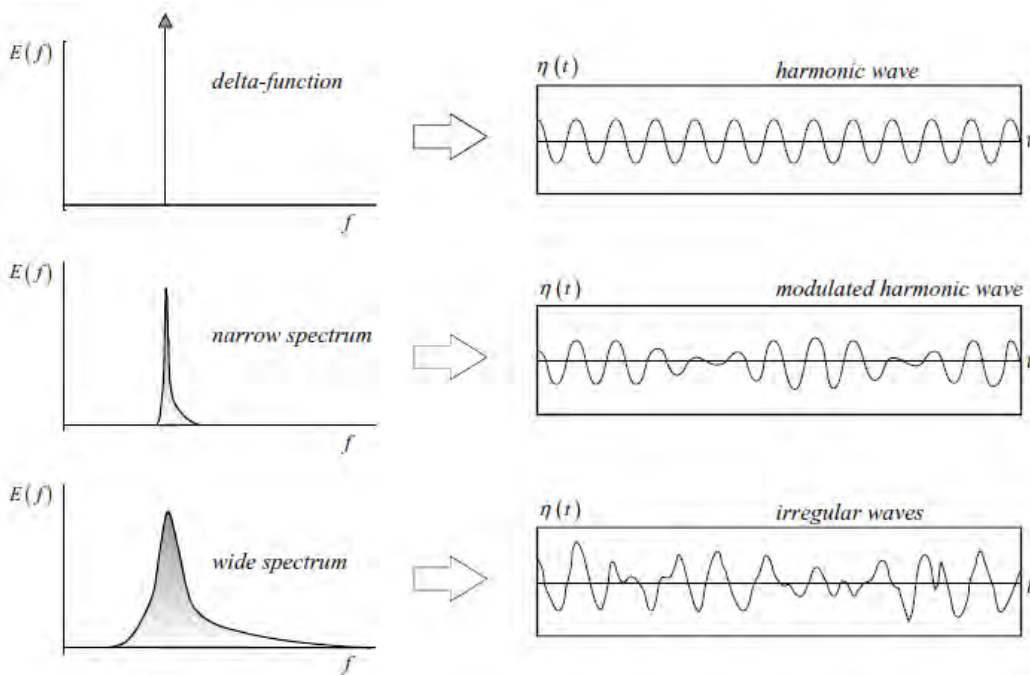


Figure 3.4. The characteristics of the waves for three different widths of the spectrum [37]

When the random sea-surface elevation is treated as a stationary, Gaussian process (reasonable assumption for the duration of a wave record, typically 15 - 30 min), all its statistical characteristics are determined by the variance density spectrum $E(f)$. These characteristics can be expressed in terms of the moments of that spectrum which are defined as

$$m_n = \int_0^{\infty} f^n E(f) df \quad \text{for } n = \dots, -3, -2, -1, 0, 1, 2, 3, \dots \quad (3.42)$$

where the moment m_n is called the n th-order moment of $E(f)$. The variance of the surface elevation is equal to the zeroth-order moment

$$\text{variance} = \overline{\eta^2} = E\{\eta^2\} = \int_0^{\infty} E(f) df = m_0 \quad \text{for } \mu_n = E\{\eta\} = 0 \quad (3.43)$$

Assuming the mean of the sea-surface elevation to be zero, the Gaussian probability density function is given by

$$p(\eta) = \frac{1}{\sqrt{2\pi m_0}} \exp\left(-\frac{\eta^2}{2m_0}\right) \quad \text{for } \mu_n = E\{\eta\} = 0 \quad (3.44)$$

where $\sqrt{m_0}$ is the standard deviation σ of the surface elevation. The integral of the Gaussian probability density function gives the probability that $\eta(t)$ is below a certain level η , or the time fraction that $\eta(t) \leq \eta$ [37]. The average of the time interval between two surface elevation crossings can be expressed in term of the spectrum as

$$\bar{T}_\eta = \frac{\sqrt{\frac{m_0}{m_2}}}{\exp\left(-\frac{\eta^2}{2m_0}\right)} \quad (3.45)$$

where m_0 and m_2 are the zeroth- and second- order moment of $E(f)$. The mean frequency of these level crossing is given by

$$\bar{f}_\eta = \bar{T}_\eta^{-1} = \sqrt{\frac{m_2}{m_0}} \exp\left(-\frac{\eta^2}{2m_0}\right) \quad (3.46)$$

A special case is the mean zero-crossing period $\bar{T}_0 = T_{m_{02}}$, which can be obtained by eq. (3.45) with $\eta=0$

$$\bar{T}_0 = T_{m_{02}} = \sqrt{\frac{m_0}{m_2}} \quad (3.47)$$

The m_2 value, and then the \bar{T}_0 value, is sensitive to small errors or variations in the measurement or analysis technique. Thus another mean period is sometimes used, which is less dependent on high-frequency noise. It is defined as the inverse of the wave spectrum mean frequency:

$$T_{m_{01}} = f_{\text{mean}}^{-1} = \sqrt{\frac{m_0}{m_1}} \quad (3.48)$$

where m_1 is the first-order moment of $E(f)$.

The wave energy period or wave spectral period $T_{m_{-10}}$ is given by

$$T_{m_{-10}} = \frac{\int_0^{\infty} E(f) \cdot f^{-1} df}{\int_0^{\infty} E(f) df} = \frac{m_{-1}}{m_0} \quad (3.49)$$

The significant wave period, defined in eq. (3.30), is also less dependent on high-frequency noise and for the waves with a narrow spectrum (called also swell waves) is equal to the peak period of the spectrum:

$$T_{1/3} \approx T_p = \frac{1}{f_p} \quad (3.50)$$

Instead, for the wind sea waves the $T_{1/3}$ value is typically 5 % shorter than the peak period of the spectrum.

For waves with a narrow spectrum in deep water the height of the waves is practically equal to twice the height of the crest, defined as maximum of the surface elevation. The probability density of the zero-crossing wave height H is a Rayleigh distribution:

$$p(H) = \frac{H}{4m_0} \exp\left(-\frac{H^2}{8m_0}\right) \quad (3.51)$$

The significant wave height, defined in eq. (3.29), can be determined from that distribution and its value in deep water, estimated from the spectrum is given by

$$H_{m_0} \approx 4\sqrt{m_0} \quad (3.52)$$

This is typically 5 % - 10 % larger than the value of $H_{1/3}$ estimated directly from measured time series, because the surface elevation is not perfectly Gaussian distributed, due to nonlinear processes, and the assumption of $H = 2\eta_{\text{crest}}$ is not entirely correct.

The characteristics of the *frequency spectra* (one-dimensional spectrum) of the sea waves have been fairly well established through analyses of a large number of records taken in

various waters of the world [39]. The spectra of a fully developed wind waves can be approximated by the Bretschneider standard formula:

$$E(f) = 0.257 H_{1/3}^2 T_{1/3}^{-4} f^{-5} \exp\left[-1.03(T_{1/3} f)^{-4}\right] \quad (3.53)$$

or by the Pierson Moskowitz formula:

$$E(f) = 0.205 H_{1/3}^2 T_{1/3}^{-4} f^{-5} \exp\left[-0.75(T_{1/3} f)^{-4}\right] \quad (3.54)$$

Wind waves rapidly developed in a fetch limited area (like the Mediterranean Sea) by very strong wind usually exhibit a spectral peak much sharper than the one given by eqs. (3.53) and (3.54) and can be approximated by the JONSWAP formula:

$$E(f) = \beta_j H_{1/3}^2 T_p^{-4} f^{-5} \exp\left[-1.25(T_p f)^{-4}\right] \cdot \gamma^{\exp\left[\frac{1}{2}\left(\frac{T_p \cdot f - 1}{\sigma}\right)^2\right]} \quad (3.55)$$

in which γ is a peak-enhancement factor and σ is a peak-width parameter (more details in Paragraph 5.1.1.2).

If the spectrum is a function of both frequency and direction (angle θ) is called *directional wave spectrum* (Figure 3.5) and is given by

$$E(f, \theta) = E(f)D(\theta | f) \quad (3.56)$$

where $D(\theta | f)$ is the directional distribution, that is the cross-section through the two-dimensional spectrum at a given frequency, normalized so that its integral over the directions is 1 [37]:

$$\int_0^{2\pi} D(\theta | f) d\theta = \int_0^{2\pi} \frac{E(f, \theta)}{E(f)} d\theta = \frac{\int_0^{2\pi} E(f, \theta) d\theta}{E(f)} = \frac{E(f)}{E(f)} = 1 \quad (3.57)$$

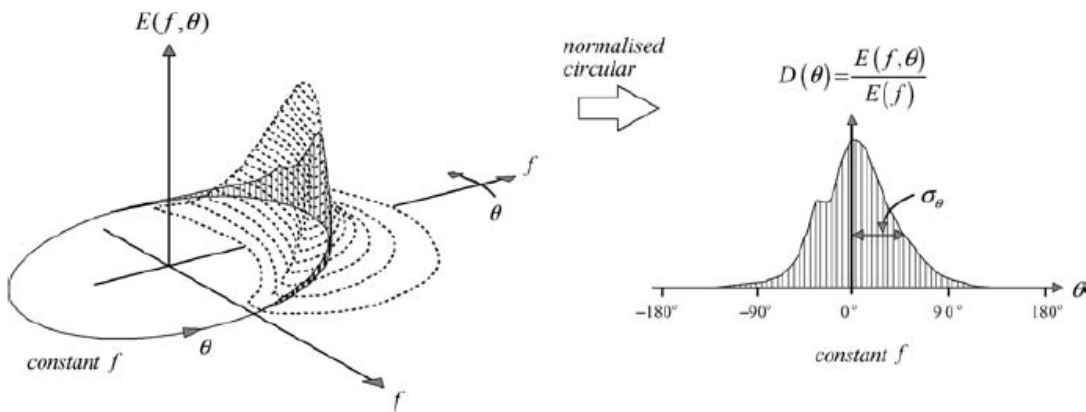


Figure 3.5. The directional energy distribution at a given frequency and its directional width σ_0 [37]

If the variance density spectrum is multiplied by ρg it yields the energy density spectrum, that shows how the wave energy is distributed over the frequencies [37]

$$E_{\text{energy}}(f) = \rho g E_{\text{variance}}(f) \quad (3.58)$$

Replacing in the eq. (3.28), the eq. (3.58) and the values in deep water of the celerity (3.18) and of n (3.21) equal to $1/2$, it yields the energy transport (called also the wave power) for the random waves in the deep water

$$P_{\text{energy}} = \rho g \int_0^{\infty} E(f) \cdot n \cdot c \cdot df = \rho g \int_0^{\infty} E(f) \cdot \frac{1}{2} \cdot \frac{g}{2\pi} T \cdot df = \frac{1}{4} \frac{\rho g^2}{\pi} \int_0^{\infty} E(f) \cdot f^{-1} df \quad (3.59)$$

Multiplying and dividing the eq. (3.59) by m_0 (3.43) and considering the relations in eqs. (3.42) and (3.52), the wave power in deep water yields

$$P_{\text{energy}} = \frac{1}{4} \frac{\rho g^2}{\pi} \frac{\int_0^{\infty} E(f) \cdot f^{-1} df}{\int_0^{\infty} E(f) df} = \frac{1}{4} \frac{\rho g^2}{\pi} T_{m_{-10}} \frac{H_{m_0}^2}{16} = \frac{1}{64} \frac{\rho g^2}{\pi} H_{m_0}^2 T_{m_{-10}} \quad (3.60)$$

3.2 Previous findings for the Mediterranean Sea

In recent years several authors presented wave energy atlas of the Mediterranean Sea relied on wave measurements obtained from buoys, satellite and output from model hindcasts. A first attempt to assess the offshore European wave energy resource using a high accurate data was made through the European Wave Energy Atlas – WERATLAS, the adopted methodology of which established the basis for the further development of some atlas at a regional scale. The WERATLAS is a software for PC that contains annual and seasonal (yearly, winter and summer) wave-climate and wave-energy statistics for a set of offshore locations distributed along the European coastline. It covers the North-eastern Atlantic Ocean, the North Sea, the Norwegian Sea, the Barents Sea and the Mediterranean Sea, the area being delimited by 49°W - 45°E and 26.5° - 73°N . The wave data used in compiling the Atlas, come from the numerical wind-wave model WAM, implemented at the European Centre for Medium-Range Weather Forecasts (ECMWF), in situ measurements and satellite (GEOSAT and Topex/Poseidon) altimeter data [40]. The

information in the Mediterranean (Figure 3.6) is presented at 44 data points, with a grid resolution of $0.5^\circ \times 0.5^\circ$. Their locations were influenced by the set of WAM grid points and the set of points for which the long-term directional wave data set were available [41]. For the Mediterranean Sea the wave parameters (significant wave height, mean period, spectral peak period, mean direction and wave power or flux of energy per unit crest length) are computed six-hourly by WAM model for the period July 1992 – December 1995 [40].

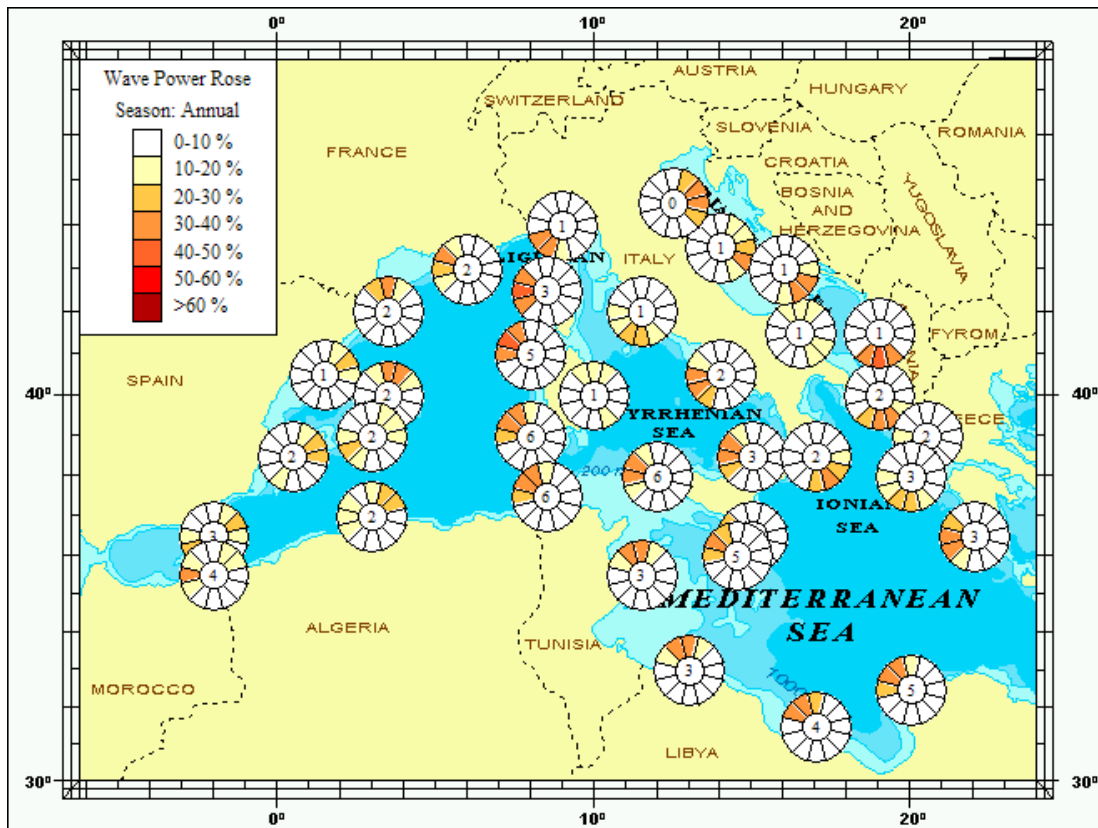


Figure 3.6. WERATLAS - Wave power rose in the Mediterranean Sea [8]

The World Wave Atlas (WWA) is PC application of the Fugro Oceanor, which can be used for geographical presentation of wave and wind statistics worldwide. The WWA, in order to provide the data at the highest resolution and accuracy is a composite of atlases, including wave atlases for any country worldwide (from Guam to Nigeria to the US), and wave atlases for a number of larger regions or sea areas (e.g., North America, the Far East, Europe, the Mediterranean, the North Sea etc.) and atlases for major shipping lanes. This atlas contains calibrated wave data from the WorldWaves wave model database [42]. The WorldWaves is a global wave and wind climate package developed through EU and industry sponsorship over many years. The offshore data incorporate global hindcast and operational wave and wind data, in the Mediterranean Sea for the period 1992 – 2004, from

ECMWF at 6-hourly intervals on a 0.5° lat/lon grid worldwide, validated and calibrated with independent satellite and buoy data [9]. The world wave power map, obtained with the WorldWaves dataset, is shown in Figure 3.7, and the detailed wave power map for the Med Sea in Figure 3.8.

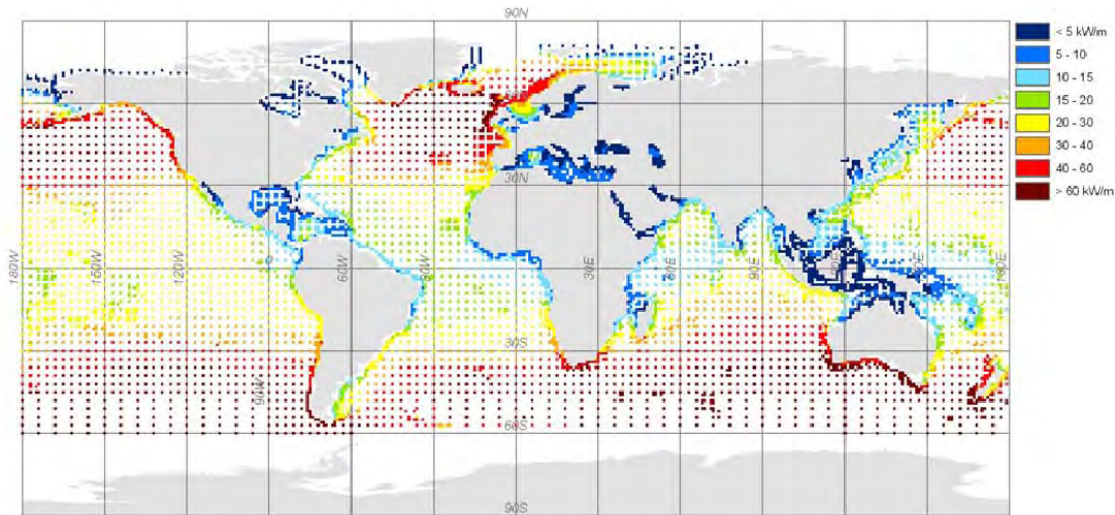


Figure 3.7. Annual global gross theoretical wave power for all WorldWaves grid points worldwide [9]

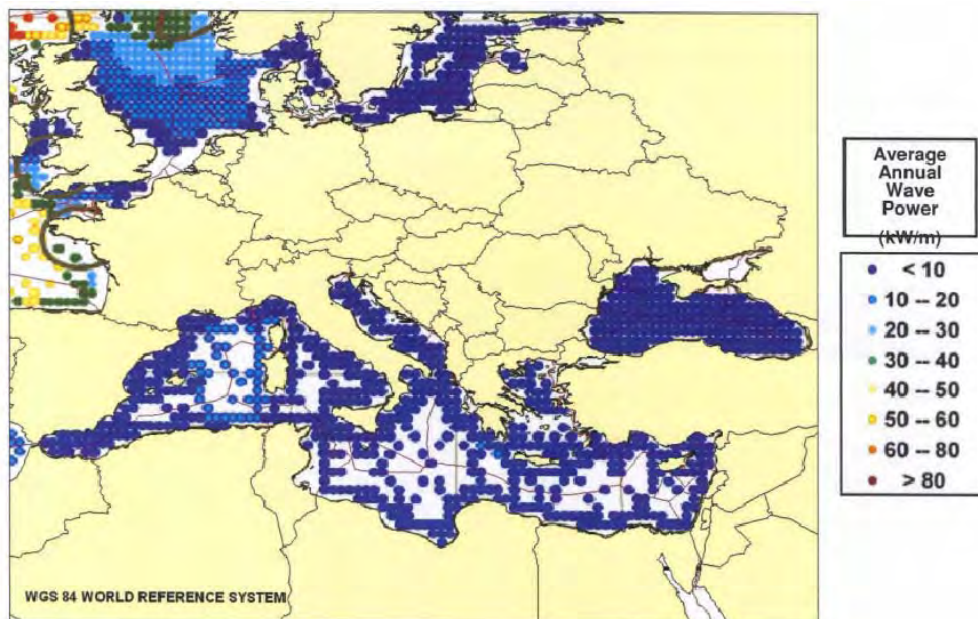


Figure 3.8. Mean yearly wave power in the Mediterranean Sea, based on WWA [43]

The most recent wind and wave atlas for the Mediterranean Sea area is the MEDATLAS. It was completed within the WW-Medatlas project and it was sponsored by the Italian, French and Greek Navies. The atlas is based on the wind and wave integrated wave parameters available from the ECMWF archive from July 1992 to June 2002 with 0.5° resolution between 6° West and 36° East for longitude, and 30° and 46° North for

latitude. These data were calibrated on the basis of the data available from the ERS1-2 and Topex satellites, because the wind, hence the wave, data are normally strongly underestimated in the enclosed seas. The calibration was done deriving the model values at each satellite position, typically at 7 km intervals [10]. The mean wave power map, based on the MEDATLAS, is shown in Figure 3.9.

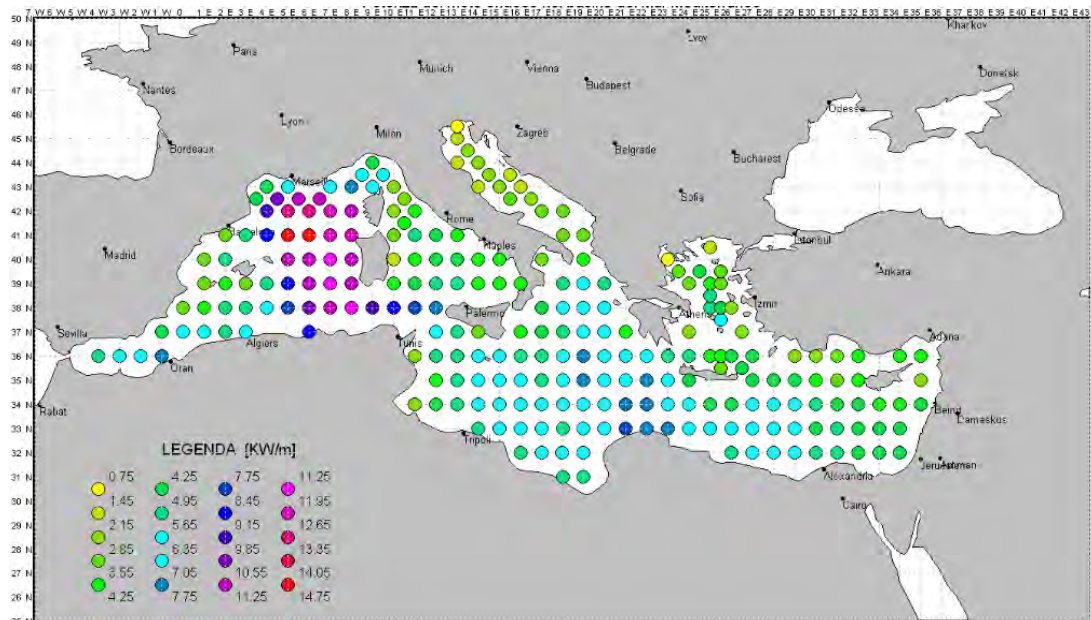


Figure 3.9. Mean wave power in the Mediterranean Sea, based on MEDATLAS [44]

Liberti et al. [11] obtained a wave energy atlas of the Mediterranean Sea by running for the 10 years period 2001 - 2010 a $1/16^\circ$ resolution a WAM wave model forced by the wind fields provided by the ECMWF. The model results were validated against Topex-POSEIDON, Jason-1, Jason-2, Envisat, ERS-2 satellites and the buoy wave measurements collected by the Italian Wave measuring Network (Rete Ondametrica Nazionale, RON). These results were analyzed to define the average wave energy availability.

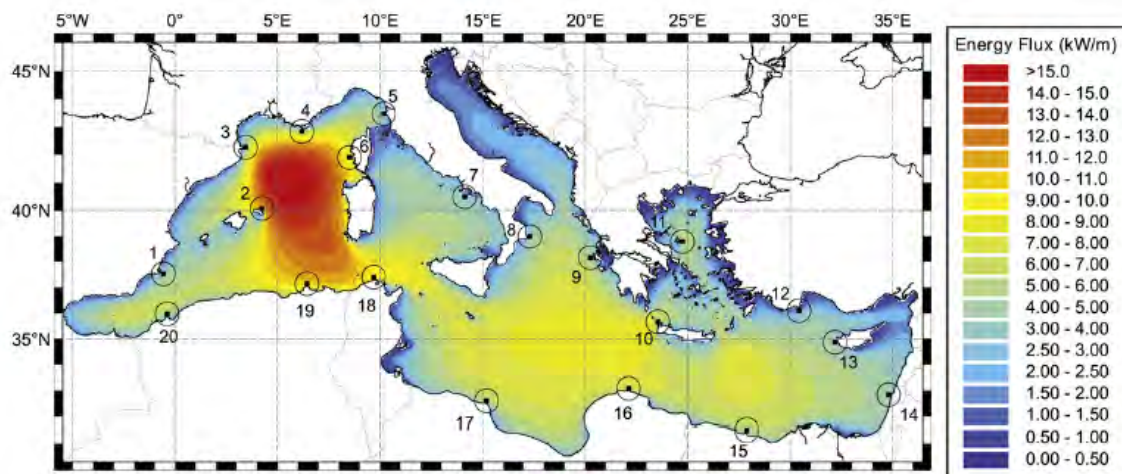


Figure 3.10. Mean wave power in the Mediterranean Sea, based on [11]

The Italian Wave measuring Network (Rete Ondametrica Nazionale RON) was activated in 1989. At the beginning it was composed by eight pitch-roll Datawell-Wavec (type directional) buoys, placed off La Spezia, Alghero, Ortona, Ponza, Monopoli, Crotona, Catania and Mazara and anchored on floors of 100 metres. In the 1999 two directional translational Datawell-Waverider buoy (Cetraro and Ancona), in the 2004 four TRIAXYS buoys located in Capo Linaro (Civitavecchia, Central Tyrrhenian Sea), Capo Gallo (Palermo, Sicily), Punta della Maestra (Northern Adriatic) and Capo Comino (East Sardinia) and in the 2007 one TRIAXYS buoy (Cagliari) were added to the network. The data acquisition occurs every three hours, with shorter intervals in case of particularly remarkable sea-storms. These transmitted data were analyzed to find the directional frequency distribution parameters, with no preliminary hypotheses concerning the form of the distribution itself. From this analysis synthetic parameters (significant wave height, peak period, mean period, mean direction) and spectral parameters (energy density, directional dispersion, asymmetry, kurtosis) were computed. The data processing and the storage centre is operating at the SIMN (ISPRA) maritime area [45].

An offshore wave energy estimation of the Italian seas based on the wave measurements carried out by the Italian Wave Buoys Network (RON), was computed by Vicinanza et al. [12]. The monthly and yearly mean wave power are summarized in Table 3.1 and their locations are shown in Figure 3.11.

Table 3.1. Mean monthly and yearly wave power at RON buoys [12]

Buoy Name	Buoy	Mean Wave Power kW/m												Yearly
		Jan	Feb	Mar	Apr	May	Jun	Jul	Aug	Sep	Oct	Nov	Dec	
Alghero	1	12.39	13.43	10.2	10.78	5.85	4.13	4.32	3.68	6.16	7.47	14.83	15.39	9.05
Ancona	2	2.75	1.24	2.23	1.23	0.69	0.46	0.74	0.66	1.56	1.94	4.49	3.8	1.82
Cagliari	3	1.85	0.91	1.02	1.98	nd	nd	0.57	0.39	0.65	1.4	3.5	2.92	1.52
Capo Comino	4	1.91	2.28	2.65	3.3	1.31	0.62	0.55	1	1.55	1.12	5.5	7.31	2.43
Capo Gallo	5	6.11	6.51	5.45	2.86	2.11	1.37	1.42	2.17	2.73	1.15	4.83	9.94	3.89
Capo Linaro	6	3.71	5.08	3.39	3.41	2.44	0.85	0.9	2.39	0.95	2.69	2.05	6.68	2.88
Catania	7	3.11	2.94	3.13	1.96	1.22	0.5	0.44	0.36	0.99	1.67	2.83	3.71	1.9
Cetraro	8	4.31	4.67	4.5	3.32	1.97	1.09	1.01	1.02	1.63	1.64	4	5.07	2.85
Crotona	9	5	4.31	3.83	2.93	1.25	0.49	0.5	0.5	1.36	2.69	4.79	6.67	2.86
La Spezia	10	3.96	4.9	3.8	3.86	2.03	1.95	1.92	1.91	3.05	4	5.32	4.89	3.46
Mazara del Vallo	11	7.16	7.33	5.6	6.68	2.86	1.82	1.44	1.52	2.62	3.46	7.03	9.44	4.75
Monopoli	12	3.56	3.35	3.15	1.73	1.03	0.74	1.04	0.93	1.12	1.81	2.46	3.7	2.05
Ortona	13	3.3	2.88	2.68	1.58	0.81	0.67	0.69	0.63	1.03	1.37	2.84	4.29	1.9
Ponza	14	4.77	4.93	3.8	4.18	2.09	1.42	1.81	1.79	3	3.01	6.62	6.93	3.7
Punta della Maestra	15	1.67	4.29	2.73	1.23	1.31	1.15	0.56	0.89	1.65	1.38	1.73	nd	1.69



Figure 3.11. RON buoys locations [12]

3.3 Offshore characterization

3.3.1 METHODOLOGY

The wave energy estimation was computed for all the Mediterranean Sea and in detail, with a higher accuracy, for the North-Western Mediterranean Sea. The wave data were provided by IFREMER (French Research Institute for Exploration of the Sea) that has developed a pre-operational system, called PREVIMER [46], aiming to provide short-term forecasts (0 – 6 days) concerning the coastal environment along the French coastlines bordering the English Channel, the Atlantic Ocean and the Mediterranean Sea. The PREVIMER wave forecasts is calculated by SHOM using the WaveWatch III (WW3) numerical code, with a third-order accuracy propagation scheme in space and time, forced by ECMWF meteorological data for large scale, provided by Météo-France. The model output are validated with in situ measurements (i.e. the swell buoys network operated by CETMEF - Centre d'Etudes Techniques Maritimes Et Fluviales) and the remote sensing (CERSAT - Center for Satellite Exploitation and Research). The model results are provided in the NetCDF format, compliant with CF-1 metadata convention mainly used for gridded

data, at 3 hour intervals and the variables are, for example, significant wave height, wave energy period, mean wave direction.

The WW3 PREVIMER model that covers all the Mediterranean Sea, from 6° W to 36.5° E of longitude and from 30° N to 46° N of latitude, with a resolution of 0.1° (≈ 11 km), is called MED-6MIN. The WW3 PREVIMER model that covers the NW Mediterranean Sea, from 1° W to 11° E of longitude and from 40° N to 45° N of latitude, with a resolution of 0.036° (≈ 4 km), is called, until the 24 November 2010, MENOR-4000M, and after the 25 November 2010, MENOR-2MIN.

The analyzed data-set covers a period of 2 years and 10 months, from 17 June 2009 for Mediterranean Sea model, and from 2 July 2009 for the NW Mediterranean Sea, to 31 March 2012.

The wave power values in each point of the domain were computed in deep water with the eq. (3.60), in which the significant wave height and mean energy period data were extracted by PREVIMER data-set using MATLAB script. The spatial distribution of the monthly mean and yearly mean wave power was computed and reported in the form of contour maps for each month, for the all Mediterranean area and in detail for the NW Mediterranean area (see Appendix B). For each monthly map the value and the location of the highest values were obtained.

In order to estimate the magnitude of the wave power variability, the coefficient of variation (COV) in eq. (3.61) was computed as proposed in [11]

$$\text{COV} = \frac{\sigma}{\mu} \quad (3.61)$$

where σ and μ are the standard deviation and the average of the yearly mean wave power flux respectively. The COV of a constant series of values is 0 while a COV of 1 means that the standard deviation equals the average value. The lowest COV values correspond to the most promising areas for wave energy production.

The PREVIMER data-set were compared directly with the Gorgona Buoy data (Paragraph 3.3.3.1), that covers the same time period, and in term of monthly and yearly mean wave power with 7 points of the WorldWaves data (Paragraph 3.3.3.2), concerning the period from July 1992 to December 2004.

Other comparisons were done with the results of the Liberti et al. [11] model (Paragraph 3.3.3.3) and the Vicinanza et al. [12] RON buoy measurements (Paragraph 3.3.3.4).

3.3.2 RESULTS

3.3.2.1 *Mediterranean Sea*

The maximum values of the monthly mean power were estimated for each month of data-set and reported in Table 3.2. It's possible to observe that the months with values above 20 kW (highlighted in red) are the winter months: October, December, January and February. The exceptions are November 2010 (with a power value near 30 kW), January and February 2011. Figure 3.12 shows the trend of the maximum monthly mean power values and Figure 3.13 depicts the localization of the related points (the coordinates are in UTM-WGS84). It is confirmed that the most energetic parts of the Mediterranean Sea are those on the western coasts of Corsica and Sardinia islands, with only some exceptions: parts near the Strait of Gibraltar (September 2009, April 2010, April 2011 and May 2011), parts near the Greek islands (August 2011 and November 2011) and parts on the northern of the African coast (February 2011 and March 2011).

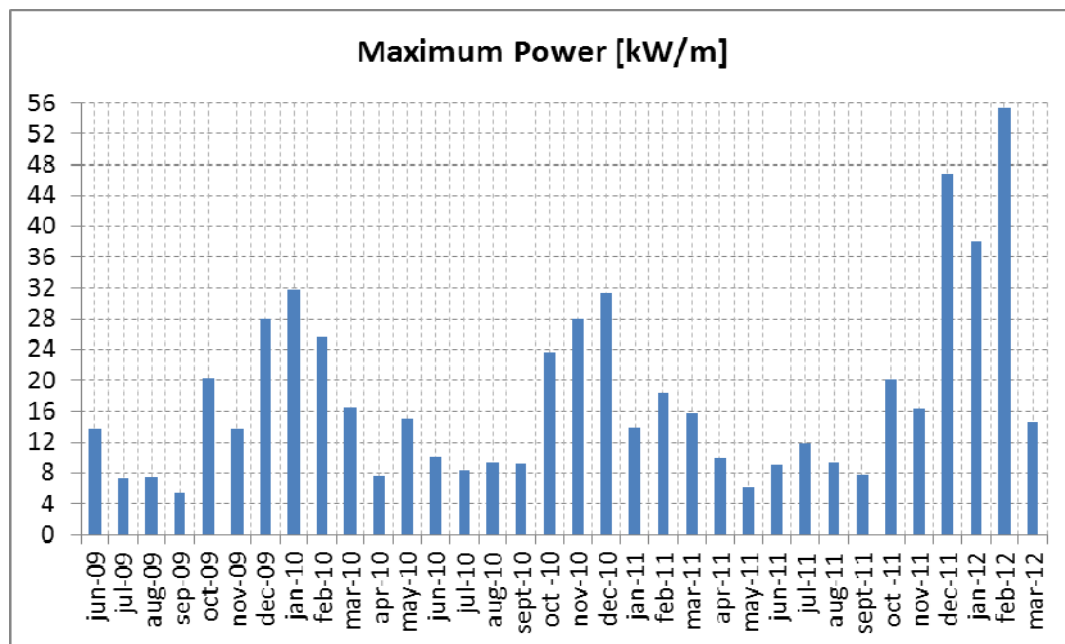


Figure 3.12. Maximum values of the monthly mean power

The mean powers change a lot from month to month with values on the order of 5 kW/m during the spring and the summer (Figure 3.14), and higher values on the order of 30-50 kW/m, in the winter and the autumn (Figure 3.15).

Table 3.2 Maximum values of the monthly mean power and their location
(the coordinates are in UTM-WGS84)

Year	Month	Pmax[kW/m]	Lat[°N]	Long[°E]
2009	6	13.66	40.9	6
2009	7	7.4	42	7.2
2009	8	7.41	37.6	25.4
2009	9	5.45	36.2	-2.7
2009	10	20.31	39.5	7
2009	11	13.75	41.5	7.8
2009	12	28.11	41	6.4
2010	1	31.72	38.1	8
2010	2	25.57	40.5	6.2
2010	3	16.4	41.8	4.7
2010	4	7.57	35.9	-4.2
2010	5	15.08	41.3	6.7
2010	6	10.09	40.9	6.2
2010	7	8.4	41.3	5.8
2010	8	9.26	41.5	6.4
2010	9	9.23	41.7	7
2010	10	23.7	41.2	5
2010	11	28.05	38	7
2010	12	31.43	41	5.2
2011	1	13.95	40.5	5.5
2011	2	18.51	34	17.4
2011	3	15.73	36	-3
2011	4	9.87	36	-3.5
2011	5	6.04	36	-3
2011	6	9.01	41.9	6.7
2011	7	11.89	41.9	7
2011	8	9.29	37.6	25.5
2011	9	7.84	41.1	7.2
2011	10	20.19	40.7	5.7
2011	11	16.37	38.3	24.6
2011	12	46.76	39.8	7.2
2012	1	38.2	40.7	6.7
2012	2	55.3	40.9	4.5
2012	3	14.61	32	28.7

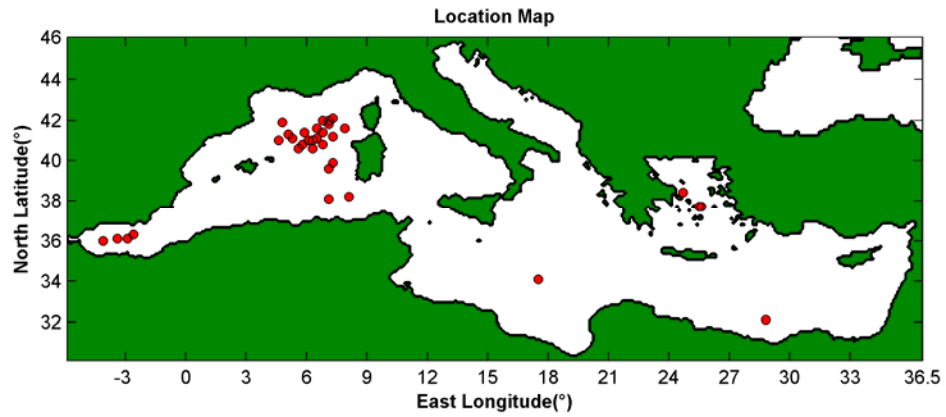


Figure 3.13. Location map of sea sites characterized by the maximum monthly mean power

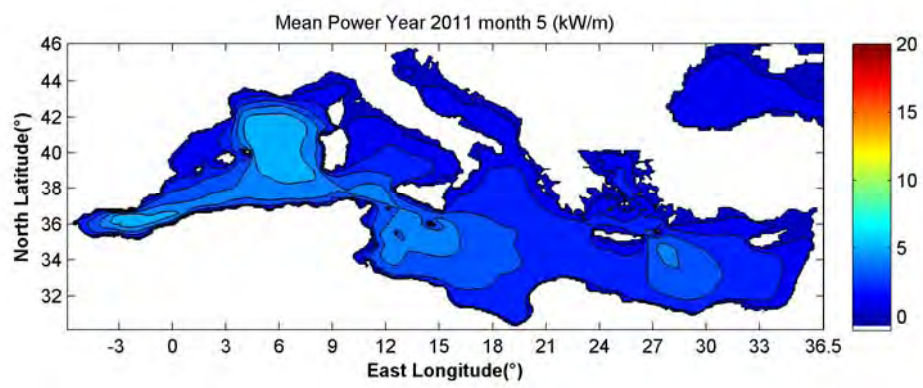


Figure 3.14. Spatial distribution of the mean power for May 2011 [kW/m]

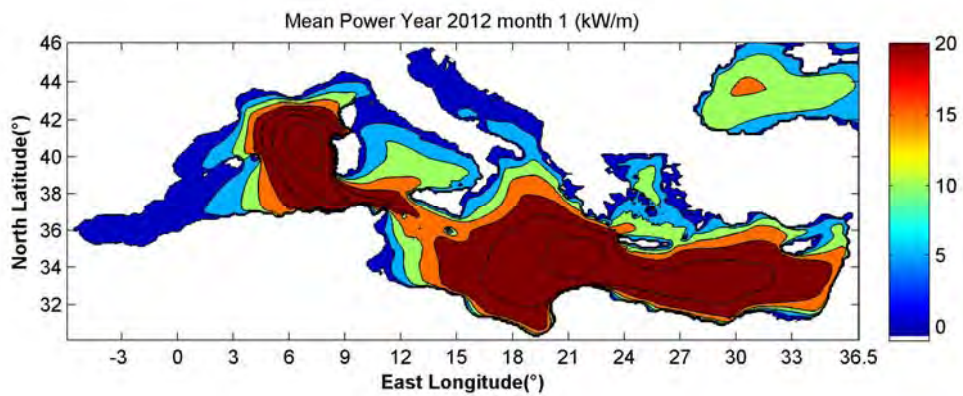


Figure 3.15. Spatial distribution of the mean power for January 2012 [kW/m]

Therefore, in order to have an idea of the mean power that it's possible to harvest in a year, the spatial distribution of the yearly mean power for the years 2010 (Figure 3.16) and 2011 (Figure 3.18) has been computed as the mean of the monthly mean powers. For the year 2010 the maximum of the yearly mean power is about 16 kW/m and for the year 2011 is lower, about 13 kW/m.

The wave power variability in the 2010 (Figure 3.17) is low (with COV value lower than 0.5) in the Gibraltar Strait, in the NW Mediterranean Sea, in the Adriatic Sea, in front of Tunisia and in the Aegean Sea. Instead, in the sheltered area and especially in the Cyprus area, the COV values are close to 1 and sometimes above 1. In the 2011 (Figure 3.19) the band between the NW Italy and the Algeria and the SW Italy area present the highest COV, with values also above 1. The Eastern and the Western Mediterranean area present values lower than 0.5.

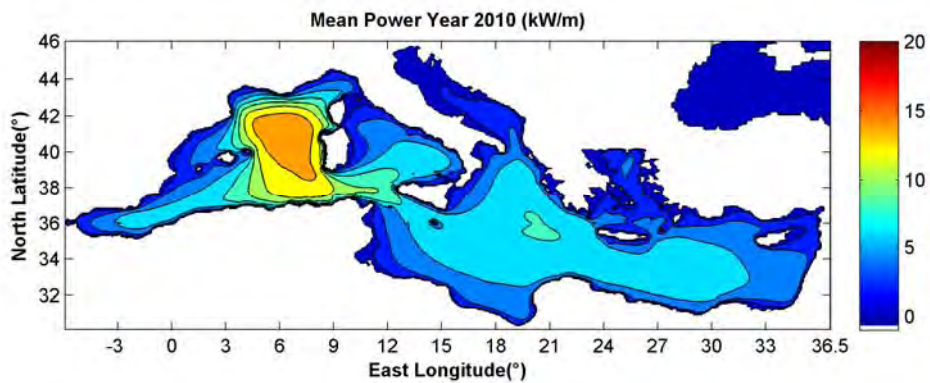


Figure 3.16. Spatial distribution of the mean power for the year 2010 [kW/m]

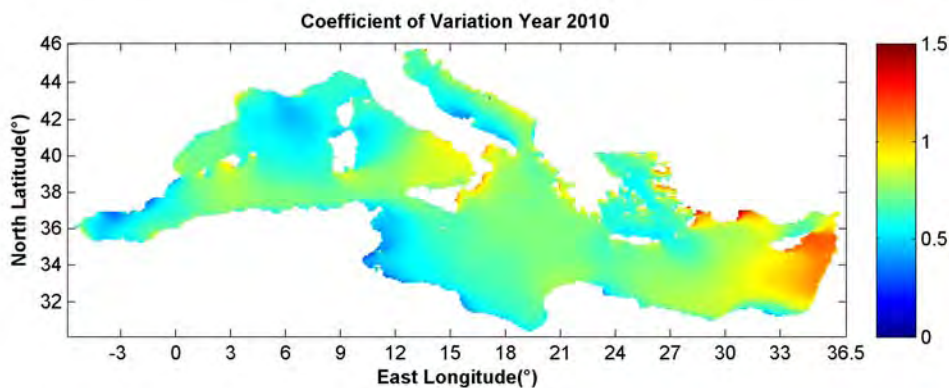


Figure 3.17. Coefficient of variation distribution for the year 2010

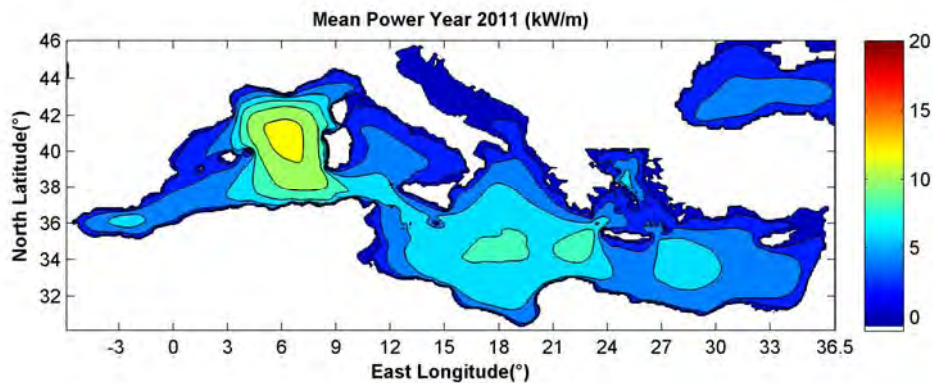


Figure 3.18. Spatial distribution of the mean power for the year 2011 [kW/m]

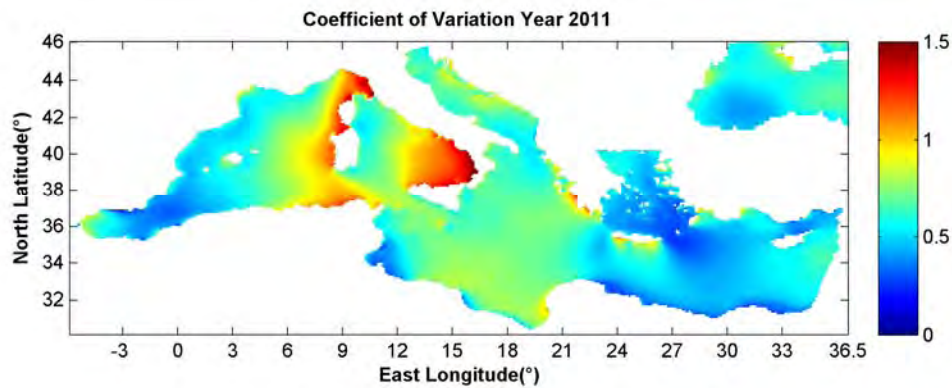


Figure 3.19. Coefficient of variation distribution for the year 2011

3.3.2.2 *North-Western Mediterranean Sea*

The same analysis of the Paragraph 3.3.2.1 was carried out in detail for the North-Western Mediterranean Sea. The Table 3.3 shows the maximum values of the monthly mean power and, highlighted in red, the values above 20 kW/m (see also the Figure 3.20). Comparing these highest values with the highest values in Table 3.2, it's interesting to note that they are very similar. This means that the locations of the highest values (the coordinates are in UTM-WGS84) are, as previously stated, in the area on the western coasts of the Corsica and Sardinia islands (Figure 3.21).

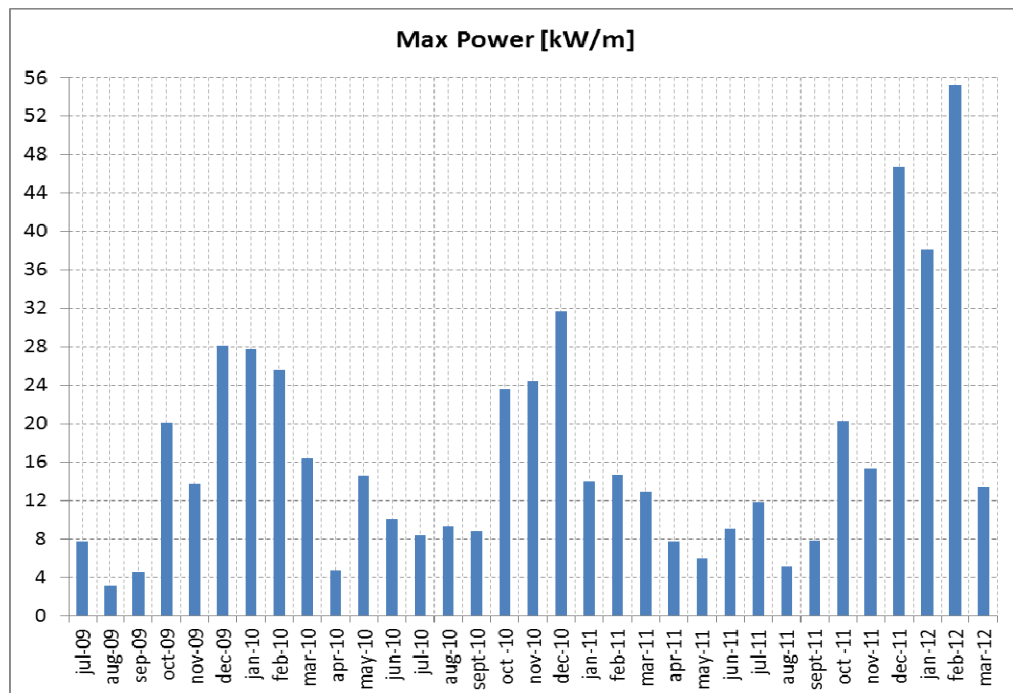


Figure 3.20. Maximum values of the monthly mean power

Table 3.3 Maximum values of the monthly mean power and its location
(the coordinates are in UTM-WGS84)

Year	Month	Pmax[kW/m]	Lat[°N]	Long[°E]
2009	7	7.77	42.00	7.20
2009	8	3.12	41.70	6.10
2009	9	4.53	41.00	4.00
2009	10	20.15	40.00	6.50
2009	11	13.76	41.50	7.80
2009	12	28.09	41.00	6.40
2010	1	27.73	40.00	7.10
2010	2	25.54	40.50	6.30
2010	3	16.35	41.80	4.80
2010	4	4.71	40.00	6.50
2010	5	14.61	41.30	6.80
2010	6	10.06	41.00	6.10
2010	7	8.37	41.20	5.90
2010	8	9.25	41.50	6.40
2010	9	8.87	41.80	7.00
2010	10	23.6	41.00	5.00
2010	11	24.38	40.00	7.40
2010	12	31.72	40.90	5.20
2011	1	13.98	40.40	5.50
2011	2	14.7	40.00	5.10
2011	3	12.9	41.10	5.50
2011	4	7.74	41.4	4.75
2011	5	5.92	41.1	5.4
2011	6	9	41.9	6.7
2011	7	11.88	41.9	7
2011	8	5.06	41.3	6.9
2011	9	7.83	41.1	7.2
2011	10	20.17	40.7	5.7
2011	11	15.26	42.3	6.9
2011	12	46.68	40	7.2
2012	1	38.17	40.7	6.7
2012	2	55.27	40.9	4.5
2012	3	13.35	40.7	4.7

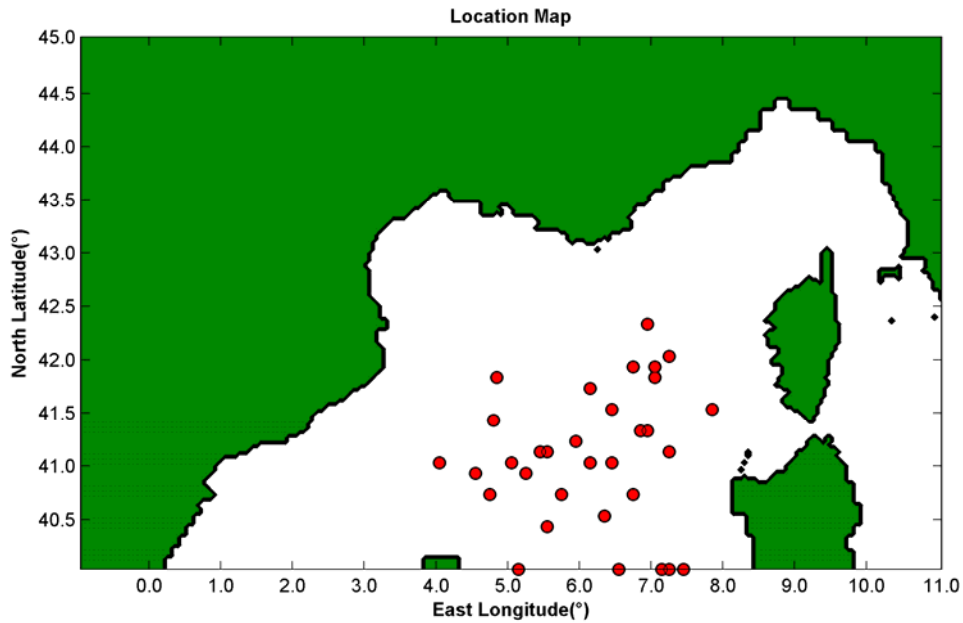


Figure 3.21. Location map of sea sites characterized by the maximum monthly mean power

The power values change a lot during the year, ranging from maximum values of 5-10 kW/m in the summer and the spring and 20-50 kW/m in the winter and in the autumn. In fact, from Figure 3.22 and Figure 3.23, it can be noticed the difference between the month of May 2011 (maximum value of 5.92 kW/m) and December 2011 (maximum value of 46.68 kW/m).

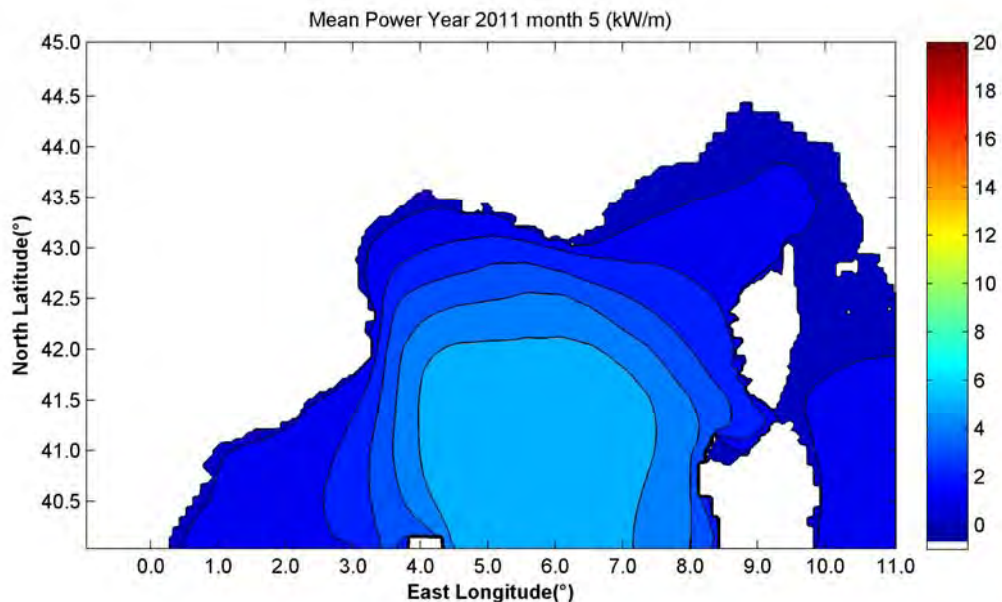


Figure 3.22. Spatial distribution of the mean power for May 2011 [kW/m]

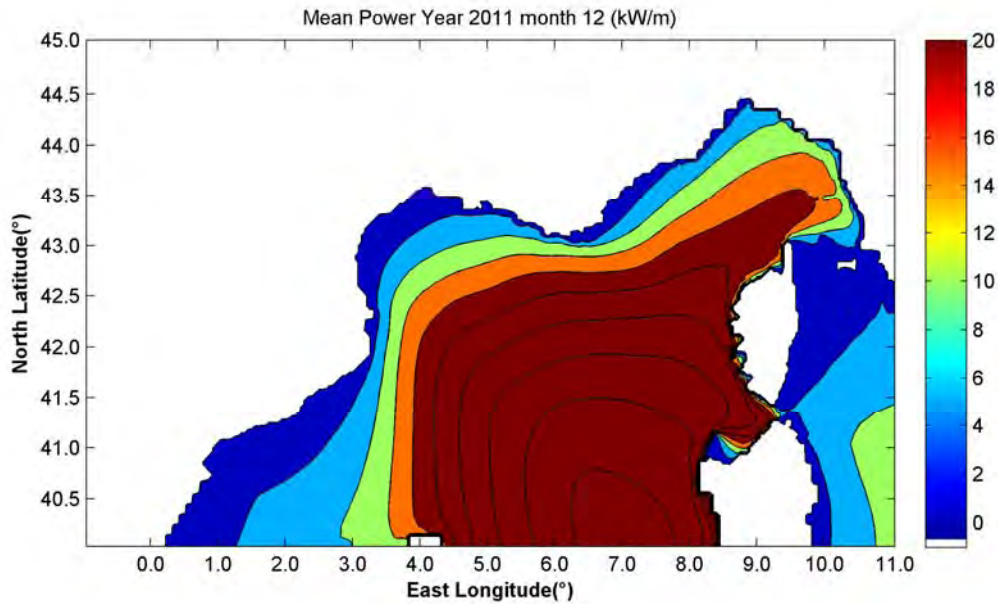


Figure 3.23. Spatial distribution of the mean power for December 2011 [kW/m]

Therefore, in order to have an idea of the mean power that it's possible to harvest in a year, the spatial distribution of the yearly mean power for the years 2010 (Figure 3.24) and 2011 (Figure 3.26) was computed as the mean of the monthly mean powers.

The results are the same of the previous analysis for the Mediterranean sea, in fact for the year 2010 the maximum of the yearly mean power is about 16 kW/m and for the year 2011 is lower, about 13 kW/m.

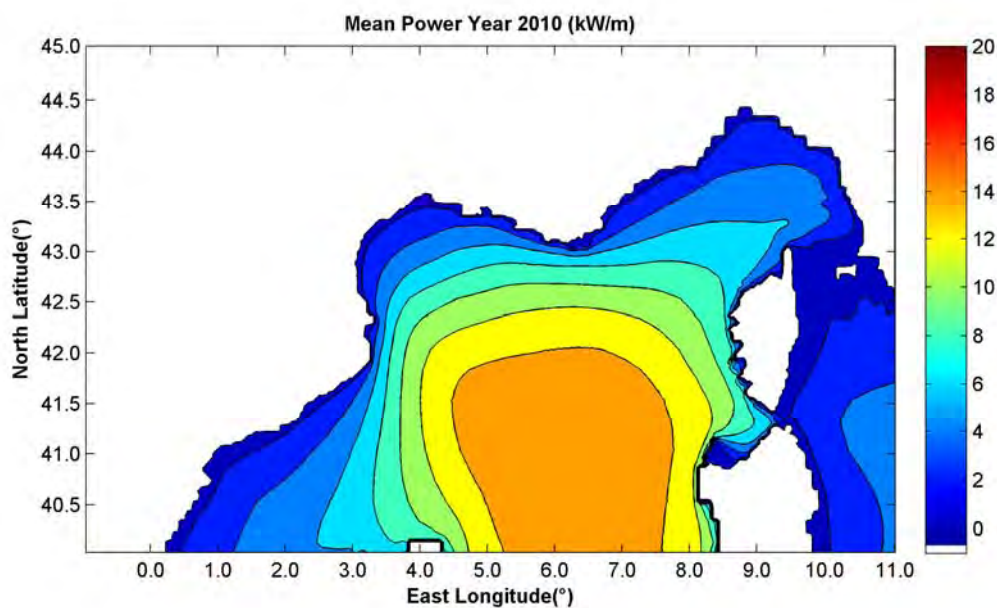


Figure 3.24. Spatial distribution of the mean power for the year 2010 [kW/m]

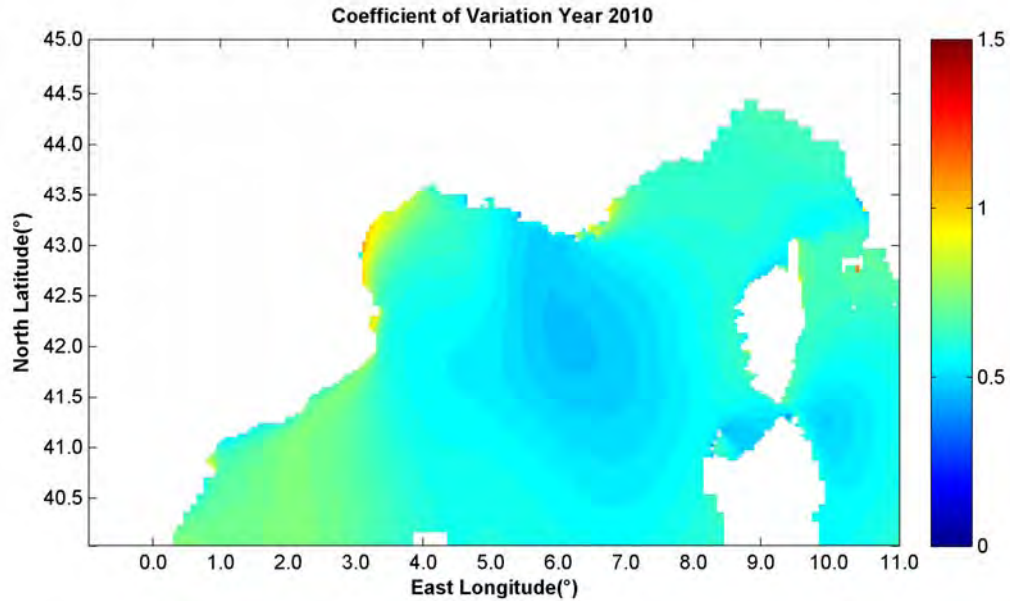


Figure 3.25. Coefficient of variation distribution for the year 2010

The wave power variability distribution for the 2010 (Figure 3.25) shows almost everywhere values lower than 0.5-0.6. The highest values, lower than 0.95, are located in the narrow sheltered area in the SE France. In the 2011 the wave power fluctuation (Figure 3.27) is higher, in fact in the area between the Northern Sardinia and Tuscany the COV values are around 1 and in the sheltered area above 1.

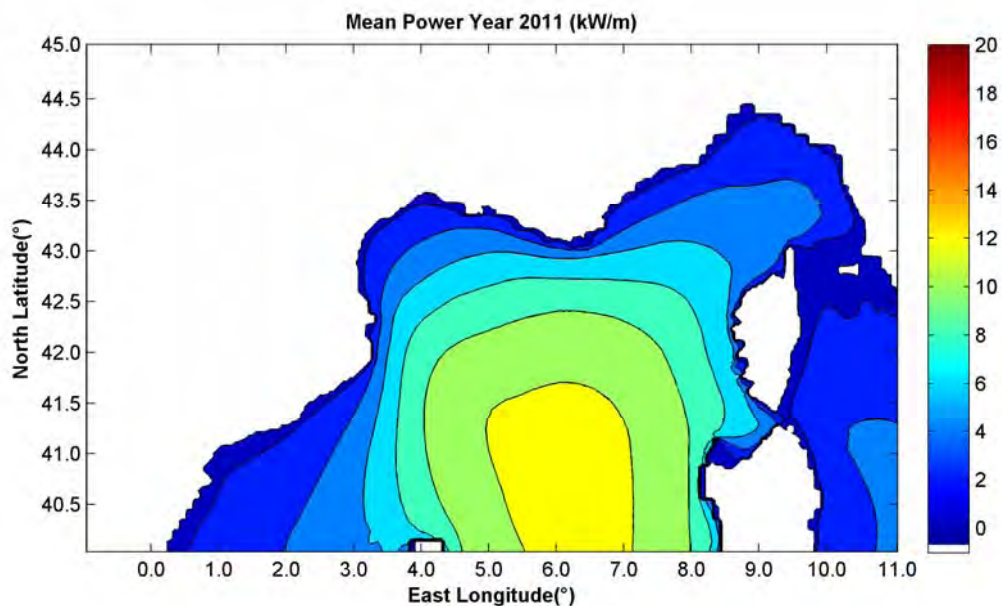


Figure 3.26. Spatial distribution of the mean power for the year 2011 [kW/m]

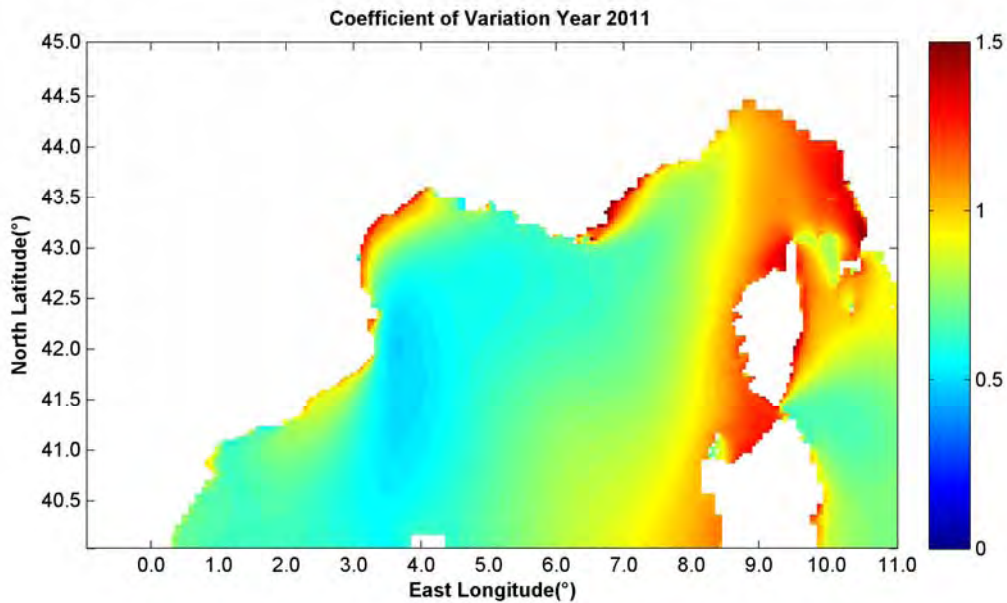


Figure 3.27. Coefficient of variation distribution for the year 2011

3.3.3 COMPARISON PREVIMER MODEL WITH OTHER DATA

3.3.3.1 Gorgona Buoy

The Gorgona buoy data covers the same period of the PREVIMER dataset, so an analysis of the correlation between the NW Med Sea model and in situ measurement wave significant height, and a comparison of the monthly mean wave power were performed.

The Gorgona buoy is a Datawell Directional Waverider MKIII buoy and was installed in front of Livorno (coordinates 43.57° N 9.96° E, see Figure 3.28) in June 2008 by Servizio Idrologico Regionale - Centro Funzionale of the Tuscany Region administration, who provided the data for this analysis.

The correlation between the significant wave height measured by the buoy and extracted at the nearest grid point by PREVIMER dataset was done with the Pearson formula given by

$$r = \frac{\sigma_{xy}}{\sigma_x \sigma_y} = 0.9 \quad (3.62)$$

that suggests a strong relation ($r > 0.7$) between the two data types.



Figure 3.28. Gorgona buoy location

The same significant correlation is shown in Figure 3.29, done comparing the same 3-h data. The two wave roses (Figure 3.30) show some differences but the direction from which the waves are more frequent and higher is SW in both.

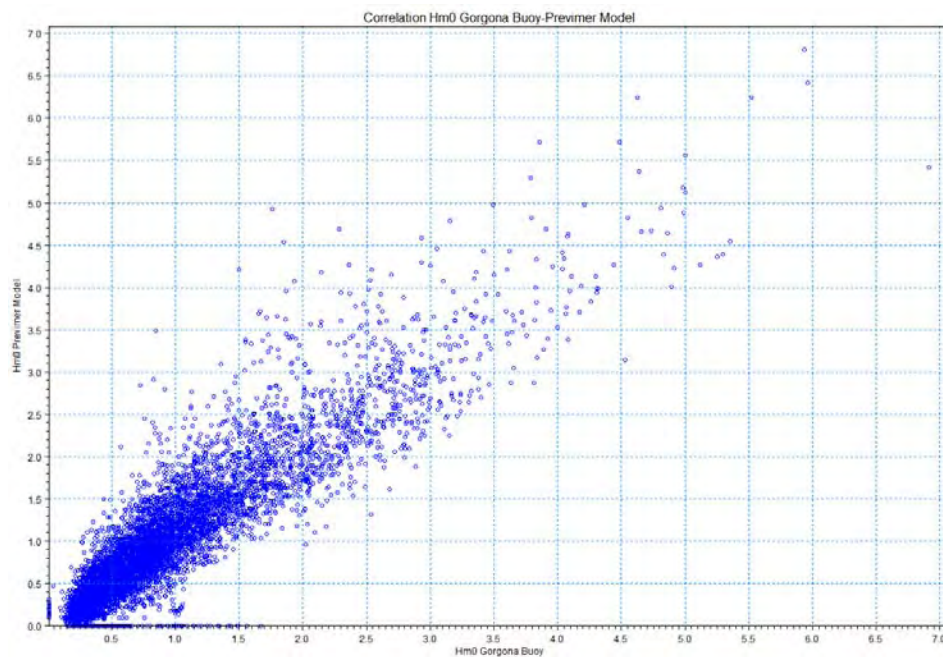


Figure 3.29. Relation between Gorgona buoy and NW Med Sea PREVIMER model

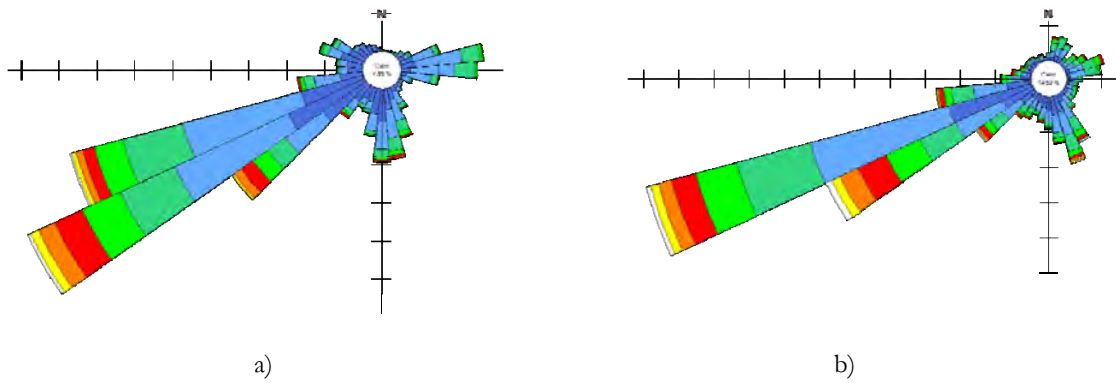


Figure 3.30. Wave rose: a) Gorgona buoy, b) NW Med Sea PREVIMER model

The Gorgona buoy wave power estimation was obtained by the eq. (3.60), in which the significant wave height was measured and the mean energy period was computed by the peak period using the relation $T_p = 1.1T_{m-1,0}$ [47]. The peak period was measured only after the 26 April 2010, so for the period July 2009–April 2010 its value was obtained by the mean period value with the relation $T_p = 1.39T_m$ in Figure 3.31, estimated by the correlation of their data measured in the period May 2010-March 2012.

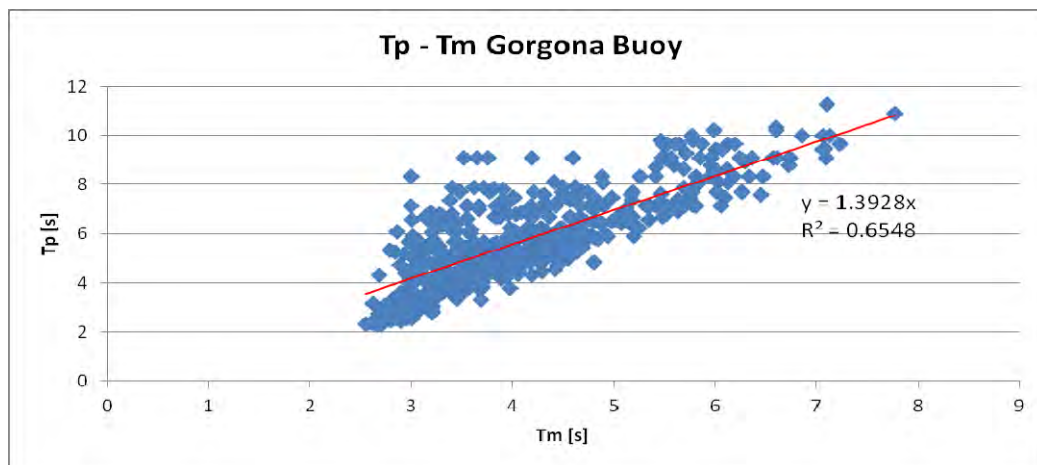


Figure 3.31. Gorgona Buoy: relation between peak period and mean period

The monthly mean wave power values of NW Med Sea PREVIMER model follow very well the buoy values in the period July 2009-December 2010, with the exception of October (Figure 3.32). In the 2011 the highest difference are in March and especially in November (PREVIMER value is two and half times the buoy value) and in the 2012 the PREVIMER values are always higher than the Gorgona buoy values.

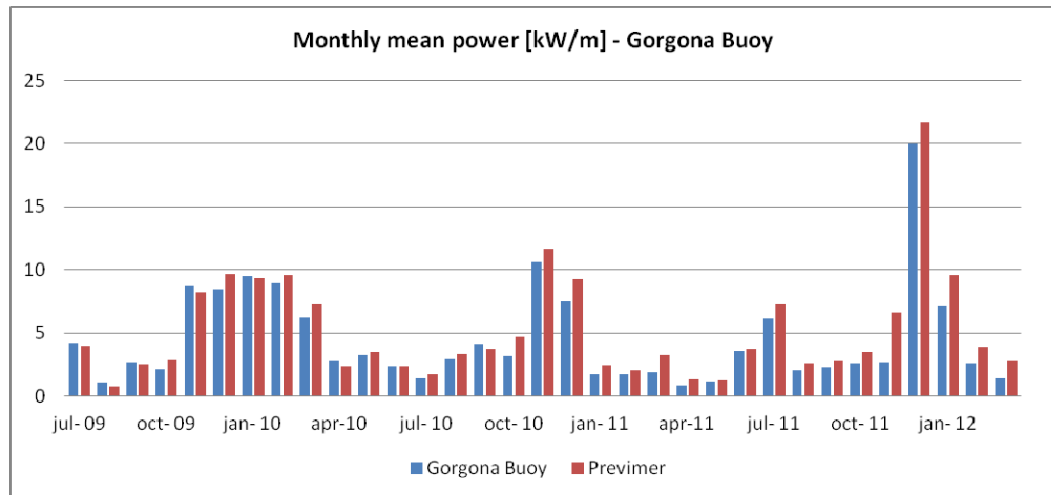


Figure 3.32. Monthly mean wave power of the Gorgona Buoy and NW Med Sea PREVIMER model

The wave power values relative to the same month were averaged over the analyzed period in order to obtain a monthly and an yearly mean power, characteristic of the site, which results are summarized in Table 3.4 and shown in Figure 3.33. The yearly mean values differ each other on the order of 13% and the largest differences, on the order of 28%, are in March and October. On the basis of these considerations the PREVIMER model data seem to be reliable.

Table 3.4. Monthly and yearly mean wave power of the Gorgona Buoy and NW Med Sea PREVIMER model

	Mean Wave Power [kW/m]												
	jan	feb	mar	apr	may	jun	jul	ago	sep	oct	nov	dec	yearly
<i>Gorgona Buoy</i>	6.15	4.43	3.16	1.81	2.21	2.96	3.92	2.02	3.04	2.64	7.33	12.00	4.31
<i>Previmer model</i>	7.12	5.15	4.48	1.85	2.36	3.05	4.36	2.24	2.98	3.67	8.84	13.51	4.97

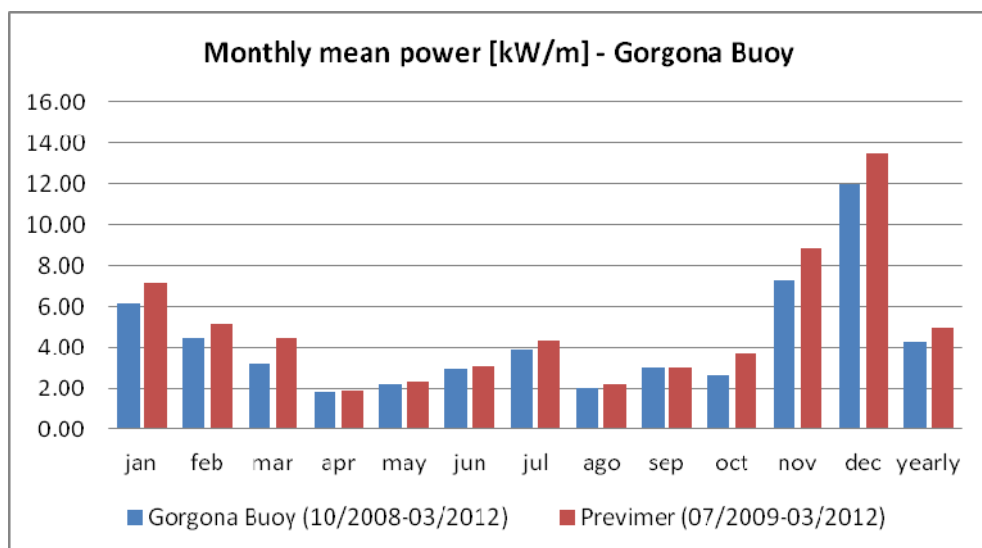


Figure 3.33. Monthly and yearly mean power of the Gorgona Buoy and NW Med Sea PREVIMER model

3.3.3.2 *WorldWaves data*

The WorldWaves data were analysed in 7 points (Figure 3.34), which significant wave height, mean energy period and mean direction data were provided by Tuscany Region administration. Their coordinates are, from north to south: (44°N, 9.5°E), (43.5°N, 9.5°E), (43.5°N, 10°E), (43°N, 10°E), (42.5°N, 10.5°E), (42°N, 11°E), (42°N, 11.5°E). These data cover the time period from July 1992 to December 2004 (Paragraph 3.2), then the comparison with the PREVIMER model data points (July 2009 – March 2012), chosen nearest to these coordinates, is qualitatively only on the monthly mean wave power. The first five points data were compared with those extracted by NW Med Sea PREVIMER model, while the southern points data were compared with those extracted by Med Sea PREVIMER model, as to out of the model domain with the highest accuracy.

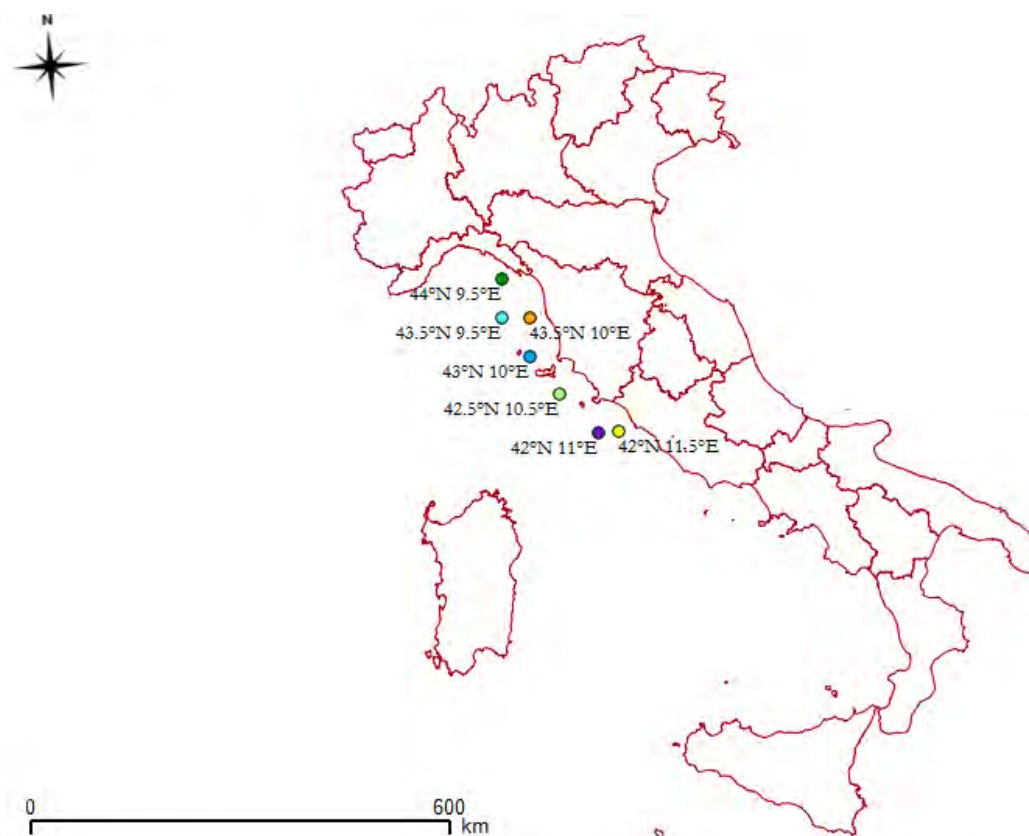


Figure 3.34. WorldWaves data points location

For each point the monthly and the yearly mean wave power of the two data type were summarized in a table (from Table 3.5 to Table 3.11) and their trends displayed in a figure (from Figure 3.35 to Figure 3.41). It is important to highlight that the differences are also due to non-perfect overlap of the point (for reasons of grid size) and to the different measurement time period.

Table 3.5. Monthly and yearly mean wave power of the (44° E, 9.5° N) point and PREVIMER model

	Mean Wave Power [kW/m]												
	jan	feb	mar	apr	may	jun	jul	ago	sep	oct	nov	dec	yearly
44° E 9.5° N	6.8	5.6	4.9	4.9	2.9	2.5	2.7	2.0	3.6	5.8	7.4	8.0	4.8
Previmer model	3.6	2.8	2.2	1.1	1.5	1.7	2.4	1.3	1.7	2.0	6.1	8.6	2.9

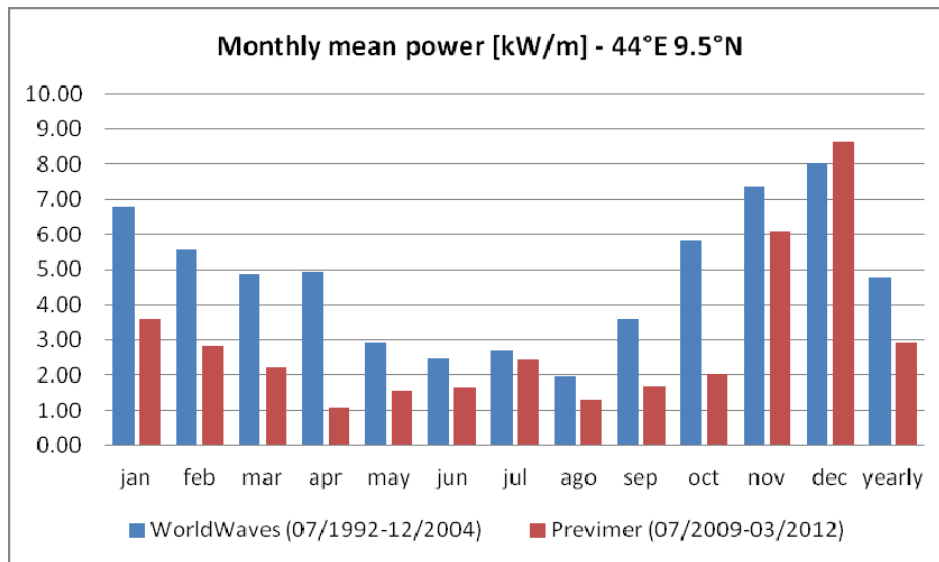


Figure 3.35. Monthly and yearly mean power of the (44° E, 9.5° N) point and PREVIMER model

Table 3.6. Monthly and yearly mean wave power of the (43.5° E , 9.5° N) point and PREVIMER model

	Mean Wave Power [kW/m]												
	jan	feb	mar	apr	may	jun	jul	ago	sep	oct	nov	dec	yearly
43.5° E 9.5° N	8.6	7.8	6.4	6.2	3.4	3.1	3.5	2.4	4.3	7.5	9.3	10.9	6.1
Previmer model	6.4	4.6	4.0	1.7	2.2	2.8	3.9	2.1	2.8	3.4	8.6	12.9	4.6

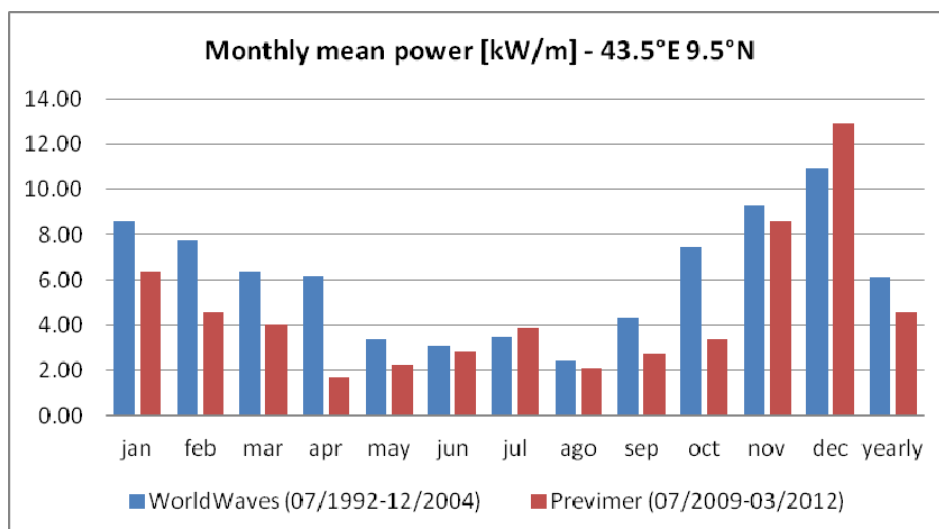


Figure 3.36. Monthly and yearly mean power of the (43.5° E , 9.5° N) point and PREVIMER model

Table 3.7. Monthly and yearly mean wave power of the (43.5° E, 10° N) point and PREVIMER model

		Mean Wave Power [kW/m]												
		jan	feb	mar	apr	may	jun	jul	ago	sep	oct	nov	dec	yearly
43.5° E	10° N	5.02	4.75	3.70	3.70	2.09	1.99	2.22	1.54	2.74	4.52	5.44	6.20	3.66
<i>Previmer model</i>		4.55	3.34	2.77	1.21	1.65	2.20	3.24	1.68	2.17	2.51	6.24	10.39	3.50

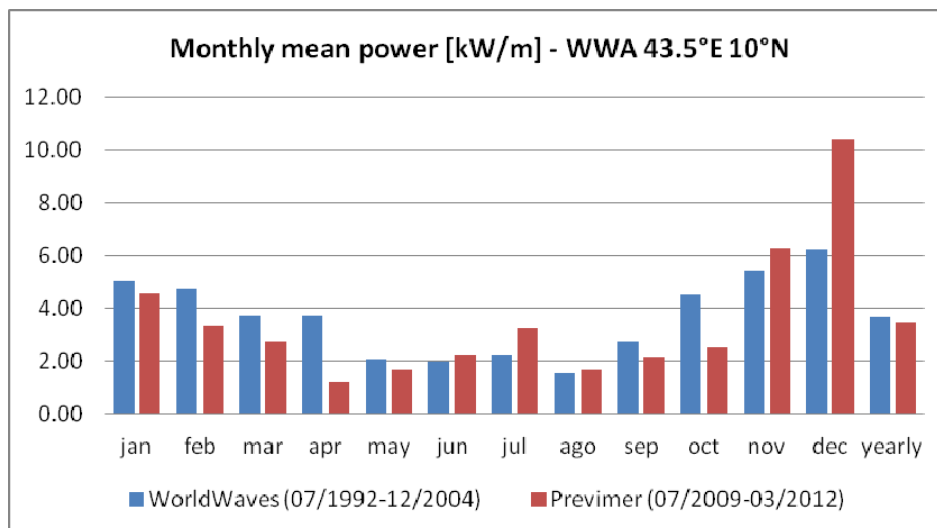


Figure 3.37. Monthly and yearly mean power of the (43.5° E, 10° N) point and PREVIMER model

Table 3.8. Monthly and yearly mean wave power of the (43° E, 10° N) point and PREVIMER model

		Mean Wave Power [kW/m]												
		jan	feb	mar	apr	may	jun	jul	ago	sep	oct	nov	dec	yearly
43° E	10° N	3.24	3.05	2.15	2.11	1.19	1.09	1.24	0.81	1.44	2.51	3.30	3.72	2.15
<i>Previmer model</i>		2.14	2.47	1.77	0.72	0.43	0.51	0.86	0.36	0.63	1.68	2.63	3.05	1.44

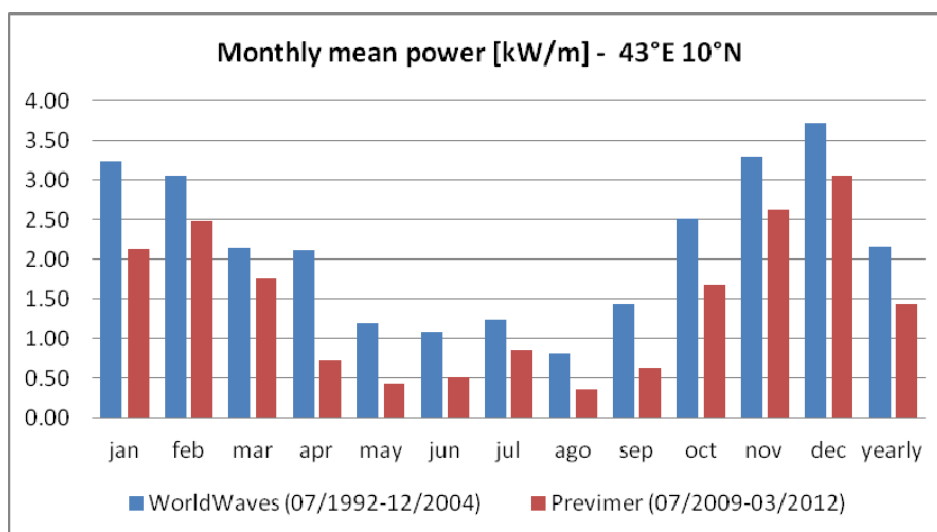


Figure 3.38. Monthly and yearly mean power of the (43° E, 10° N) point and PREVIMER model

Table 3.9. Monthly and yearly mean wave power of the (42.5° E, 10.5° N) point and PREVIMER model

	jan	feb	mar	apr	may	jun	jul	ago	sep	oct	nov	dec	yearly
42.5° E 10.5° N	3.90	2.86	2.95	3.04	1.48	1.26	1.05	0.77	1.87	2.83	5.27	5.19	2.71
<i>Previmer model</i>	2.04	2.73	2.27	1.09	0.77	0.70	0.73	0.32	0.82	2.16	4.37	3.77	1.81

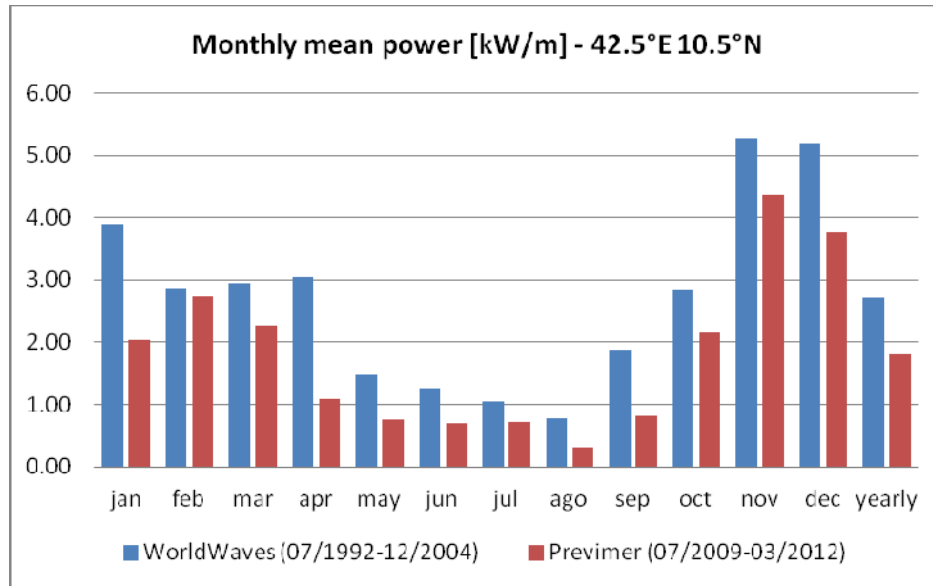


Figure 3.39. Monthly and yearly mean power of the (42.5° E, 10.5° N) point and PREVIMER model

Table 3.10. Monthly and yearly mean wave power of the (42° E, 11° N) point and PREVIMER model

	Mean Wave Power [kW/m]												
	jan	feb	mar	apr	may	jun	jul	ago	sep	oct	nov	dec	yearly
42° E 11° N	4.81	3.69	3.56	3.64	1.88	1.55	1.24	0.95	2.35	3.45	6.60	6.73	3.37
<i>Previmer model</i>	3.48	3.99	3.02	1.53	1.29	1.37	1.43	0.65	1.56	2.86	5.62	5.92	2.73

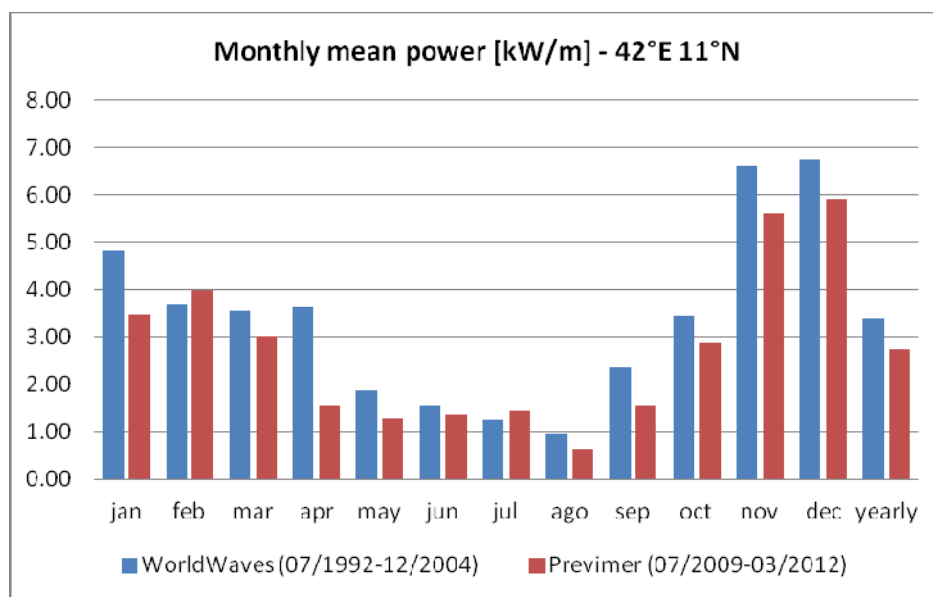


Figure 3.40. Monthly and yearly mean power of the (42° E, 11° N) point and PREVIMER model

Table 3.11. Monthly and yearly mean wave power of the (42° E, 11.5° N) point and PREVIMER model

	Mean Wave Power [kW/m]												
	jan	feb	mar	apr	may	jun	jul	ago	sep	oct	nov	dec	yearly
42° E 11.5° N	4.85	3.76	3.60	3.71	1.93	1.58	1.26	0.97	2.40	3.51	6.66	6.81	3.42
Previmer model	3.32	3.60	2.70	1.30	1.37	1.36	1.43	0.66	1.55	2.52	5.51	6.22	2.63

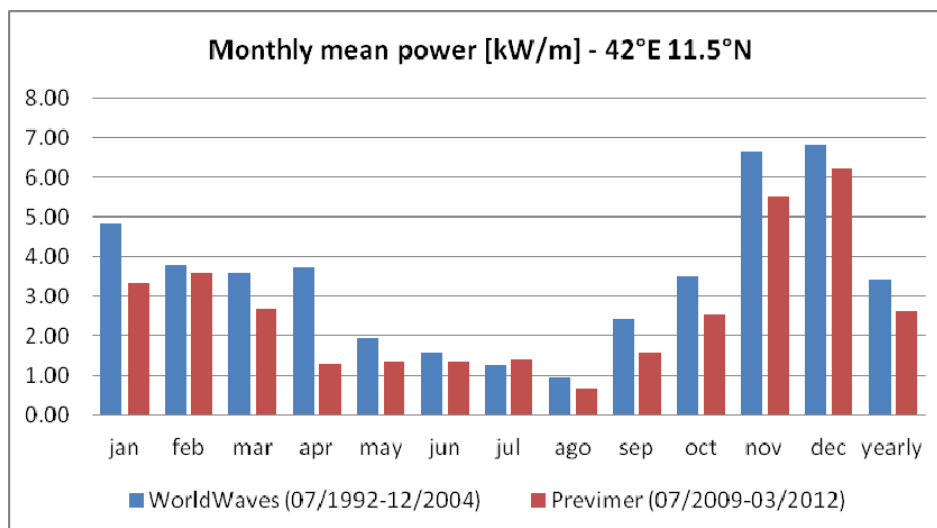


Figure 3.41. Monthly and yearly mean power of the (42° E, 11.5° N) point and PREVIMER model

The results in the point (43.5° E, 10° N) (Table 3.7 and Figure 3.37) shows that the PREVIMER model trend values follow fairly well the WorldWave data, with the exception of the April and December months (differences of the order of 60 %). In fact the yearly mean power values differ each other of 4 %, while in the other points are much higher. The highest difference (≈ 38 %) are for the point (44° E, 9.5° N) (Table 3.5 and Figure 3.35), in which the best results are for the December (≈ 7 %). The points (43° E, 10° N) (Table 3.8 and Figure 3.38) and (42.5° E, 10.5° N) (Table 3.9 and Figure 3.39) present a difference of the yearly mean value around 30 % and WorldWaves monthly mean values always higher than the PREVIMER model data. Instead, the difference of yearly mean values in the point (43.5° E, 9.5° N) (Table 3.6 and Figure 3.36) is around the 20%, in which the best result is for November (≈ 7 %). Also in the two most southern points, (42° E, 11° N) (Table 3.10 and Figure 3.40) and (42° E, 11.5° N) (Table 3.11 and Figure 3.41) the yearly difference is around 20 %, but the best result is for February in both (≈ 5 %).

In each of the analyzed points the worst month is April, with differences that reach also the 70 %, and the PREVIMER data mean values are lower than those of WorldWaves.

3.3.3.3 *Med Sea model*

The yearly mean wave power values, computed by Liberti & al. [11] model in 20 locations around all the Mediterranean Sea (see Figure 3.10), were compared with PREVIMER model. The comparison (Table 3.12 and Figure 3.42) shows that the highest differences ($\approx 30\%$) are in the point 1, 5, 12, 13, 14 and the lowest differences ($\approx 1\%$) are in the points 8, 9, 10, 16. In the other points the differences are lower than 13%. Considering that the time periods are different the results seem comparable.

Table 3.12. Yearly mean wave power in 20 points Liberti & al. [11] model and PREVIMER model

	Location	Liberti&al.	Previmer
Yearly mean wave power [kW/m]	1 Cabo de Palos (Es)	3.91	2.73
	2 Menorca (Es)	10.9	9.69
	3 Cabo Creus (Es)	5.34	4.94
	4 Hyères (Fr)	6.47	5.87
	5 Livorno (It)	3.24	2.28
	6 Ajaccio (Fr)	8.44	7.56
	7 Napoli (It)	3.51	3.27
	8 Crotone (It)	3.7	3.66
	9 Kefallonia (Gr)	4.91	4.84
	10 Ag. Gramvousa (Gr)	7.1	6.99
	11 Skyros (Gr)	5.16	4.45
	12 Gelydonia Burnu (Tr)	2.26	2.85
	13 Peyia (Cy)	3.83	5.17
	14 Haifa (Il)	4.02	5.55
	15 Ras El-Kanayis (Eg)	5.3	5.03
	16 Ras Al Hilal (Ly)	6.59	6.49
	17 Misrata (Ly)	5.68	5.45
	18 Ras Angela (Tn)	9.25	8.17
	19 Cap Bougaouni (Dz)	10.33	9.22
	20 Orano (Dz)	5.15	4.7

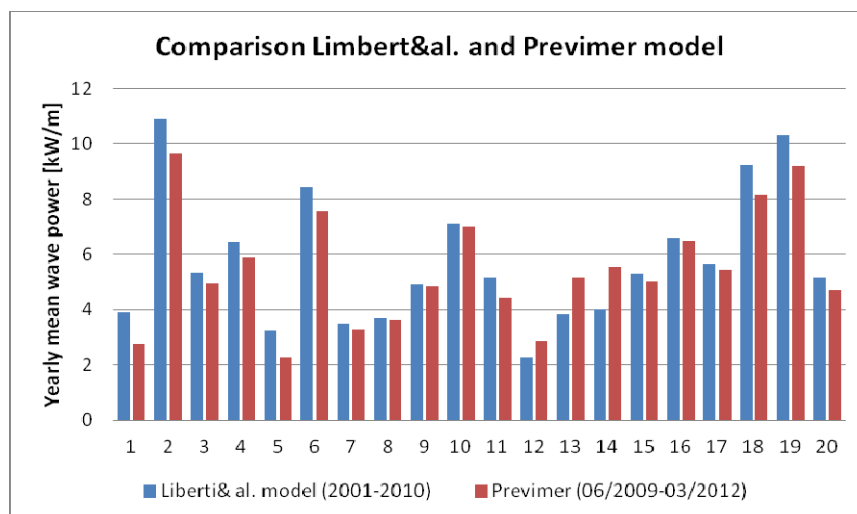


Figure 3.42. Yearly mean power in 20 points Liberti & al. [11] model and PREVIMER model

3.3.3.4 *RON wave buoy measurements data*

Vicinanza et al. [12] computed the yearly and the monthly mean wave power in the 15 buoys of the Italian Wave Buoys Network (RON). Their results were compared with the results obtained by the PREVIMER model, extracted in the grid points nearest to the buoy coordinates (see Figure 3.11 in Paragraph 3.2).

Table 3.13. Yearly mean wave power in the 15 RON buoy: Vicinanza&al. [12] and PREVIMER values

	Buoy	Vicinanza&al.	Previmer
Yearly mean wave power [kW/m]	1 Alghero	9.05	10.97
	2 Ancona	1.82	1.54
	3 Cagliari	1.52	1.47
	4 Capo Comino	2.43	1.91
	5 Capo Gallo	3.89	3.93
	6 Capo Linaro	2.88	2.28
	7 Catania	1.9	1.02
	8 Cetraro	2.85	3.06
	9 Crotone	2.86	2.91
	10 La Spezia	3.46	2.75
	11 Mazara del Vallo	4.75	4.07
	12 Monopoli	2.05	1.57
	13 Ortona	1.9	1.20
	14 Ponza	3.7	3.66
	15 Punta della Maestra	1.69	1.09

The yearly mean power values in Table 3.13 differ each other, in the Catania (7), Ortona (13) and Punta della Maestra (15) buoy more than 35 %, in the Cagliari (3), Capo Gallo (5), Crotone (9) and Ponza (14) buoy lower than 3 %, in the others among 10 % – 20 %. The buoys number 7 (Figure 3.49), 13 (Figure 3.55) and 15 (Figure 3.57) monthly mean wave power do not follow the trend of the PREVIMER model and present always larger values. Also in La Spezia (Figure 3.52) the buoy values are always higher than those of PREVIMER, except in December. The trend of the buoys 3 (Figure 3.45), 5 (Figure 3.47), 8 (Figure 3.50), 9 (Figure 3.51), 11 (Figure 3.53), 12 (Figure 3.54) and 14 (Figure 3.56) follow very well the PREVIMER one, with the exception of some months. Alghero (Figure 3.43) monthly mean power values do not differ a lot from PREVIMER values, except for December, where the PREVIMER value is two times the buoy value. The Ancona (Figure 3.44), Capo Comino (Figure 3.46) and Capo Linaro (Figure 3.48) buoys present remarkable differences in April and August, with buoy values three times higher than the PREVIMER values, and, at a lower rate in November and December.

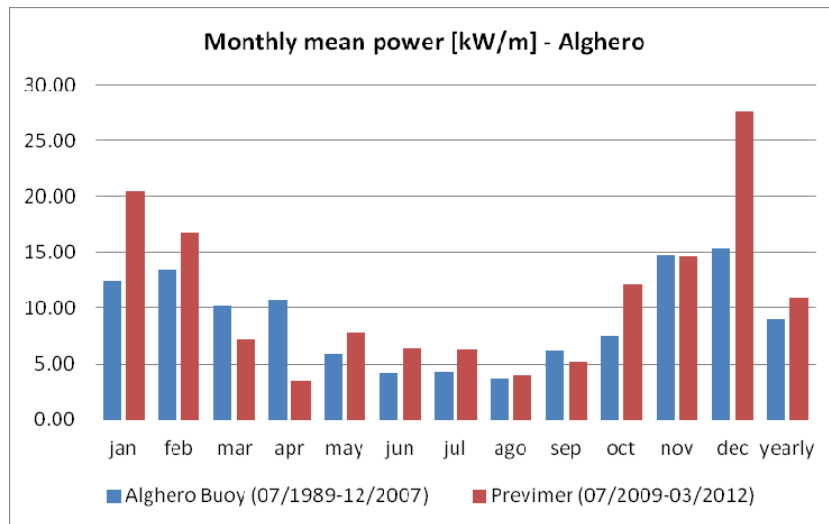


Figure 3.43. Monthly and yearly mean power in the Alghero Buoy

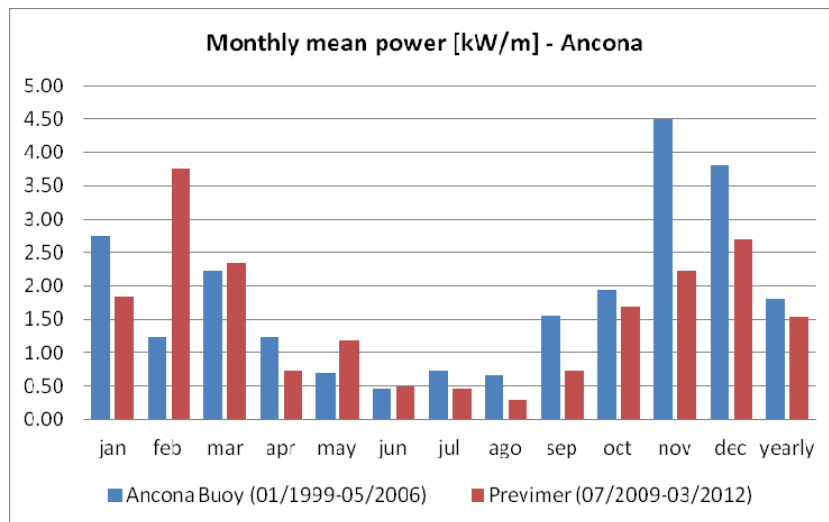


Figure 3.44. Monthly and yearly mean power in the Ancona Buoy

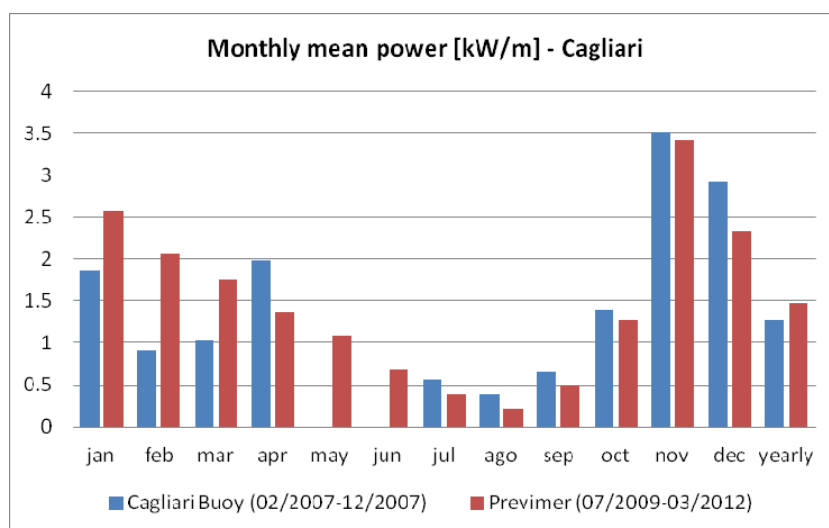


Figure 3.45. Monthly and yearly mean power in the Cagliari Buoy

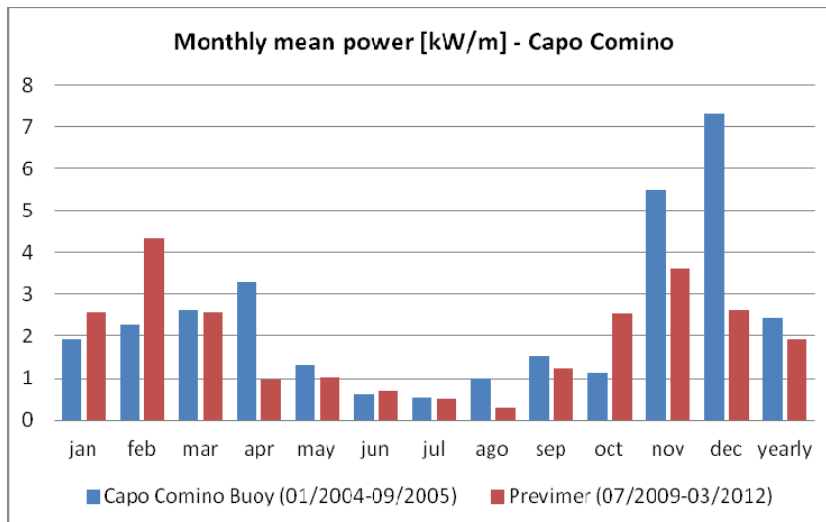


Figure 3.46. Monthly and yearly mean power in the Capo Comino Buoy

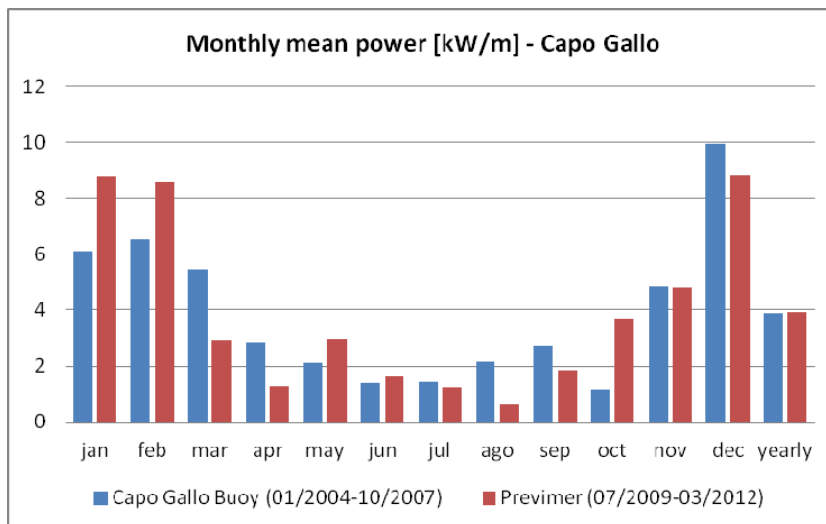


Figure 3.47. Monthly and yearly mean power in the Capo Gallo Buoy

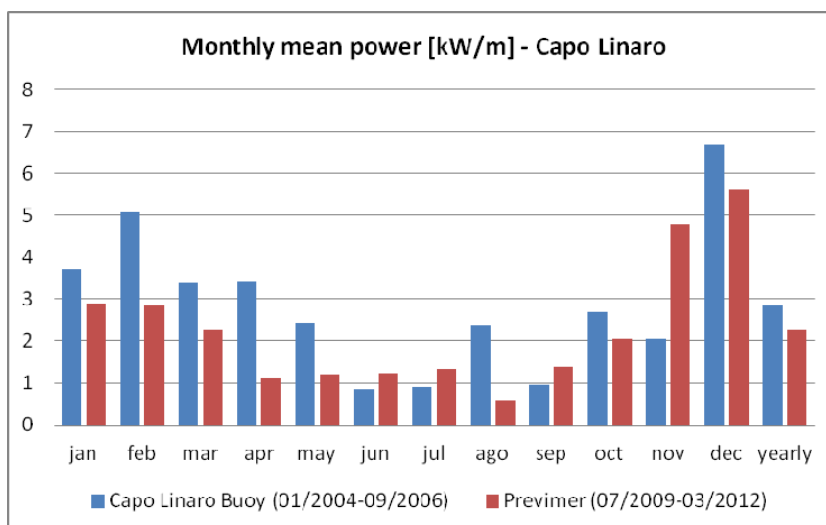


Figure 3.48. Monthly and yearly mean power in the Capo Linaro Buoy

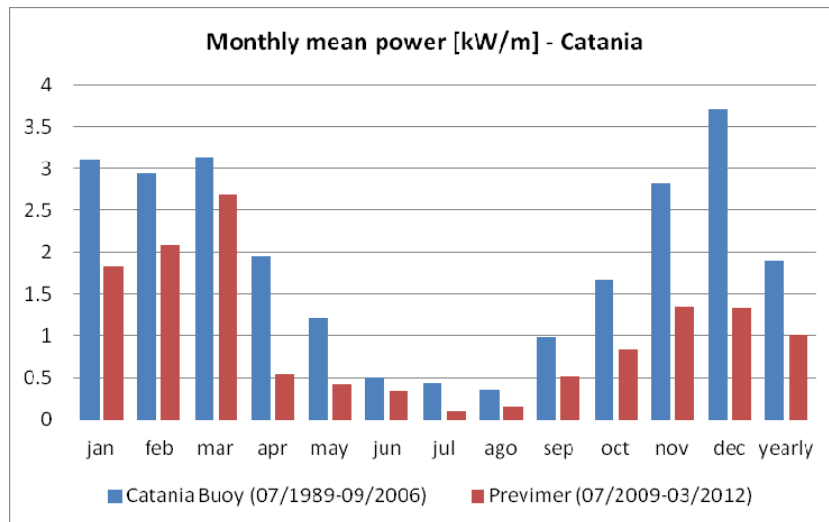


Figure 3.49. Monthly and yearly mean power in the Catania Buoy

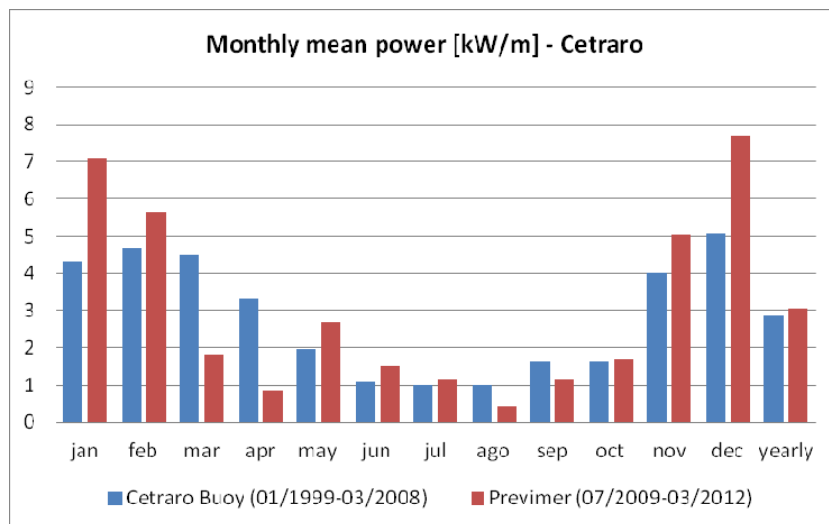


Figure 3.50. Monthly and yearly mean power in the Cetraro Buoy

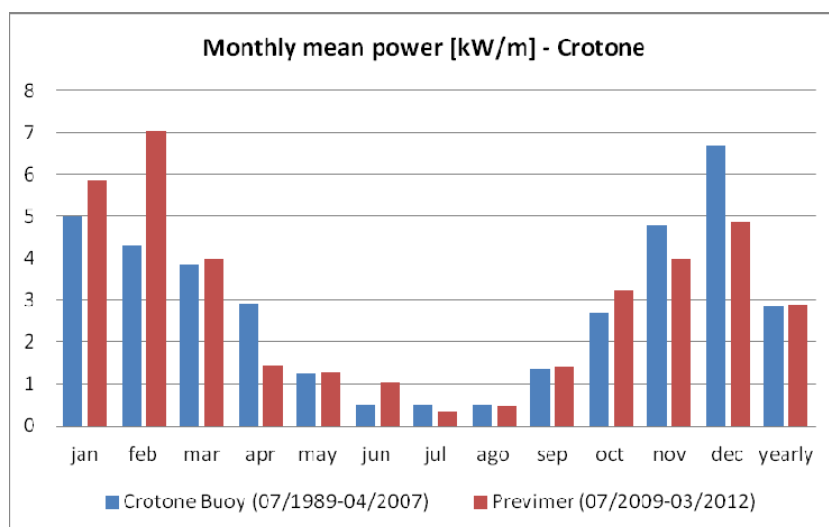


Figure 3.51. Monthly and yearly mean power in the Crotona Buoy

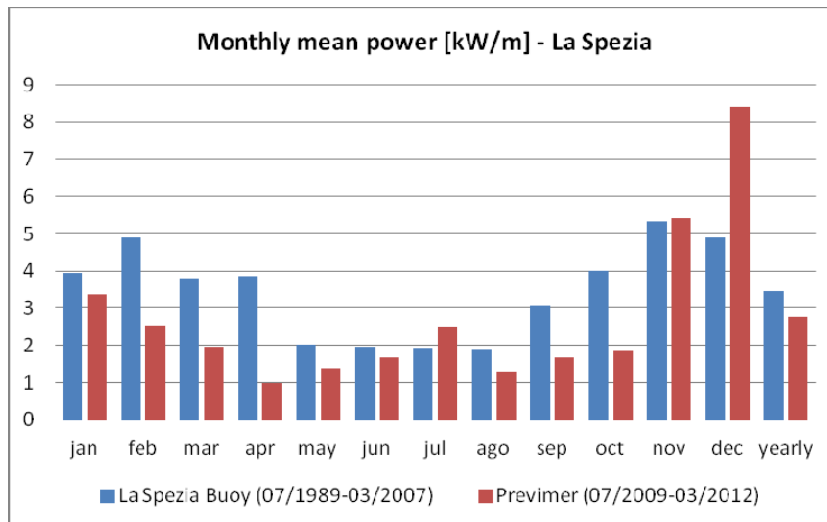


Figure 3.52. Monthly and yearly mean power in the La Spezia Buoy

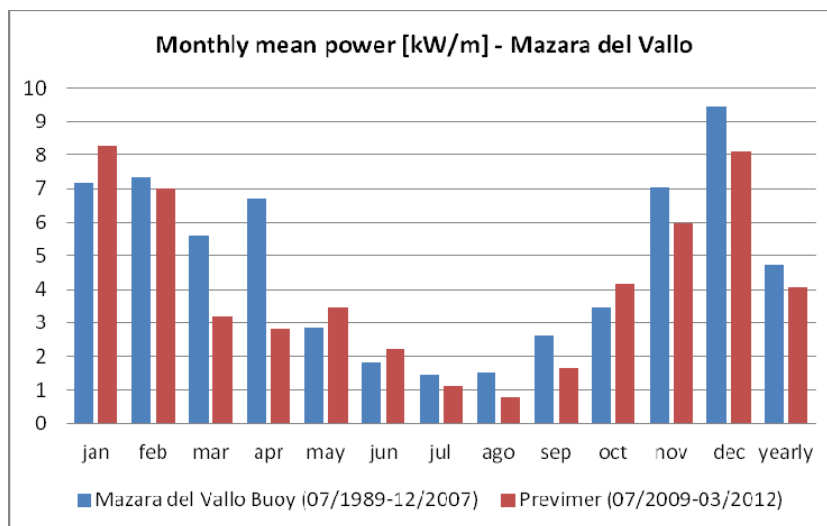


Figure 3.53. Monthly and yearly mean power in the Mazara del Vallo Buoy

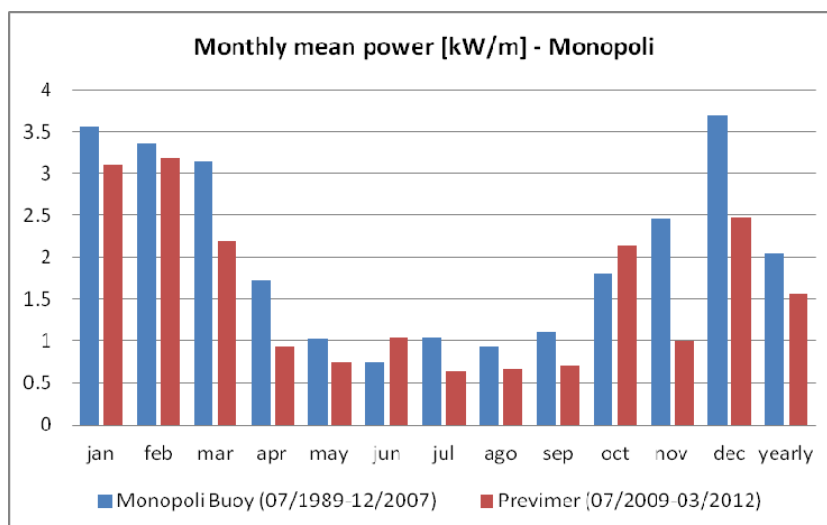


Figure 3.54. Monthly and yearly mean power in the Monopoli Buoy

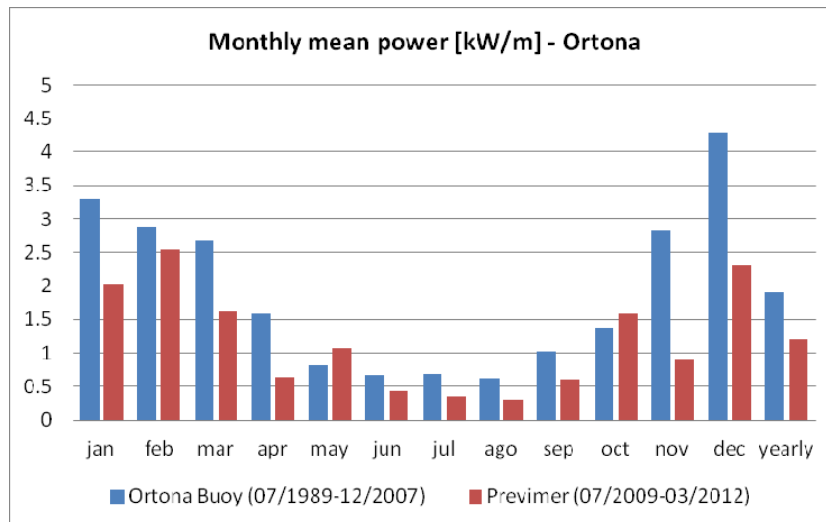


Figure 3.55. Monthly and yearly mean power in the Ortona Buoy

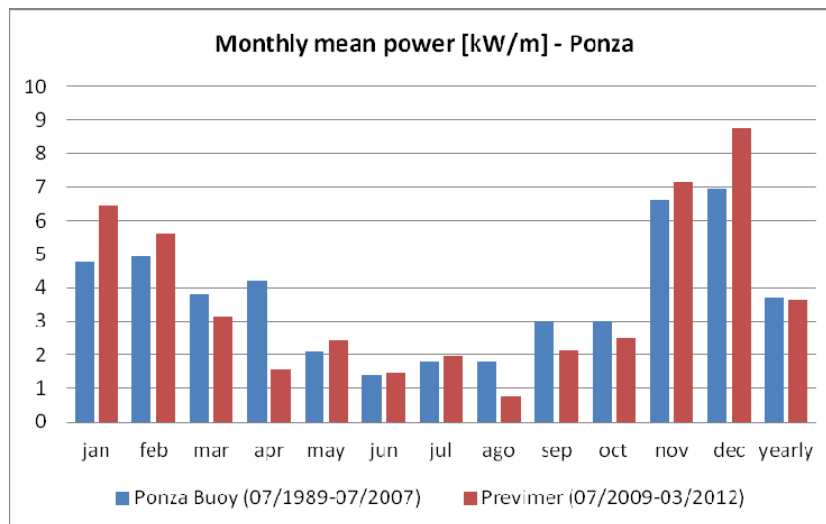


Figure 3.56. Monthly and yearly mean power in the Ponza Buoy

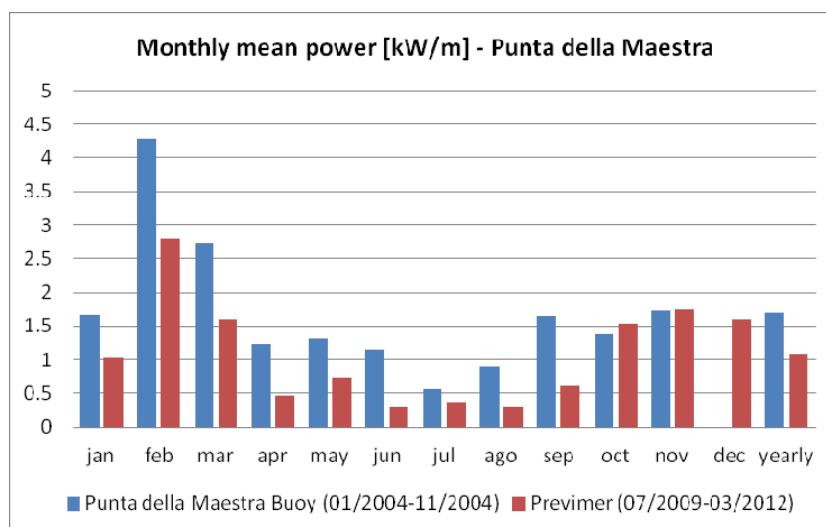


Figure 3.57. Monthly and yearly mean power in the Punta della Maestra Buoy

CHAPTER 4

NEARSHORE WAVE ENERGY CHARACTERIZATION

4.1. Description of the numerical model used

Although the offshore wave energy potential is known from the analysis in the Chapter 3, the processes affecting the waves as they propagate towards the nearshore can modify its values, leading to reductions or, sometimes, local enhancements due to focusing mechanisms. To quantify these processes, and then select the most energetic locations, numerical simulations were performed to propagate the power time series from deepwater into the nearshore area of the selected test sites.

The numerical simulations were carried out by MIKE 21-Spectral Wave (MIKE 21 SW) of the DHI Institute. The SW is a third generation spectral wind-wave model based on unstructured mesh that allows the simulation of the following physical phenomena: non-linear wave-wave interaction, dissipation due to white-capping, dissipation due to bottom friction, dissipation due to depth-induced wave breaking, refraction and shoaling due to depth variations. The model includes two different formulations: the fully spectral formulation, based on the wave action conservation equation, and the directional decoupled parametric formulation, based on a parameterisation of the wave action conservation equation.

The discretization of the governing equation is performed using the cell-centred volume technique. The time integration, in the non-stationary formulation, is performed using a fractional step time integration with a multi-sequence explicit method for the propagation, and, in the quasi-stationary formulation, is solved using the modified Newton-Raphson iteration or the iteration in the time domain [48].

4.1.1 MODEL EQUATIONS

The dynamics of the gravity waves are described by the transport equation for wave action density. The wave action density spectrum $N(\sigma, \theta)$ varies in time and space and is a function of two wave phase parameters: the relative angular frequency $\sigma = 2\pi f$ and the direction of wave propagation θ . It is related to the energy density $E(\sigma, \theta)$ by

$$N = \frac{E}{\sigma} \quad (4.1)$$

For wave propagation over slowly varying depths and currents the relation between the relative angular frequency σ and the absolute angular frequency ω is given by the linear dispersion relation

$$\sigma = \sqrt{gk \tanh(kd)} = \omega - \bar{k} \cdot \bar{U} \quad (4.2)$$

where g is the gravity acceleration, d the water depth, \bar{U} is the current velocity vector and \bar{k} is the wave number vector.

In the MIKE 21 SW fully spectral formulation, the governing equation is the wave action balance, that formulated in horizontal Cartesian co-ordinates can be written as

$$\frac{\partial N}{\partial t} + \nabla \cdot (\bar{v}N) = \frac{S}{\sigma} \quad (4.3)$$

where $N(\bar{x}, \sigma, \theta, t)$ is the action density, t the time, $\bar{x} = (x, y)$ the Cartesian co-ordinates, ∇ is the four dimensional differential operator in the \bar{x}, σ, θ space, $\bar{v} = (c_x, c_y, c_\sigma, c_\theta)$ the propagation velocity of a wave group in the four dimensional phase space and S is the source term for the energy balance.

The source function term, S , represents the superposition of source functions that describe various physical phenomena

$$S = S_{in} + S_{nl} + S_{ds} + S_{bot} + S_{surf} \quad (4.4)$$

where S_{in} represents the momentum transfer of wind energy to wave generation, S_{nl} the energy transfer due to non-linear wave-wave interaction, S_{ds} the dissipation of wave energy due to white-capping, S_{bot} the dissipation due to bottom friction, S_{surf} the dissipation of wave energy due to depth-induced breaking [49]. The S_{bot} term becomes important in the shallow water and the S_{surf} term in the extremely shallow water.

The wind input S_{in} is based on the Janssen's quasi-linear theory [50] of wind wave generation, where the moment transfer from the wind to the sea not only depends on the wind stress, but also on the sea itself, and it can be expressed as

$$S_{in}(f, \theta) = \max(\alpha, \gamma E(f, \theta)) \quad (4.5)$$

where α is the linear growth and γ is the nonlinear growth rate (for more details see [49]).

The nonlinear energy transfer (S_{nl}) amongst the different wave components of a directional-frequency spectrum plays a crucial role for the temporal and spatial evolution of a wave field. In deep water it is used the quadruplet-wave interaction, that controls the shape-stabilisation of the high-frequency part of the spectrum, the downshift of energy to lower frequencies and the frequency-dependent redistribution of directional distribution functions. In the SW module it is described by the Discrete Interaction Approximate (DIA) [51]. In the shallow water instead the triad-wave interaction becomes important and the exchanges of energy are obtained between three interacting wave modes. Nonlinear transformation of irregular waves in shallow water involves the generation of bound sub- and super-harmonics and near-resonant triad interactions, where substantial cross-spectral energy transfer can take place in relatively short distance. The triad-wave interaction is modelled using the simplified approach proposed by Eldeberky and Battjes [52] (for more details see [49]).

The source function describing the dissipation due to white-capping (deep water wave breaking) S_{ds} is based on the theory of Hasselmann [53], that obtained a function linear in both the spectral density and frequency, expressed by

$$S_{ds} \approx \omega E \quad (4.6)$$

With the introduction of Janssens description of wind input [50], it was realized that the dissipation source function needs to be adjusted in order to obtain a proper balance between the wind input and the dissipation at high frequencies, and can be expressed by

$$S_{ds}(f, \theta) = -C_{ds} \left(\frac{\hat{\alpha}}{\hat{\alpha}_{PM}} \right)^m \left\{ (1-\delta) \frac{k}{\bar{k}} + \delta \left(\frac{k}{\bar{k}} \right)^2 \right\} \bar{\sigma} E(f, \theta) \quad (4.7)$$

where C_{ds} , δ , m are constant, \bar{k} is the mean wave number, $\hat{\alpha}_{PM}$ is the value of $\hat{\alpha} = \bar{k} \sqrt{E_{tot}}$ for the Pierson-Moskowitz spectrum, E is the energy of energy spectrum.

The rate dissipation due to bottom friction [49] is given by

$$S_{bot}(f, \theta) = - \left(C_f + \frac{f_c(\bar{u} \cdot \bar{k})}{k} \right) \frac{k}{\sinh 2kd} E(f, \theta) \quad (4.8)$$

where C_f is a friction coefficient, k the wave number, d the water depth, f_c the friction coefficient for current and u the current velocity.

Depth-induced breaking occurs when waves propagate into very shallow areas, and the wave height can no longer be supported by the water depth. The formulation of wave breaking is based on the breaking model by Battjes and Janssen [54] and of its spectral version proposed by Eldeberky and Battjes [55], in which the spectral shape is not influenced by breaking, and then the source term S_{surf} can be written as [49]

$$S_{surf}(f, \theta) = - \frac{2\alpha_{BJ} Q_b \bar{f}}{X} E(f, \theta) = - \frac{\alpha_{BJ} Q_b H_m^2 \bar{f}}{4} \frac{E(f, \theta)}{E_{tot}} \quad (4.9)$$

where α_{BJ} is a calibration constant, Q_b is the fraction of breaking waves, \bar{f} is the mean frequency, X the ratio of the total energy E_{tot} in the random wave train to the energy in a wave train with the maximum wave height $H_m = \gamma d$, d the water depth and γ the free breaking parameter. In the directional decoupled parametric formulation the parameterisation of the wave action conservation equation follows these equations [56]

$$\left\{ \begin{array}{l} \frac{\partial(m_0)}{\partial t} + \frac{\partial(c_x m_0)}{\partial x} + \frac{\partial(c_y m_0)}{\partial y} + \frac{\partial(c_\theta m_0)}{\partial \theta} = T_0 \\ \frac{\partial(m_1)}{\partial t} + \frac{\partial(c_x m_1)}{\partial x} + \frac{\partial(c_y m_1)}{\partial y} + \frac{\partial(c_\theta m_1)}{\partial \theta} = T_1 \end{array} \right. \quad (4.10)$$

where $m_0(x, y, \theta)$ and $m_1(x, y, \theta)$ are the zeroth and first moment of action spectrum $N(x, y, \sigma, \theta)$ respectively, $T_0(x, y, \theta)$ and $T_1(x, y, \theta)$ are the source functions based on the action spectrum, that takes into account the effect of local wind generation and energy dissipation due to bottom friction and wave breaking.

4.1.2 MODEL OUTPUT

Four different types of output can be obtained from MIKE 21 SW, at each mesh point and for each time step [49]:

- integral wave parameters divided into wind sea and swell;
- input parameters (e.g. water level, current velocity, wind speed and direction);
- model parameters (e.g. bottom friction parameter, breaking parameter, Courant number, time step factor, roughness length);
- directional-frequency wave spectra at selected grid points and or areas as well as direction and frequency spectra.

In the integral wave parameter the distinction between wind-sea and swell can be calculated using either a constant threshold frequency (4.11) or a dynamic threshold frequency with an upper frequency limit (4.12).

$$f < f_{threshold} \quad or \quad \cos(\theta - \theta_w) < 0 \quad (4.11)$$

where θ is the wave propagation, θ_w is the wind direction, $f_{threshold}$ is the constant threshold frequency (default value equal to 0.125 Hz)

$$\begin{cases}
 \text{version 1} \left\{ \begin{array}{l}
 f < f_{\text{threshold}} \quad \text{or} \quad \cos(\theta - \theta_w) < 0 \\
 f_{\text{threshold}} = 0.7 f_{p,PM} \left(\frac{E_{PM}}{E_{\text{model}}} \right)^{0.31} = 0.7 \cdot 0.14 \frac{g}{U_{10}} \left(\frac{\left(\frac{U_{10}}{1.4g} \right)^4}{E_{\text{model}}} \right)^{0.31}
 \end{array} \right. \\
 \text{version 2} \left\{ \frac{U_{10}}{c} \cos(\theta - \theta_w) < 0.83
 \end{cases} \quad (4.12)$$

where θ is the wave propagation, θ_w is the wind direction, $f_{\text{threshold}}$ is the dynamic threshold frequency, $f_{p,PM}$ and E_{PM} are the peak frequency and the total wave energy for a fully developed wind-sea described by a Pierson-Moskowitz spectrum respectively, U_{10} is the wind speed, c the phase speed.

Some of the integral wave parameters are the significant wave height [m] (3.52), the peak period [s] (3.50), the wave energy mean period [s] (eq. 3.49), the mean wave direction [°] (4.13), the directional standard deviation [°] (4.14), the omni-directional wave power [kW/m] (4.15).

$$\bar{\theta} = 270 - \tan^{-1} \left(\frac{b}{a} \right) \quad \text{with} \quad \begin{cases}
 a = \frac{1}{m_0} \int_0^{2\pi} \int_0^{\infty} \cos \left(\frac{3}{2} \pi - \theta \right) E(f, \theta) df d\theta \\
 b = \frac{1}{m_0} \int_0^{2\pi} \int_0^{\infty} \sin \left(\frac{3}{2} \pi - \theta \right) E(f, \theta) df d\theta
 \end{cases} \quad (4.13)$$

$$\sigma = \left[2 \left(1 - (a^2 + b^2)^{1/2} \right)^{1/2} \right] \cdot \frac{180}{\pi} \quad (4.14)$$

$$P_{\text{energy}} = \rho g c_g E = \rho g \int_0^{2\pi} \int_0^{\infty} c_g(f, \theta) E(f, \theta) df d\theta \quad (4.15)$$

where m_n is the spectral moment of order n , f_p is the peak frequency, ρ the water density, g the gravity acceleration, c_g the group velocity and E the energy density.

4.2. Nearshore characterization

Four Italian areas (Figure 4.1) were selected as cases of study for the nearshore characterization: the Tuscany, divided for computational reasons in the Northern Tuscany between La Spezia and Livorno and the Central Tuscany between Livorno and Piombino, the Western Liguria between Ventimiglia and Imperia, the North Western Sardinia between Stintino and Alghero.



Figure 4.1. Sites selected location

4.2.1 **METHODOLOGY**

The wave propagation was computed from the offshore sites characterized by a maximum water depth of approximately 100 m toward the coastal sites.

Computational domain

The bathymetries were obtained by the digitalization of the nautical charts (1:100.000), for Tuscany area “Da Portofino a San Rossore” and “Da San Rossore al Canale di Piombino”, for Liguria area “Da Cannes a Imperia”, for Sardinia area “Da Capo Caccia a Castelsardo e Isola Asinara” and “Da Capo S.Marco a Capo Caccia”.

The model domains were about:

- 1) 30 km x 85 km for the Northern Tuscany,
- 2) 25 km x 80 km for the Central Tuscany,
- 3) 7 km x 75 km for the Western Liguria,
- 4) 30 km x 70 km for the North-Western Sardinia.

The model meshes were flexible and different resolutions were adopted within each numerical spatial domains. The meshes in the Tuscany areas were characterized by a triangular side of about 2000 m in water depths over 50 m, a side of about 1000 m in water depths between 50 m and 30 m, a side of about 500 m until the water depth of 20 m and of about 300 m until the coast sites. The meshes in the Liguria and Sardinia areas, were characterized by a triangular side of about 1000 m in water depths over 50 m, a side of about 500 m in water depths between 50 m and 30 m, a side of about 300 m until the water depth of 20 m and a side of about 200 m until the coast line. The meshes with higher resolution in Liguria and Sardinia areas were due to the fact that the slope of the bottom near the coast is higher, and this requires a larger number of nodes to properly simulate the phenomena of transformation of the wave motion. The total number of nodes was equal to 13188 for the Northern Tuscany (Figure 4.2), 8246 for the Central Tuscany (Figure 4.3), 4521 for the Liguria (Figure 4.4) and 5461 for the Sardinia (Figure 4.5).

As offshore boundary conditions the values of significant wave height, peak period, average direction and spreading factor of all the 8028 events in the time period between July 2009 and March 2012 were used. These values were extracted by the PREVIMER model on a series of equidistant points, located along the boundary on a water depth of 100 m (Table 4.1), among which the values vary linearly. In the boundaries perpendicular

to the coast, it was imposed the lateral boundary condition, that consists a one-dimensional calculation of the basic equations solved along the boundary line. The information of the incoming waves in the start point and in the end point of the line are obtained from the connected boundary lines.

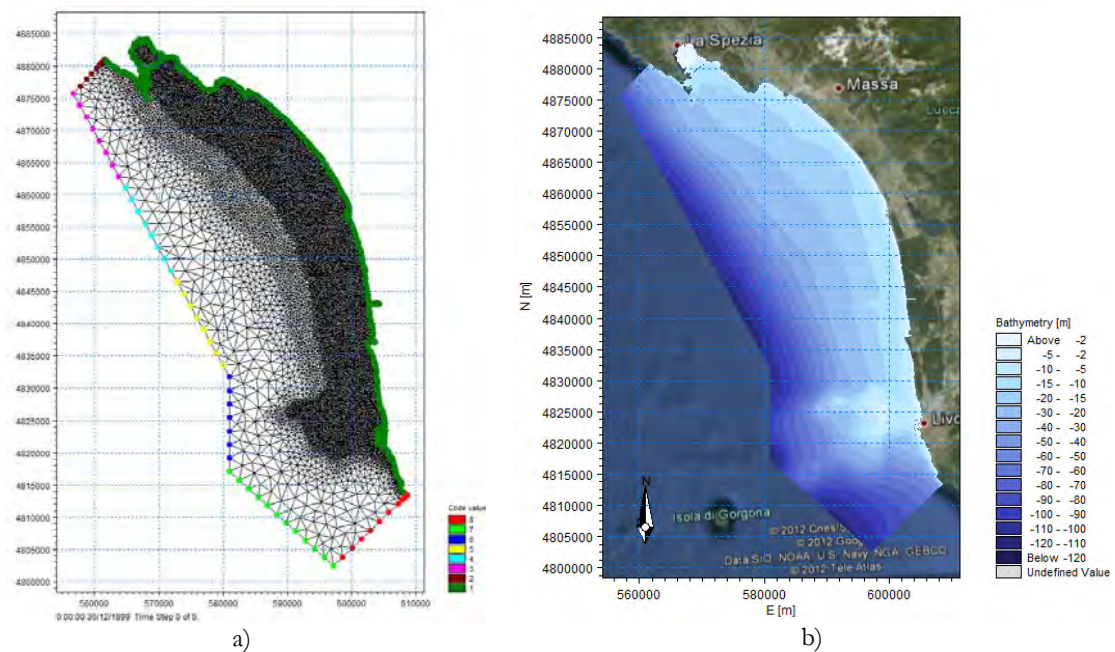


Figure 4.2. Northern Tuscany: a) mesh and boundaries, b) bathymetry

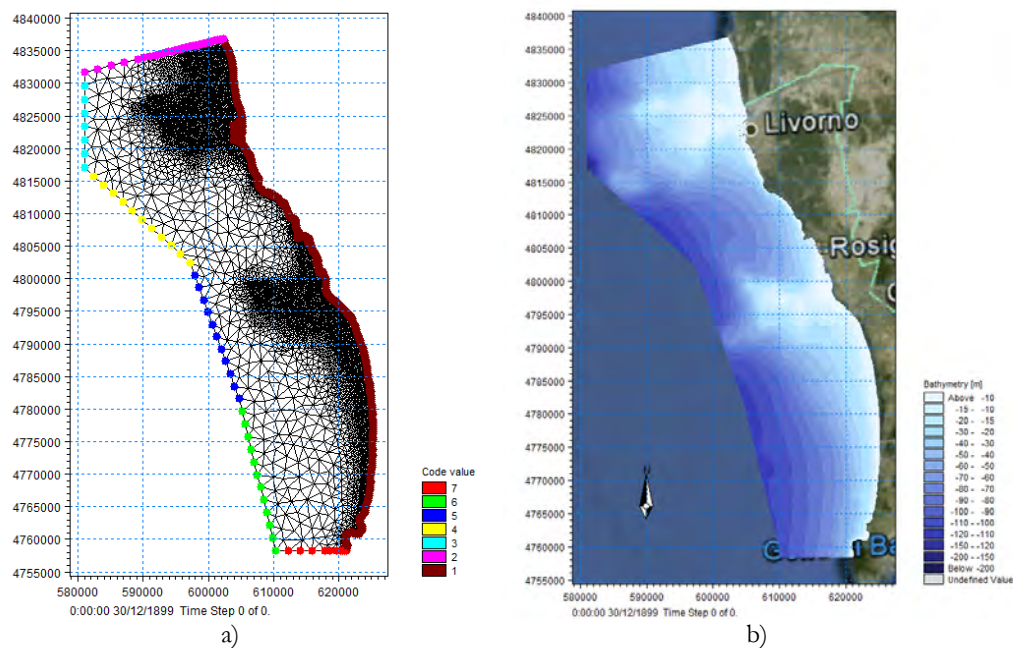


Figure 4.3. Central Tuscany: a) mesh and boundaries, b) bathymetry

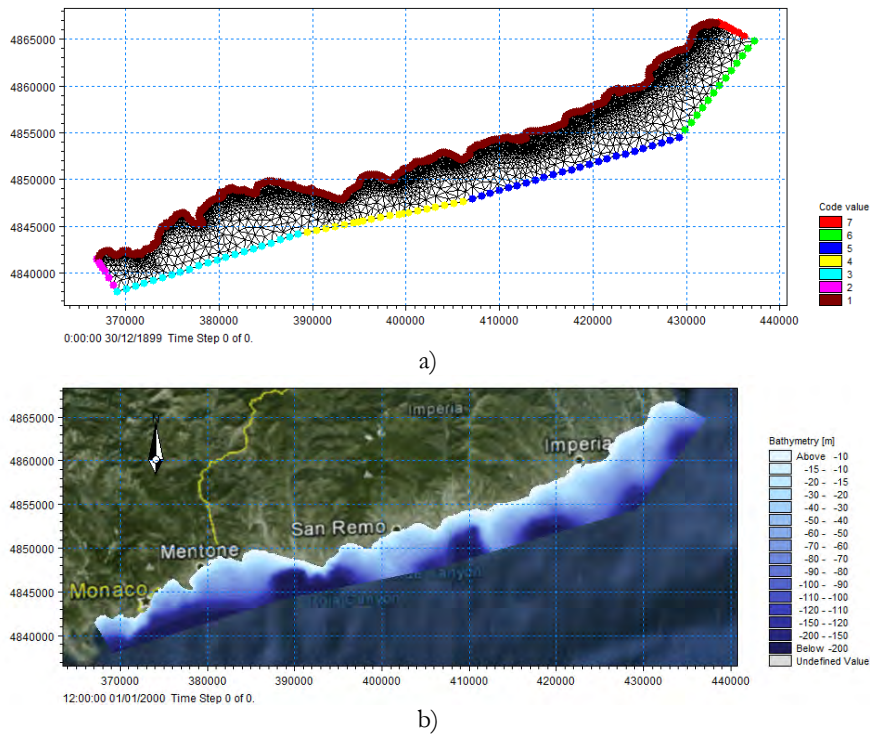


Figure 4.4. Liguria: a) mesh and boundaries, b) bathymetry

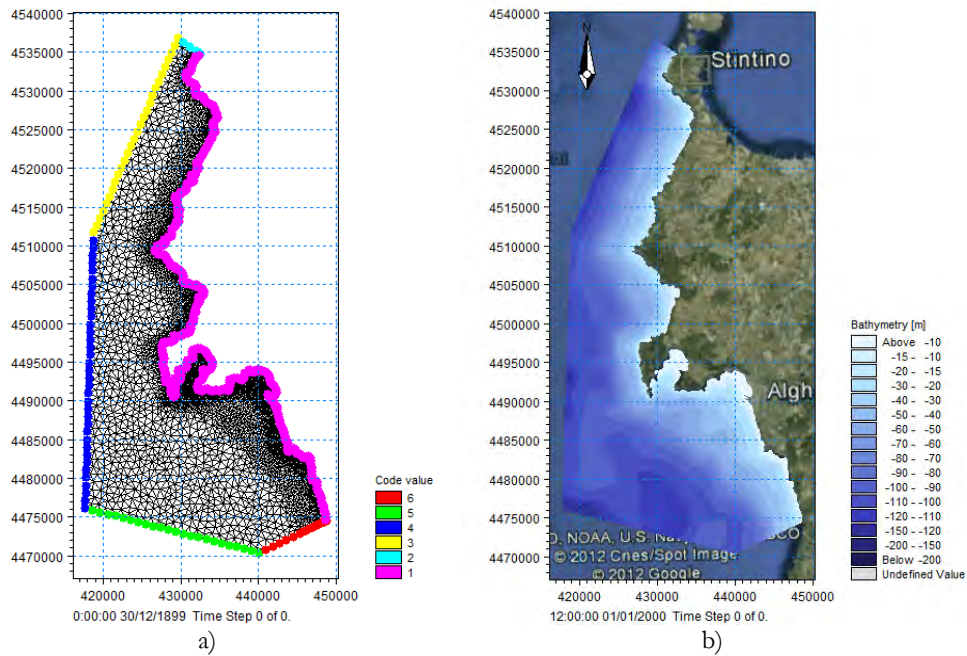


Figure 4.5. Sardinia: a) mesh and boundaries, b) bathymetry

Table 4.1. Coordinates and yearly mean wave power values at the offshore boundary points extracted by the PREVIMER dataset

	<i>Latitude</i> (WGS84-UTM32)	<i>Longitude</i> (WGS84-UTM32)	<i>Mean Wave Power</i> 2010 (kW/m)	<i>Mean Wave Power</i> 2011 (kW/m)
<i>Northern Tuscany</i>				
1	4875712	556673	3.25	2.58
2	4861033	564800	3.38	2.64
3	4846398	572906	3.79	2.94
4	4831764	581011	3.70	2.90
5	4817130	581011	4.03	3.22
6	4802473	597199	3.52	2.81
<i>Central Tuscany</i>				
1	4831764	581011	3.70	2.90
2	4817130	581011	4.03	3.22
3	4802473	597199	3.52	2.81
4	4781616	604685	2.00	1.77
5	4758265	610350	0.25	0.04
<i>Liguria</i>				
1	4837980	369096	1.45	1.31
2	4844161	388493	1.68	1.47
3	4847686	406126	1.74	1.55
4	4854467	429257	1.88	1.68
5	4864782	437241	1.50	1.37
<i>Sardinia</i>				
1	4536798	429614	11.70	8.37
2	4511710	418763	11.35	8.23
3	4476116	417706	12.61	8.97
4	4470415	440105	10.04	6.28

Spectral Wave module specifications

The 8028 events of the PREVIMER data-set were propagated like a time series with the fully spectral and quasi-stationary formulation.

The spectral discretization was performed on frequency and direction. The frequency discretization was of logarithmic type with a number of frequencies equal to 25, a minimum frequency value equal to 0.04 and a frequency factor equal to 1.12. The direction discretization was performed on a 360 degree rose and the number of directions was chosen equal to 16. In the wave breaking model the gamma value was chosen constant and equal to 0.8, while the alpha value was 1. The Nikuradse formulation for the bottom friction was employed with a constant value equal to 4 cm in the whole computational

domain as well as a constant values for the two dissipation coefficients, C_{dis} , equal to 4.5, that is a proportional factor on the white capping dissipation source function and thus control the overall dissipation rate, and $DELTA_{dis}$, equal to 0.5, that is controlling the weight of dissipation in the energy/action spectrum. The spectra from empirical formulas were used as initial condition where the formulas type was the JONSWAP fetch growth expression with the classical parameters ($\sigma_a = 0.07, \sigma_b = 0.09, \gamma = 3.3$).

Maps of the variation of the significant wave height, peak period, mean spectral period, mean direction and wave power were obtained in output for each event of the time series.

4.2.2 RESULTS

The values of the variables H_{m0} , T_p , $T_{m-1,0}$, Dir , P were computed in each point of the analysed domains. In the Figure 4.6, Figure 4.7 and Figure 4.8 examples of the power distribution maps are shown for each site for the event of the 5 January 2012, at 18.00, characterized by the sea state values (on a point of the offshore boundary) in Table 4.2.

Table 4.2. Sea state values

	H_{m0} (m)	T_p (s)	Dir ($^\circ$)
Northern Tuscany (point 5)	4.20	10.5	245
Central Tuscany (point 2)	4.20	10.5	245
Western Liguria (point 4)	2.45	9.9	220
North-Western Sardinia (point 1)	6.05	11.1	296

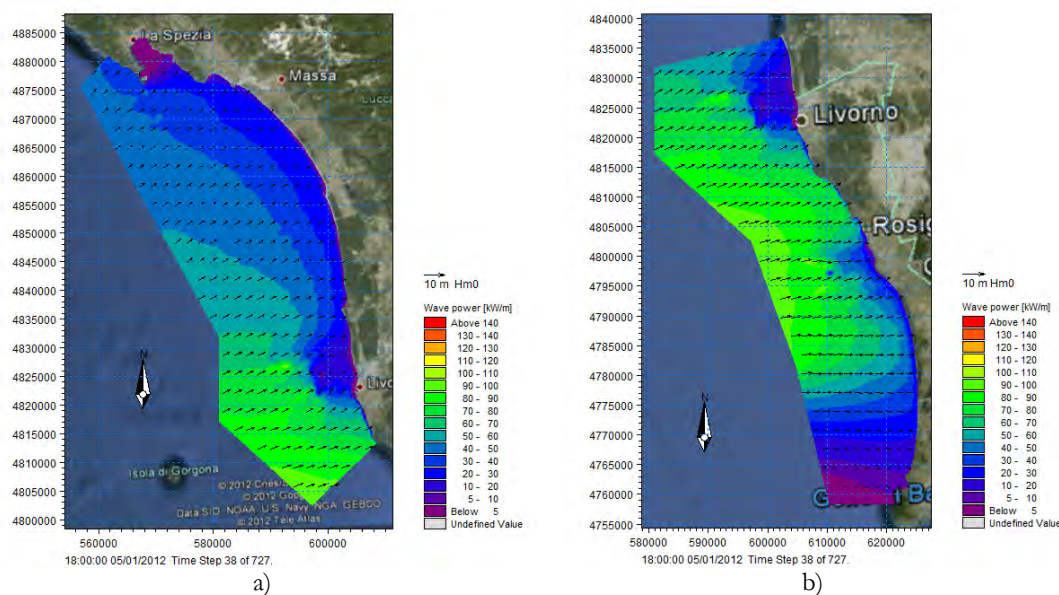


Figure 4.6. Power map of Tuscany for the event 5th of January 2012 hour 18:00: a) Northern, b) Central

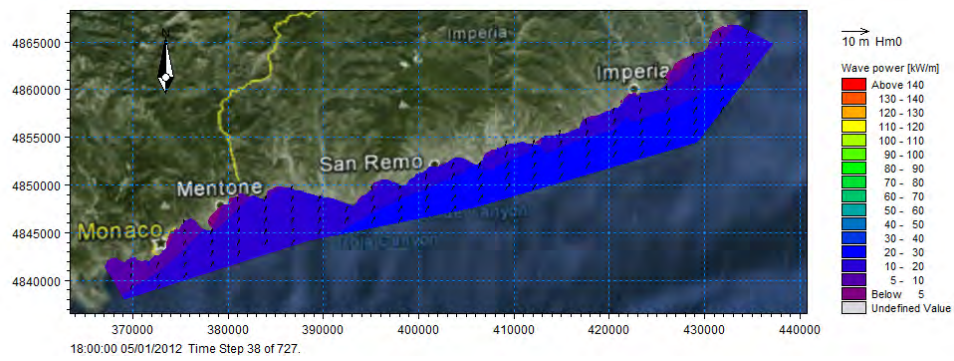


Figure 4.7. Power map of Liguria for the event 5th of January 2012 hour 18.00

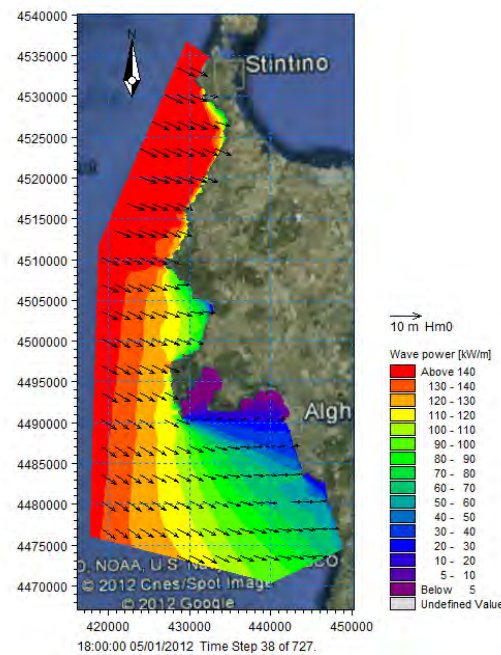


Figure 4.8. Power map of Sardinia for the event 5th of January 2012 hour 18.00

In the Figure 4.6 it is important to note the wave height decay (the arrows in the Figure) from offshore to the coast line, mainly in the area south of Rosignano, and the focusing mechanism on the Meloria shoals (Secche della Meloria) in front of Livorno, due to the bathymetry conformation. The detailed power map centred on the Meloria shoals (Figure 4.9a) highlights that there is a simultaneous increase in both the significant wave height (Figure 4.9b) and the energetic period (Figure 4.9c). Of course, the increment of wave height affects strongly, i.e. more than the increment of the energetic period, the power value, considering that this parameter is proportional to the square of it. In the Meloria shoals area close to the harbour of Livorno there is a wave height decay due to the wave breaking phenomenon and a consequent wave power decay, even if the energetic period values are high and almost reach the peak period (Figure 4.9d). This may indicate that the

energy density moves toward the values associated to the peak frequencies of the energy spectrum.

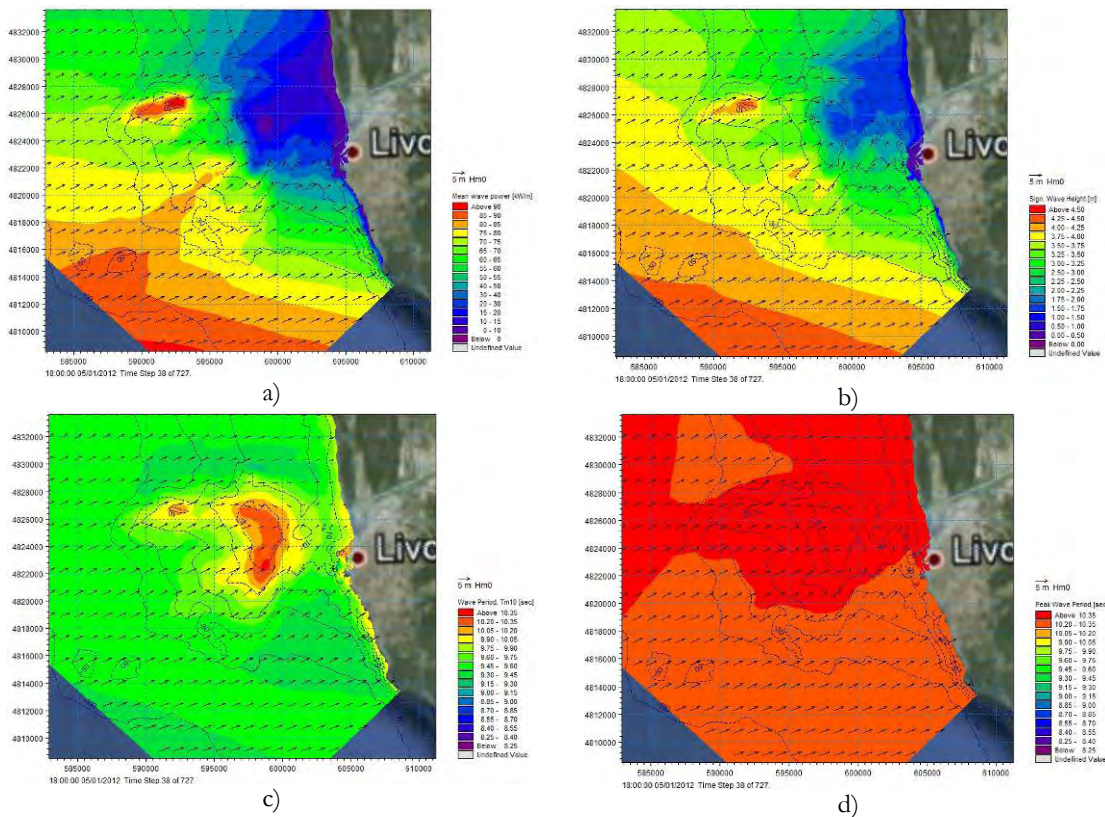


Figure 4.9. Meloria shoals details of the event of 5 January 2012 at 18:00: a) power map, b) significant wave height map, c) energetic period map, d) peak period map

In Liguria (Figure 4.7) the wave power decay mainly occurs in the Ventimiglia area, while in Sardinia (Figure 4.8) it is possible to see a maintenance of high values in the Stintino area and an high decay of the wave heights (arrows in Figure) and wave power values in the Alghero area, due to the refraction and diffraction phenomena.

The monthly mean wave power maps were computed for each month from July 2009 to March 2012 (see Appendix C) while the yearly mean wave power maps were produced only for the years 2010 (Figure 4.10, Figure 4.12, Figure 4.15, Figure 4.18) and 2011 (Figure 4.11, Figure 4.13, Figure 4.16, Figure 4.19). Analysing the yearly mean wave power maps it is possible to see that on average the year 2010 was more energetic than the year 2011.

In the Northern Tuscany (Figure 4.10a and Figure 4.11a) the decay of the wave power is uniform with the water depth decrease, except for the Meloria shoals area, where the highest values, equal to 4.78kW/m in the 2010 and to 3.55 kW/m in the 2011, are located on a water depth of 12.5 m (Figure 4.14). The normalized maps (Figure 4.10 b and Figure 4.11 b) are very useful to understand the importance of the exact location of an

hypothetical wave energy farm. In fact the area above the threshold of 4.5 kW/m, for the 2010, is about 17.60 ha only, and the area above 3.3 kW/m, for the 2011, is about 38.22 ha (Table 4.3). Moving away from the highest wave power points, the values decay abruptly: for example, in only a kilometre away, the mean value of the available power reduces by 30%.

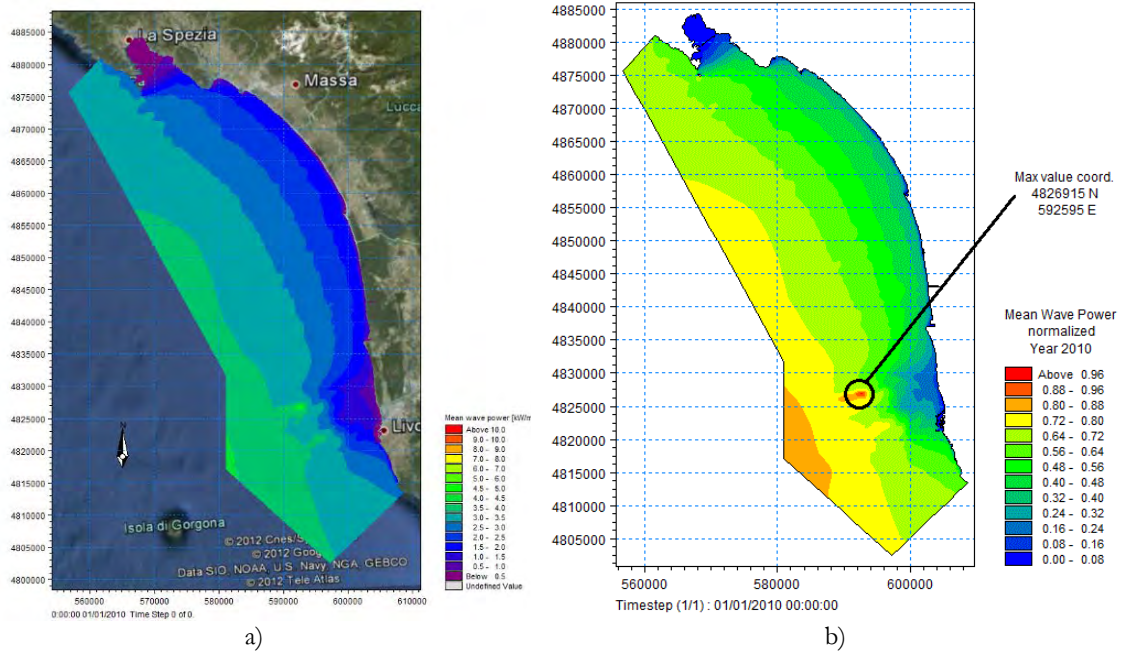


Figure 4.10. Northern Tuscany 2010: a) yearly mean wave power, b) yearly mean wave power normalized

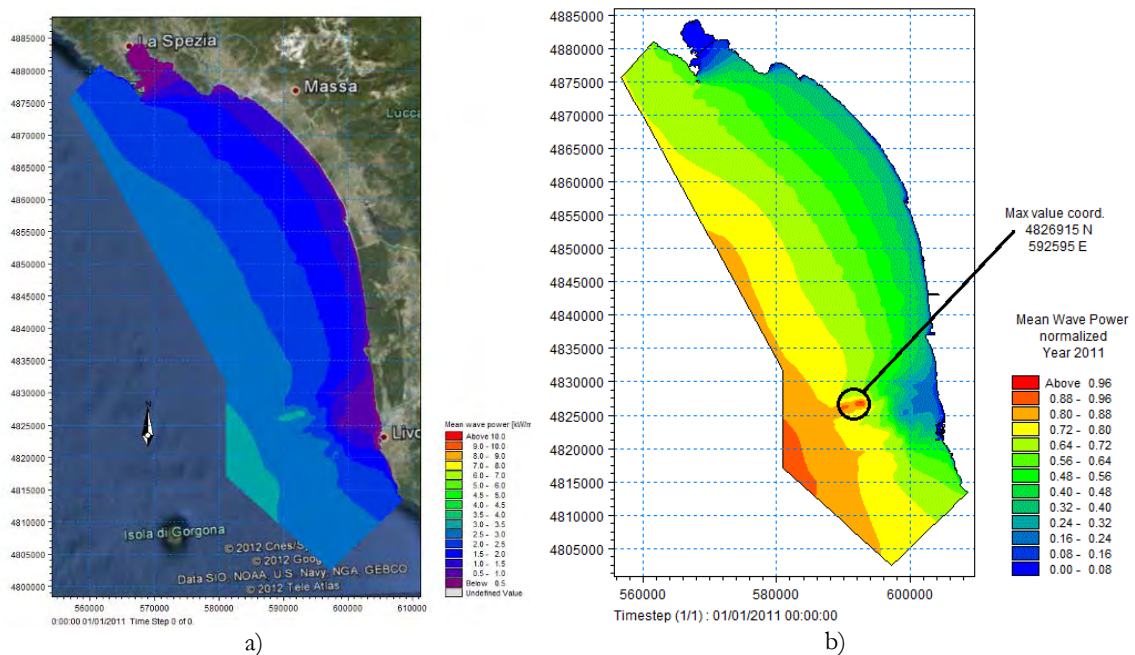


Figure 4.11. Northern Tuscany 2011: a) yearly mean wave power, b) yearly mean wave power normalized by using the maximum wave power within the model spatial domain

In the Central Tuscany (Figure 4.12 and Figure 4.13) the decay of wave power is particularly evident on the area south of Rosignano, probably due to the presence of Corsica Island. The highest values are located on the same points of the Northern Tuscany and then the considerations are similar.

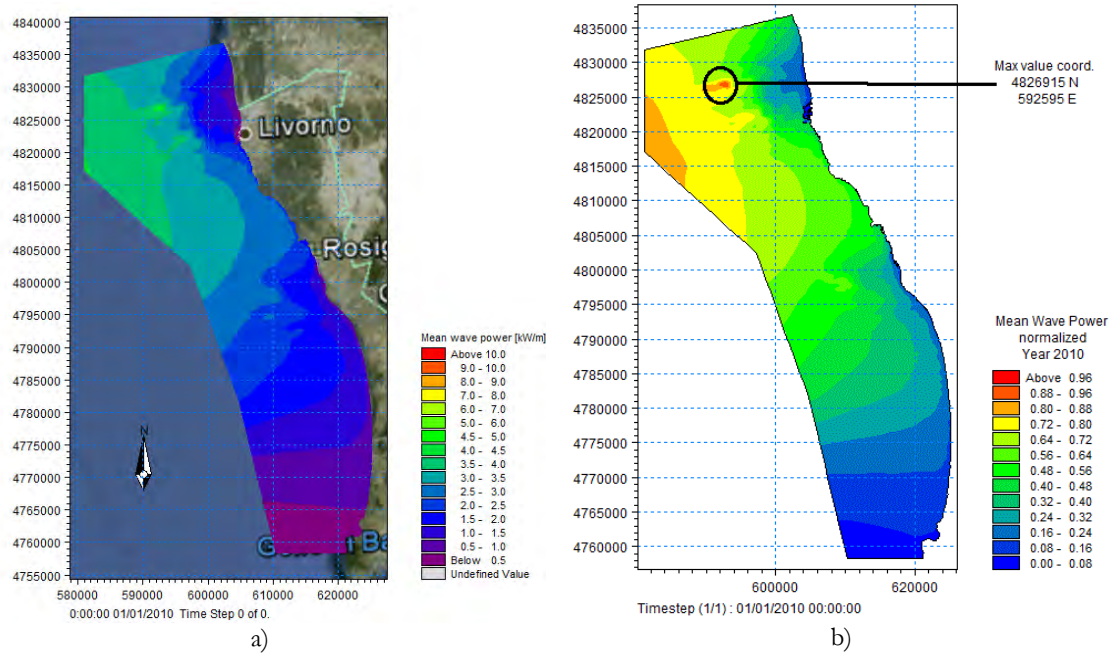


Figure 4.12. Central Tuscany 2010: a) yearly mean wave power, b) yearly mean wave power normalized by using the maximum wave power within the model spatial domain

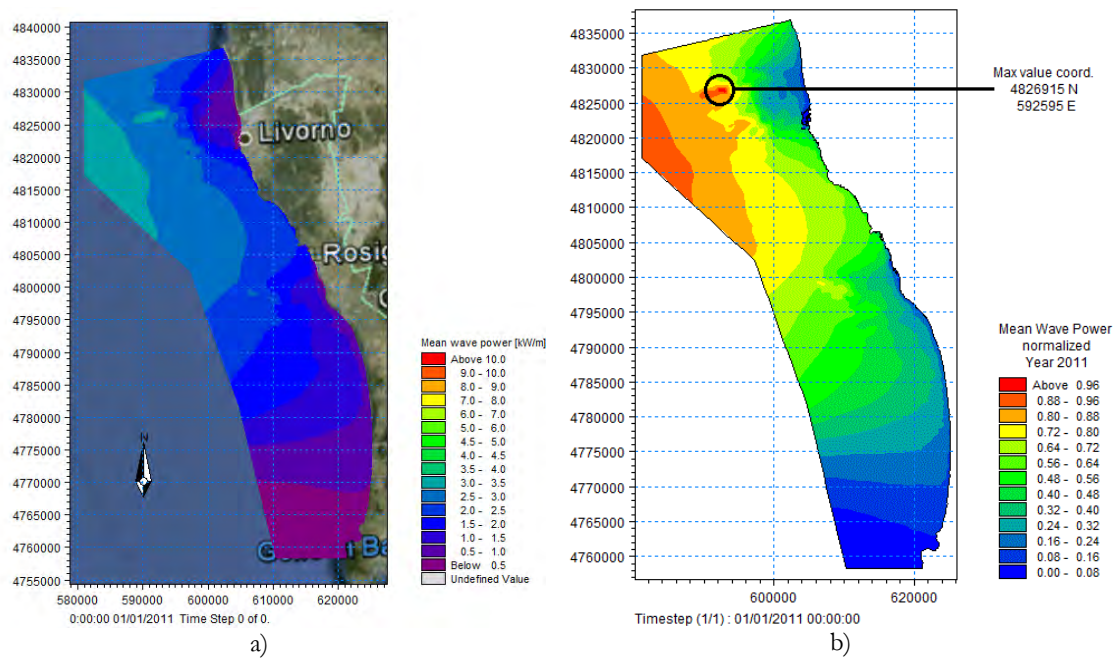


Figure 4.13. Central Tuscany 2011: a) yearly mean wave power, b) yearly mean wave power normalized by using the maximum wave power within the model spatial domain

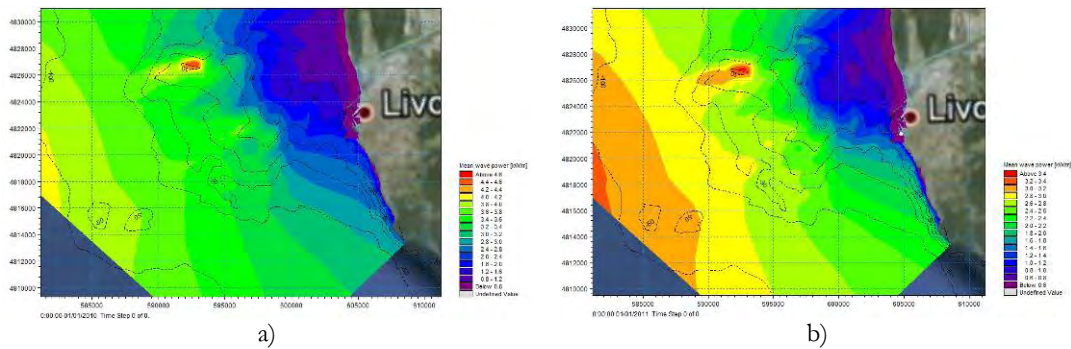


Figure 4.14. Northern Tuscany detailed yearly mean wave power map: a) 2010, b) 2011

In Liguria (Figure 4.15 and Figure 4.16) the wave power decrease is uniform from offshore to coastline. The focusing mechanisms are less emphasized with respect to the Meloria shoals area, but anyway it generates, near some headlands, local maximum values of the same order of the highest values on the offshore boundary in front of Imperia (Table 4.1). The maximum values are due to a submerged cusp in the bathymetry (Figure 4.17), and are equal to 1.84 kW/m for the 2010 and to 1.59 kW/m for the 2011 (Table 4.3) and are located in front of an headland between Sanremo and Imperia, on a water depth around 28 m. In the wave power normalized maps the area above the threshold of 1.80 kW/m, for the 2010, covers about 13.60 ha and the area above the threshold of 1.55 kW/m, for the 2011, covers about 25.59 ha.

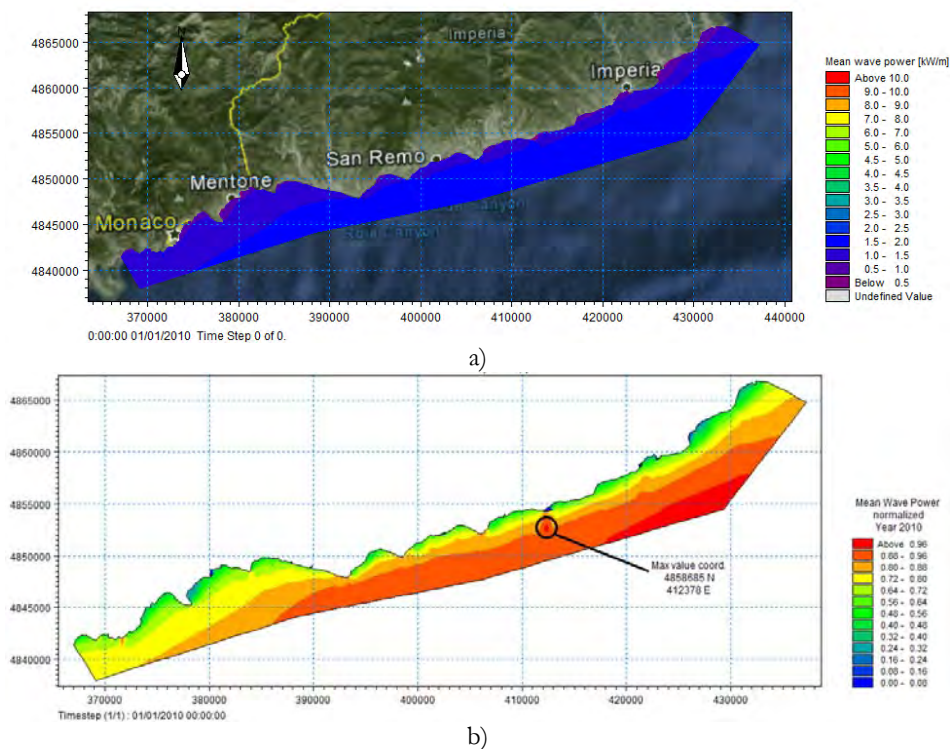


Figure 4.15. Liguria 2010: a) yearly mean wave power, b) yearly mean wave power normalized

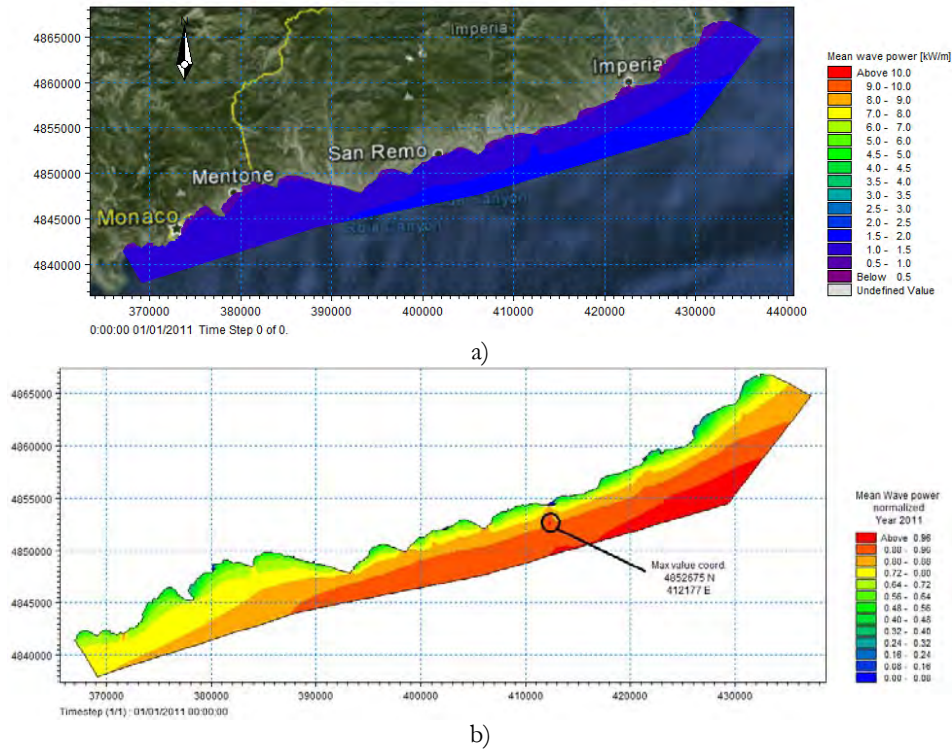


Figure 4.16. Liguria 2011: a) yearly mean wave power, b) yearly mean wave power normalized by using the maximum wave power within the model spatial domain

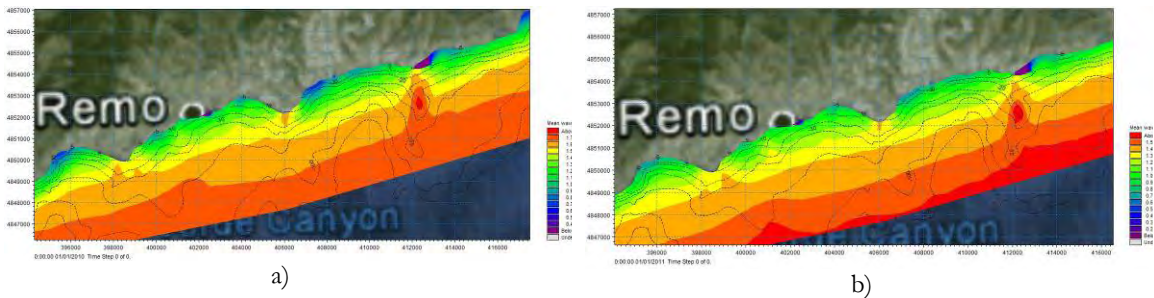


Figure 4.17. Liguria detailed yearly mean wave power map: a) 2010, b) 2011

In Sardinia (Figure 4.18 a and Figure 4.19 a), accordingly to the results of the PREVIMER model focused on deep waters, the wave power values are much higher than the other analyzed sites, especially in the north, where the seabed is characterized by high slopes that allow the obtainment of these high values also close to the coast. Indeed in the upper North-Western coast of the spatial domain (West of Stintino), the 100 m water depth is far about 3600 m by the shoreline, according to the nautical chart values. The focusing mechanisms occur near the headlands on the area south of the Western coast of Stintino, due to refraction effect during the wave propagation (Figure 4.20). The maximum values are equal to 12.16 kW/m for the 2010 and to 8.45 kW/m for the 2011 on a water depth of about 20 m. In the wave power normalized maps (Figure 4.18 b and Figure 4.19

b) the area above the threshold of 11.80 kW/m, for the 2010, covers about 9.30 ha while the area above the value of 8.20 kW/m, for the 2011, covers about 7.81 ha (Table 4.3).

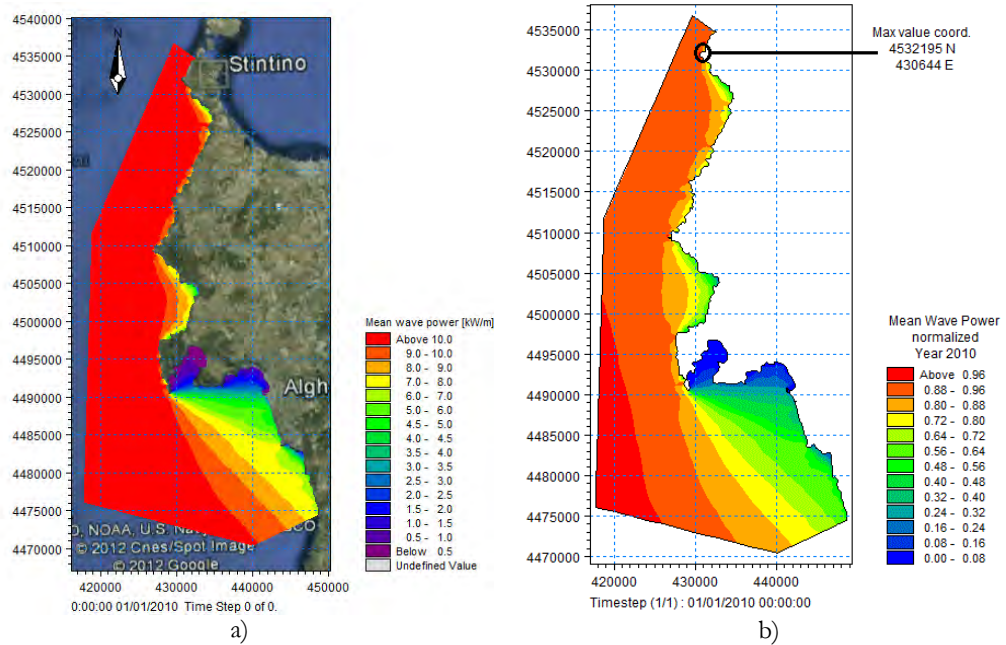


Figure 4.18. Sardinia 2010: a) yearly mean wave power, b) yearly mean wave power normalized

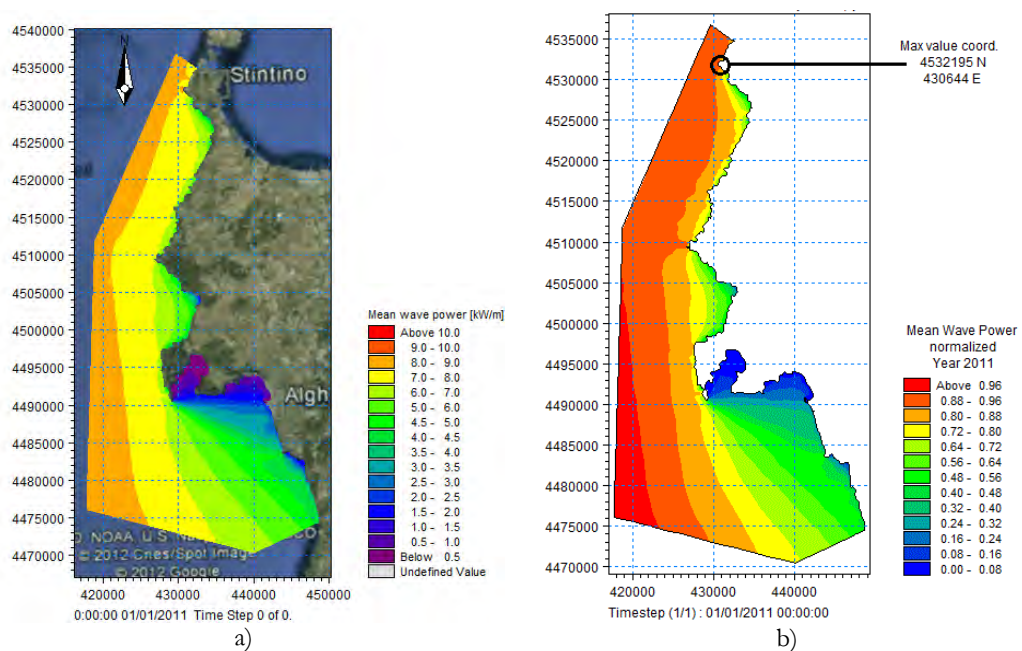


Figure 4.19. Sardinia 2011: a) yearly mean wave power, b) yearly mean wave power normalized

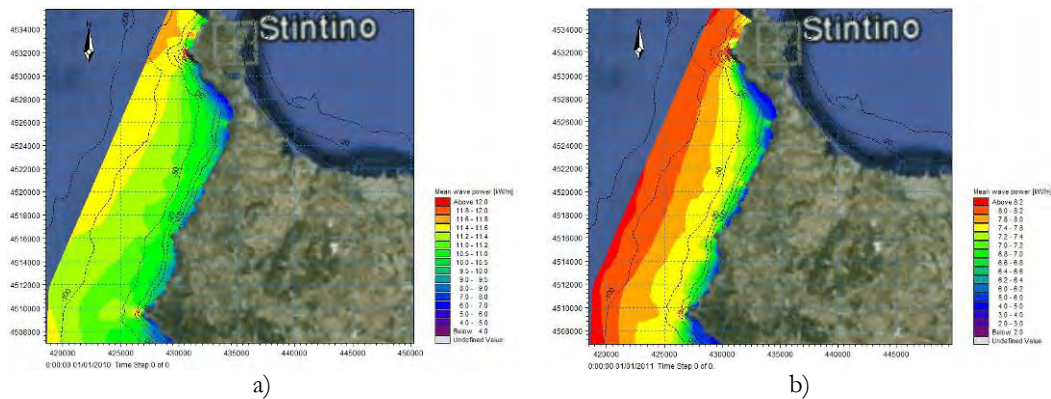


Figure 4.20. Sardinia detailed yearly mean wave power map: a) 2010, b) 2011

Table 4.3. Value, location, water depth of the maximum yearly mean wave power nearshore and area above the threshold selected. All the wave power values of the years 2010 and 2011 were used to compute the “yearly mean wave power”

	<i>Latitude</i> (UTM32)	<i>Longitude</i> (UTM32)	<i>Max Mean Power</i> <i>nearshore (kW/m)</i>	<i>Water</i> <i>depth(m)</i>	<i>Threshold</i> (kW/m)	<i>Area ≥</i> <i>Threshold (ha)</i>
<i>Northern and Central Tuscany</i>						
2010	4826915	592595	4.78	-12.5	4.50	17.60
2011	4826915	592595	3.55	-12.5	3.30	38.22
<i>Liguria</i>						
2010	4852685	412378	1.84	-23.0	1.80	13.60
2011	4852675	412177	1.59	-21.0	1.55	25.59
<i>Sardinia</i>						
2010	4532195	430644	12.16	-20.0	11.80	9.30
2011	4532195	430644	8.45	-20.0	8.20	7.81

To better describe the wave energy potential within the studied spatial domain, 36 points (10 for Northern Tuscany and Liguria, 8 for Central Tuscany and Sardinia) were selected on 15 m and 50 m water depths.

For each of these points the wave roses and the time series of the computed wave power values were extracted.

The wave roses show the directional distribution of the incident waves (Figure 4.22, Figure 4.25, Figure 4.28 and Figure 4.32).

The time series maps were obtained for each month of the PREVIMER dataset (July 2009 – March 2012) in order to show the trend of the wave power values (for all maps see Appendix D). The Figure 4.21a shows the wave power values trend on the December 2010 in the 10 points extracted in the Northern Tuscany on 15m water depth and the Figure 4.21b shows the trend of the other 10 points extracted in the Northern Tuscany on 50 m water depth. This grouping is useful in order to observe the wave energy losses next to the

peaks in the wave propagation from offshore to coast. In fact, for example, on 18th December at 0.00 there is a decrease above 10 kW/m between the point 9 (15 m water depth) and the point 19 (50 m water depth).

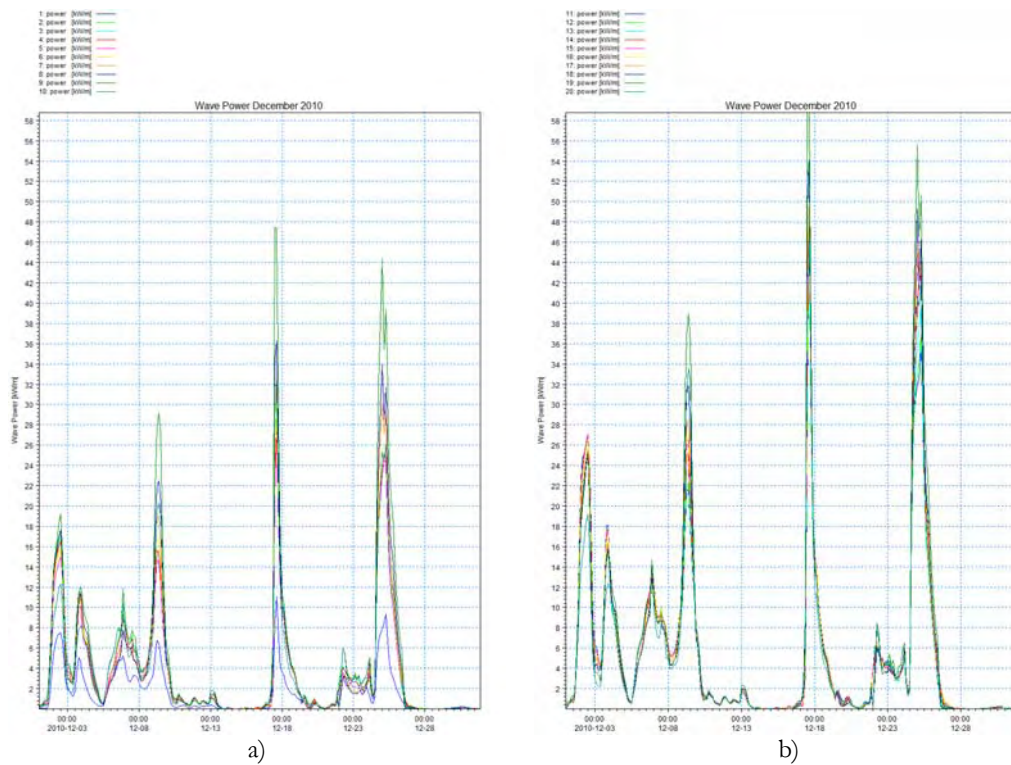


Figure 4.21. Wave power values trend in December 2010 in the 20 points extracted in the Northern Tuscany : a) on 15m water depth, b) on 50m water depth

The two points of each analysed site, one on 15 m water depth and the other on 50 m water depth, with the highest wave power values, were selected and highlighted in the Table 4.4 for the Northern Tuscany, Table 4.7 for the Central Tuscany, Table 4.10 for the Liguria and Table 4.14 for the Sardinia. For each one of them, using all the time series values, a scatter diagram was produced (Table 4.5, Table 4.6, Table 4.8, Table 4.9, Table 4.11, Table 4.12, Table 4.13, Table 4.15 and Table 4.16), showing the occurrence frequencies (in %) of the 168 sea states combinations. The latter were obtained considering the 14 significant wave heights classes (average values between 0.25 m and 6.75 m, interval of 0.5 m) and the 12 energetic periods classes (average values between 0.25 m and 6.75 m, interval of 0.5 m). The scatter diagram is a joint-distribution function, created by counting the number of individual sea-states falling within the selected classes and dividing by the total number. The graphs (Figure 4.23, Figure 4.24, Figure 4.26, Figure 4.27, Figure 4.29, Figure 4.30, Figure 4.31, Figure 4.33 and Figure 4.34) show the mean annual energy per meter of wave front (in kWh/m), to varying the sea states combinations of the scatter diagrams, referred to wave power isolines (in kW/m).

Table 4.4. Northern Tuscany – location and yearly mean wave power values of the extracted points

	<i>Latitude (UTM32)</i>	<i>Longitude (UTM32)</i>	<i>Mean Wave Power 2010 (kW/m)</i>	<i>Mean Wave Power 2011 (kW/m)</i>	<i>Water depth (m)</i>
<i>Northern Tuscany</i>					
1	4877617	570360	0.97	0.72	-15
2	4875864	576280	2.23	1.55	-15
3	4873346	580984	2.23	1.61	-15
4	4869348	584866	2.21	1.61	-15
5	4866065	590940	2.06	1.48	-15
6	4855970	595210	2.16	1.60	-15
7	4847299	597533	2.28	1.71	-15
8	4836886	598325	2.44	1.86	-15
<u>9</u>	<u>4823741</u>	<u>595661</u>	<u>2.89</u>	<u>2.23</u>	<u>-15</u>
10	4820939	603681	2.10	1.60	-15
11	4871836	563641	3.16	2.51	-50
12	4868070	566903	3.16	2.50	-50
13	4863990	570922	3.23	2.54	-50
14	4859240	574575	3.33	2.61	-50
15	4854171	578192	3.40	2.66	-50
16	4850244	580744	3.38	2.65	-50
17	4844741	584137	3.31	2.60	-50
18	4835729	588582	3.36	2.65	-50
<u>19</u>	<u>4821420</u>	<u>589516</u>	<u>3.63</u>	<u>2.93</u>	<u>-50</u>
20	4816251	600089	3.07	2.43	-50

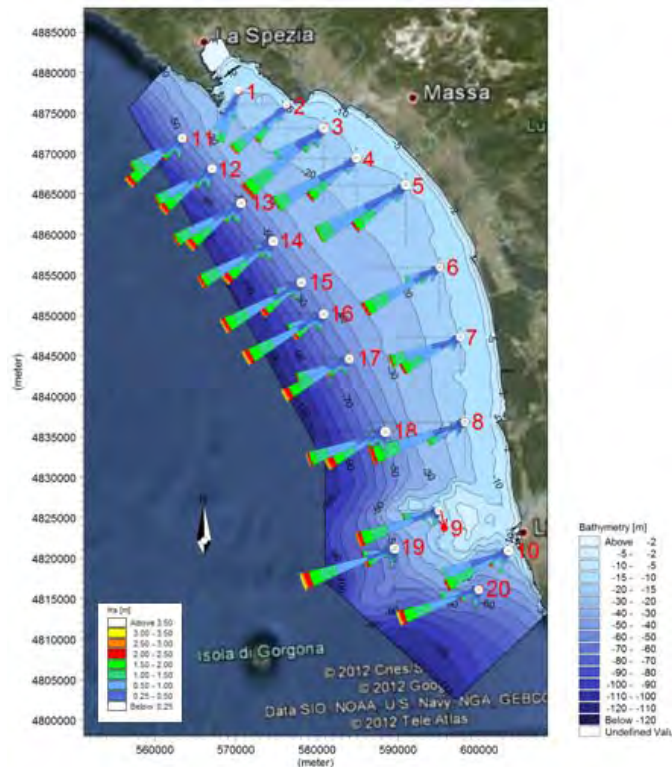


Figure 4.22. Northern Tuscany - location and wave roses of the extracted points

In the Northern Tuscany the points with the highest values of wave power are the point 9, that reaches a value of 2.9 kW/m in the 2010 and 2.2 kW/m in the 2011 on 15 m water depth, and the point 19, that reaches values of 3.6 kW/m in the 2010 and 2.9 kW/m in the 2011 on 50 m water depth (Table 4.4). Their locations are on the Meloria shoals (Figure 4.22), where there is an important focusing mechanism which was also observed in the previous analysis. The wave roses of these two points show that the main wave direction is SW.

Table 4.5. Northern Tuscany - scatter diagram (%) of H_{m0} and T_e at the point 9

		H_{m0} [m]													
		< 0.5	0.5	1.0	1.5	2.0	2.5	3.0	3.5	4.0	4.5	5.0	5.5	6.0	>= 6.5
Te [s]	< 1.5	0.27	0	0	0	0	0	0	0	0	0	0	0	0	0
	1.5	11.34	0	0	0	0	0	0	0	0	0	0	0	0	0
	3	27.19	3.46	0	0	0	0	0	0	0	0	0	0	0	0
	4.5	14.59	9.37	2.53	0.04	0	0	0	0	0	0	0	0	0	0
	6	4.62	5.88	3.66	2.82	0.30	0	0	0	0	0	0	0	0	0
	7.5	1.67	3.60	3.29	1.31	0.95	0.49	0.14	0	0	0	0	0	0	0
	9	0.21	0.31	0.66	0.59	0.21	0.16	0.12	0.10	0.02	0.01	0	0	0	0
	10.5	0	0	0.01	0	0.04	0.02	0.01	0	0.01	0	0	0	0	0
	12	0	0	0	0	0	0	0	0	0	0	0	0	0	0
	13.5	0	0	0	0	0	0	0	0	0	0	0	0	0	0
	15	0	0	0	0	0	0	0	0	0	0	0	0	0	0
	>= 16.5	0	0	0	0	0	0	0	0	0	0	0	0	0	0

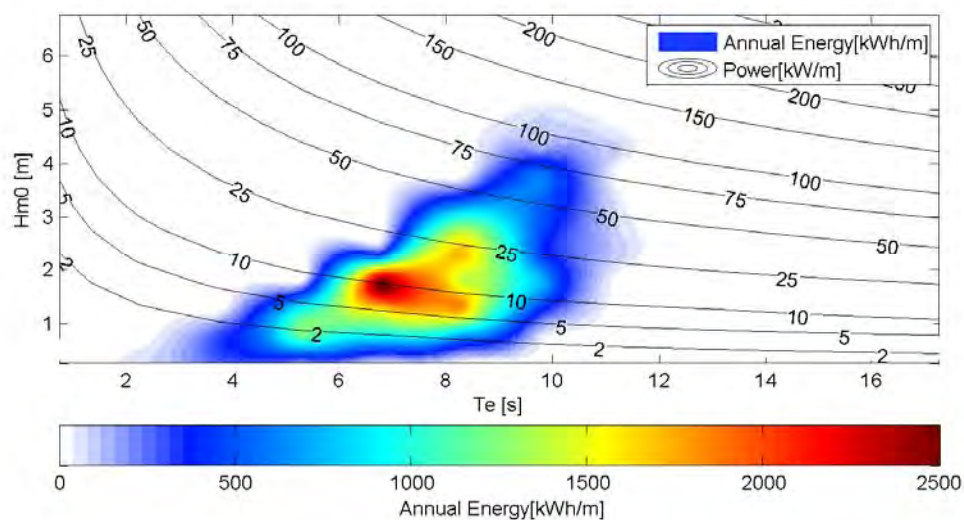


Figure 4.23. Northern Tuscany – Annual energy at the point 9

At the point 9 the combination $H_{m0} \approx 2\text{m}$ and $T_e \approx 7\text{s}$, that occurs for less than the 2.8% of the year (Table 4.5), produces the highest annual energy value on the order of 2.5

MWh/m (Figure 4.23). The annual energy values above 1.25 MWh/m are obtained with H_{m0} between 1 m and 2.5 m and T_e between 6 s and 9 s, that occur for the 12.8%. The 50% of the sea states have a H_{m0} under 0.5 m and T_e between 1.5 s and 6s.

At the point 19 the combination characterized by annual energy values higher than 2.5 MWh/m (Figure 4.24) are obtained for $2\text{ m} \leq H_{m0} \leq 2.5\text{ m}$ and $6.5\text{ s} \leq T_e \leq 7.5\text{ s}$, combination that occurs in the 1.7 % of the time (Table 4.6). The combinations $1\text{ m} \leq H_{m0} \leq 2.5\text{ m}$ for $6.5\text{ s} \leq T_e \leq 7.5\text{ s}$ and $1\text{ m} \leq H_{m0} \leq 3.5\text{ m}$ for $7.5\text{ s} \leq T_e \leq 9\text{ s}$ (15.6 % of the time) provide an annual energy above 1.25 MWh/m.

Table 4.6. Northern Tuscany - scatter diagram (%) of H_{m0} and T_e at the point 19

		H_{m0} [m]													
		< 0.5	0.5	1.0	1.5	2.0	2.5	3.0	3.5	4.0	4.5	5.0	5.5	6.0	>= 6.5
T_e [s]	< 1.5	1.38	0	0	0	0	0	0	0	0	0	0	0	0	0
	1.5	10.86	0	0	0	0	0	0	0	0	0	0	0	0	0
	3	25.44	4.10	0	0	0	0	0	0	0	0	0	0	0	0
	4.5	12.59	9.04	3.57	0.30	0	0	0	0	0	0	0	0	0	0
	6	4.33	5.82	3.23	2.91	1.71	0.25	0	0	0	0	0	0	0	0
	7.5	1.16	3.74	3.26	1.97	0.88	0.65	0.51	0.20	0.05	0	0	0	0	0
T_e [s]	9	0.14	0.11	0.46	0.47	0.31	0.17	0.11	0.07	0.09	0.02	0.05	0	0	0
	10.5	0	0	0.01	0	0	0.01	0	0	0	0	0	0	0	0
	12	0	0	0	0	0	0	0	0	0	0	0	0	0	0
	13.5	0	0	0	0	0	0	0	0	0	0	0	0	0	0
	15	0	0	0	0	0	0	0	0	0	0	0	0	0	0
	>= 16.5	0	0	0	0	0	0	0	0	0	0	0	0	0	0

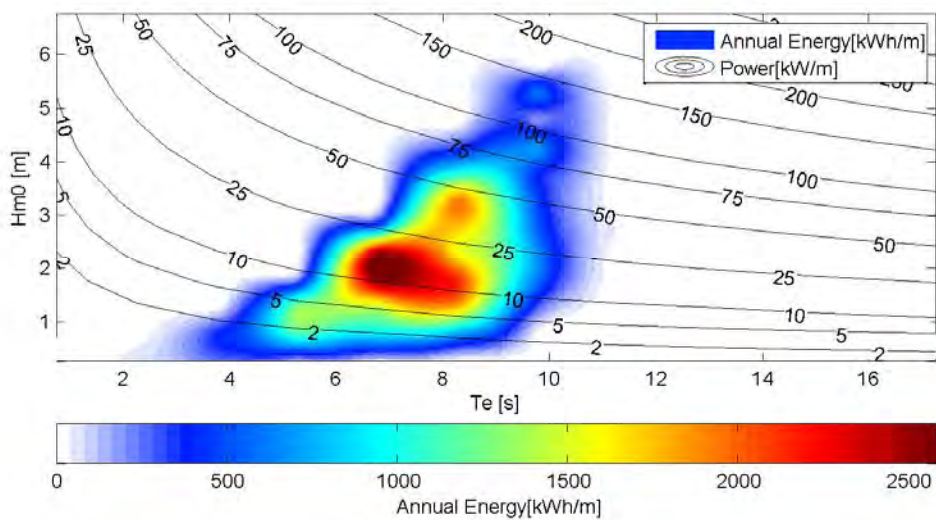


Figure 4.24. Northern Tuscany – Annual energy at the point 19

Table 4.7. Central Tuscany – location and yearly mean wave power values of the extracted points

	<i>Latitude</i> (UTM32)	<i>Longitude</i> (UTM32)	<i>Mean Wave Power</i> 2010 (kW/m)	<i>Mean Wave Power</i> 2011 (kW/m)	<i>Water depth</i> (m)
<i>Central Tuscany</i>					
1	4830284	599583	1.51	1.24	-15
2	4823741	595661	2.89	2.32	-15
3	4816119	606514	2.68	2.17	-15
4	4805420	614802	2.16	1.81	-15
5	4796680	608172	2.53	2.2	-15
6	4792310	619473	1.40	1.17	-15
7	4775282	623693	0.92	0.76	-15
8	4761569	622337	0.34	0.23	-15
9	4829229	589185	3.32	2.66	-50
10	4821420	589516	3.63	2.93	-50
11	4814913	604254	2.92	2.38	-50
12	4804365	610583	2.64	2.21	-50
13	4797100	605460	2.61	2.24	-50
14	4788844	613145	1.93	1.67	-50
15	4775131	619775	1.04	0.86	-50
16	4762172	620378	0.40	0.24	-50

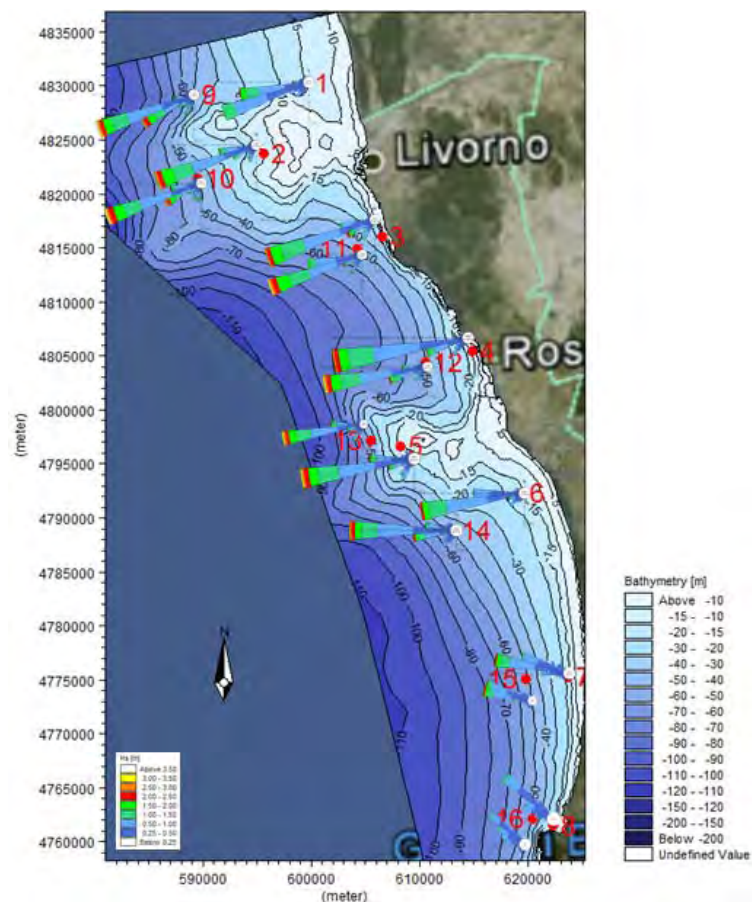


Figure 4.25. Central Tuscany - location and wave roses of the extracted points

In the Central Tuscany the highest values of wave power are located in the Meloria Shoals area on the points 2 and 10 (Table 4.7) are equal to those of the points 9 and 19 in the Table 4.4, previously described. After these, the values with highest wave power are located, for the 15 m water depth, in the point 3 in the Livorno south area, with a value of 2.7 kW/m in the 2010 and 2.2 kW/m in the 2011, and for 50 m water depth, on the point 10 on the north of Meloria shoals, with a value of 3.3 kW/m in the 2010 and 2.7 kW/m in the 2011. Moreover it is important to note that in the south area of the domain the wave power values hardly reaches 1 kW/m. In fact after the Vada Shoals (points 5 and 13) the wave power decreases rapidly. Due to these considerations the Southern Tuscany was not analysed.

Table 4.8. Central Tuscany - scatter diagram (%) of H_{m0} and T_e at the point 3

		H_{m0} [m]													
		< 0.5	0.5	1.0	1.5	2.0	2.5	3.0	3.5	4.0	4.5	5.0	5.5	6.0	>= 6.5
Te [s]	< 1.5	0.149	0	0	0	0	0	0	0	0	0	0	0	0	0
	1.5	12.13	0	0	0	0	0	0	0	0	0	0	0	0	0
	3	28.34	2.09	0	0	0	0	0	0	0	0	0	0	0	0
	4.5	15.35	9.08	1.51	0.01	0	0	0	0	0	0	0	0	0	0
	6	4.91	6.14	4.29	2.19	0.27	0	0	0	0	0	0	0	0	0
	7.5	1.84	3.40	3.34	1.37	0.90	0.51	0.14	0	0	0	0	0	0	0
	9	0.21	0.25	0.52	0.42	0.26	0.11	0.14	0.06	0.05	0	0	0	0	0
	10.5	0.01	0	0	0	0	0	0	0	0	0	0	0	0	0
	12	0	0	0	0	0	0	0	0	0	0	0	0	0	0
	13.5	0	0	0	0	0	0	0	0	0	0	0	0	0	0
	15	0	0	0	0	0	0	0	0	0	0	0	0	0	0
	>= 16.5	0	0	0	0	0	0	0	0	0	0	0	0	0	0

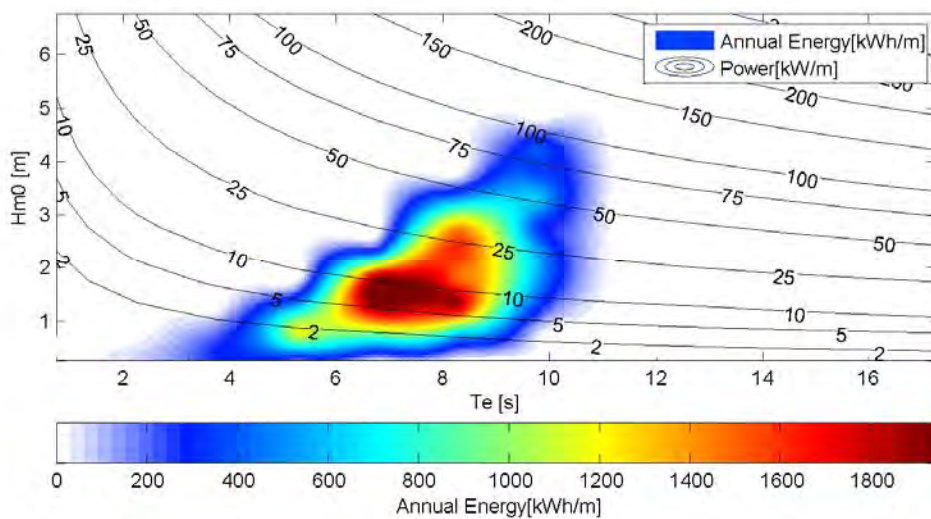


Figure 4.26. Central Tuscany – Annual energy at the point 3

At the point 3 the combination $1.5\text{ m} \leq H_{m0} \leq 2\text{ m}$ and $6.5\text{ s} \leq T_e \leq 8.5\text{ s}$, with an occurrence frequency of 3.6 %, produces the highest annual energy value on the order of 1.8 MWh/m (Figure 4.26). The mean annual energy values above 1 MWh/m are obtained with the combinations $H_{m0} \approx 0.5\text{ m}$ and $T_e \approx 5\text{ s}$, $1\text{ m} \leq H_{m0} \leq 2\text{ m}$ and $6\text{ s} \leq T_e \leq 7.5\text{ s}$, $1\text{ m} \leq H_{m0} \leq 3\text{ m}$ and $7.5\text{ s} \leq T_e \leq 9\text{ s}$ (28% of the time, see Table 4.8).

At the point 9 the area characterized by annual energy values higher than 2.5 MWh/m (Figure 4.26) are obtained for $H_{m0} \approx 2\text{ m}$ and $T_e \approx 7\text{ s}$, with an occurrence frequency of 1.25% (Table 4.9 Figure 4.24). The combinations $1\text{ m} \leq H_{m0} \leq 2.5\text{ m}$ and $6.5\text{ s} \leq T_e \leq 7.5\text{ s}$, $1\text{ m} \leq H_{m0} \leq 3.5\text{ m}$ and $7.5\text{ s} \leq T_e \leq 9\text{ s}$ (13% of the time) give an annual energy value above 1.25 MWh/m.

Table 4.9. Central Tuscany - scatter diagram (%) of H_{m0} and T_e at the point 9

		H_{m0} [m]													
		< 0.5	0.5	1.0	1.5	2.0	2.5	3.0	3.5	4.0	4.5	5.0	5.5	6.0	>= 6.5
Te [s]	< 1.5	1.31	0	0	0	0	0	0	0	0	0	0	0	0	0
	1.5	11.46	0	0	0	0	0	0	0	0	0	0	0	0	0
	3	24.34	3.00	0	0	0	0	0	0	0	0	0	0	0	0
	4.5	13.94	9.35	3.05	0.07	0	0	0	0	0	0	0	0	0	0
	6	4.85	5.93	3.30	3.11	1.25	0.19	0	0	0	0	0	0	0	0
	7.5	1.67	3.94	3.30	1.74	0.95	0.71	0.39	0.11	0.04	0	0	0	0	0
	9	0.21	0.17	0.51	0.42	0.24	0.16	0.07	0.05	0.07	0.02	0.01	0	0	0
	10.5	0	0	0	0.04	0.01	0	0	0	0	0	0	0	0	0
	12	0	0	0	0	0	0	0	0	0	0	0	0	0	0
	13.5	0	0	0	0	0	0	0	0	0	0	0	0	0	0
	15	0	0	0	0	0	0	0	0	0	0	0	0	0	0
	>= 16.5	0	0	0	0	0	0	0	0	0	0	0	0	0	0

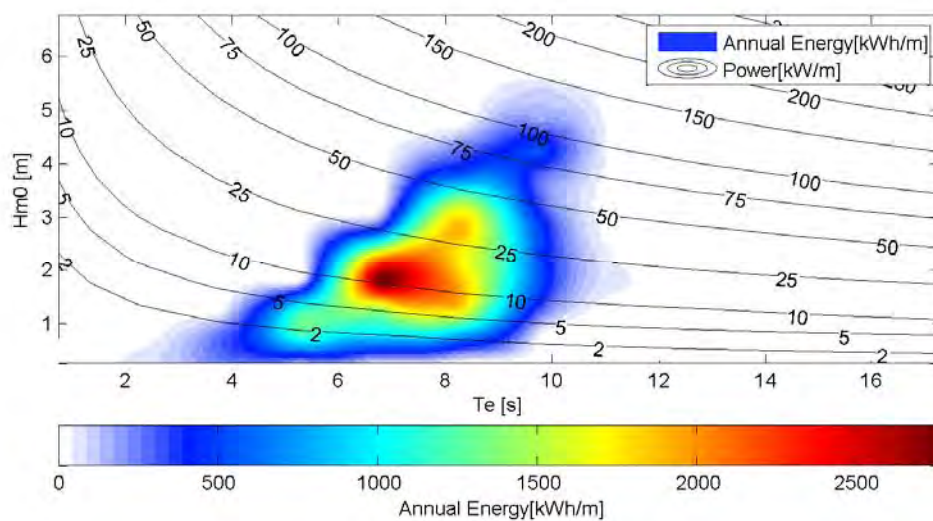


Figure 4.27. Central Tuscany – Annual energy at the point 9

Table 4.10. Liguria – location and yearly mean wave power values of the extracted points

	<i>Latitude</i> (UTM32)	<i>Longitude</i> (UTM32)	<i>Mean Wave Power</i> 2010 (kW/m)	<i>Mean Wave Power</i> 2011 (kW/m)	<i>Water depth</i> (m)
<i>Liguria</i>					
1	4842881	373064	1.00	1.00	-15
2	4845264	378302	1.30	1.22	-15
3	4848133	383989	1.40	1.23	-15
4	4847655	393258	1.58	1.37	-15
5	4849884	397327	1.40	1.15	-15
6	4851945	402602	1.17	1.04	-15
7	<u>4853354</u>	<u>412140</u>	<u>1.70</u>	<u>1.45</u>	<u>-15</u>
8	4855553	417204	1.36	1.21	-15
9	4858467	422469	1.24	1.11	-15
10	4864134	430676	1.10	1.04	-15
11	4842672	373279	1.19	1.11	-50
12	4845010	378673	1.36	1.23	-50
13	4846968	384175	1.43	1.25	-50
14	4847138	393338	1.66	1.43	-50
15	4848813	397080	1.60	1.37	-50
16	4850338	403344	1.63	1.41	-50
17	<u>4850951</u>	<u>412322</u>	<u>1.74</u>	<u>1.55</u>	<u>-50</u>
18	4854520	417720	1.63	1.43	-50
19	<u>4855656</u>	<u>423617</u>	<u>1.74</u>	<u>1.55</u>	<u>-50</u>
20	4863108	431727	1.48	1.33	-50



Figure 4.28. Liguria - location and wave roses of the extracted points

In Liguria the highest wave power values are in the point 7, for the 15 m water depth and in the points 17 and 19, for the 50 m water depth. The values are similar for all of these points: 1.70 kW/m in the 2010 and 1.50 kW/m in the 2011 (Table 4.10). The points

7 and 17 are located in front of an headland among Sanremo and Imperia, and the point 19 in front of Imperia (Figure 4.28). Their wave roses show that the main wave direction is S-SW.

Table 4.11. Liguria - scatter diagram (%) of H_{m0} and T_e at the point 7

		H_{m0} [m]													
		< 0.5	0.5	1.0	1.5	2.0	2.5	3.0	3.5	4.0	4.5	5.0	5.5	6.0	≥ 6.5
T_e [s]	< 1.5	0	0	0	0	0	0	0	0	0	0	0	0	0	0
	1.5	9.95	0	0	0	0	0	0	0	0	0	0	0	0	0
	3	31.65	7.59	0.01	0	0	0	0	0	0	0	0	0	0	0
	4.5	8.81	15.72	2.35	0.01	0	0	0	0	0	0	0	0	0	0
	6	3.86	4.35	3.61	0.95	0.15	0	0	0	0	0	0	0	0	0
	7.5	2.59	2.78	1.44	0.73	0.27	0.14	0.01	0	0	0	0	0	0	0
T_e [s]	9	0.91	0.65	0.39	0.14	0.21	0.10	0.01	0	0	0	0	0	0	0
	10.5	0.19	0.15	0.04	0.02	0.09	0.05	0.01	0.01	0	0	0	0	0	0
	12	0	0.05	0	0	0	0	0	0	0	0	0	0	0	0
	13.5	0	0	0	0	0	0	0	0	0	0	0	0	0	0
	15	0	0	0	0	0	0	0	0	0	0	0	0	0	0
	≥ 16.5	0	0	0	0	0	0	0	0	0	0	0	0	0	0

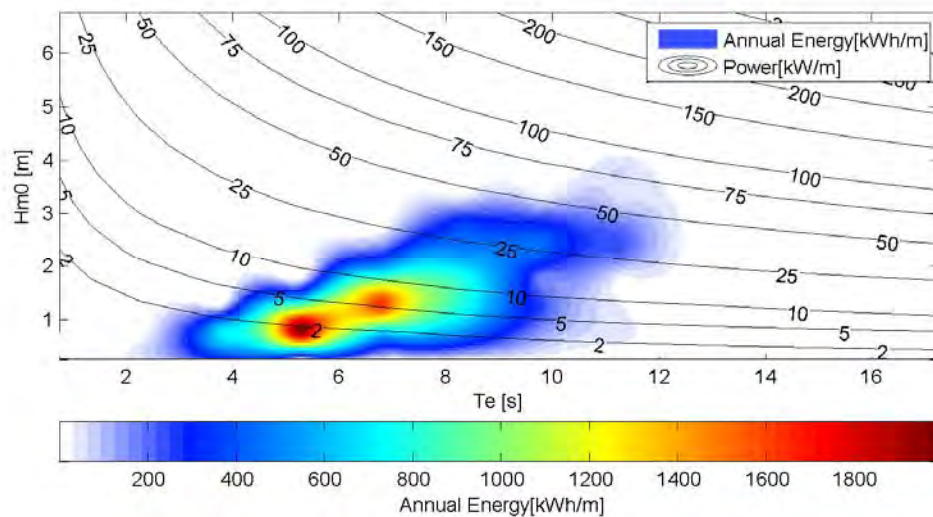


Figure 4.29. Liguria – Annual energy at the point 7

At the point 7 the combination $H_{m0} \approx 1\text{m}$ and $T_e \approx 5\text{s}$, with an occurrence frequency of 3.8%, produces the highest annual energy value on the order of 1.8 MWh/m (Figure 4.29). The mean annual energy values above 1.2 MWh/m are obtained for the 19.3% of the time (Table 4.11), with the combinations $0.5\text{m} \leq H_{m0} \leq 1\text{m}$ and $4.5\text{s} \leq T_e \leq 6\text{s}$,

$1\text{m} \leq H_{m0} \leq 1.5\text{m}$ and $6\text{s} \leq T_c \leq 7.5\text{s}$. The 50% of the sea states are in the wave height class below 0.5 m and in the period class below 6 s.

Table 4.12. Liguria - scatter diagram (%) of H_{m0} and T_c at the point 17

		H_{m0} [m]													
		< 0.5	0.5	1.0	1.5	2.0	2.5	3.0	3.5	4.0	4.5	5.0	5.5	6.0	≥ 6.5
T _c [s]	< 1.5	0	0	0	0	0	0	0	0	0	0	0	0	0	0
	1.5	10.04	0	0	0	0	0	0	0	0	0	0	0	0	0
	3	27.95	9.43	0.04	0	0	0	0	0	0	0	0	0	0	0
	4.5	8.55	15.28	3.81	0.11	0	0	0	0	0	0	0	0	0	0
	6	4.09	4.46	3.86	1.38	0.37	0.02	0	0	0	0	0	0	0	0
	7.5	2.52	2.85	1.43	0.78	0.34	0.15	0.05	0	0	0	0	0	0	0
	9	0.75	0.55	0.34	0.11	0.17	0.07	0.04	0	0	0	0	0	0	0
	10.5	0.19	0.10	0.01	0.02	0.07	0.02	0	0	0	0	0	0	0	0
	12	0.01	0.01	0	0	0	0	0	0	0	0	0	0	0	0
	13.5	0	0	0	0	0	0	0	0	0	0	0	0	0	0
	15	0	0	0	0	0	0	0	0	0	0	0	0	0	0
	≥ 16.5	0	0	0	0	0	0	0	0	0	0	0	0	0	0

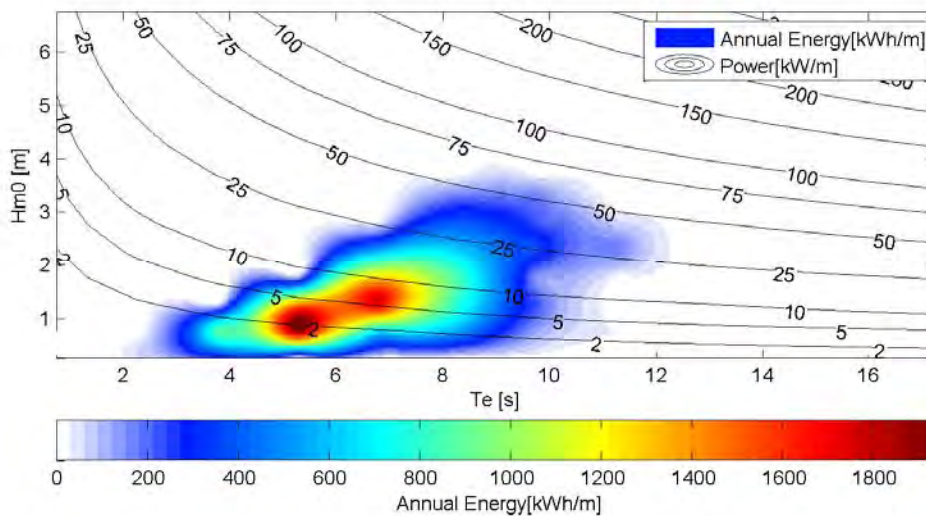


Figure 4.30. Liguria – Annual Energy at the point 17

At the point 17 the area characterized by annual energy values higher than 1.8 MWh/m (Figure 4.30) are obtained, similarly to the point 7, for $H_{m0} \approx 1\text{m}$ and $T_c \approx 5\text{s}$, with an occurrence frequency of 3.81% (Table 4.12). The combinations $0.5\text{m} \leq H_{m0} \leq 1.5\text{m}$ and $5\text{s} \leq T_c \leq 6\text{s}$, $1\text{m} \leq H_{m0} \leq 2\text{m}$ and $6\text{s} \leq T_c \leq 7\text{s}$ (24.3% of the time) provide an annual energy value above 1.2 MWh/m.

Table 4.13. Liguria - scatter diagram (%) of H_{m0} and T_e at the point 19

		H_{m0} [m]													
		< 0.5	0.5	1.0	1.5	2.0	2.5	3.0	3.5	4.0	4.5	5.0	5.5	6.0	>= 6.5
T_e [s]	< 1.5	0	0	0	0	0	0	0	0	0	0	0	0	0	0
	1.5	10.36	0	0	0	0	0	0	0	0	0	0	0	0	0
	3	28.36	10.36	0.04	0	0	0	0	0	0	0	0	0	0	0
	4.5	8.18	14.26	4.22	0.09	0	0	0	0	0	0	0	0	0	0
	6	3.66	4.29	3.70	1.35	0.35	0.02	0	0	0	0	0	0	0	0
	7.5	2.50	2.96	1.52	0.83	0.34	0.15	0.09	0	0	0	0	0	0	0
	9	0.73	0.42	0.35	0.14	0.20	0.09	0.02	0	0	0	0	0	0	0
	10.5	0.16	0.10	0	0.02	0.06	0.02	0	0	0	0	0	0	0	0
	12	0.02	0	0	0	0	0	0	0	0	0	0	0	0	0
	13.5	0	0	0	0	0	0	0	0	0	0	0	0	0	0
	15	0	0	0	0	0	0	0	0	0	0	0	0	0	0
	>= 16.5	0	0	0	0	0	0	0	0	0	0	0	0	0	0

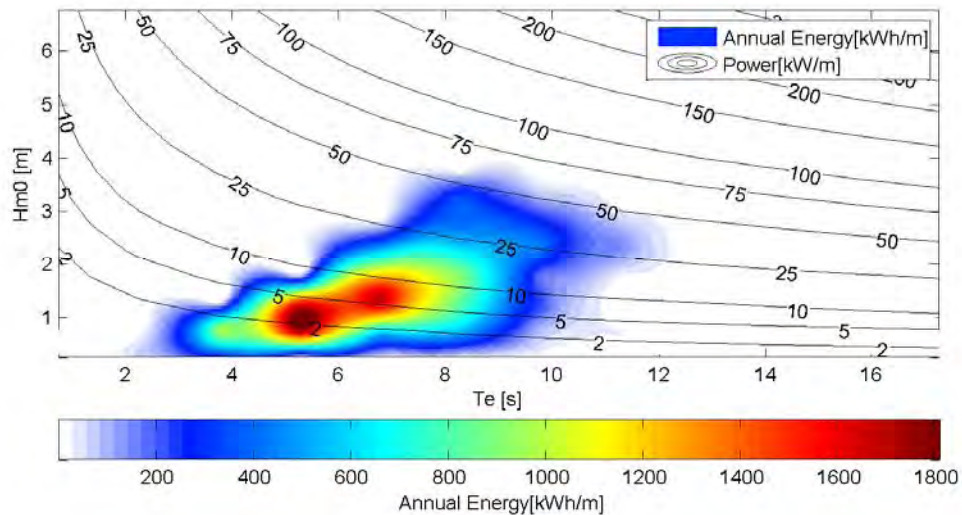


Figure 4.31. Liguria – Annual energy at the point 19

At the point 19 two different peaks are present (Figure 4.31) : the first one with a value of annual energy above 1.8 MWh/m for $H_{m0} \approx 1$ m and $T_e \approx 5.5$ s (occurrence frequency of 4.22%), the second one with a value around 1.8 MWh/m for $H_{m0} \approx 1.5$ m and $T_e \approx 7$ s (occurrence frequency of 1.35%). The same combinations of the point 17 ($H_{m0} \approx 0.5-1.5$ m and $T_e \approx 5-6$ s, $H_{m0} \approx 1-2$ m and $T_e \approx 6-7.5$ s) provide an annual energy value above 1.1 MWh/m and hold over the 23.5% of the time (Table 4.13).

Table 4.14. Sardinia – location and yearly mean wave power values of the extracted points

	<i>Latitude (UTM32)</i>	<i>Longitude (UTM32)</i>	<i>Mean Wave Power 2010 (kW/m)</i>	<i>Mean Wave Power 2011 (kW/m)</i>	<i>Water depth (m)</i>
<i>Sardinia</i>					
<u>1</u>	<u>4532021</u>	<u>430592</u>	<u>12.02</u>	<u>8.33</u>	<u>-15</u>
2	4525707	433632	9.86	6.46	-15
3	4516244	429216	10.88	7.38	-15
4	4509652	426722	11.30	7.61	-15
5	4497472	427645	10.27	6.76	-15
6	4490442	429136	7.59	4.74	-15
7	4490107	440652	3.86	2.32	-15
8	4479800	446537	6.72	4.06	-15
<u>9</u>	<u>4532021</u>	<u>429802</u>	<u>11.48</u>	<u>8.00</u>	<u>-50</u>
10	4525588	431498	10.87	7.35	-50
11	4516570	427478	11.18	7.70	-50
12	4509971	424733	11.26	7.78	-50
13	4497543	425905	11.05	7.47	-50
14	4489600	429065	9.77	6.20	-50
15	4485876	436103	7.60	4.61	-50
16	4478310	443061	7.89	4.79	-50

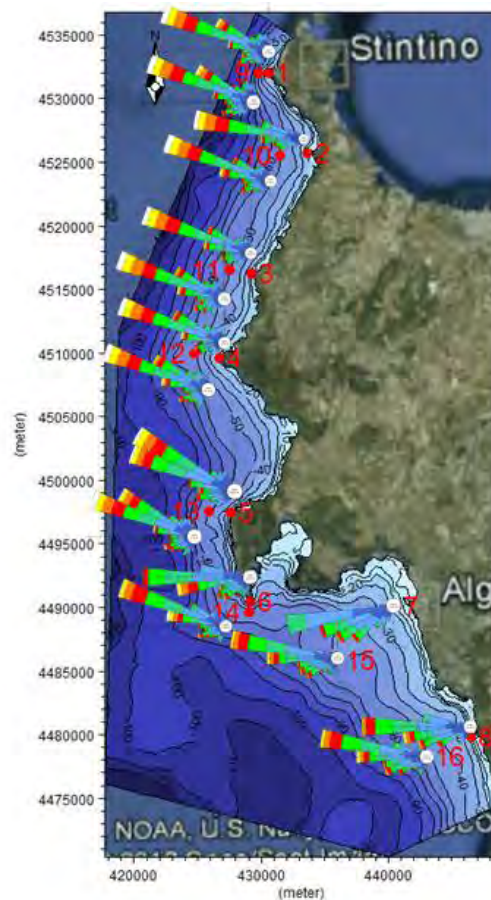


Figure 4.32. Sardinia - location and wave roses of the extracted points

In Sardinia the points with the highest values of wave power are the point 1, that reaches a value of 12 kW/m in the 2010 and 8.3 kW/m in the 2011 on 15 m water depth, and the point 9, that reaches values of 11.5 kW/m in the 2010 and 8 kW/m in the 2011 on 50 m water depth (Table 4.14). The wave power value in the point 1 higher than the value in the point 9 is due to the focusing mechanism that occurs in front of the headland in the northern part of the domain, on the West of Stintino (Figure 4.32). The wave roses of these two points show that the main wave direction is NW.

Table 4.15. Sardinia - scatter diagram (%) of H_{m0} and T_c in the point 1

		H_{m0} [m]													
		< 0.5	0.5	1.0	1.5	2.0	2.5	3.0	3.5	4.0	4.5	5.0	5.5	6.0	>= 6.5
T_c [s]	< 1.5	0.05	0	0	0	0	0	0	0	0	0	0	0	0	0
	1.5	5.63	0	0	0	0	0	0	0	0	0	0	0	0	0
	3	19.44	4.10	0.02	0	0	0	0	0	0	0	0	0	0	0
	4.5	8.28	16.04	5.00	0.59	0	0	0	0	0	0	0	0	0	0
	6	0.46	4.83	7.88	5.74	2.28	0.36	0	0	0	0	0	0	0	0
	7.5	0.02	0.21	1.46	3.03	3.43	2.68	1.56	0.65	0.12	0	0	0	0	0
	9	0	0.01	0.09	0.12	0.45	0.88	1.00	1.35	0.91	0.49	0.27	0.15	0.01	0
	10.5	0	0	0	0	0	0	0	0.10	0.01	0.02	0.05	0.10	0.06	0.05
	12	0	0	0	0	0	0	0	0	0	0	0	0	0	0
	13.5	0	0	0	0	0	0	0	0	0	0	0	0	0	0
	15	0	0	0	0	0	0	0	0	0	0	0	0	0	0
	>= 16.5	0	0	0	0	0	0	0	0	0	0	0	0	0	0

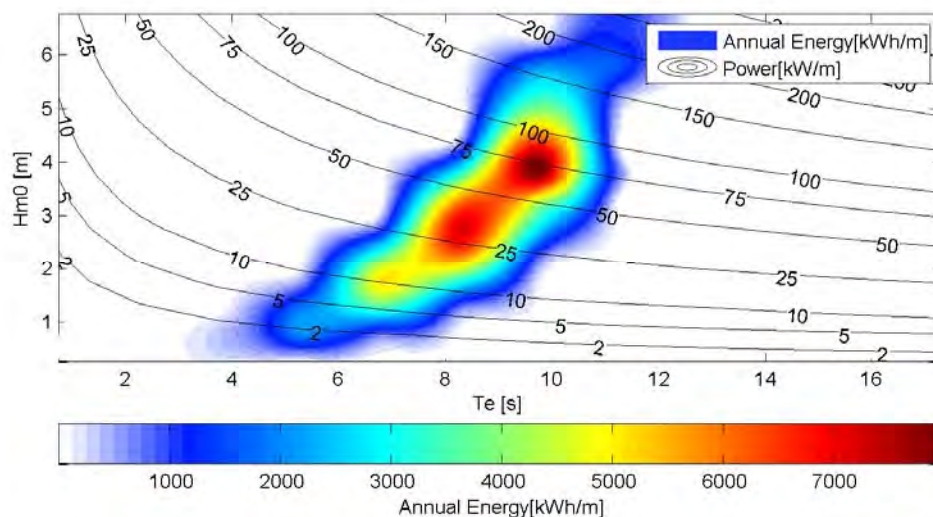


Figure 4.33. Sardinia – Annual energy at the point 1

In the point 1 the combination $H_{m0} \approx 4$ m and $T_c \approx 9.5$ s, that occurs for the 0.9% of the year (Table 4.15), produces the highest annual energy value, equal to more than 7

MWh/m (Figure 4.33). The mean annual energy values above 3 MWh/m are obtained for the 35.2% of the time with H_{m0} between 1m and 5.5 m and T_c between 6 s and 11 s, while the values above 2 MWh/m are obtained with H_{m0} between 0.5 m and 6 m and T_c between 5 s and 12 s, with an occurrence frequency of 61.8%. Therefore it is important to highlight that for an occurrence frequency above 60 % the mean annual energy values are higher or similar to the highest values of Liguria and Tuscany areas, that occur for no more than the 5% of the time.

Table 4.16. Sardinia - scatter diagram (%) of H_{m0} and T_c at the point 9

		H_{m0} [m]													
		< 0.5	0.5	1.0	1.5	2.0	2.5	3.0	3.5	4.0	4.5	5.0	5.5	6.0	>= 6.5
Te [s]	< 1.5	0.10	0	0	0	0	0	0	0	0	0	0	0	0	0
	1.5	5.68	0	0	0	0	0	0	0	0	0	0	0	0	0
	3	18.82	4.50	0.04	0	0	0	0	0	0	0	0	0	0	0
	4.5	7.60	15.83	5.42	0.71	0	0	0	0	0	0	0	0	0	0
	6	0.46	3.92	8.35	5.97	2.70	0.65	0.02	0	0	0	0	0	0	0
	7.5	0.02	0.17	1.22	3.09	3.46	2.86	1.68	1.07	0.29	0.01	0	0	0	0
	9	0	0	0.05	0.07	0.30	0.71	0.85	1.17	0.85	0.55	0.34	0.12	0.01	0
	10.5	0	0	0	0	0	0	0.07	0.02	0	0.02	0.02	0.07	0.06	0.04
	12	0	0	0	0	0	0	0	0	0	0	0	0	0	0
	13.5	0	0	0	0	0	0	0	0	0	0	0	0	0	0
	15	0	0	0	0	0	0	0	0	0	0	0	0	0	0
	>= 16.5	0	0	0	0	0	0	0	0	0	0	0	0	0	0

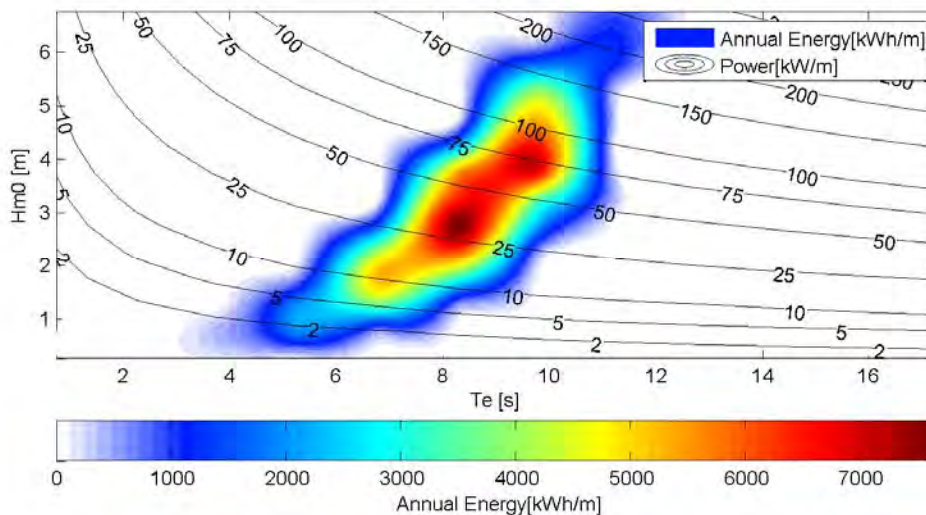


Figure 4.34. Sardinia – Annual energy at the point 9

In the point 9 two different peaks are present with annual energy values above 7 MWh/m (Figure 4.34): the first one for $H_{m0} \approx 3$ m and $T_c \approx 8.5$ s (occurrence frequency of 1.68 %), the second for $H_{m0} \approx 4.5$ m and $T_c \approx 9.5$ s (occurrence frequency of 0.55 %). The

mean annual energy values above 3 MWh/m are obtained for the 36.3 % of the time with H_{m0} between 1 m and 5.5 m and T_c between 6 s and 10.5 s, while the values above 2 MWh/m are obtained with H_{m0} between 0.5 m and 6 m and T_c between 5 s and 11 s, with an occurrence frequency of 62.6 %. The 50 % of the sea states are in a wave height class below 1 m and a period class below 6 s.

4.3. Non-technical barriers

In order to assess the installation of a wave energy farm a test site for WECs, non-technical barriers, as the environmental, logistical and social constraints, have to be taken into account, in addition to the energy potentials studied in the Paragraph 4.2.2.

In particular the marine protected area, the distance from the coast, the distance from harbour facility, the navigation routes and the population density were analysed.

The marine protected areas are an important non-technical barrier because a wave energy installations within its boundaries can be seen as an human interference, posing an hazard to the environment. Wave energy devices seeking to be sited within marine reserves will need to go through extra and probably lengthy planning permission approval, unless the marine protected area law allow the renewable energy installations [57].

The hot-spot assessment should also consider factors as the closeness to coast, closeness to nearest harbour as well as closeness to nearest grid connection. The closeness to the coast is due to the high cost of the purchase and installation of the offshore cables (Table 4.17 and Table 4.18). A rock coverage will be required for the first kilometre for the cable, and a rough cost per km, is of approximately 1M €/km [58]. Therefore only hotspots that are within a 5 km distance from the coast can be considered, unless the price of cabling reduces in the future [57].

Table 4.17. Range cable costs [58]

Range MW	kV	Supply Cost per km
0.25-7 MW	20	€ 59000
8.1-20 MW	38	€ 173000
21 -110 MW	110	€ 288000

Table 4.18. Pelamis cable laying costs [58]

Pelamis cable laying costs	
cable laying /km trenched	€ 282000
cable laying /km untrenched	€ 100000
Cable/rock coverage/km	€ 939000

The closeness to the harbour is important in order to have an easy access to service harbour and an availability of skilled labour with appropriate equipment, that are essential factors for a wave energy industry development. Moreover wave energy installations need to be serviced regularly via small survey boats and a suitable distance that are economical to travel are about 20-30 km [59].

Ideally, the power production is located as close as possible to population centres to reduce energy loss via cable transmission and to reduce the onshore cabling connection costs, necessary to reach the grid infrastructure, closed to the coast where there are the major population centres [57].

Wave energy farms adjacent to busy navigation routes can strongly increase the potential of shipping hazard due to collisions, and are therefore unlikely to be allowed within a rather large perimeter around shipping routes even outside the main ones. However this aspect might be alleviated with the establishment of adequate and reliable signalling systems by the navigation authorities [60].

4.3.1 METHODOLOGY

The bathymetry, coastline, harbour [61], marine protected area [62], administrative boundaries, population density [63], navigation route [64] information, in the geospatial vector data format, were analysed, manipulated and visualized in the geographic information systems software Quantum GIS. The data layers are in the Universal Transverse Mercator (UTM) projection, World Geodetic System 84 (WGS84) datum, zone 32 North.

The analysis was focused on the points with the highest wave power, selected in the Paragraph 4.2.2, following the criteria described above.

4.3.2 RESULTS

The Pelagos Sanctuary for Mediterranean Marine Mammals is a marine protected area aimed at the protection of marine mammals (cetaceans). It covers an area of approximately 87.000 km² (Figure 4.35), comprising the waters between Toulon (French Riviera), Capo Falcone (western Sardinia), Capo Ferro (eastern Sardinia) and Fosso Chiarone (Tuscany). The sanctuary was established on 25 November 1999 with an International Agreement between France, Italy and the Principality of Monaco. The Articles n.4-5-6-7-8-9 of this International Agreement prohibit all pollution forms, toxic waste, new fishing equipment harming the marine mammals or their food and the competition of high-speed motorboat in order to guarantee a favourable conservation status of marine mammals and their habitat [65]. These constraints do not seem to prevent the WEC installation, but anyway a permission approval will be required. In fact one of the new offshore LNG power plants, that are under construction in Italy, is located in front of the Tuscany Coast that is comprised inside this area.

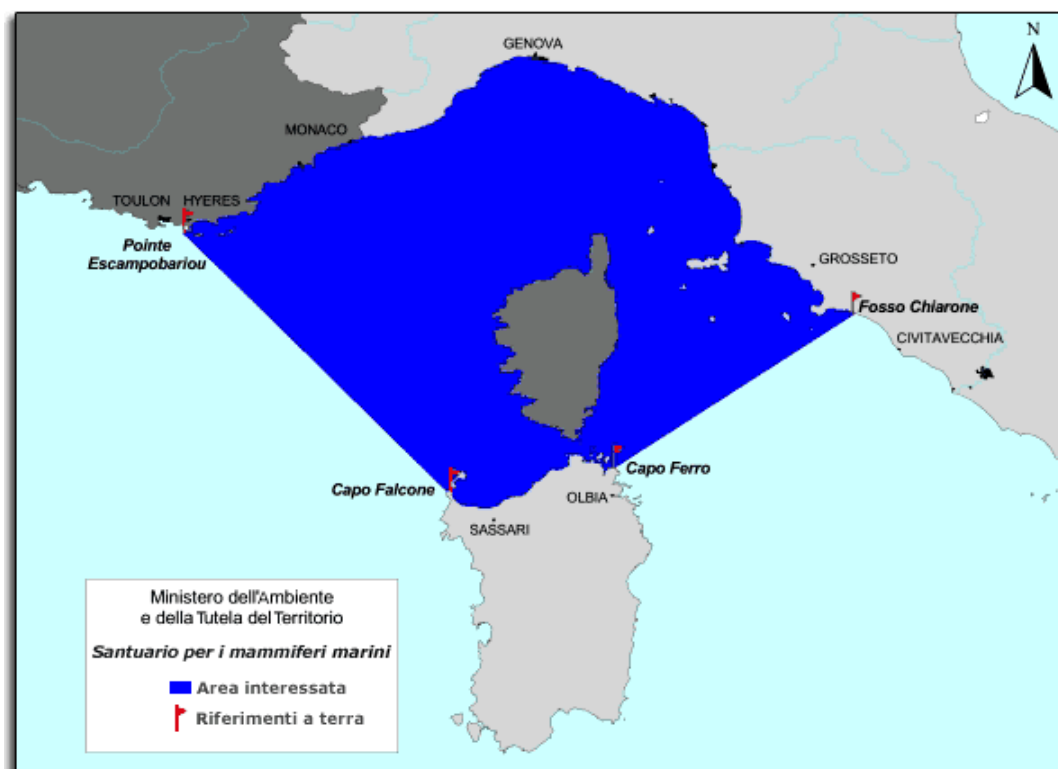


Figure 4.35. Perimeter of Pelagos Sanctuary [65]

The area, population and population density are summarized for Tuscany, Liguria and Sardinia in the Table 4.19.

Table 4.19. Area, population [63] and population density of the selected Region

Region	Area [km ²]	Population 2001	Population Density
Tuscany	22984.43	3497806	152.18
Liguria	5415.46	1571783	290.24
Sardinia	24094.17	1631880	67.73

The navigation routes for maritime and goods transport are shown in Figure 4.36.

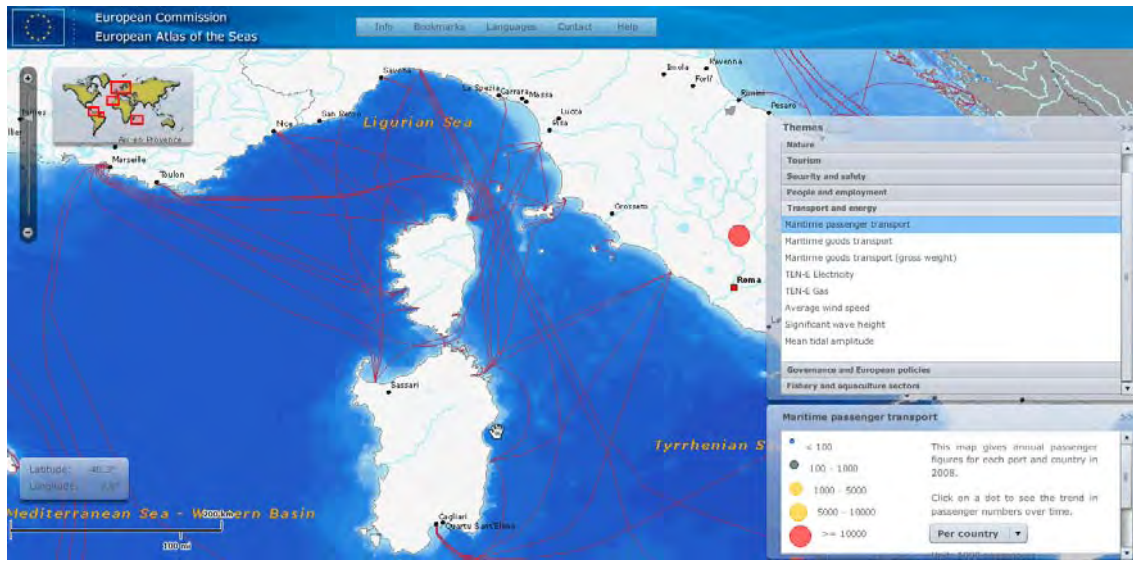


Figure 4.36. Navigation routes [64]

4.3.2.1 *Tuscany area*

In Tuscany in addition to the Pelagos Sanctuary the Meloria Shoals (Secche della Meloria) marine protected area is present, located in the most energetic area of the Tuscany. The perimeter of the area are highlighted in pink and called “Secche della Marina Area C” in Figure 4.37. The Italian Decree n.217/2009 establish that the area C is a partial reserve area and the area A is an integral reserve. In the area A the only allowed activities are: i) the control and rescue activities, ii) service activities carried out by the administrator of the marine protected area, iii) the scientific research activities authorized by the administrator of the marine protected area.

The point 9 selected for the Northern Tuscany is inside the area A of the Secche della Meloria marine protected area and then it is excluded from this analysis. On the opposite, the point 19 selected for the Northern Tuscany and the point 9 for the Central Tuscany are just out the area C, but are far from the coastline, about 15.4 km and 14.8 km respectively.

The point 3 for the Central Tuscany is very close to the coast, only 580 m far, and it's located in front of Livorno, a large population centre and a commercial harbour, also famous for the shipbuilding. The main navigation routes do not cover this area and so it results most suitable to install a device.

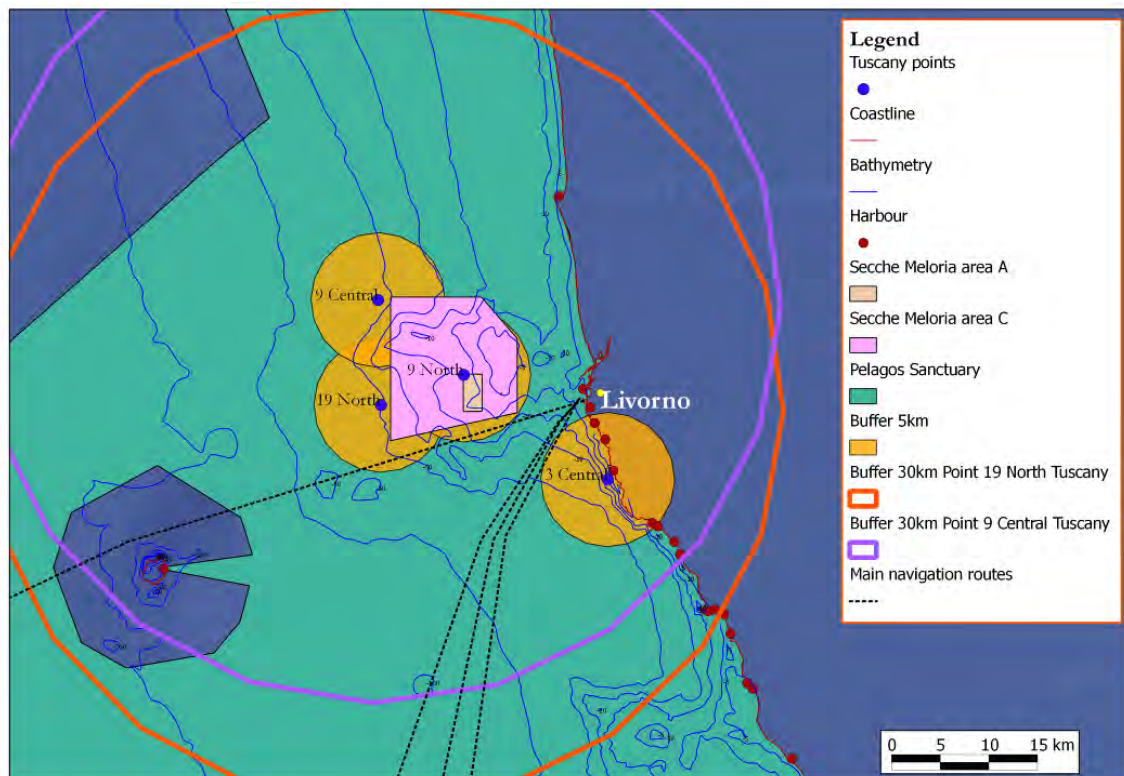


Figure 4.37. Tuscany area: analysis of the non-technical barriers

Other interesting points in terms of WEC installation, with a distance from the coast lower than 5 km, are the point 8 of the Northern Tuscany and the points 4 and 12 of the Central Tuscany.

The point 8 of the Northern Tuscany is located in front of Viareggio harbour and its mean wave power values are equal to 2.44 kW/m in the 2010 and equal to 1.86 kW/m in the 2011.

The point 4 of the Central Tuscany, on the 15 m water depth, and the point 12, on the 50 m water depth, are located in front of Rosignano harbour and their mean wave power values are larger than 2 kW/m. The points located on the Vada Shoals (points 5 and 13) have larger mean wave power values than the points 4 and 12, but their distances from the coast exceed 10 km.

4.3.2.2 *Liguria area*

In Liguria there is the Pelagos Sanctuary but not others marine protected area with integral reserve. All the points 7, 17, 19 are very close to the coastline, only 1 km, 3.5 km and 4 km respectively and a lot of harbours are less than 20-30 km far (Figure 4.38). The main navigation routes bound to Genova do not interfere with these sites, but the point 19 is just outside of the commercial Imperia harbour entrance and so it may not be suitable for the installation.

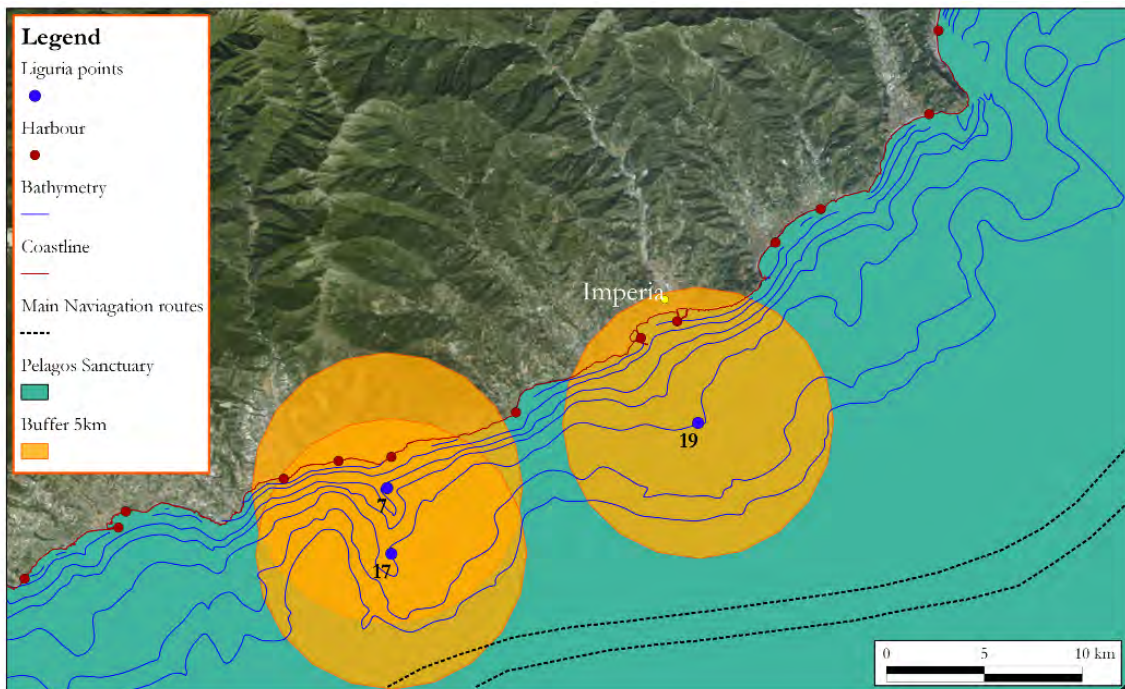


Figure 4.38. Liguria area: analysis of the non-technical barriers

4.3.2.3 *Sardinia area*

The Pelagos Sanctuary is on the Northern Sardinia, so outside of the analyzed area (Figure 4.39).

The points 1 and 9 are very close to the coastline, 100 m and 1000 m respectively and the main navigation routes depart from Porto Torres harbour and do not interfere with the Stintino area.

The harbours in the Northern Sardinia are less than 30 km far and small boats can go across the shallow water depths around the Piana Island, between Stintino and Asinara Island. On the opposite, the largest boats need to sail more than 60 km far if coming from

the Porto Torres harbour circumnavigating the Asinara Island or coming from Alghero harbour.

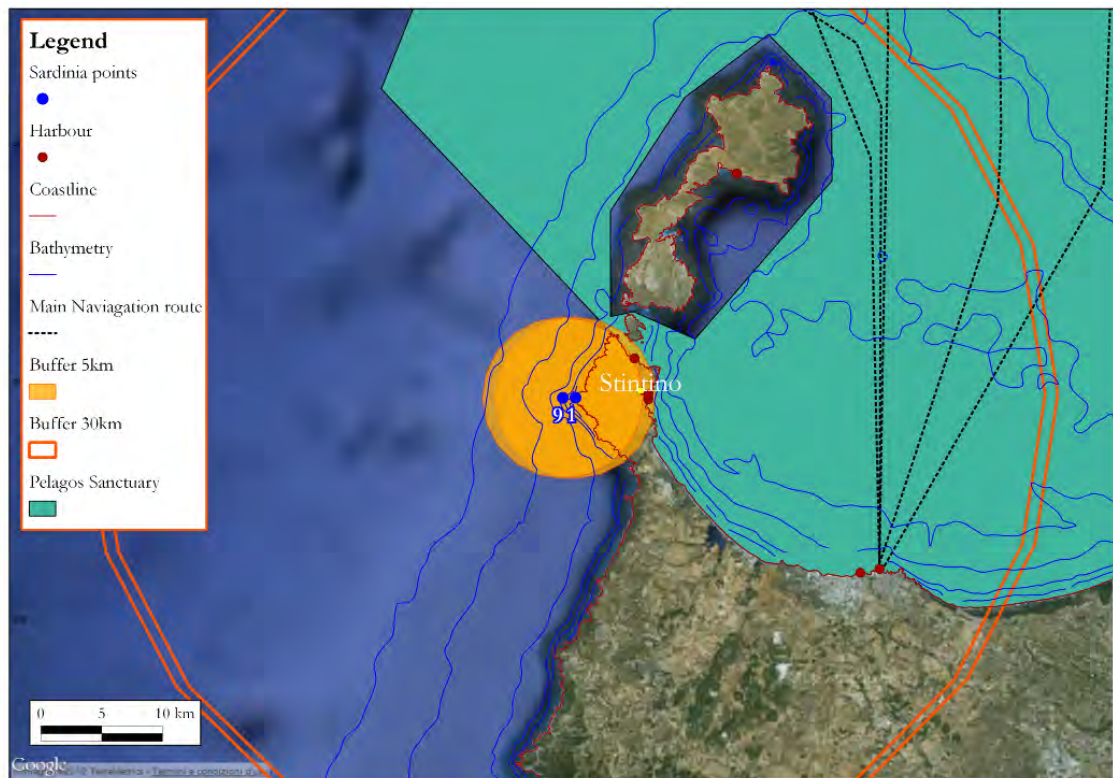


Figure 4.39. Sardinia area: analysis of the non-technical barriers

It is important to highlight that all the points north of Punta Cristallo (points from 1 to 5, on 15 m water depth, and points from 9 to 13, on 50 m water depth) could be taken into account in the installation of a WEC, because the mean wave power values are significant (above 9.8 kW/m in the 2010 and above 6.5 kW/m in the 2011) and the distances from the coast are lower than 5 km.

CHAPTER 5

HYDRODYNAMICS OF WAVE ENERGY ABSORPTION BY A FLOATING DEVICE

5.1. Governing equations

In wave energy studies, the purpose of the mathematical modelling is usually to determine the performance of the device. In fact, if a device is found to be a poor wave energy absorber, it is not worthwhile carrying on its development. The analysis is restricted to those devices that operate offshore and particularly to floating structures. A general rigid body motion (Figure 5.1) is composed of three translational modes of motion (surge, sway, heave) and three rotational modes of motion (roll, pitch, yaw) in the directions of the (x, y, z) coordinate axis [27].

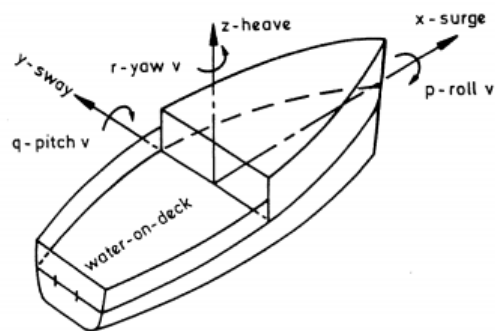


Figure 5.1. Degrees of freedom of a rigid body [66]

5.1.1. SINGLE BODY

The simplest case, analysed in this paragraph, is a system composed by a single floating body, oscillating in heave (coordinate x , with $x=0$ in absence of waves), and linked to the seabed by means of a PTO mechanism (Figure 5.2). This approximation is realistic from the hydrodynamic point of view if an axisymmetric buoy is selected, because the hydrodynamic interference between the heave mode and other modes is practically negligible (theoretically equal to zero)[67].

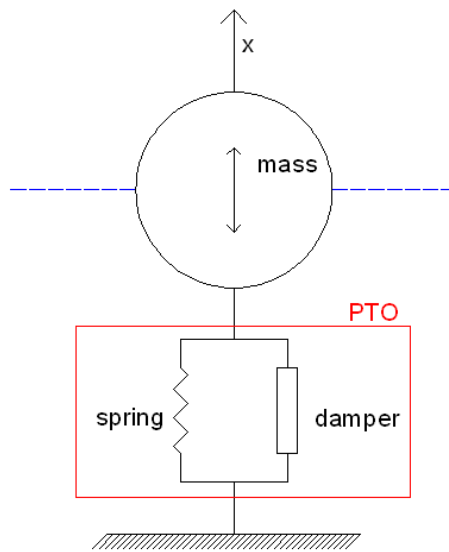


Figure 5.2. Schematic representation of a single body oscillating in heave

In a general approach the equation of motion for a single body oscillating in heave is expressed by use of the Newton's law:

$$m\ddot{x} = f_h(t) + f_{PTO}(t) \quad (5.1)$$

where m is the mass of the buoy, \ddot{x} is the acceleration, f_h is the vertical component of the force due to the water pressure on the wetted surface of the body (hydrodynamic force), and f_{PTO} is the vertical component of the force applied on the buoy by the power take off system.

If the amplitudes of the waves and the body motions are small, and then the system may be regarded as linear from the wave hydrodynamic view point, and the force f_h can be separated in three components:

$$f_h = f_d + f_r + f_{hs} \quad (5.2)$$

where f_d is the force produced by the incident waves on the assumed fixed body (excitation or diffraction force), f_r is the radiation force and f_{hs} is the hydrodynamic force. The last force is the buoyancy force on the device and can be written in the linearized form

$$f_{hs} = -\rho g S x \quad (5.3)$$

where ρ is the water density, g is the acceleration of gravity and S is the buoy cross sectional area, defined by the undisturbed water free surface [68].

5.1.1.1 Linear system in regular waves: frequency domain analysis

The power take-off system is assumed to be linear and consists of a linear spring of stiffness K and a linear damper with coefficient C . The force can be written as

$$f_{PTO} = -Kx - C\dot{x} \quad (5.4)$$

where $-Kx$ represents the spring effect (which may exist or not) and $-C\dot{x}$ ($C > 0$) is the damping effect associated with the energy extraction.

Since the incident waves are regular and the system is linear, the coordinate x and the forces are simple-harmonic functions of time and so it is useful to make use of complex variables and write

$$x(t) = \text{Re}(X_0 e^{i\omega t}), \quad f_d(t) = \text{Re}(F_d e^{i\omega t}) \quad (5.5)$$

where X_0, F_d are complex amplitudes, $\text{Re}()$ means real part of (a notation that may be omitted) and $e^{i\omega t} = \cos \omega t + i \sin \omega t$.

The radiation force corresponds to the force experienced by the body due to its oscillatory movement in absence of an incident wave field and is proportional to the amplitude of the displacement in the linear theory [27]. It is useful to decompose this force in two components, one in phase with the body acceleration and the other in phase with the body velocity:

$$f_r(t) = -A(\omega)\ddot{x} - B(\omega)\dot{x} \quad (5.6)$$

where $A(\omega)$ is the added mass and $B(\omega)$ is the radiation damping coefficient (B cannot be negative because $B < 0$ would mean that it is possible to extract energy in the absence of incident waves). These coefficients depend on the body geometry and on the frequency ω ; they can be calculated analytically only for simple geometries.

Since the system is linear, F_d is proportional to the incident wave amplitude A_w (assumed real and positive) and it can be written as

$$|F_d| = \Gamma(\omega)A_w \quad (5.7)$$

where $\Gamma(\omega)$ is a real positive excitation force coefficient. For the bodies with a vertical axial symmetry oscillating in heave, it is possible to use the Haskind relation [68]:

$$\Gamma(\omega) = \left(\frac{2g^3 \rho B(\omega)}{\omega^3} \right)^{1/2} \quad (5.8)$$

Replacing equations (5.3), (5.4) and (5.6), into equation (5.1), it is obtained

$$(m + A)\ddot{x} + (B + C)\dot{x} + (\rho gS + K)x = f_d \quad (5.9)$$

If the equation (5.5) is also replaced in equation (5.1), it yields

$$X_0 = \frac{F_d}{-\omega^2(m + A) + i\omega(B + C) + \rho gS + K} \quad (5.10)$$

The instantaneous power extracted from the oscillating body with the energy conversion system is

$$P_m(t) = -\dot{x}f_m = \dot{x}(Kx + C\dot{x}) = Kx\dot{x} + C\dot{x}^2 \quad (5.11)$$

and its time-averaged is

$$\bar{P}_m = \frac{1}{2}C\omega^2|X_0|^2 \quad (5.12)$$

In the same way the instantaneous power generated by the fluid (hydrodynamic) forces is

$$P_h(t) = -\dot{x}f_h = -\dot{x}(f_d + f_r + f_{hs}) \quad (5.13)$$

and the time-averaged power can be written as

$$\bar{P}_h = \frac{1}{8B}|F_d|^2 - \frac{B}{2} \left| U_0 - \frac{F_d}{2B} \right|^2 \quad (5.14)$$

Since the body, in average, cannot store energy, it must be $\bar{P}_m = \bar{P}_h = \bar{P}$, that is the average value of the power extracted by the body. For a given body and for fixed incident wave frequency and amplitude, the maximum value of \bar{P} is given by the first term on the

right-hand side of (5.14) and occurs when the second term takes its minimum value, which is zero [37], and it yields

$$\bar{P}_{\max} = \frac{1}{8B} |F_d|^2 = \frac{1}{8B} \Gamma^2 A_w^2 \quad (5.15)$$

or, replacing the eq. (5.8) inside the eq. (5.15)

$$\bar{P}_{\max} = \frac{g^3 \rho A_w^2}{4\omega^3} \quad (5.16)$$

Therefore the value is maximum when

$$U_0 = \frac{F_d}{2B} \rightarrow \begin{cases} B = C \\ \omega = \sqrt{\frac{k + \rho g S}{m + A}} \end{cases} \quad (5.17)$$

That is, when the radiation damping is equal to the PTO damping and in resonance condition.

The capture width L measures the power absorbing capability of the device and is defined as the ratio between the absorbed power and the energy flux of incident wave per unit crest length

$$L = \frac{\bar{P}}{E} \quad (5.18)$$

The maximum capture width is

$$L_{\max} = \frac{\bar{P}_{\max}}{E} \quad (5.19)$$

In the deep water the energy flux of incident wave per unit crest length is equal to

$$E = \frac{g^2 \rho A_w^2}{4\omega} \quad (5.20)$$

and

$$\frac{\omega^2}{g} = k = \frac{2\pi}{\lambda} \quad (5.21)$$

where k is the wave number and λ the wavelength.

Replacing the eqs.(5.16), (5.20) and (5.21) inside the eq.(5.19), it is obtained

$$L_{\max} = \frac{\lambda}{2\pi} \quad (5.22)$$

5.1.1.2 JONSWAP spectrum formulation

The sea waves can be analysed like an infinite number of wavelets with different frequencies and directions. The distribution of the energy of these wavelets plotted against the frequency and the direction is called the wave spectrum. In particular if the distribution is referred to the frequency alone it is called frequency spectrum while if it is a function of both frequency and direction it is called wave directional spectrum.

The spectra observed during JONSWAP (Joint North Sea Wave Project) appear to have a sharper peak than the Pierson–Moskowitz (PM) spectrum. To account for this in a parameterisation of the observations, the scientists of JONSWAP chose to take the shape of the Pierson–Moskowitz spectrum (Figure 5.3) and to enhance its peak with a peak-enhancement function $G(f)$:

$$G(f) = \gamma \exp \left[-\frac{1}{2} \left(\frac{T_p \cdot f - 1}{\sigma} \right)^2 \right] \quad (5.23)$$

in which γ is a peak-enhancement factor and σ is a peak-width parameter ($\sigma = \sigma_a$ for $f \leq f_p$ and $\sigma = \sigma_b$ for $f > f_p$ to account for the slightly different widths on the two sides of the spectral peak).

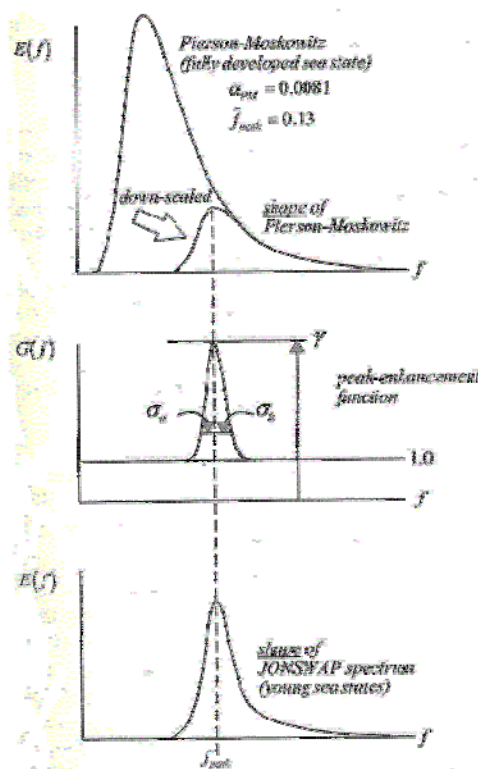


Figure 5.3. The shapes of the PM spectrum and the JONSWAP spectrum [37]

The JONSWAP spectrum formula can be written in terms of the parameters of the wave height and the period as follows [39]:

$$E(f) = \beta_j H_{1/3}^2 T_p^{-4} f^{-5} \exp[-1.25(T_p f)^{-4}] \cdot G(f) \quad (5.24)$$

in which

$$\beta_j = \frac{0.0624}{0.23 + 0.0336\gamma - 0.185(1.9 + \gamma)^{-1}} [1.094 - 0.01915 \cdot \ln \gamma] \quad (5.25)$$

$$T_p \approx \frac{T_{1/3}}{\left[1 - 0.132(\gamma + 0.2)^{-0.559}\right]} \quad (5.26)$$

If the equation (5.24) is written in terms of the spectral period T_e ($= 0.8997 \cdot T_{1/3}$ [69]) and the angular frequency $\omega = 2\pi f$, the following expression is obtained

$$E(\omega) = \frac{1}{2\pi} \beta_j H_s^2 T_e^{-4} \left(\frac{\omega}{2\pi}\right)^{-5} \exp\left[-1.25\left(T_e \cdot \left(\frac{\omega}{2\pi}\right)\right)^{-4}\right] \cdot G(\omega) \quad (5.27)$$

The values of the parameters γ , σ_a and σ_b are shown in the Table 5.1 [70] for the areas of interest in two different points of the R.O.N. (the Italian National Sea Wave Measurements Network): Alghero for the Sardinia area and La Spezia for the Tuscany and Liguria area.

Table 5.1. Shape parameters for the JONSWAP spectrum

	<i>Mean Values</i>		
	γ	σ_b	σ_a
<i>Alghero</i>	1.86	0.076	0.089
<i>La Spezia</i>	2.02	0.073	0.096

5.1.1.3 Linear system in irregular waves: frequency domain analysis

Real irregular waves may be represented, at least approximately, as a superposition of many different frequencies, by defining a spectrum. Usually only statistical information is available for the amplitude, the phase and the direction of propagation for each individual harmonic wave [48]. Since the floating device is axisymmetric and insensitive to wave direction, it is possible to consider a one-dimensional spectrum. In wave energy studies the

significant wave height, the spectral period and the JONSWAP spectrum (5.27) are usually adopted.

Since linear water wave theory is adopted and the system is assumed linear, the coordinate x , and the other forces, can be obtained by linear superposition:

$$x(t) = \sum_{i=1}^N x_i = \text{Re} \left(\sum_{i=1}^N X_{0i} e^{i\omega_i t} \right) \quad (5.28)$$

The time-averaged power output in irregular waves is computed as

$$\bar{P}_{irr}(H_s, T_e) = \int_0^\infty \bar{P}_1(\omega) \cdot E(\omega) d\omega \quad (5.29)$$

where $\bar{P}_1(\omega)$ is the time-averaged power absorbed from regular waves of frequency ω and unit amplitude. A dimensionless time-averaged power is defined as

$$\bar{P}_{irr}^* = \bar{P}_{irr} / \bar{P}_{max,irr} \quad (5.30)$$

where

$$\bar{P}_{max,irr} = \frac{g^3 \rho}{4} \int_0^\infty \omega^{-3} \cdot E(\omega) d\omega \quad (5.31)$$

is the maximum power that can be extracted by an asymmetric body in deep water oscillating in heave from a sea state represented by the spectral distribution.

5.1.2 SPAR-BUOY OWC

The Spar-Buoy OWC is an axisymmetric floating OWC that was studied at Institute of Mechanical Engineering (IDMEC) of the Instituto Superior Técnico (IST) in Lisbon, where I spent a foreign research period of three months.

One of the main advantages of floating OWC devices is to widen the range of frequencies within which the system performs well. A floating OWC device may be regarded as a two-body system, the OWC being one of the bodies. Two-body system are expected to have two resonance peaks, due to the dynamics of each body, and if these two peaks are closed to the dominant wave frequency a better performance is reached [72].

The analyzed device consists of a cylindrical floater pierced by a hollow cylinder opened at the bottom to the sea water and the top to the OWC chamber (Figure 5.4). The floater provides the radiation and diffraction of the waves, required for an efficient wave energy

absorption [48]. The small thickness tube (STT) separates the floater and the large thickness tube (LTT), and reduces the interference between them that would negatively affect the radiation/diffraction capabilities of the floater. The submerged LTT produces an added mass that is used to tune the floating device to the frequency of incoming waves and to enhance the pitching stability. If a device is supposed to oscillate in heave, it is important to increase the distance between the centre of buoyancy and centre of gravity, to increase the pitching mode natural period and move it away from the range of periods characterizing the sea waves [72].

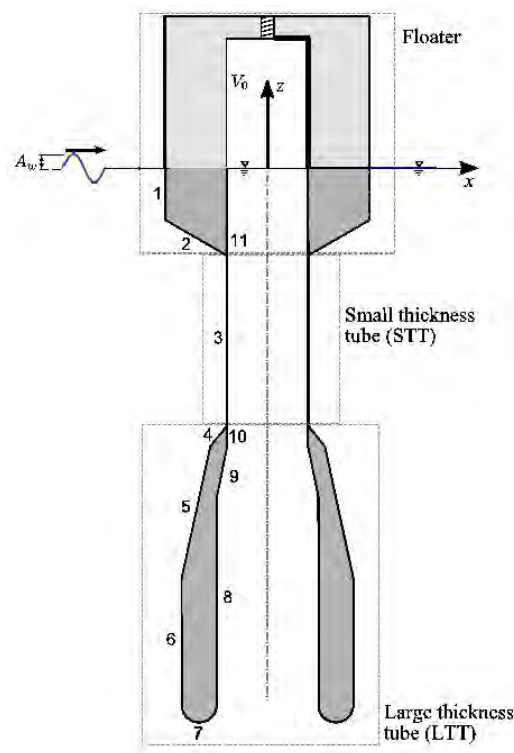


Figure 5.4. Spar-Buoy OWC cross section view [72]

5.1.2.1 Linear system in regular waves: frequency domain analysis

The Spar-Buoy OWC can be schematized as a two-body heaving system, where the body 1 is the floater and the body 2 is the rigid piston. The time-dependent coordinates of the heaving bodies 1 and 2 are $z_1(t)$ and $z_2(t)$ respectively, increasing upwards and equal to zero at the equilibrium condition. The linear water wave theory is applied by assuming wave amplitude and body motions much smaller than the wavelength. Moreover the incompressible and irrotational water flow is assumed [72].

The motion equations of the bodies 1 and 2, acted upon by sinusoidal waves of frequency ω , are given by [73]

$$\begin{cases} m_1 \ddot{z}_1(t) + \rho_w g S_1 z_1(t) - S_2 p(t) = f_{e1}(t) + f_{r1}(t) \\ m_2 \ddot{z}_2(t) + \rho_w g S_2 z_2(t) + S_2 p(t) = f_{e2}(t) + f_{r2}(t) \end{cases} \quad (5.32)$$

where ρ_w is the water density equal to 1025 kg/m^3 , g is the acceleration of gravity, m_1 the floater mass, m_2 the piston mass, S_1 is the cross sectional area of the floater defined by the undisturbed free surface, $p(t)$ is the pressure oscillation inside the chamber, S_2 is the inner free surface area, f_{ei} is the hydrodynamic excitation force on body i and f_{ri} is the hydrodynamic radiation force on body i .

The mass flow rate of air leaving the chamber through the turbine is

$$\dot{m} = -\frac{d(\rho_a V)}{dt} \quad (5.33)$$

where ρ_a is the air density, assumed equal to 1.2041 kg/m^3 in atmospheric condition for a temperature of 20° C and pressure 101.325 kPa , and V is the volume of air inside the chamber. The expression of the time-dependent air volume is

$$V(t) = V_0 + (z_1(t) - z_2(t)) \cdot S_2 \quad (5.34)$$

where $V_0 (= S_1 \cdot h_c)$, h_c being the averaged height of the OWC chamber under undisturbed conditions) is the the undisturbed value of V . Assuming air as a perfect gas ($p/\rho = RT$) and air compression inside the chamber as an isentropic process ($\rho p^{-1/\gamma} = \text{constant}$) [74], the equation (5.33) can be written as

$$\dot{m} = \rho_a q - (V_0 + (z_1 - z_2) \cdot S_2) \frac{1}{c^2} \frac{dp}{dt} \quad (5.35)$$

where $q (= S_2(\dot{z}_1 - \dot{z}_2))$ is the volume flow rate of air displaced by the relative motion of the piston and c is the speed of sound in air, assumed equal to 343.8 m/s in atmospheric condition for a temperature of 20° C .

In order to relate \dot{m} to p the turbine characteristic curves are introduced. Applying dimensional analysis to incompressible flow turbomachinery and taking the dimensionless pressure coefficient Ψ as the independent variable [69], it is possible to write

$$\Phi = f_m(\Psi) \quad (5.36)$$

$$\Pi = f_p(\Psi) \quad (5.37)$$

where

$$\Psi = \frac{p}{\rho_a N^2 D^2} \quad (5.38)$$

$$\Phi = \frac{\dot{m}}{\rho_a N D^3} \quad (5.39)$$

$$\Pi = \frac{P_t}{\rho_a N^3 D^5} \quad (5.40)$$

Here Ψ is the non-dimensional pressure head, Φ the non-dimensional flow rate, Π the non-dimensional turbine power turbine, N the rotational speed (rad/s), D the turbine rotor diameter and P_t the turbine power output (mechanical losses are ignored).

In the frequency domain analysis the eq.(5.36) can be assumed approximately linear, $\Phi=K \Psi$, with K constant depending on turbine geometry but not on its size or rotational speed.

Therefore, in dimensional form, the relation between \dot{m} and p is given by

$$\dot{m} = \frac{KD}{N} p = kp \quad (5.41)$$

where k is the dimensional damping of the turbine. Replacing the eq. (5.41) in eq.(5.35), it yields

$$\frac{V_0}{c^2} \frac{dp}{dt} + \frac{KD}{N} p = \rho_a q \quad (5.42)$$

Since the eq.(5.36) is assumed linear, the system is linear and time-invariant and so it is possible to apply a Fourier transformation to the time-dependent quantities [72]

$$\{z_i, \dot{z}_i, \ddot{z}_i, p, q, f_{ei}, f_{ri}\} = \{Z_i, i\omega Z_i, -\omega^2 Z_i, P, Q, A_w \Gamma_i, F_{ri}\} e^{i\omega t} \quad (5.43)$$

where $Z_i, P, Q, \Gamma_i, F_{ri}$ are complex quantities, Γ_i is the excitation coefficient on body i , A_w is the incident wave amplitude and F_{ri} the frequency dependent radiation force amplitude, given by

$$F_{ri}(\omega) = (-\omega^2 A_{ii} + i\omega B_{ii})Z_i + (-\omega^2 A_{ij} + i\omega B_{ij})Z_j \quad (5.44)$$

where $A_{ii}(\omega)$ is the added mass, $B_{ii}(\omega)$ the radiation damping coefficient, A_{ij} and B_{ij} the coefficients of the hydrodynamic force on one of the bodies as affected by the motion of the other.

Replacing the equations (5.42), (5.43), (5.44) in eq.(5.32) it yields

$$\begin{cases} \left[-\omega^2(m_{1+}A_{11}) + i\omega B_{11} + \rho_w g S_1 \right] Z_1 + \left[-\omega^2 A_{12} + i\omega B_{12} \right] Z_2 - S_2 P = A_w \Gamma_1 \\ \left[-\omega^2(m_{2+}A_{22}) + i\omega B_{22} + \rho_w g S_2 \right] Z_2 + \left[-\omega^2 A_{21} + i\omega B_{21} \right] Z_1 + S_2 P = A_w \Gamma_2 \\ P = \Lambda Q \end{cases} \quad (5.45)$$

where $Q = -i\omega S_2(Z_1 - Z_2)$ and Λ is the transfer function of the pressure p frequency response to the volume flow rate q and is given by

$$\Lambda = \left(i\omega \frac{V_0}{\rho_a c^2} + \frac{KD}{\rho_a N} \right)^{-1} \quad (5.46)$$

The instantaneous power output of the turbine [69] is given by eqs. (5.38) and (5.40)

$$P_t = \rho_a N^3 D^5 f_p \left(\frac{p(t)}{\rho_a N^2 D^2} \right) \quad (5.47)$$

The instantaneous pneumatic power available to the turbine is

$$P_{avai} = \frac{\dot{m}}{\rho_a} p \quad (5.48)$$

and the instantaneous turbine efficiency is

$$\eta = \frac{P_t}{P_{avai}} = \frac{\Pi}{\Phi\Psi} \quad (5.49)$$

or, if eq.(5.36) is linear, is

$$\eta = \frac{P_t}{P_{avai}} = \frac{\Pi}{K\Psi^2} \quad (5.50)$$

The time-averaged value of the power available to the turbine [72] is given by

$$\bar{P}_{avai} = \frac{KD}{2\rho_a N} |P|^2 = \frac{k}{2\rho_a} |P|^2 \quad (5.51)$$

5.1.2.2 Linear system in irregular waves: frequency domain analysis

The first assumption is that each of the sea states, that represent the local wave climate, is a stationary stochastic ergodic process. For each sea state, at a fixed position, it is assumed that the probability density function $f(\zeta)$ of the surface elevation ζ is a Gaussian [69], and so it is possible to write

$$f(\zeta) = \frac{1}{\sqrt{2\pi}\sigma_\zeta} \exp\left(-\frac{\zeta^2}{2\sigma_\zeta^2}\right) \quad (5.52)$$

where σ_ζ^2 is the variance and σ_ζ the standard deviation of ζ . The variance is related to the energy density spectrum by

$$\sigma_\zeta^2 = \int_0^\infty E_\omega(\omega) d\omega \quad (5.53)$$

where $E_\omega(\omega)$ is a one-sided wave energy density spectrum (see 5.1.1.2). Since the system is linear, the pressure oscillation $p(t)$ is a Gaussian probability density function and its variance is given by

$$\sigma_p^2 = \int_0^\infty E_\omega(\omega) |P(\omega)|^2 d\omega \quad (5.54)$$

Taking into account the eq.(5.47) and the eq.(5.54) the average value of the power output of the turbine can be written as [69]

$$\bar{P}_t = \frac{\rho_a N^3 D^5}{\sqrt{2\pi}\sigma_p} \int_0^\infty \exp\left(-\frac{p^2}{2\sigma_p^2}\right) f_p\left(\frac{p}{\rho_a N^2 D^2}\right) dp \quad (5.55)$$

or in the dimensionless form as

$$\bar{\Pi} = \frac{1}{\sqrt{2\pi}\sigma_\psi} \int_0^\infty \exp\left(-\frac{\psi^2}{2\sigma_\psi^2}\right) f_p(\psi) d\psi \quad (5.56)$$

where $\bar{\Pi}$ is the averaged value of Π and

$$\sigma_\psi = \frac{\sigma_p}{\rho_a N^2 D^2} \quad (5.57)$$

The averaged value of the power available to the turbine is given by

$$\bar{P}_{avai} = \int_0^{\infty} P_{avai} f(p) dp = \frac{1}{\rho_a \sqrt{2\pi\sigma_p}} \int_0^{\infty} \dot{m} p \exp\left(-\frac{p^2}{2\sigma_p^2}\right) dp \quad (5.58)$$

or in the dimensionless form as

$$\bar{\Pi}_{avai} = \frac{\bar{P}_{avai}}{\rho_a N^3 D^5} = \frac{1}{\sqrt{2\pi\sigma_\Psi}} \int_0^{\infty} f_m(\Psi) \exp\left(-\frac{\Psi^2}{2\sigma_\Psi^2}\right) \Psi d\Psi \quad (5.59)$$

If $\Phi = K\Psi$, i.e. if the turbine is linear, the equation (5.59) can be written as

$$\bar{\Pi}_{avai} = K\sigma_\Psi^2 \quad (5.60)$$

and the eq.(5.50) as

$$\bar{\eta} = \Pi(K\sigma_\Psi^2)^{-1} \quad (5.61)$$

5.2. Numerical simulation for devices optimization

5.2.1 SINGLE BODY

The single body device optimization was performed for the geometry (radius in a range between 0.5 m and 20 m with a step of 0.5 m) and for the PTO damping coefficient (range between 5×10^4 kg/s and 10×10^5 kg/s with a step of 5×10^4 kg/s).

In this study 9 local wave climates, each consisting of a set of sea states were considered. Each sea state was characterized by a spectral distribution and a frequency of occurrence, and was an element of the wave climate matrix. The optimization, whose results are presented here, was performed for a wave climate off the coast of Tuscany, Sardinia and Liguria (see Paragraph 4.2.2).

The optimization procedure was implemented in MATLAB environment and followed different criteria that consisted in maximizing three objective functions, in order to consider the cost (5.62), particularly useful in the fully commercial stage, the efficiency (5.63) and the performance (5.64) of the device:

$$F_1(\nu) = \frac{\bar{P}_{ann}}{V_{sub}^\alpha} = \frac{\sum_{i=1}^N \phi_n \bar{P}_{irr,n}}{V_{sub}^\alpha} \quad \alpha = 0, 0.25, 0.5, 0.75 \quad (5.62)$$

where \bar{P}_{ann} is the annual average of the power extracted by the body, V_{sub} is the total submerged volume of the device and V_{sub}^α is a parameter approximately proportional to the total cost of the device (project, construction, maintenance, operation and decommissioning).

$$F_2(\nu) = \bar{P}_{ann}^* = \sum_{i=1}^N \phi_n \bar{P}_{irr,n} / \bar{P}_{max,irr,n} \quad (5.63)$$

$$F_3(\nu) = \bar{L}_{ann}^* = \sum_{i=1}^N \phi_n \bar{P}_{irr,n} / (\bar{E}_{w,n} \cdot d) \quad (5.64)$$

where d is the diameter of the floater and $\bar{E}_{w,n}$ (in kW/m) is the average flux of energy transported by the waves. The values of $\bar{E}_{w,n}$ on a 50 m water depth for the points 17 and 19 in Liguria, 19 in North of Tuscany, 9 in South of Tuscany and 9 in Sardinia and the values on a 15 m water depth for the points 7 in Liguria, 9 in North of Tuscany, 3 in South of Tuscany and 1 in Sardinia, were extracted by the results of the Mike21-SW simulations, inasmuch as the condition of deep water is not applicable.

For each optimization criterion a map of values of each combination (diameter, turbine damping coefficient) normalized with respect to the maximum value (see Appendix E) was obtained. Some examples are reported in Figure 5.7 for the Northern Tuscany, in Figure 5.12 for the Central Tuscany, in Figure 5.19 for the Liguria and in Figure 5.24 for the Sardinia.

5.2.1.1 Northern Tuscany area

The results of the optimization of the objective functions $F_{1,2,3}(\nu)$ are shown in the Table 5.2 for the point 9 and in the Table 5.3 for the point 19.

For each combination of radius and PTO damping coefficients in the Table 5.2 and Table 5.3 the ratio X_0 / A_w and P / P_{max} for the regular waves (Figure 5.5 and Figure 5.8), and the ratio P_{irr} / H_s^2 and $P_{irr} / P_{irr,max}$ for the irregular waves (Figure 5.6 and Figure 5.9) were computed. It is possible to note that the best results in terms of power and efficiency are given by the $F_{1,\alpha=0}$ with $T_c=6-7$ s, $F_{1,\alpha=0.25}$ and F_2 with $T_c=5-6$ s.

Table 5.2. Optimized values for the point 9 Northern Tuscany

Point 9 Northern Tuscany			
	F value	r	C
$F_1, \alpha=0$	16.49	15.5	1000000
$F_1, \alpha=0.25$	2.08	9.5	1000000
$F_1, \alpha=0.5$	0.40	4	450000
$F_1, \alpha=0.75$	0.25	1	50000
F_2	0.40	9	850000
F_3	0.26	3	100000

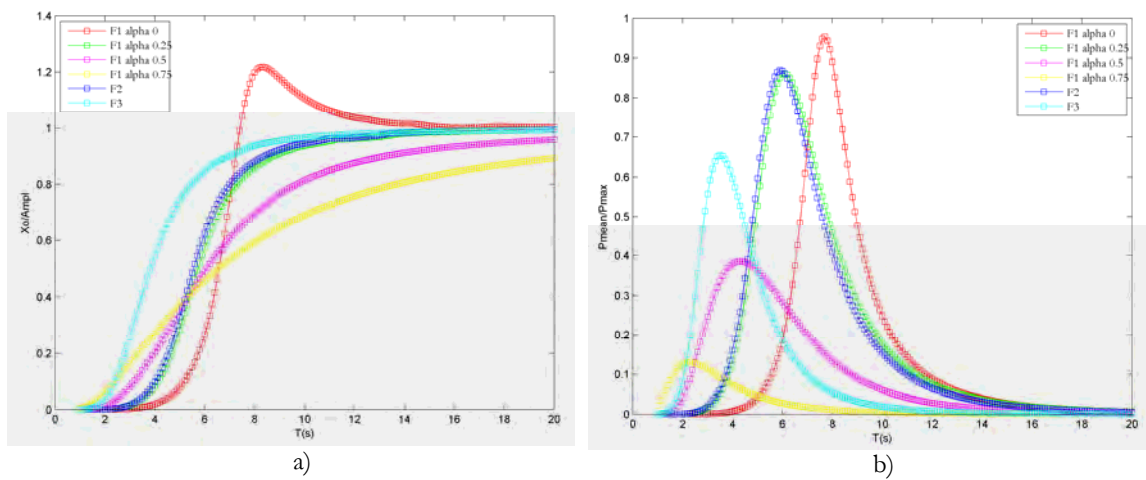


Figure 5.5. Point 9 – Regular waves for each optimization criterion: a) X_0/ampl , b) P/P_{max}

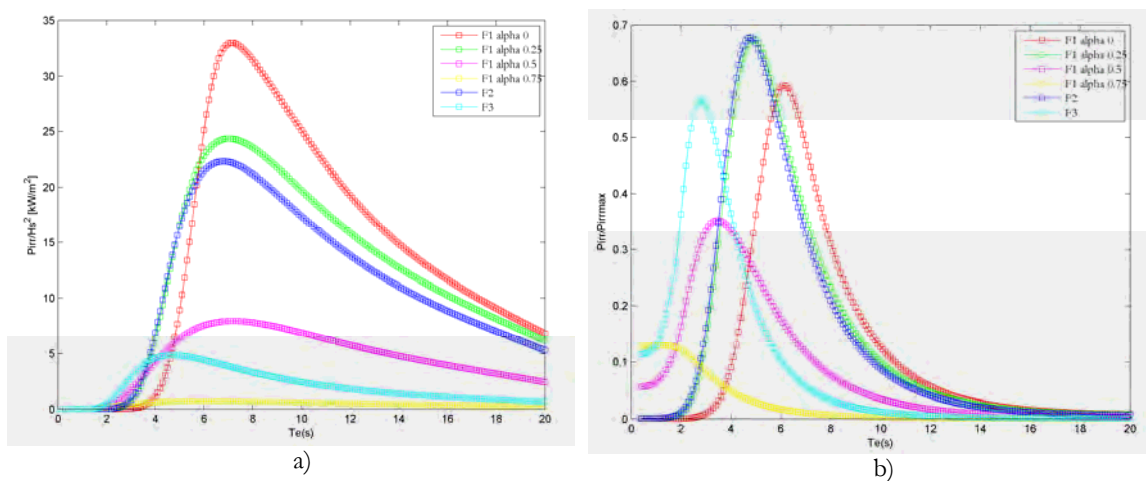


Figure 5.6. Point 9 – Irregular waves for each optimization criterion: a) P_{irr}/H_s^2 , b) $P_{\text{irr}}/P_{\text{maxirr}}$

Table 5.3. Optimized values for the point 19 Northern Tuscany

Point 19 Northern Tuscany			
	F value	r	C
$F_1, \alpha=0$	23.19	15.5	1000000
$F_1, \alpha=0.25$	2.89	10	1000000
$F_1, \alpha=0.5$	0.55	4	450000
$F_1, \alpha=0.75$	0.34	1	50000
F_2	0.39	9.5	1000000
F_3	0.27	4	200000

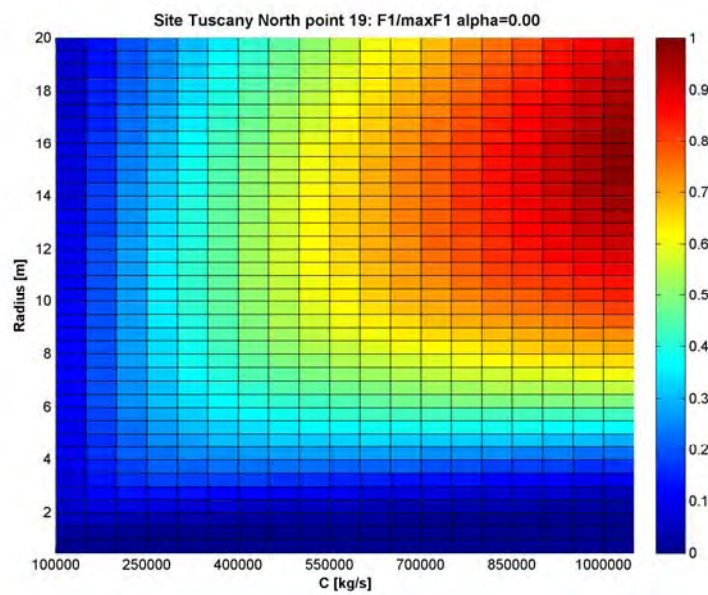


Figure 5.7. Point 19 – results of $F_1 \alpha=0$ normalized to the maximum value

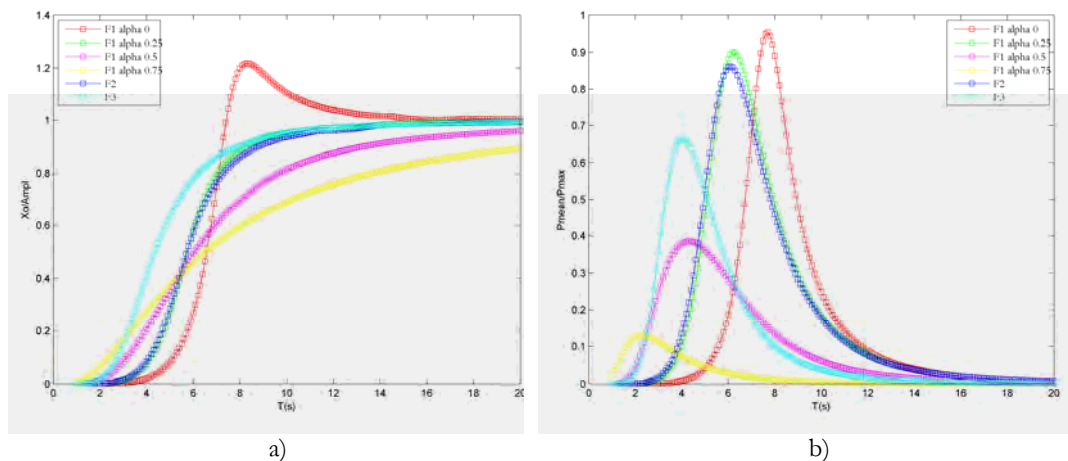


Figure 5.8. Point 19 – Regular waves for each optimization criterion: a) X_0/ampl , b) P/Pmax

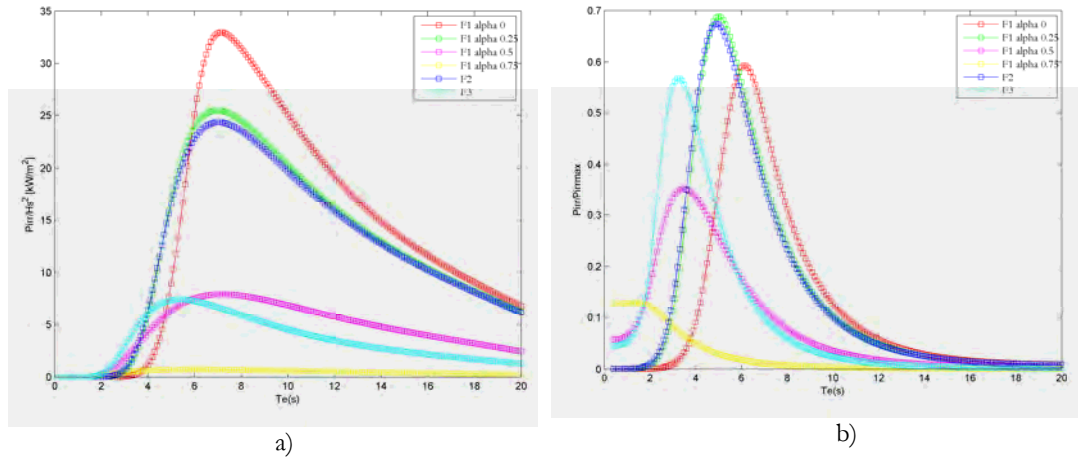


Figure 5.9. Point 19 – Irregular waves for each optimization criterion: a) P_{irr}/H_s^2 , b) P_{irr}/P_{maxirr}

5.2.1.2 Central Tuscany area

The results from the optimization of the objective functions $F_{1,2,3}(v)$ are shown in Table 5.4 for the point 3 and in Table 5.5 for the point 9.

For all the diameter-PTO damping coefficient combinations in Table 5.4 and Table 5.5, the trend of X_0/A_w and P/P_{max} for the regular waves (Figure 5.10 and Figure 5.13), and the trend of P_{irr}/H_s^2 and P_{irr}/P_{irrmax} for the irregular waves (Figure 5.11 and Figure 5.14) were computed.

The best results in terms of power and efficiency are given by the $F_{1,\alpha=0}$ with a value of P_{irr}/H_s^2 over 30 kW/m² for $T_e=7$ s, $F_{1,\alpha=0.25}$ and F_2 with a value of P_{irr}/H_s^2 around 20-25 kW/m² for $T_e=6-7$ s.

Table 5.4. Optimized values for the point 3 Central Tuscany

Point 3 Central Tuscany			
	F value	r	C
$F_1, \alpha=0$	15.60	15.5	1000000
$F_1, \alpha=0.25$	1.95	9.5	1000000
$F_1, \alpha=0.5$	0.37	4	450000
$F_1, \alpha=0.75$	0.23	1	50000
F_2	0.40	9	900000
F_3	0.29	2	50000

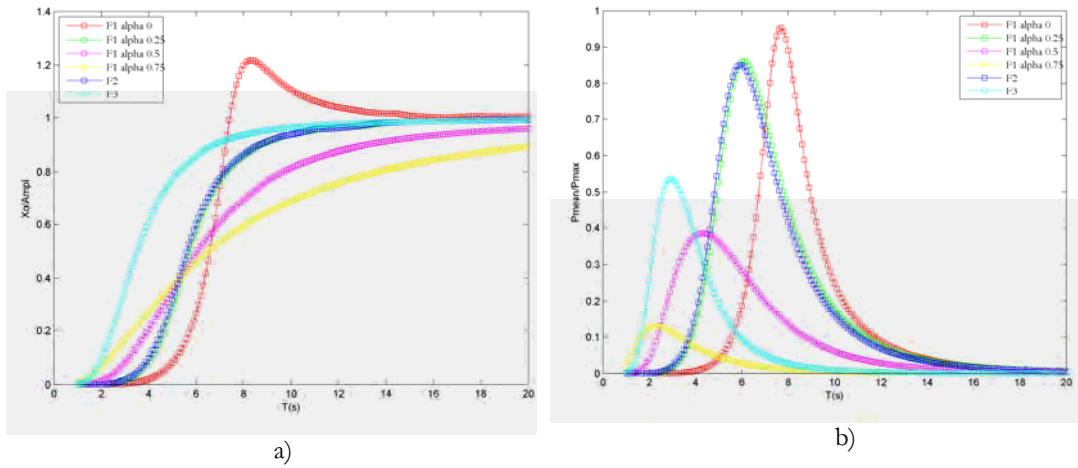


Figure 5.10. Point 3 – Regular waves for each optimization criterion: a) $X_0/ampl$, b) P/P_{max}

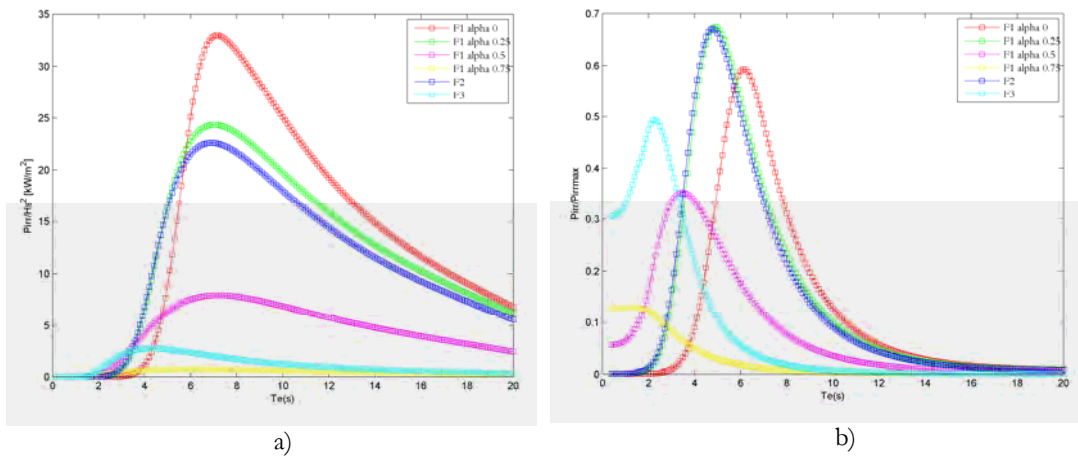


Figure 5.11. Point 3 – Irregular waves for each optimization criterion: a) P_{max}^2/Hs^2 , b) P_{max}/P_{maxirr}

Table 5.5. Optimized values for the point 9 Central Tuscany

Point 9 Central Tuscany			
	F value	r	C
$F_1, \alpha=0$	20.99	15.5	1000000
$F_1, \alpha=0.25$	2.61	10	1000000
$F_1, \alpha=0.5$	0.50	4	450000
$F_1, \alpha=0.75$	0.30	1	50000
F_2	0.39	9.5	1000000
F_3	0.27	3.5	150000

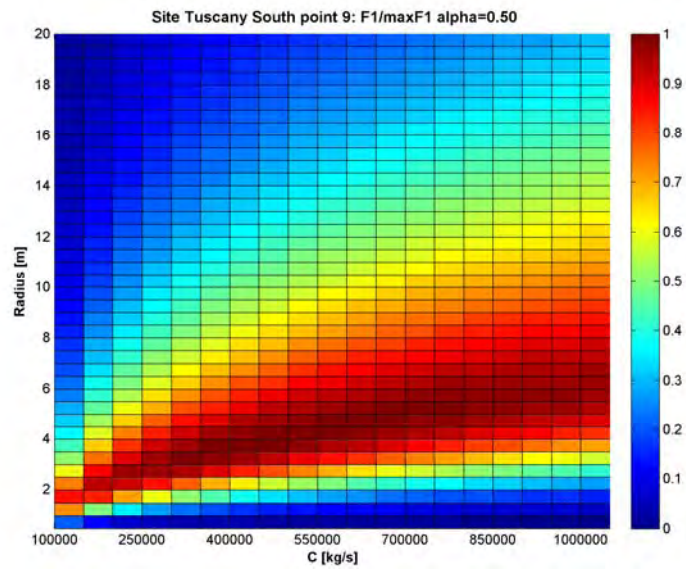


Figure 5.12. Point 9 – results of $F_1 \alpha=0.5$ normalized to the maximum value

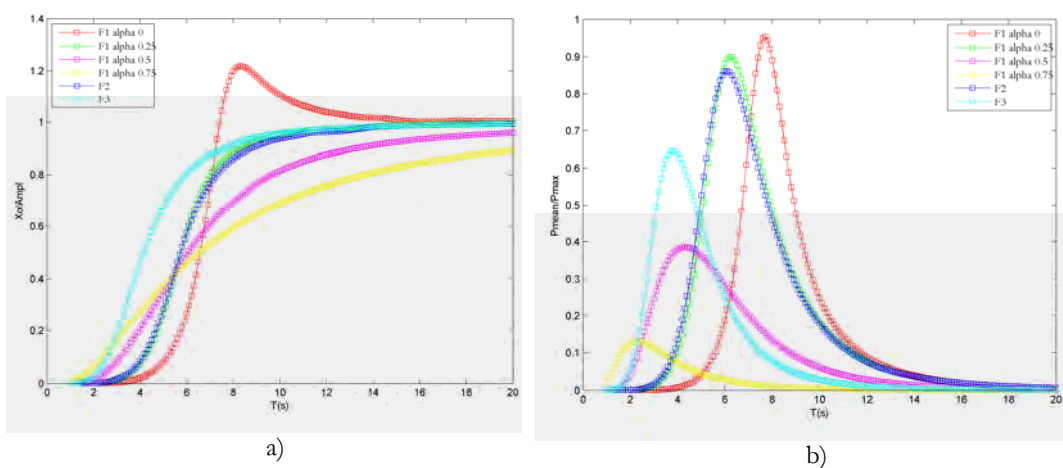


Figure 5.13. Point 9 – Regular waves for each optimization criterion: a) $X_o/ampl$, b) P/P_{max}

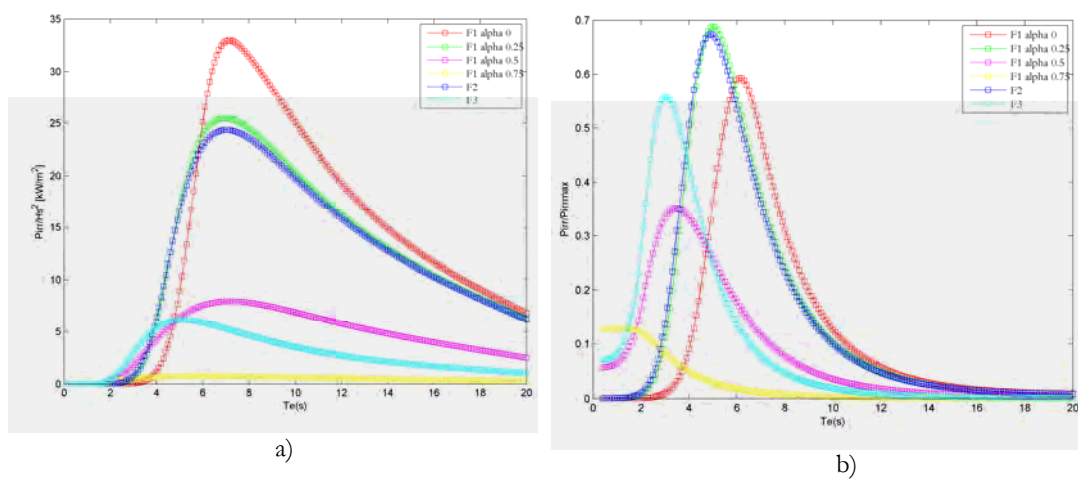


Figure 5.14. Point 9 – Irregular waves for each optimization criterion: a) $Pirr/Hs^2$, b) $Pirr/P_{maxirr}$

5.2.1.3 Liguria area

The results of the optimization of the objective functions $F_{1,2,3}(v)$ are shown in Table 5.6 for the point 7, in Table 5.7 for the point 17 and in Table 5.8 for the point 19.

For the 18 combinations of diameter-PTO damping coefficients in Table 5.6, Table 5.7 and Table 5.8 the X_0 / A_w and P / P_{\max} for the regular waves (Figure 5.15, Figure 5.17 and Figure 5.20), and the P_{irr} / H_s^2 and $P_{\text{irr}} / P_{\text{irr}\max}$ for the irregular waves (Figure 5.16, Figure 5.18 and Figure 5.21) were computed. The best results in terms of power are given by the $F_{1,\alpha=0}$ with a value of P_{irr} / H_s^2 over 30 kW/m² for $T_c=6$ s and $F_{1,\alpha=0.25}$ with a value of P_{irr} / H_s^2 around 20-25 kW/m² for $T_c=6$ s. In term of efficiency the F_2 also reaches high values.

Table 5.6. Optimized values for the point 7 Liguria

Point 7 Liguria			
	F value	r	C
F1, a=0	9.71	13	1000000
F1, a=0.25	1.32	9.5	1000000
F1, a=0.5	0.27	2.5	150000
F1, a=0.75	0.17	1	50000
F2	0.43	7	450000
F3	0.25	3.5	150000

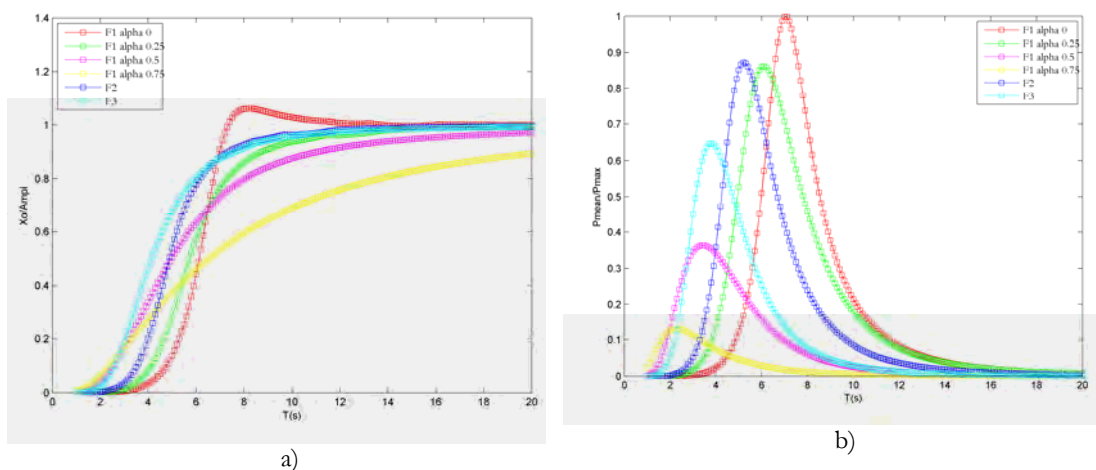


Figure 5.15. Point 7 – Regular waves for each optimization criterion: a) X_0/ampl , b) P/P_{\max}

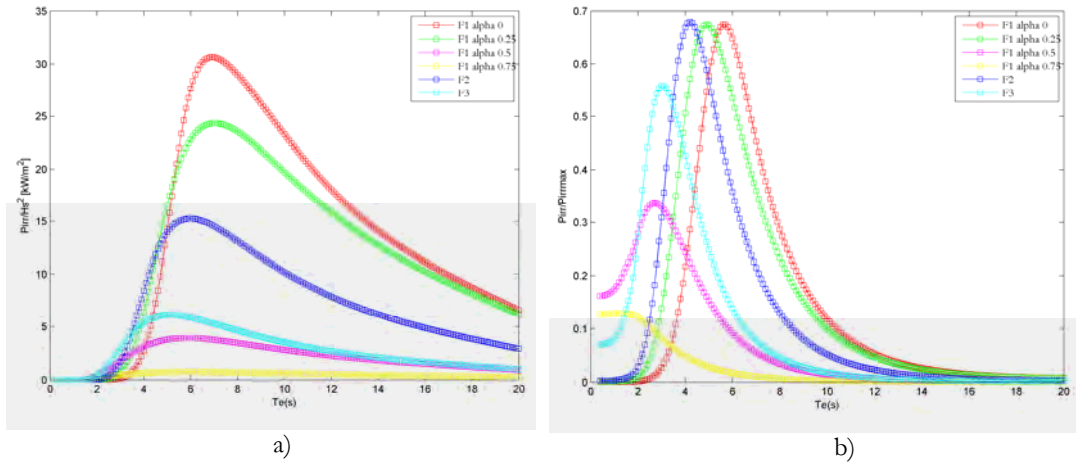


Figure 5.16. Point 7 – Irregular waves for each optimization criterion: a) P_{irr}/H_s^2 , b) P_{irr}/P_{maxirr}

Table 5.7. Optimized values for the point 17 Liguria

Point 17 Liguria			
	F value	r	C
F1, a=0	11.15	13	1000000
F1, a=0.25	1.51	9.5	1000000
F1, a=0.5	0.31	2.5	150000
F1, a=0.75	0.20	1	50000
F2	0.43	7.5	500000
F3	0.26	4	200000

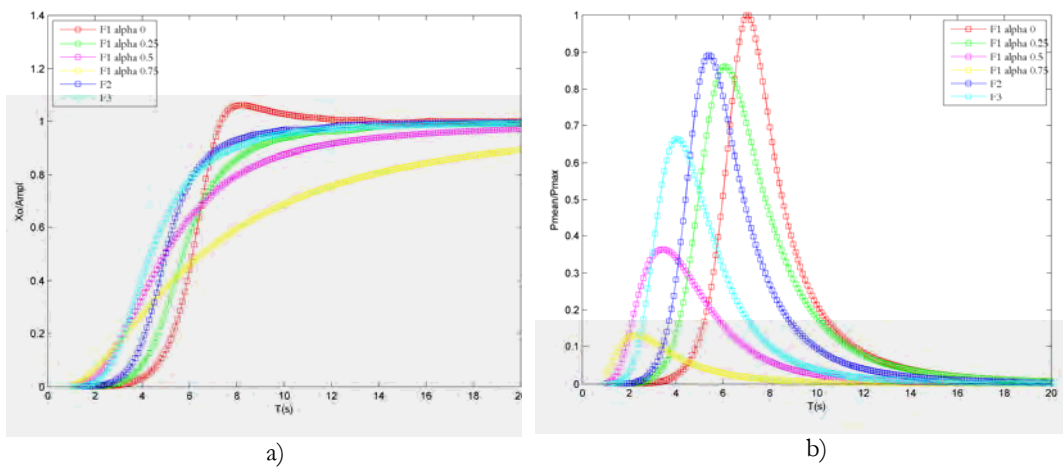


Figure 5.17. Point 17 – Regular waves for each optimization criterion: a) $X_0/ampl$, b) P/P_{max}

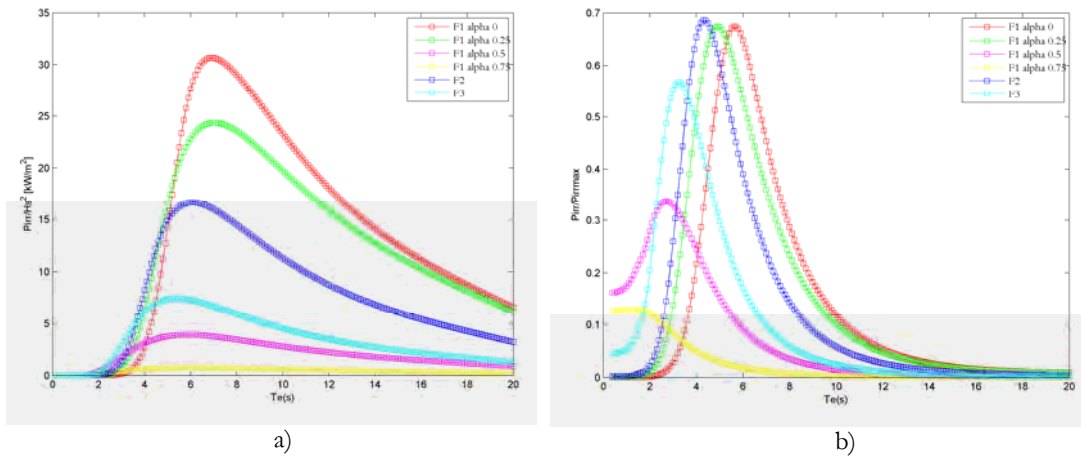


Figure 5.18. Point 17 – Irregular waves for each optimization criterion: a) P_{irr}/H_s^2 , b) P_{irr}/P_{maxirr}

Table 5.8. Optimized values for the point 19 Liguria

	Point 19 Liguria		
	F value	r	C
F1, a=0	11.22	13	1000000
F1, a=0.25	1.52	9.5	1000000
F1, a=0.5	0.32	2.5	150000
F1, a=0.75	0.20	1	50000
F2	0.43	7	450000
F3	0.26	4	200000

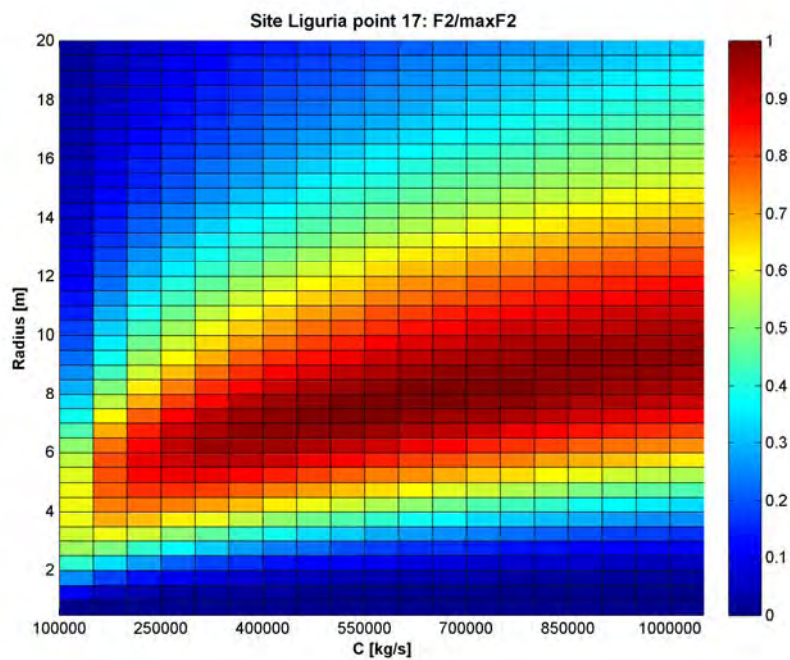


Figure 5.19. Point 17 – results of F_2 normalized to the maximum value

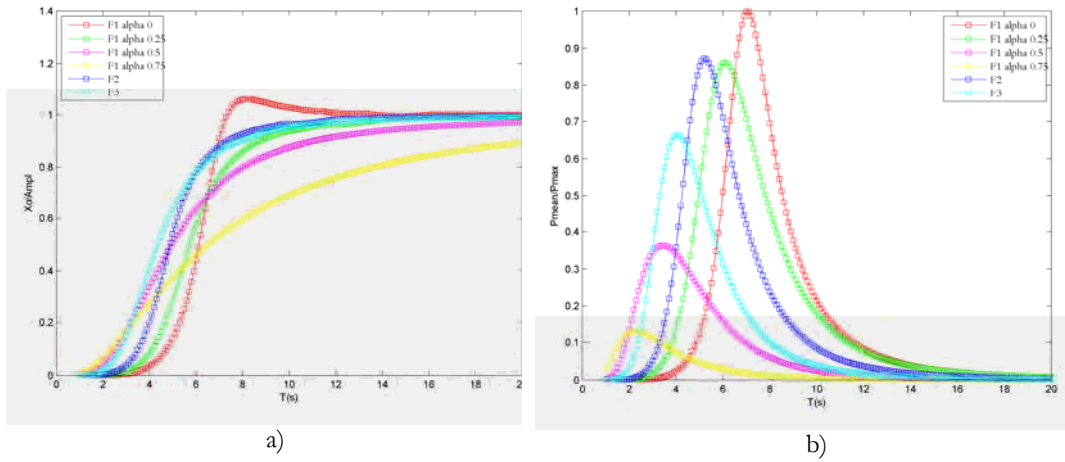


Figure 5.20. Point 19 – Regular waves for each optimization criterion: a) $X_0/ampl$, b) P/P_{max}

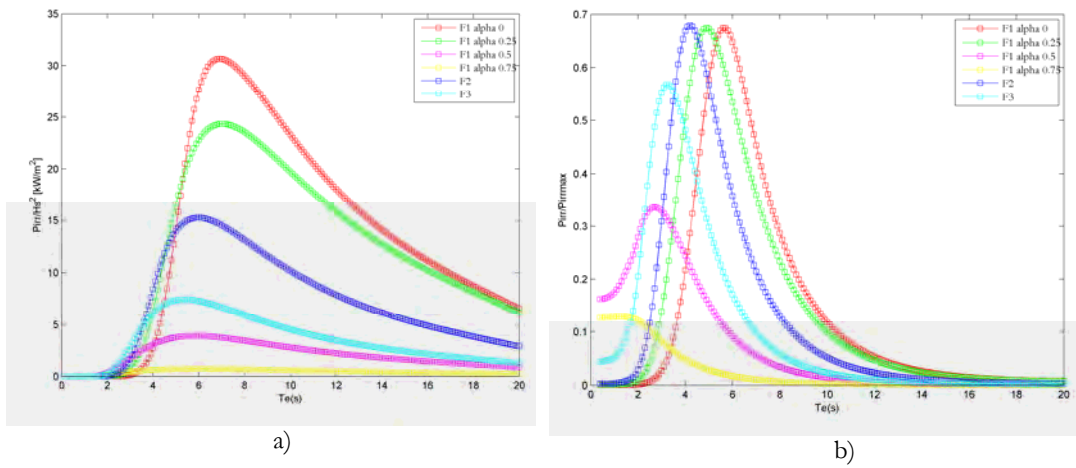


Figure 5.21. Point 19 – Irregular waves for each optimization criterion: a) P_{irr}/H_s^2 , b) P_{irr}/P_{maxirr}

5.2.1.4 Sardinia area

The results of the optimization of the objective functions $F_{1,2,3}(v)$ are shown in Table 5.9, for the point 1, and in Table 5.10 for the point 9.

For each combination of diameter-PTO damping coefficient in Table 5.9 and in Table 5.10 the values of X_0/A_w and P/P_{max} for the regular waves (Figure 5.22 and Figure 5.25), and the value of P_{irr}/H_s^2 and P_{irr}/P_{maxirr} for the irregular waves (Figure 5.23 and Figure 5.26) were computed. Like for the previous site, the best results in terms of power are obtained with the functions $F_{1,\alpha=0}$ with a value of P_{irr}/H_s^2 over 30 kW/m² for $T_e=7$ s and

$F_{1,\alpha=0.25}$ with a value of P_{irr} / H_s^2 near 25 kW/m² for $T_e=7$ s. But in terms of efficiency results the better functions are $F_{1,\alpha=0.25}$ for $T_e=5$ s and F_3 for $T_e=4$ s.

Table 5.9. Optimized values for the point 1 Sardinia

Point 1 Sardinia			
	F value	r	C
F1, a=0	64.29	17	1000000
F1, a=0.25	7.80	9.5	1000000
F1, a=0.5	1.51	5	800000
F1, a=0.75	0.88	1	50000
F2	0.41	10	1000000
F3	0.25	6	500000

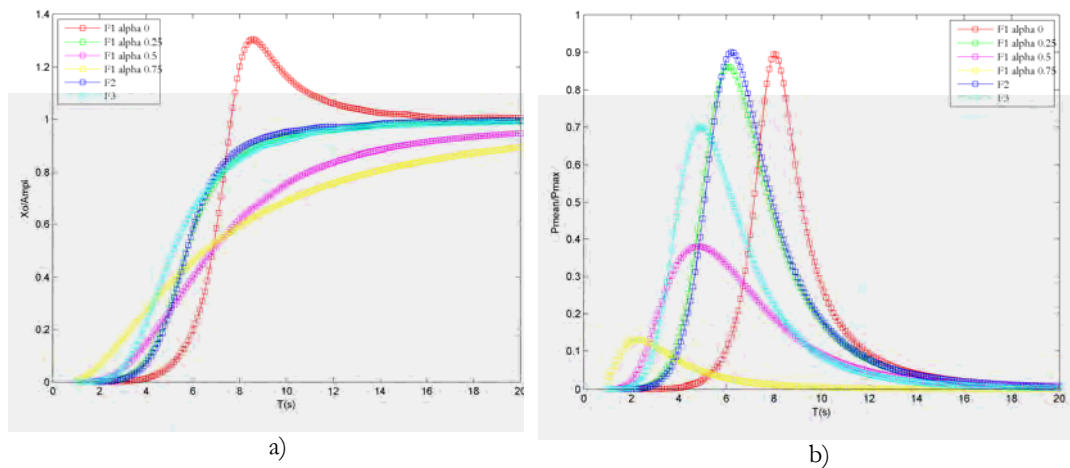


Figure 5.22. Point 1 – Regular waves for each optimization criterion: a) X_0/ampl , b) P/P_{max}

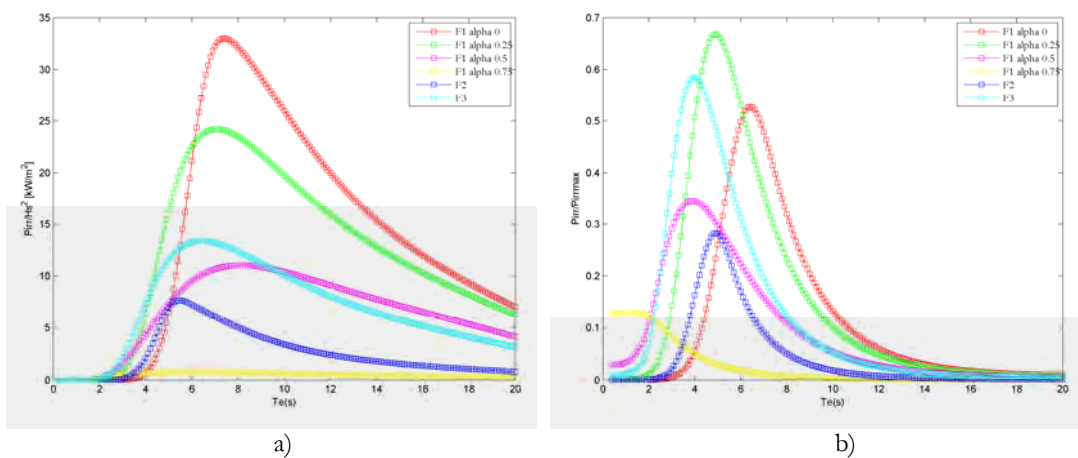


Figure 5.23. Point 1 – Irregular waves for each optimization criterion: a) P_{irr}/H_s^2 , b) $P_{irr}/P_{\text{maxirr}}$

Table 5.10. Optimized values for the point 9 Sardinia

Point 9 Sardinia			
	F value	r	C
F1, a=0	67.76	16.5	1000000
F1, a=0.25	8.21	9.5	1000000
F1, a=0.5	1.58	5	750000
F1, a=0.75	0.92	1	50000
F2	0.41	10	1000000
F3	0.27	6.5	600000

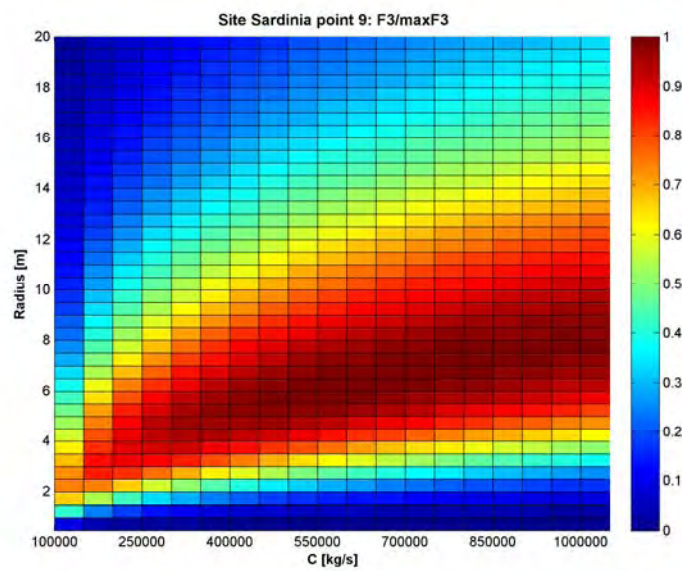


Figure 5.24. Point 9 – results of F₃ normalized to the maximum value

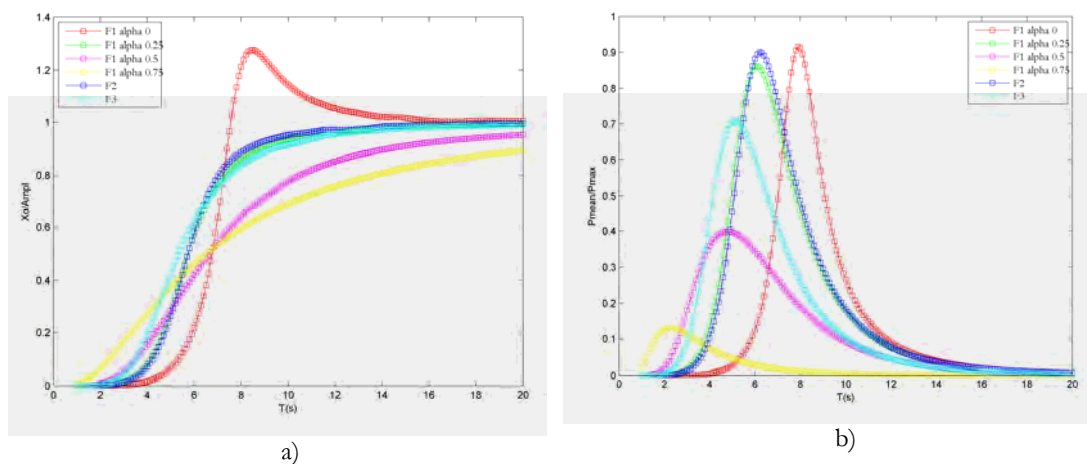


Figure 5.25. Point 9 – Regular waves for each optimization criterion: a) X_0/ampl , b) P/Pmax

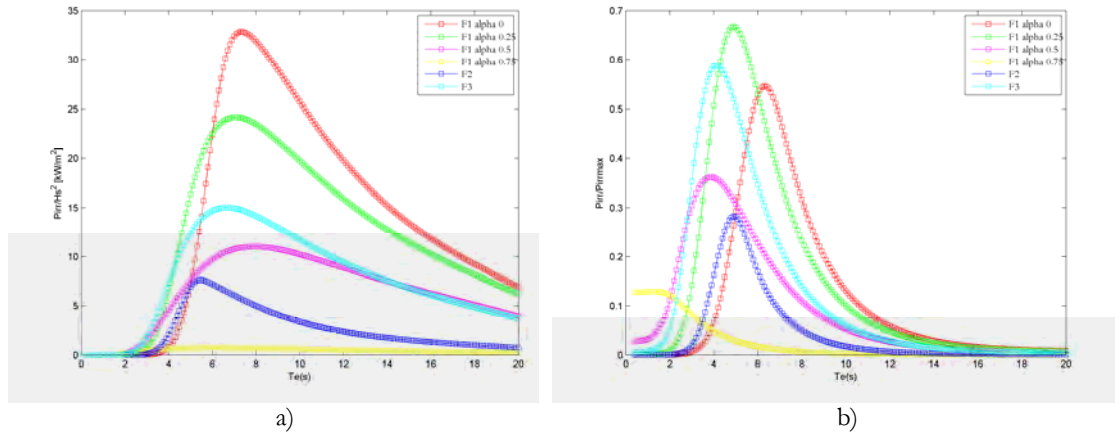


Figure 5.26. Point 9 – Irregular waves for each optimization criterion: a) P_{irr}/H_s^2 , b) P_{irr}/P_{maxirr}

5.2.2 SPAR-BUOY OWC

The Spar-Buoy OWC geometries summarized in Table 5.11 were analyzed in order to optimize the turbine rotor diameter (range between 1 m and 3.5 m with a step of 0.1 m) and the turbine rotational speed (range between 50 rad/s and 200 rad/s with a step of 10 rad/s), following the two criteria represented by the objective functions in eqs. (5.65) and (5.66).

$$F_1(v) = \frac{\bar{P}_{t,ann}}{V_{sub}^\alpha} = \frac{\sum_{i=1}^N \phi_n \bar{P}_{t,n}}{V_{sub}^\alpha} \quad \alpha = 0, 0.25, 0.5, 0.75 \quad (5.65)$$

In the eq. (5.65) $\bar{P}_{t,ann}$ is the annual average of the power output of the turbine, V_{sub} is the total submerged volume of the floater and V_{sub}^α is a parameter approximately proportional to the total cost of the device (project, construction, maintenance, operation and decommissioning). It is important to highlight that the $F_1(v)$ with $\alpha = 0$ represents the value of the annual power output of the turbine.

$$F_2(v) = \bar{L}_{ann}^* = \sum_{i=1}^N \phi_n \bar{P}_{t,n} / (\bar{E}_{w,n} \cdot d_1) \quad (5.66)$$

In the eq. (5.66) d_1 is the diameter of the floater and $\bar{E}_{w,n}$ (in kW/m) is the average flux of energy transported by the waves. The values of $\bar{E}_{w,n}$ on a 50 m water depth for the points 17 and 19 in Liguria, 19 in North of Tuscany, 9 in South of Tuscany and 9 in

Sardinia were extracted by the results of the Mike21-SW simulations, inasmuch as the condition of deep water is not applicable.

Table 5.11. Analyzed Spar-Buoy OWC geometries [72]

Case	l_{max} (m)	d_1 (m)	d_2 (m)
A	24	8	3.7
B	36	8	2.7
E	24	12	5.9
F	36	12	4.8
I	24	16	9.4
J	36	16	7.1
M	24	20	12
N	36	20	9.7

This optimization procedure was performed for a wave climate off the western coast of Tuscany, Sardinia and Liguria on 50 m water depth (see Paragraph 4.2.2). The points on 15 m water depth were not considered because the draught of the device is 24 m or 36 m.

The frequency dependent linear hydrodynamic coefficients (A_{11} , $A_{12} = A_{21}$, A_{22} , B_{11} , $B_{12} = B_{21}$, B_{22} , Γ_1 and Γ_2) were computed for 52 frequencies equally spaced between 0.205 and 2.500 rad/s assuming the deep water condition [72]. These results were obtained by the IDMEC-IST researchers in Lisbon, using the commercial boundary element method (BEM) WAMIT.

The turbine considered in this analysis is a biradial self-rectifying air turbine, that was studied at IDMEC-IST. The biradial turbine is an alternative to the self-rectifying axial-flow impulse turbine. The turbine is symmetrical with respect to a plane perpendicular to its axis of rotation, and is a radial-flow machine at both inlet and outlet [75].

Assuming that, for the frequency domain analysis, the biradial turbine is linear, with $K=0.28401$, the dimensionless curves are given by

$$\Phi = K\Psi = 0.28401\Psi \quad (5.67)$$

$$\begin{cases} \eta = -231.75\Phi^2 + 41.526\Phi - 1.0917 & (\Psi \leq 0.07) \\ \eta = 2166.7\Phi^3 - 720\Phi^2 + 78.383\Phi - 2.022 & (0.07 < \Psi \leq 0.105) \\ \eta = 0.4444\Phi^3 + 0.4762\Phi^2 - 1.3821\Phi + 0.9183 & (0.105 < \Psi \leq 0.4) \\ \eta = -0.95\Phi + 0.8475 + 0.0022 & (\Psi > 0.4) \end{cases} \quad (5.68)$$

The eqs.(5.67) and (5.68) are based on results from the numerical simulation of the air flow through the turbine computed at IDMEC-IST.

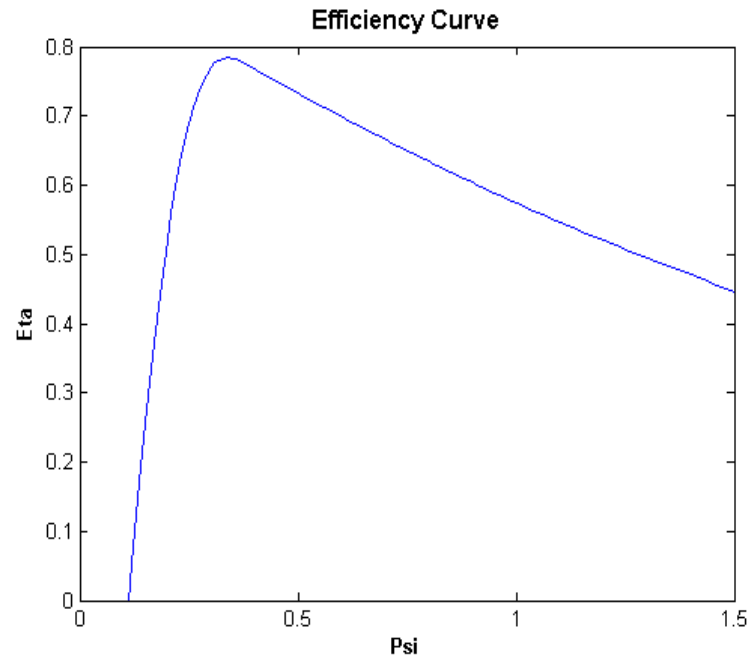


Figure 5.27. Efficiency curve

The Figure 5.27 shows the efficiency curve for psi values between 0 and 1.5, obtained from the eqs. (5.67) and (5.68) .

For each optimization criterion a map of values, for the optimum geometry, of each combination (turbine rotor diameter, turbine rotational speed) normalized with respect to the maximum value (see Appendix E) was obtained. Some examples are reported in Figure 5.29 for the Northern Tuscany, in Figure 5.32 for the Central Tuscany, in Figure 5.35 and Figure 5.36 for the Liguria and in Figure 5.39 for the Sardinia.

The chamber height h needs to be high enough to prevent green water from reaching the turbine. Analysing the two bodies (floater and piston) oscillations it was assumed that the chamber height was constant and equal to 10 m for the hot-spots in Tuscany and Liguria and equal to 12 m in Sardinia. Fixing the chamber height, the volume of the chamber (V_0) only depends on the diameter of the hollow cylinder body. The chamber volume is known to broaden the power absorption spectrum due to the spring-like effect of air compressibility [72].

Figure 5.28 shows the influence of the chamber height on the \bar{L}_{ann}^* values of the eq. (5.66), obtained with the optimum geometry selected for each site. The lowest objective function values are for the Liguria hot-spots, while the highest values are for the Sardinia

hot-spot (Table 5.12). E.g: for a chamber height between 14 m and 30 m, the optimum value of the turbine rotational speed of Central Tuscany hot-spot decreases from 60 rad/s to 50 rad/s, and between 18 m and 30 m, the optimum geometry of the Sardinia hot-spot switches from the case E in Table 5.11 to the case J.

Table 5.12. $L_{c,ann}^*$ values on varying of chamber height

	h [m]					
	0	10	20	30	40	50
Point 19 Northern Tuscany	0.073	0.076	0.079	0.079	0.077	0.075
Point 9 Central Tuscany	0.075	0.077	0.080	0.080	0.078	0.076
Point 17 Liguria	0.058	0.062	0.065	0.064	0.062	0.061
Point 19 Liguria	0.058	0.061	0.064	0.064	0.061	0.060
Point 9 Sardinia	0.091	0.093	0.095	0.097	0.096	0.096

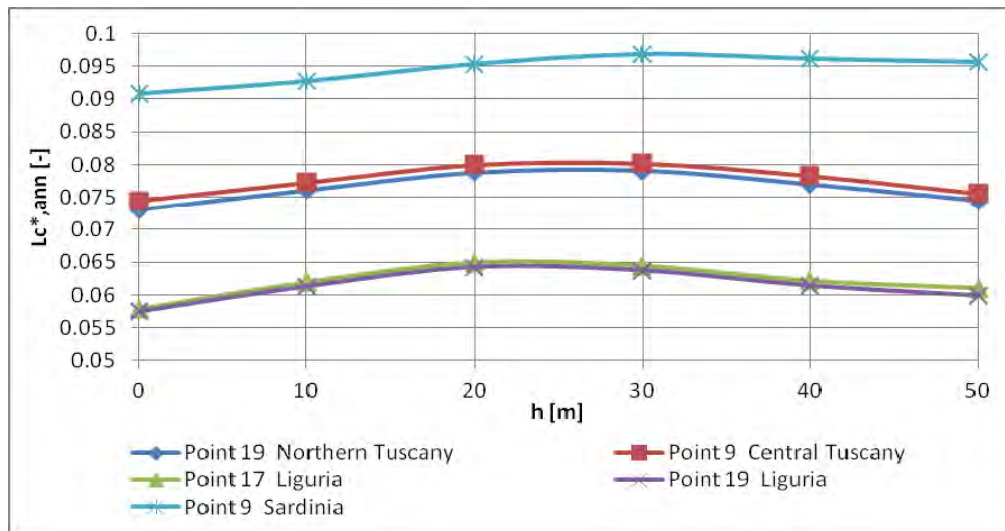


Figure 5.28. The influence of the chamber height on the performance of the optimized devices

5.2.2.1 Northern Tuscany area

The results of the optimization of the objective functions $F_{1,2}(v)$ are shown in Table 5.13. For each combination of geometry, turbine rotor diameter and the turbine rotational speed (shown in Table 5.13), the values of $X/ampl$ and $Y/ampl$ and $L_{c,reg}$ for the regular waves (Figure 5.30), and the value of P_t/H_s^2 and $L_{c,irr}$ for the irregular waves (Figure 5.31) were computed. The best results in terms of power and in terms of

performance ($L_{c,irr}$) are obtained with the function $F_{1,\alpha=0-0.25}$ with a value, for $T_c=9$ s, of P_t / H_s^2 about 25 kW/m^2 and of $L_{c,irr}$ about 0.08. In the regular waves, in the case of the function $F_{1,\alpha=0.5-0.75}$, the piston oscillations reaches, for $\omega = 0.6$ a height of 9 m, and for $\omega = 0.75$ a height of 6 m. In this second peak the piston oscillations ($Y / ampl$) are in phase with the floater oscillations ($X / ampl$), in fact the capture length value reaches 0.8, while for the first peak is lower than 0.3.

Table 5.13. Optimized values for the point 19 Northern Tuscany

Point 19 Northern Tuscany				
	F value	N [rad/s]	D [m]	Geometry
F1, a=0 (Pt)	11.60	60	1.9	N
F1, a=0.25	1.62	60	1.9	N
F1, a=0.5	0.32	100	1.1	B
F1, a=0.75	0.08	100	1.1	B
F2	0.08	60	1.4	J

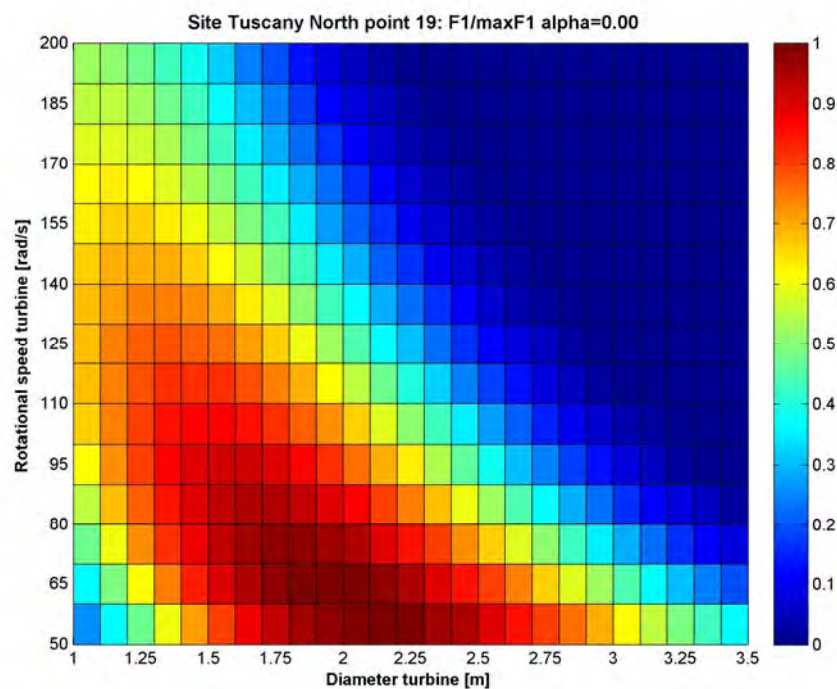


Figure 5.29. Point 19 – results of $F_1 \alpha=0$ normalized to the maximum value (geometry N)

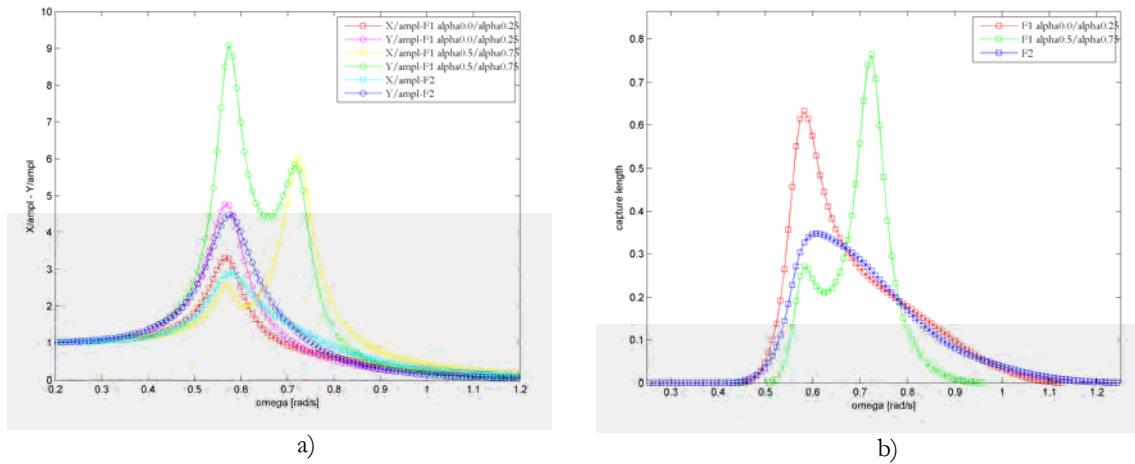


Figure 5.30. Point 19 – Regular waves for each optimization criterion: a) $X/ampl$ and $Y/ampl$, b) $L_{c,reg}$

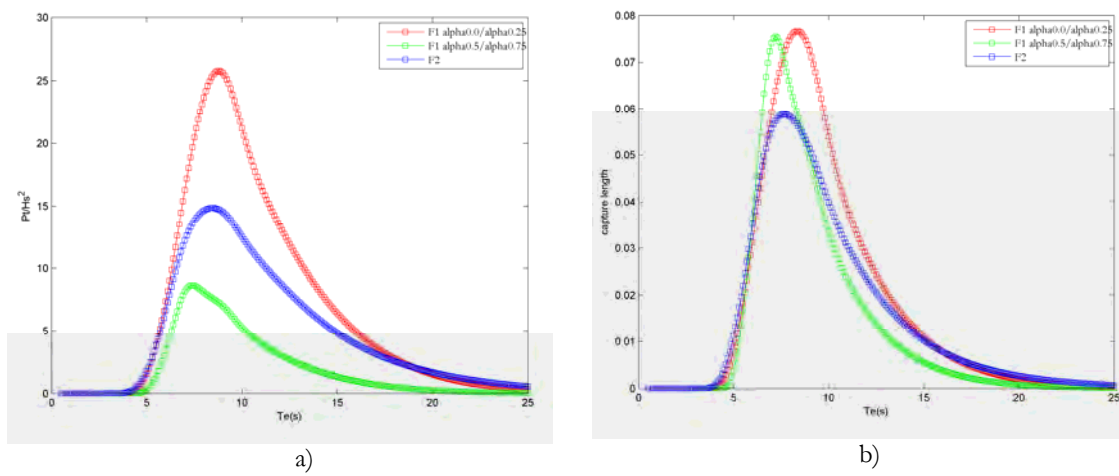


Figure 5.31. Point 19 – Irregular waves for each optimization criterion: a) P_t/H_s^2 , b) $L_{c,irr}$

5.2.2.2 Central Tuscany area

The results of the optimization of the objective functions $F_{1,2}(v)$ are shown in Table 5.14. For each combination of geometry, turbine rotor diameter and turbine rotational speed (shown in Table 5.14), the values of $X / ampl$ and $Y / ampl$ and $L_{c,reg}$ for the regular waves (Figure 5.33), and the value of P_t / H_s^2 and $L_{c,irr}$ for the irregular waves (Figure 5.34) were computed.

The best results in terms of power are obtained with the function $F_{1,\alpha=0-0.25}$ with a value, for $T_c=9$ s, of P_t / H_s^2 about 25 kW/m² and in terms of performance are obtained with the function $F_{1,\alpha=0.5-0.75}$ with a value, for $T_c=7.5$ s of $L_{c,irr}$ about 0.075. In the regular waves the results are similar to those obtained for the Northern Tuscany hot-spot.

Table 5.14 Optimized values for the point 9 Central Tuscany

Point 9 Central Tuscany				
	F value	N [rad/s]	D [m]	Geometry
F1, a=0 (Pt)	10.81	50	2	N
F1, a=0.25	1.51	50	2	N
F1, a=0.5	0.29	100	1.1	B
F1, a=0.75	0.08	100	1.1	B
F2	0.08	60	1.4	J

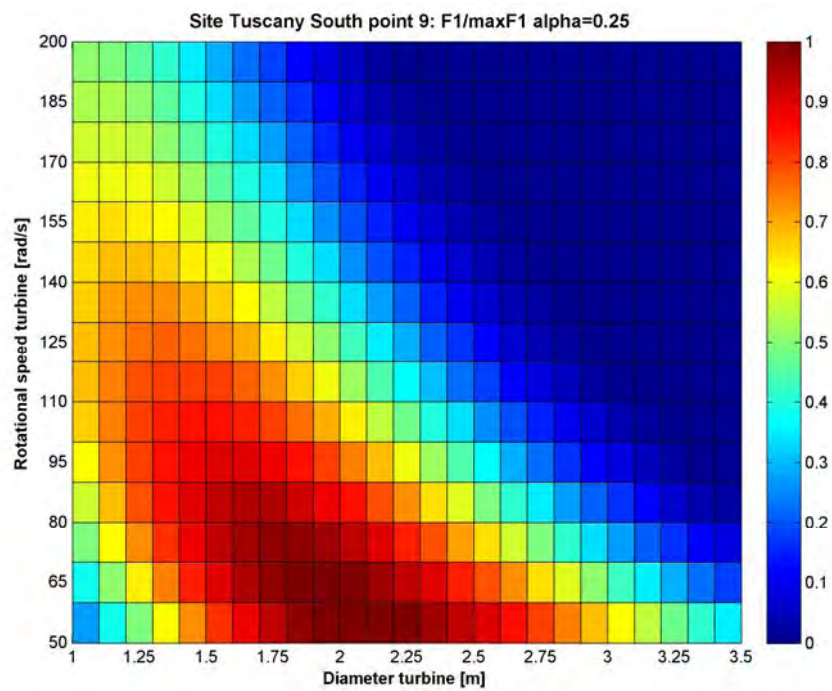


Figure 5.32. Point 9 – results of $F_1 \alpha=0.25$ normalized to the maximum value (geometry N)

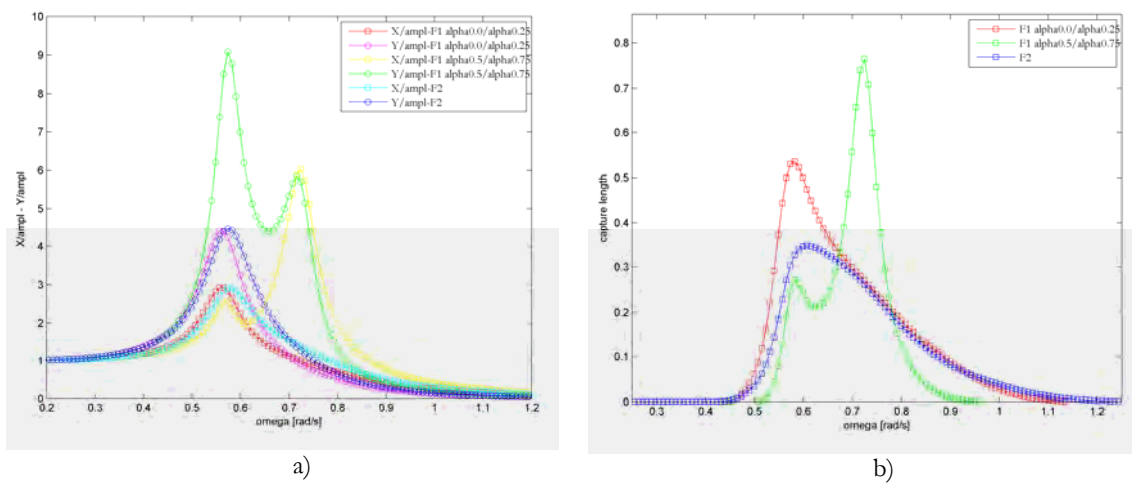


Figure 5.33. Point 9 – Regular waves for each optimization criterion: a) $X/ampl$ and $Y/ampl$, b) $L_{c,reg}$

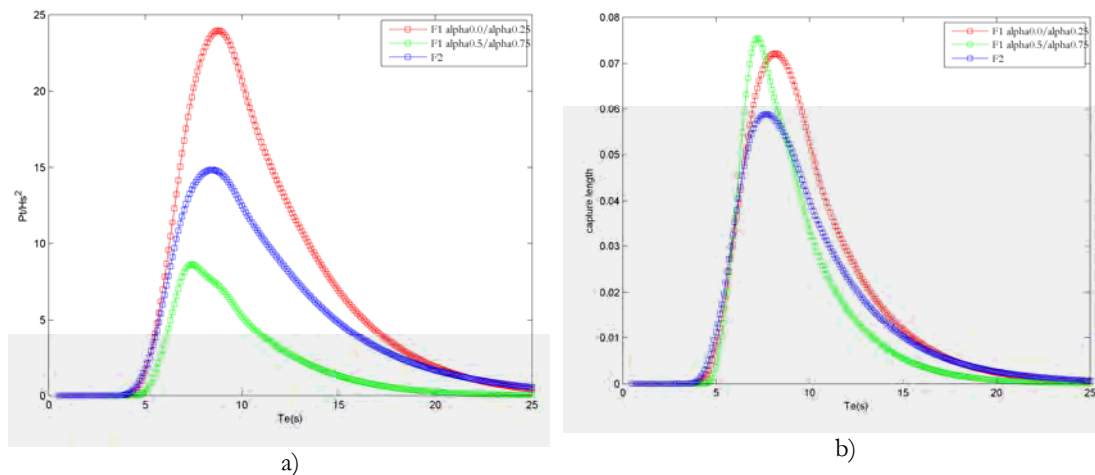


Figure 5.34. Point 9 – Irregular waves for each optimization criterion: a) P_t/H_s^2 , b) $L_{c,irr}$

5.2.2.3 Liguria area

The results of the optimization of the objective functions $F_{1,2}(v)$ are shown in Table 5.15, for the point 17, and in Table 5.16, for the point 19.

For each combination of geometry, turbine rotor diameter and turbine rotational speed (shown in Table 5.15 and Table 5.16), the values of $X / ampl$ and $Y / ampl$ and $L_{c,reg}$ for the regular waves (Figure 5.37), and the value of P_t / H_s^2 and $L_{c,irr}$ for the irregular waves (Figure 5.38) were computed.

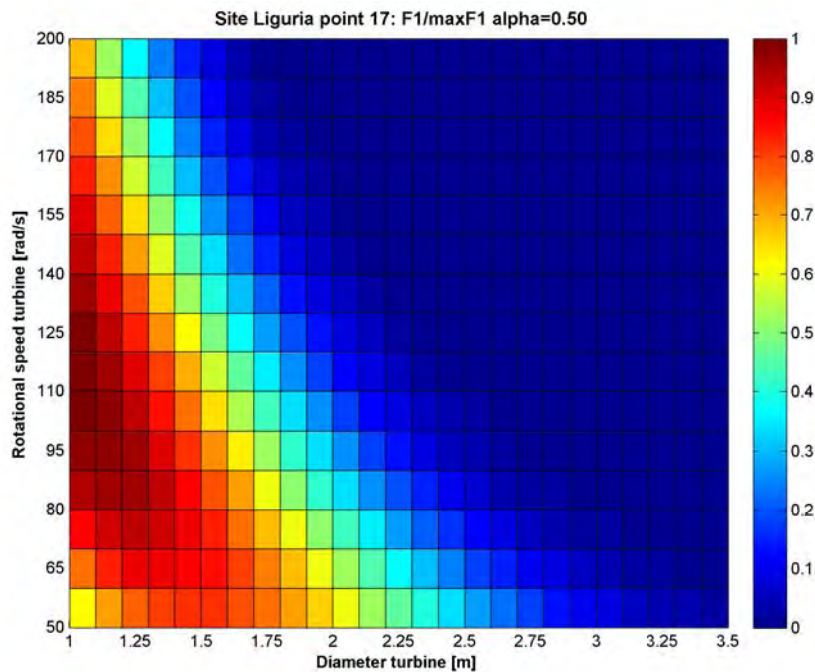
Table 5.15. Optimized values for the point 17 Liguria

Point 17 Liguria				
	F value	N [rad/s]	D [m]	Geometry
F1, a=0 (Pt)	5.20	50	1.9	N
F1, a=0.25	0.72	50	1.9	N
F1, a=0.5	0.14	110	1	B
F1, a=0.75	0.04	110	1	B
F2	0.06	50	1.3	J

Table 5.16. Optimized values for the point 19 Liguria

Point 19 Liguria				
	F value	N [rad/s]	D [m]	Geometry
F1, a=0 (Pt)	5.29	50	1.9	N
F1, a=0.25	0.74	50	1.9	N
F1, a=0.5	0.14	110	1	B
F1, a=0.75	0.04	110	1	B
F2	0.06	50	1.3	J

The best results in terms of power are obtained with the function $F_{1,\alpha=0-0.25}$ with a value, for $T_c=9$ s, of P_i/H_s^2 about 25 kW/m² and in terms of $L_{c,irr}$ are obtained with the function $F_{1,\alpha=0.5-0.75}$ with a value, for $T_c=7$ s of $L_{c,irr}$ about 0.075. In the regular waves, in the case of the function $F_{1,\alpha=0.5-0.75}$, the piston oscillations reaches, for $\omega=0.6$ an height of 8 m, and for $\omega=0.75$ an height of 5 m. In this second peak the piston oscillations ($Y / ampl$) are in phase with the floater oscillations ($X / ampl$), in fact the capture length value reaches 0.65, while for the first peak is lower than 0.3.

Figure 5.35. Point 17 – results of $F_1 \alpha=0.5$ normalized to the maximum value (geometry B)

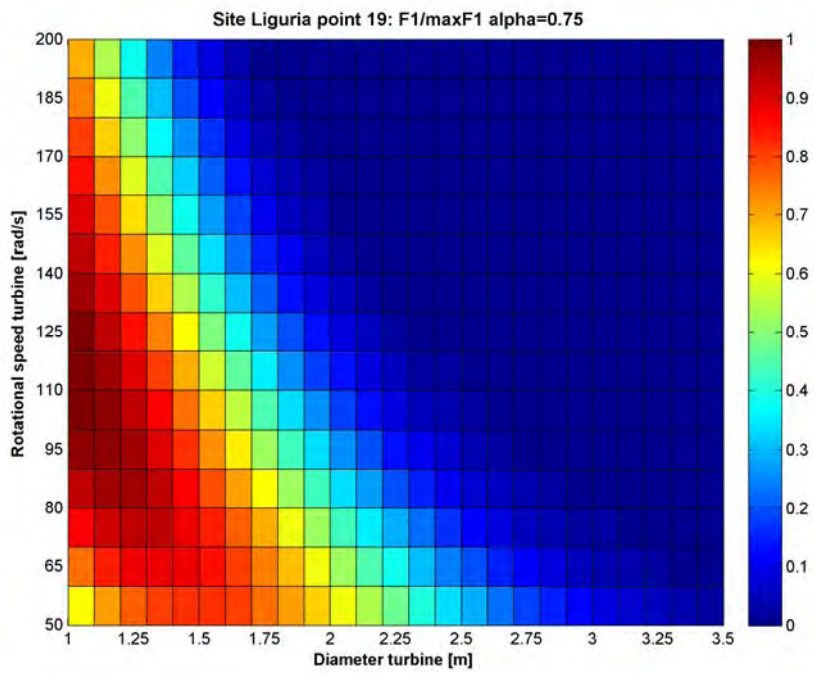


Figure 5.36. Point 19 – results of $F_1 \alpha=0.75$ normalized to the maximum value (geometry B)

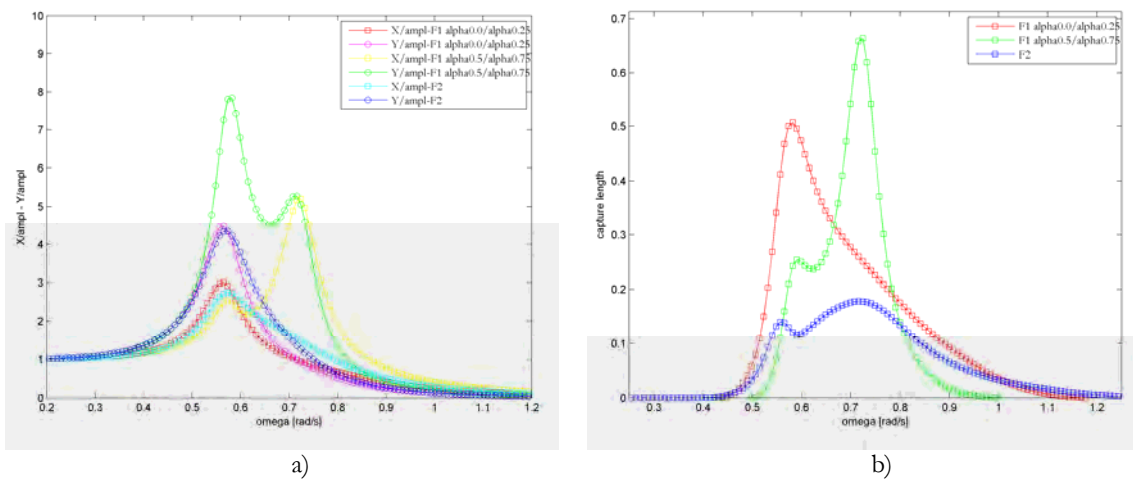


Figure 5.37. Regular waves for each optimization criterion: a) $X/ampl$ and $Y/ampl$, b) $L_{c,reg}$

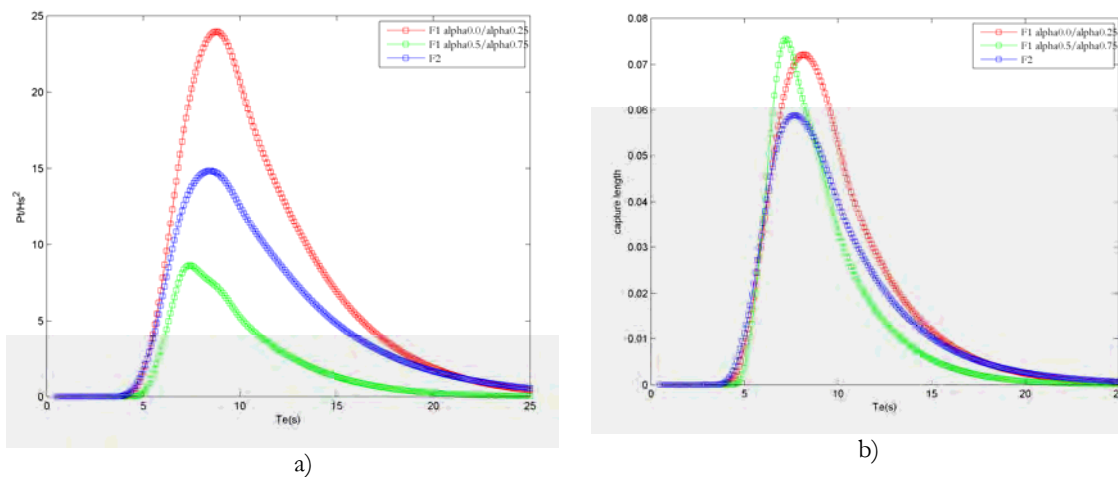


Figure 5.38. Irregular waves for each optimization criterion: a) Pt/Hs^2 , b) $L_{c,irr}$

5.2.2.4 Sardinia area

The results of the optimization of the objective functions $F_{1,2}(\nu)$ are shown in Table 5.17.

For the 5 combinations of geometry, turbine rotor diameter and turbine rotational speed in Table 5.17 the values of $X / ampl$ and $Y / ampl$ and $L_{c,reg}$ for the regular waves (Figure 5.40Figure 5.37), and the values of P_t / H_s^2 and $L_{c,irr}$ for the irregular waves (Figure 5.41) were computed.

The best results in terms of power and in terms of performance ($L_{c,irr}$) are given by the function $F_{1,\alpha=0-0.25}$ with a value, for $T_c=9-10$ s, of P_t / H_s^2 about 28 kW/m² and of $L_{c,irr}$ equal to 0.08.

In the regular waves, in the case of the function $F_{1,\alpha=0.5-0.75}$, the piston oscillations reaches, for $\omega = 0.6$ a height of 12 m, and for $\omega = 0.75$ a height of 7-8 m. This is the reason why a chamber height of 14 m, higher with respect to the other sites, was selected. In this second peak the piston oscillations ($Y / ampl$) are in phase with the floater oscillations ($X / ampl$), in fact the capture length value reaches 1.15, while for the first peak ($\omega = 0.6$) is lower than 0.4.

Table 5.17. Optimized values for the point 9 Sardinia

Point 9 Sardinia				
	F value	N [rad/s]	D [m]	Geometry
F1, a=0 (Pt)	29.68	80	1.8	N
F1, a=0.25	4.14	80	1.8	N
F1, a=0.5	0.83	90	1.4	B
F1, a=0.75	0.22	90	1.4	B
F2	0.09	50	1.6	E

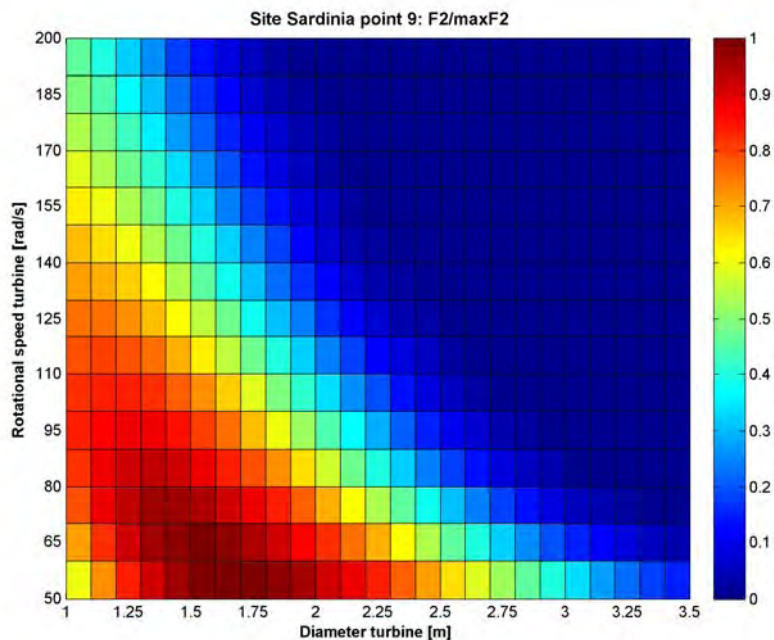


Figure 5.39. Point 9 – results of F_2 normalized to the maximum value (geometry E)

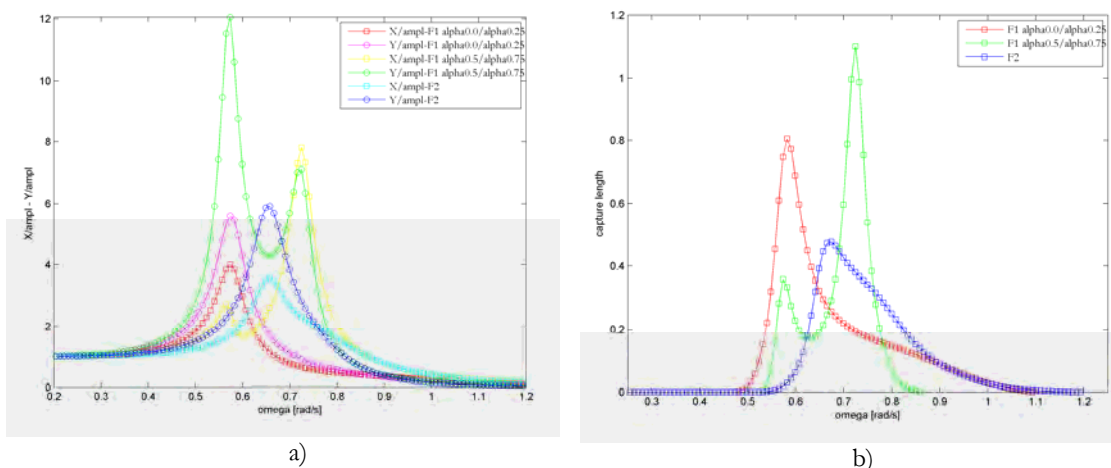


Figure 5.40. Point 9 – Regular waves for each optimization criterion: a) $X/ampl$ and $Y/ampl$, b) $L_{c,reg}$

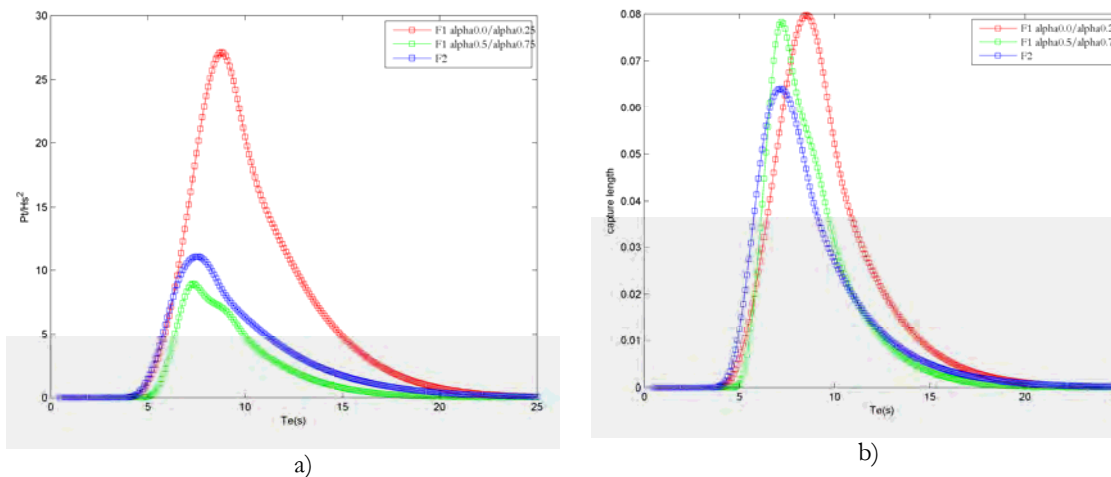


Figure 5.41. Point 9 – Irregular waves for each optimization criterion: a) P_t/H_s^2 , b) $L_{c,irr}$

CHAPTER 6

CONCLUSIONS

Currently in the research activity in the renewable energy, the possibilities of producing electrical energy from the waves in the sea is also emerging. At present a large number of WECs have been proposed with a wide variety of wave technologies, based on different ways in which energy can be captured (or power take off), water depth and location, type of the device and operating principle. In the first part of the thesis an update of present world state of art was done and the actual procedure to develop a device was defined.

In the Chapter 3 a characterization of the offshore regions in the Mediterranean Sea in terms of available wave energy was performed. The wave data were provided by IFREMER (French Research Institute for Exploration of the Sea) that developed the pre-operational system PREVIMER. The PREVIMER models employed in this thesis are the MED-6MIN that covers all the Mediterranean Sea with a resolution of 0.1° in latitude and longitude and the MENOR-4000M that covers the NW Mediterranean Sea with a resolution of 0.033° in latitude and 0.05° in longitude. The analyzed data-set covers a period of 2 years and 10 months, from 17 June 2009 for Mediterranean Sea model, and from 2 July 2009 for the NW Mediterranean Sea, to 31 March 2012.

The wave power values in each point of the domain were computed considering the deep water condition and extracting the significant wave height and mean energy period data by PREVIMER data-set. The spatial distributions of the monthly mean and yearly mean wave power were computed and reported in the form of contour maps for each month, for the all Mediterranean area and in detail for the NW Mediterranean area. The

winter and autumn months are more energetic than the other ones and the resulted monthly highest values are mainly located on the western coasts of the islands of Corsica and Sardinia, with only some exceptions. Moreover it was obtained that in the year 2010 the maximum of the yearly mean power is about 16 kW/m, higher than the corresponding value for the year 2011, about 13 kW/m.

These results were compared with the available Gorgona Buoy measurement data, that covers the same time period. It is evident that there is a significant agreement between the measured and extracted significant wave heights.

The monthly and yearly mean wave power values were also compared with those obtained in 7 points of the WorldWaves data, concerning the period from July 1992 to December 2004, and with those of other models existing in literature. The results constitute an up-date of previous older studies and a deepening of the knowledge, in terms of spatial resolution, of wave energy potentials also with respect to more recent studies.

Although the offshore wave energy potential was assessed, it must be considered that the processes affecting the waves as they propagate towards the nearshore can modify the wave energy potential, leading to reductions or, sometimes, local enhancements due to focusing mechanisms. To quantify these processes, and then select the most energetic locations, numerical simulations were performed to propagate the power time series from deepwater into the nearshore area of the selected test sites. In the Chapter 4 the numerical simulations of wave propagation from the offshore sites, where a maximum water depth of approximately 100 m is present, toward the coastal sites, were carried out by the MIKE 21-Spectral Wave (MIKE 21 SW) numerical model. As offshore boundary conditions the values of significant wave height, peak period, average direction and spreading factor extracted by the MENOR-4000M PREVIMER model on a series of equidistant points, located along the boundary on a water depth of 100 m were used. The 8028 events (time period between July 2009 and March 2012) of the PREVIMER data-set were propagated like a time series with the fully spectral formulation and quasi-stationary formulation. Maps of the variation of the significant wave height, peak period, mean spectral period, mean direction and wave power were obtained in output for each event of the time series. From these results the monthly mean wave power maps and the yearly mean wave power maps for the years 2010 and 2011 were computed. For the nearshore characterization four areas were selected: the Northern Tuscany between La Spezia and Livorno, the Central Tuscany between Livorno and Piombino, the Western Liguria between Ventimiglia and Imperia and the North Western Sardinia between Stintino and Alghero.

The results of the analysis indicate that the most energetic area, with yearly mean wave power value that reaches 12 kW/m in the 2010 and 8.4 kW/m in the 2011, is the Sardinia (around West Stintino), while the lowest energetic area, with yearly mean wave power values that not exceed 2 kW/m, is the Liguria. In the Tuscany area the yearly mean wave power value reaches 4.7 kW/m in the 2010 and 3.5 kW/m in the 2011.

Moreover the local values of the yearly mean wave power in 36 points (10 for Northern Tuscany and Liguria, 8 for Central Tuscany and Sardinia), on 15 m water depth and as many on 50 m water depths, were extracted in order to estimate the best location for a possible wave energy farm installation. The numerical simulations highlighted a considerable spatial variability of wave energy resource and the formation of hot-spots due to focusing mechanisms on the Meloria shallows (Tuscany), on headlands among Sanremo and Imperia (Liguria) and headland on the northern part of the studied Sardinia nearshore.

In order to assess the installation of a WEC/wave energy farm production or a WEC test site, the hot-spot assessment should also consider, besides the wave power values, factors as the marine protected area, the navigation routes, the closeness to coast, the closeness to nearest harbour as well as closeness to nearest grid connection. This analysis was done for the points with the highest values of yearly mean wave power in each nearshore area. It shows that the point on the 15 m water depth selected for the Northern Tuscany is inside the area A of the Meloria Shoals marine protected area and then it is not suitable for a WEC installation. Also the two points on the 50 m water depth selected for the Northern and Central Tuscany, located on the Meloria Shoals, are not very suitable for the WEC installation because the distance from the coast is around 15 km, unless the cable cost decreases. The other hot-spot in the Central Tuscany, located close to the coast south of Livorno, the hot-spots in Liguria and the hot-spots in Sardinia, located at a distance of less than 1 km, are considered to be very suitable for the WEC installation.

In the Chapter 5, despite these considerations, with a view to a technological development or a change in the regulatory context, for all the hot-spots wave climates selected for each area a device optimization was performed. The optimized devices were a single floating body linked to the seabed by means of a PTO mechanism (the simplest case of study) and of the Spar Buoy Oscillating Water Column (OWC), an axisymmetric floating OWC.

The single floating body optimization procedure followed different criteria that consisted in maximizing three objective functions, in order to consider the cost, particularly

useful in the fully commercial stage, the efficiency and the performance (dimensionless capture length) of the device. In the case of the hot-spot on 50 m water depth selected for the Northern Tuscany, the single floating body geometry optimized, considering the annual average of the extracted power and neglecting any cost parameters, has a radius of 15.5 m and a damping coefficient of 10^6 kg/s. While considering the performance, the optimal radius is 4 m and a the optimal damping coefficient is 2×10^5 kg/s. It is important to highlight how the radius decreases significantly considering different objective functions. Considering a high device cost the buoy radius and the PTO damping coefficient reach the minimum values of the range. For the hot-spot on 50 m water depth in Liguria, the optimal radius is 13 m and the optimal damping coefficient is 10^6 kg/s, considering the annual average of the absorbed power, while, if it is considered the performance, the results are the same of the Tuscany point. For the hot-spot on 50 m water depth in Sardinia, the most energetic area, the body geometry optimized is characterized, for the first objective function, by a radius of 16.5 m and a damping coefficient of 10^6 kg/s. Maximizing the performance function the optimal buoy radius is equal to 6.5 m and the optimal damping coefficient is equal to 6×10^5 kg/s.

The Spar Buoy OWC optimization procedure was performed for the wave climate off the coast of Tuscany, Sardinia and Liguria on 50 m water depth because the device draught is 24 m or 36 m, and maximized two objective functions, considering the cost and the device performance.

To define the optimal design parameters of the turbine (rotor diameter and rotational speed), eight Spar-Buoy OWC geometries, with known hydrodynamic coefficients, were analysed. For the hot-spot selected for the Northern Tuscany, the optimal device geometry has a floater diameter equal to 20 m and a draught equal to 36 m, and the optimal turbine has a rotational speed of 60 rad/s and a rotor diameter equal to 1.9 m, considering the annual average of the power output of the turbine. Instead, considering the performance, the best device geometry has a floater diameter equal to 16 m and the same draught, with a turbine rotational speed of 60 rad/s and a turbine rotor diameter equal to 1.4 m. For the hot-spot in Liguria the optimal device geometries are the same of the hot-spot in Tuscany, but with a lower value of the optimal turbine rotational speed. In term of the power production the hot-spot in Sardinia presents the highest annual average value, equal to 29.7 kW. In this case the optimal device geometry is the same of the other sites, but with a turbine rotational speed of 80 rad/s and a turbine rotor diameter equal to 1.8 m. Instead, considering the performance, the optimal floater diameter is 12 m, with a draught equal to

24 m, the optimal turbine rotational speed is 50 rad/s and the optimal turbine rotor diameter is 1.6 m.



In conclusion in this thesis a methodology that may be adopted as preliminary investigation for the site selection was developed. The wave energy assessment of some hot-spots located in nearshore areas of the Italian coast, poorly or none studied, had as value added, in addition to the update assessment of the Mediterranean Sea scale, the consideration of the “non-technical” factors. These factors, not yet widely considered in the literature and surely not in study of the Mediterranean Sea areas, are fundamental in order to consider not only the energetic aspect, but also the regulatory and planning context in which the WEC will be installed, at the purpose of taking into account a wider context of energy production planning of the territory.

The optimization procedure carried out allowed to select the most suitable devices for each area in order to maximize the production of energy taking into account at the same time the technical specification of the single turbine and the characteristics of each site. This procedure is able to evaluate not only the simple average annual power, but also factors that consider the cost and the performance.



With regard to the future developments, further studies could focus on the experimental tests of the Spar Buoy OWC, in order to compare with the numerical results and extend the analysis to other nearshore areas of the Mediterranean Sea.

APPENDIX A





WEC DATA SHEET

WAVESTAR		COMPANY DATA																																																																																																														
	<i>Name</i>	Wave Star Energy																																																																																																														
	<i>Main investors/ Project partners</i>	Privately held																																																																																																														
	<i>Country</i>	 Denmark																																																																																																														
	<i>Story</i>	The concept was invented IN 2000 by Niels and Keld Hansen																																																																																																														
	<i>Founded</i>	2003																																																																																																														
	<i>EU & State support</i>	FP6 (1.71 M€)																																																																																																														
	<i>Technical referent</i>	Laurent Marquis																																																																																																														
	<i>Contact</i>	Web: http://wavestarenergy.com Phone: +45 4040 4696 Email: info@wavestarenergy.com																																																																																																														
DEVICE TECHNOLOGY SPECIFICATION																																																																																																																
<i>Category</i>	Multi point absorber	<input checked="" type="checkbox"/> single device	<input type="checkbox"/> farm																																																																																																													
<i>Position</i>	<input type="checkbox"/> shoreline	<input checked="" type="checkbox"/> nearshore	<input type="checkbox"/> offshore																																																																																																													
<i>Power Matrix: (600 kW)</i>																																																																																																																
	<table border="1"> <thead> <tr> <th rowspan="2">Wave height H_{m0} (m)</th> <th colspan="12">Wave period $T_{0,1}$ (s)</th> </tr> <tr> <th>2-3</th> <th>3-4</th> <th>4-5</th> <th>5-6</th> <th>6-7</th> <th>7-8</th> <th>8-9</th> <th>9-10</th> <th>10-11</th> <th>11-12</th> <th>12-13</th> </tr> </thead> <tbody> <tr> <td>0.0 - 0.5</td> <td>0</td> <td>0</td> <td>0</td> <td>0</td> <td>0</td> <td>0</td> <td>0</td> <td>0</td> <td>0</td> <td>0</td> <td>0</td> </tr> <tr> <td>0.5 - 1.0</td> <td>0</td> <td>49</td> <td>73</td> <td>85</td> <td>96</td> <td>83</td> <td>78</td> <td>72</td> <td>67</td> <td>63</td> <td>59</td> </tr> <tr> <td>1.0 - 1.5</td> <td>54</td> <td>136</td> <td>193</td> <td>205</td> <td>196</td> <td>182</td> <td>167</td> <td>153</td> <td>142</td> <td>132</td> <td>123</td> </tr> <tr> <td>1.5 - 2.0</td> <td>106</td> <td>265</td> <td>347</td> <td>347</td> <td>322</td> <td>294</td> <td>265</td> <td>244</td> <td>224</td> <td>207</td> <td>193</td> </tr> <tr> <td>2.0 - 2.5</td> <td>175</td> <td>429</td> <td>522</td> <td>499</td> <td>457</td> <td>412</td> <td>372</td> <td>337</td> <td>312</td> <td>288</td> <td>267</td> </tr> <tr> <td>2.5 - 3.0</td> <td>262</td> <td>600</td> <td>600</td> <td>600</td> <td>600</td> <td>540</td> <td>484</td> <td>442</td> <td>399</td> <td>367</td> <td>340</td> </tr> <tr> <td>3.0 -</td> <td colspan="12" style="text-align: center;">Storm protection</td> </tr> </tbody> </table>	Wave height H_{m0} (m)	Wave period $T_{0,1}$ (s)												2-3	3-4	4-5	5-6	6-7	7-8	8-9	9-10	10-11	11-12	12-13	0.0 - 0.5	0	0	0	0	0	0	0	0	0	0	0	0.5 - 1.0	0	49	73	85	96	83	78	72	67	63	59	1.0 - 1.5	54	136	193	205	196	182	167	153	142	132	123	1.5 - 2.0	106	265	347	347	322	294	265	244	224	207	193	2.0 - 2.5	175	429	522	499	457	412	372	337	312	288	267	2.5 - 3.0	262	600	600	600	600	540	484	442	399	367	340	3.0 -	Storm protection													
Wave height H_{m0} (m)	Wave period $T_{0,1}$ (s)																																																																																																															
	2-3	3-4	4-5	5-6	6-7	7-8	8-9	9-10	10-11	11-12	12-13																																																																																																					
0.0 - 0.5	0	0	0	0	0	0	0	0	0	0	0																																																																																																					
0.5 - 1.0	0	49	73	85	96	83	78	72	67	63	59																																																																																																					
1.0 - 1.5	54	136	193	205	196	182	167	153	142	132	123																																																																																																					
1.5 - 2.0	106	265	347	347	322	294	265	244	224	207	193																																																																																																					
2.0 - 2.5	175	429	522	499	457	412	372	337	312	288	267																																																																																																					
2.5 - 3.0	262	600	600	600	600	540	484	442	399	367	340																																																																																																					
3.0 -	Storm protection																																																																																																															
<i>Nominal Power</i>	110 kW (n=2), 600kW (n=20)	<i>Patent</i>	<input checked="" type="checkbox"/> yes <input type="checkbox"/> no <input type="checkbox"/> no info																																																																																																													
<i>PTO</i>	<input type="checkbox"/> linear generator	<input checked="" type="checkbox"/> hydraulic motor/generator	<input type="checkbox"/> water turbine <input type="checkbox"/> air turbine																																																																																																													
<i>Power transmission system</i>	<input checked="" type="checkbox"/> electrical energy		<input type="checkbox"/> AC/DC in converter																																																																																																													
DEVICE DEVELOPMENT STRATEGY																																																																																																																
<i>Phase</i>	<i>Scale</i>	<i>Facility</i>	<i>Rating</i>	<i>Date</i>																																																																																																												
1	1:40 (d=0.25m)	Aalborg University, Denmark	-	2004-2005																																																																																																												
2	-																																																																																																															
3	1:10 (d=1m,n=40)	Nissum Bredning	1.8 kW	2006-2008																																																																																																												
4	1:2 (d=5m, n=2)	Hanstholm	110 kW (600kW con n=20)	2009-2010 (2012-2013)																																																																																																												
5																																																																																																																
<i>Scientific Paper</i>	[76]																																																																																																															
ECONOMIC DATA		PREDICTABLE IMPACT																																																																																																														
<i>Joint stock composition</i>		<i>Noise</i>																																																																																																														
<i>R&D costs (€/kW)</i>		<i>Visual impact</i>	< wind turbine																																																																																																													
<i>Commercial costs (€/kW)</i>		<i>Social impact</i>																																																																																																														
<i>Project costs</i>	4.04 M€ ¹	<i>Pollutant loss</i>																																																																																																														
<i>Device price</i>		<i>Seabed variation</i>																																																																																																														
<i>Selling energy (€/kWh)</i>	<i>Cost:</i> <i>Price:</i>	<i>Water temperature variation</i>																																																																																																														




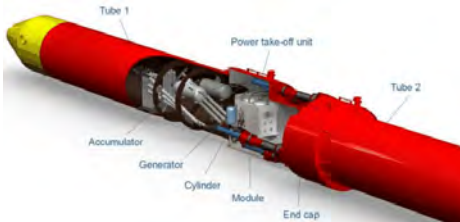

¹ http://cordis.europa.eu/fetch?CALLER=FP6_PROJ&ACTION=D&DOC=1&CAT=PROJ&RCN=86577

WAVEROLLER		COMPANY DATA		
	<i>Name</i>	AW-Energy Oy		
	<i>Main investors/ Project partners</i>	Private Holding/Venture Capital – Eneolica		
	<i>Country</i>	 Finland		
	<i>Story</i>	To commercialise the Rauno Koivusaari idea		
	<i>Founded</i>	2002		
	<i>EU & State support</i>	FP7 (3M€)		
	<i>Technical referent</i>	Mr. John Liljelund (CEO)		
	<i>Contact</i>	Web: www.aw-energy.com Email: info@aw-energy.com Phone/fax: +358 9 726 2404		
DEVICE TECHNOLOGY SPECIFICATION				
<i>Category</i>	OB - submerged	<input type="checkbox"/> single device	<input checked="" type="checkbox"/> farm	
<i>Position</i>	<input type="checkbox"/> shoreline	<input checked="" type="checkbox"/> nearshore	<input type="checkbox"/> offshore	
<i>Power Matrix</i>				
<i>Nominal Power</i>	100 kW	<i>Patent</i>	<input checked="" type="checkbox"/> yes <input type="checkbox"/> no <input type="checkbox"/> no info	
<i>PTO</i>	<input type="checkbox"/> linear generator	<input checked="" type="checkbox"/> hydraulic motor/generator	<input type="checkbox"/> water turbine <input type="checkbox"/> air turbine	
<i>Power transmission system</i>	<input checked="" type="checkbox"/> electrical energy <input type="checkbox"/> AC/DC in converter			
DEVICE DEVELOPMENT STRATEGY				
<i>Phase</i>	<i>Scale</i>	<i>Facility</i>	<i>Rating</i>	<i>Date</i>
2/3	1:3	Gulf of Finland	-	2003
1/2	-	Helsinki University, Finland	-	2004
3	1:3	Ecuador, EMEC, Scotland	-	2005
4	1:1 (3.5*4.5*6m)	Peniche, Portugal	2 x 15 kW	2007-2008
5	1:1	Peniche, Portugal	3X100 kW	2012 - ?
<i>Scientific Paper</i>				
ECONOMIC DATA		PREDICTABLE IMPACT		
<i>Joint stock composition</i>		<i>Noise</i>	no	
<i>R&D costs (€/kW)</i>	3000 ²	<i>Visual impact</i>	no	
<i>Commercial costs (€/kW)</i>	800-1300	<i>Social impact</i>		
<i>Project costs</i>	5.7 M€ (Surge Project)	<i>Pollutant loss</i>	no	
<i>Device price</i>		<i>Seabed variation</i>	minimal	
<i>Selling energy (€/kWh)</i>	<i>Cost:0.03-0.05</i> <i>Price:</i>	<i>Water temperature variation</i>		

² Based on an estimated nominal power output of 15kW per individual WaveRoller plate.

OYSTER		COMPANY DATA								
  	<i>Name</i>	Aquamarine Power								
	<i>Main investors/ Project partners</i>	ABB, SEP, SSE, Scottish Enterprise, Sigma Capital Group, Oregon Wave Energy Trust/ Queen's University Belfast								
	<i>Country</i>	 Scotland								
	<i>Story</i>	In 2001 Professor Trevor Whittaker's research and development team at Queen's University, Belfast began to research flap-type wave power devices and in 2005 Allan Thomson set up Aquamarine Power to bring Oyster wave power technology to the commercial market.								
	<i>Founded</i>	2005								
	<i>EU & State support</i>	2007: SSE 6.3M£ (≈7.6M€), Sigma Capital Group plc 1.5M£ (≈1.8M€) 2010: ABB 8M£ (≈9.6M€), Oregon Wave Energy Trust 50k\$ (≈39.2k€), Scottish Enterprise 3M£ (≈3.6M€), UK Government 5M£ (≈6M€)								
<i>Technical referent</i>	Dr Paddy O'Kane									
<i>Contact</i>	Web: www.aquamarinepower.com/ Email: info@aquamarinepower.com Phone: +44 131 524 1440									
DEVICE TECHNOLOGY SPECIFICATION										
<i>Category</i>	OB - submerged	X single device <input type="checkbox"/> farm								
<i>Position</i>	<input type="checkbox"/> shoreline	X nearshore <input type="checkbox"/> offshore								
<i>Power Matrix</i>										
Significant wave height (m)	Energy period (secs)									
		5.0	6.0	7.0	8.0	9.0	10.0	11.0	12.0	13.0
	0.5	idle	idle	idle	idle	idle	idle	1	3	3
	1.0	20	30	38	42	44	44	45	47	45
	1.5	80	85	92	97	102	103	104	100	104
	2.0	140	147	152	158	155	155	160	161	156
	2.5	192	197	208	202	203	209	211	201	204
	3.0	241	237	237	241	243	230	236	231	235
	3.5	-	271	272	269	268	267	270	260	260
	4.0	-	291	290	290	280	287	276	278	277
	4.5	-	291	290	290	280	287	276	278	277
	5.0	-	-	290	290	280	287	276	278	277
5.5	-	-	290	290	280	287	276	278	277	
6.0	-	-	290	290	280	287	276	278	277	
<i>Nominal Power</i>	800 kW		<i>Patent</i>	<input type="checkbox"/> yes <input type="checkbox"/> no X no info						
<i>PTO</i>	<input type="checkbox"/> linear generator <input type="checkbox"/> hydraulic motor/generator		X water turbine <input type="checkbox"/> air turbine							
<i>Power transmission system</i>	X electrical energy		<input type="checkbox"/> AC/DC in converter							

DEVICE DEVELOPMENT STRATEGY				
<i>Phase</i>	<i>Scale</i>	<i>Facility</i>	<i>Rating</i>	<i>Date</i>
1	1:40	Queen's Uni., Belfast	-	2003-2005
2	1:25	Queen's Uni., Belfast	-	2003-2005
3				
4	1:1 (PTO)	NaREC, UK - Billia Croo in Orkney (EWEC) (dim 18X12m) - Billia Croo in Orkney (EWEC) (dim 26X12m)	170 kW - 315kW - 800 kW x 3=2.40 MW	2009 - 2009 - da 2011 a 2013
5				
<i>Scientific Paper</i>		[77]		
ECONOMIC DATA			PREDICTABLE IMPACT	
<i>Joint stock composition</i>			<i>Noise</i>	
<i>R&D costs (€)</i>		1.2-1.6M [78]	<i>Visual impact</i>	minimal
<i>Commercial costs (€/kW)</i>			<i>Social impact</i>	
<i>Project costs (€/kW)</i>		1600 [78]	<i>Pollutant loss</i>	
<i>Device price</i>			<i>Seabed variation</i>	
<i>Selling energy (€/kWh)</i>		<i>Cost: 0.35</i> <i>Price:</i>	<i>Water temperature variation</i>	

PELAMIS		COMPANY DATA	
   	<i>Name</i>	Pelamis Wave Power	
	<i>Main investors/ Project partners</i>	Privately owned/ Vattenfall	
	<i>Country</i>	 Scotland	
	<i>Story</i>	Founded in 1998 by Pelamis inventor Dr Richard Yemm. Before September 2007 the company name was Ocean Power Delivery.	
	<i>Founded</i>	1998	
	<i>EU & State support</i>	2008: 4.8M€ Scottish government 2011: 1.3M€ Scottish Funding Council	
	<i>Technical referent</i>	Ross Henderson, Technology Director	
<i>Contact</i>	Web: http://www.pelamiswave.com Email: enquiries@pelamiswave.com Phone: +44 131 554 8444		

DEVICE TECHNOLOGY SPECIFICATION

<i>Category</i>	Attenuator – OB	<input type="checkbox"/> single device	<input checked="" type="checkbox"/> farm
<i>Position</i>	<input type="checkbox"/> shoreline	<input type="checkbox"/> nearshore	<input checked="" type="checkbox"/> offshore (depth>50m, 2-10km from the coast)

Power Matrix


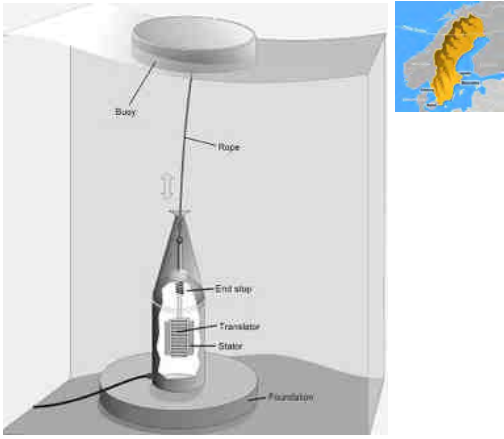


Significant wave height (H_{sig} , m)	Power period (T_{pow} , s)																
	5.0	5.5	6.0	6.5	7.0	7.5	8.0	8.5	9.0	9.5	10.0	10.5	11.0	11.5	12.0	12.5	13.0
0.5	idle	idle	idle	idle	idle	idle	idle	idle	idle	idle	idle	idle	idle	idle	idle	idle	idle
1.0	idle	22	29	34	37	38	38	37	35	32	29	26	23	21	idle	idle	idle
1.5	32	50	65	76	83	86	86	83	78	72	65	59	53	47	42	37	33
2.0	57	88	115	136	148	153	152	147	138	127	116	104	93	83	74	66	59
2.5	89	138	180	212	231	238	238	230	216	199	181	163	146	130	116	103	92
3.0	129	198	260	305	332	340	332	315	292	266	240	219	210	188	167	149	132
3.5	-	270	354	415	438	440	424	404	377	362	326	292	260	230	215	202	180
4.0	-	-	462	502	540	546	530	499	475	429	384	366	339	301	267	237	213
4.5	-	-	544	635	642	648	628	590	562	528	473	432	382	356	338	300	266
5.0	-	-	-	739	726	731	707	687	670	607	557	521	472	417	369	348	328
5.5	-	-	-	750	750	750	750	750	737	667	658	586	530	496	446	395	355
6.0	-	-	-	-	750	750	750	750	750	750	711	633	619	558	512	470	415
6.5	-	-	-	-	750	750	750	750	750	750	750	743	658	621	579	512	481
7.0	-	-	-	-	-	750	750	750	750	750	750	750	750	676	613	584	525
7.5	-	-	-	-	-	-	750	750	750	750	750	750	750	750	686	622	593
8.0	-	-	-	-	-	-	-	750	750	750	750	750	750	750	750	690	625

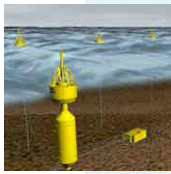



<i>Nominal Power</i>	750 kW	<i>Patent</i>	<input type="checkbox"/> yes	<input type="checkbox"/> no	<input checked="" type="checkbox"/> no info
<i>PTO</i>	<input type="checkbox"/> linear generator	<input checked="" type="checkbox"/> hydraulic motor/generator	<input type="checkbox"/> water turbine	<input type="checkbox"/> air turbine	
<i>Power transmission system</i>	<input checked="" type="checkbox"/> electrical energy		<input type="checkbox"/> AC/DC in converter		


DEVICE DEVELOPMENT STRATEGY



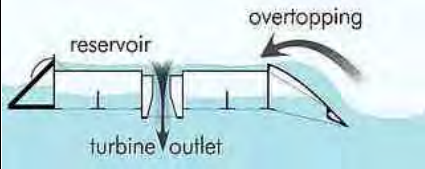

<i>Phase</i>	<i>Scale</i>	<i>Facility</i>	<i>Rating</i>	<i>Date</i>
1	1:80	Edinburgh Uni. Scotland	-	1998-2001

2	1:35	Edinburgh Uni. Scotland	-	1999-2001
3	1:7	ECN, Nantes, France	-	2001-2003
3	1:7	Firth of the Forth, Scotland	-	2001-2003
4	1:1	EMEC, Scotland	750 kW	2004-2007
5	1:1	Agucadoura, Portugal (D=3.5m, length=120m)	3 x 750 kW	2008-2009
5	1:1	EMEC, Scotland (P2 Pelamis)	750 kW	2010 -
5	1:1	Shetland, Scotland	14 x 750 kW=10.5MW	in development
5	1:1	Great Bernera – Western Islands, Scotland	26 x 750 kW=20MW	2013/2014
<i>Scientific Paper</i>		[79] [80] [81]		
ECONOMIC DATA			PREDICTABLE IMPACT	
<i>Joint stock composition</i>	Vattenfall (72M€)		<i>Noise</i>	some noise through movement of chains or sound of generators
<i>R&D costs (€)</i>	54M [79]		<i>Visual impact</i>	1.68m above sea level
<i>Commercial costs (€)</i>	0.75M		<i>Social impact</i>	
<i>Project costs (€/kW)</i>	4300 (only initial cost) [82]		<i>Pollutant loss</i>	
<i>Device price</i>			<i>Seabed variation</i>	no
<i>Selling energy (€/kWh)</i>	<i>Cost:</i>	<i>Price:</i>	<i>Water temp.var.</i>	

DIRECT DRIVE LINEAR GENERATOR		COMPANY DATA		
  		<i>Name</i>	Seabased AB	
		<i>Main investors/ Project partners</i>	Vattenfall, Swedish Energy Agency, Ångpanneföreningen research foundation, Gothenburg Energy, Draka Holding N.V./Uppsala University	
		<i>Country</i>	 Sweden	
		<i>Story</i>	Spin-off Company from Uppsala University. The Professor Mats Leijon and the Associate Professor Hans Bernhoff are the founders and majority owners of the company.	
		<i>Founded</i>	2001	
		<i>EU & State support</i>	2011: Swedish government €15M	
		<i>Technical referent</i>	Mats Leijon , Billy Johansson (CEO)	
		<i>Contact</i>	Web: http://www.seabased.com Email: info@seabased.com Phone: +46 (0)18 504 810	
DEVICE TECHNOLOGY SPECIFICATION				
<i>Category</i>	Point absorber	<input type="checkbox"/> single device <input checked="" type="checkbox"/> farm		
<i>Position</i>	<input type="checkbox"/> shoreline	<input checked="" type="checkbox"/> nearshore (25m)	<input type="checkbox"/> offshore	
<i>Power Matrix</i>				
<i>Nominal Power</i>	10kW	<i>Patent</i>	<input checked="" type="checkbox"/> yes <input type="checkbox"/> no <input type="checkbox"/> no info	
<i>PTO</i>	<input checked="" type="checkbox"/> linear generator	<input type="checkbox"/> hydraulic motor/generator	<input type="checkbox"/> water turbine <input type="checkbox"/> air turbine	
<i>Power transmission system</i>	<input type="checkbox"/> electrical energy <input checked="" type="checkbox"/> AC/DC in converter			
DEVICE DEVELOPMENT STRATEGY				
<i>Phase</i>	<i>Scale</i>	<i>Facility</i>	<i>Rating</i>	<i>Date</i>
1				
2	1:2 (PTO)	Angstrom, Uppsala University	10kW	2003-2004
3	1:2	Lysekil, Sweden	10x10kW	2005-
4	1:1 (d=3m)	Lysekil, Sweden (n=42 → n=420)	10kW (L1,L2,L3)	2005-2014/2015
5				
<i>Scientific Paper</i>				
ECONOMIC DATA		PREDICTABLE IMPACT		
<i>Joint stock composition</i>		<i>Noise</i>		
<i>R&D costs (€)</i>	37.5M	<i>Visual impact</i>	no	
<i>Commercial costs (€/kW)</i>		<i>Social impact</i>		
<i>Project costs</i>		<i>Pollutant loss</i>	minimal	
<i>Device price</i>		<i>Seabed variation</i>		
<i>Selling energy (€/kWh)</i>	<i>Cost:</i> <i>Price:</i>	<i>Water temperature variation</i>		

WAVEBOB		COMPANY DATA		
  		<i>Name</i>	Wavebob Ltd	
		<i>Main investors/ Project partners</i>	Privately-held / Chevron, Vattenfal, Lockheed Martin	
		<i>Country</i>	 Ireland	
		<i>Story</i>	1999 Original patents filed	
		<i>Founded</i>	2001	
		<i>EU & State support</i>	EU FP7: 5M€ US Dep. of Energy 1.8M€ EU STANDPOINT 8.5M€	
		<i>Technical referent</i>	Andrew Parish (CEO), William Dick (Inventor)	
<i>Contact</i>	Web: http://wavebob.com/ Phone: +353(0) 1 6510177 Fax: +353(0)1 6510175 Email: info@wavebob.com			
DEVICE TECHNOLOGY SPECIFICATION				
<i>Category</i>	Point absorber	X single device <input type="checkbox"/> farm		
<i>Position</i>	<input type="checkbox"/> shoreline	<input type="checkbox"/> nearshore	X offshore (75-100m)	
<i>Power Matrix:</i>				
<i>Nominal Power</i>	15kW	<i>Patent</i>	X yes <input type="checkbox"/> no <input type="checkbox"/> no info	
<i>PTO</i>	<input type="checkbox"/> linear generator	X hydraulic motor/generator	<input type="checkbox"/> water turbine <input type="checkbox"/> air turbine	
<i>Power transmission system</i>	X electrical energy <input type="checkbox"/> AC/DC in converter			
DEVICE DEVELOPMENT STRATEGY				
<i>Phase</i>	<i>Scale</i>	<i>Facility</i>	<i>Rating</i>	<i>Date</i>
1	1:50	HMRC, UCC, Ireland	-	2002
2	1:20	Hanover, Germany	-	2003
3	1:4 (Ø20m)	Galway Bay, Ireland	15kW	2007-2008
4				
5	1:1 (Ø14m)	Portugal	4*300kW	2013 [83]
<i>Scientific Paper</i>				
ECONOMIC DATA		PREDICTABLE IMPACT		
<i>Joint stock composition</i>	Vattenfall acquired 51% of Wavebob Ltd	<i>Noise</i>		
<i>R&D costs (€/kW)</i>		<i>Visual impact</i>		
<i>Commercial costs (€/kW)</i>		<i>Social impact</i>		
<i>Project costs</i>		<i>Pollutant loss</i>		
<i>Device price</i>		<i>Seabed variation</i>	-	
<i>Selling energy (€/kWh)</i>	<i>Cost:</i>	<i>Price:</i>	<i>Water temp. variation</i>	

OE BUOY		COMPANY DATA		
		<i>Name</i>	OceanEnergy Ltd	
		<i>Main investors/ Project partners</i>	Private/ Enterprise Ireland, HMRC, Marine Institute, SEI, MRIA	
		<i>Country</i>	 Ireland	
		<i>Story</i>		
		<i>Founded</i>	2002	
		<i>EU & State support</i>	2002-2004 SEI € 131.157 2003 EI € 80.000	
		<i>Technical referent</i>	John Keating	
		<i>Contact</i>	Web: www.oceanenergy.ie Email: info@oceanenergy.ie Phone: 00353-21-4816779 Fax: 00353-21-4816778	
DEVICE TECHNOLOGY SPECIFICATION				
<i>Category</i>	OWC - floating	X single device <input type="checkbox"/> farm		
<i>Position</i>	<input type="checkbox"/> shoreline	<input type="checkbox"/> nearshore	X offshore (>50m)	
<i>Power Matrix</i>				
<i>Nominal Power</i>	1.5MW (full scale)	<i>Patent</i>	<input type="checkbox"/> yes <input type="checkbox"/> no X no info	
<i>PTO</i>	<input type="checkbox"/> linear generator	<input type="checkbox"/> hydraulic motor/generator	<input type="checkbox"/> water turbine	X air turbine
<i>Power transmission system</i>	X electrical energy		<input type="checkbox"/> AC/DC in converter	
DEVICE DEVELOPMENT STRATEGY				
<i>Phase</i>	<i>Scale</i>	<i>Facility</i>	<i>Rating</i>	<i>Date</i>
1	1:50	HMRC, UCC, Ireland	-	2002-2003
2	1:15	ECN, Nantes, France	-	2004
3	1:4 (Hull)	Galway Bay, Ireland	20kW	2006-2008
3	1:4 (PTO) (50X25 m)	Galway Bay, Ireland	20kW	2008-2009
4	1:1	Wave Hub, Cornwall	1.5MW	Planned end 2012
5				
<i>Scientific Paper</i>				
ECONOMIC DATA		PREDICTABLE IMPACT		
<i>Joint stock composition</i>		<i>Noise</i>		
<i>R&D costs (€/kW)</i>		<i>Visual impact</i>		
<i>Commercial costs (€/kW)</i>		<i>Social impact</i>		
<i>Project costs</i>		<i>Pollutant loss</i>		
<i>Device price</i>		<i>Seabed variation</i>		-
<i>Selling energy (€/kWh)</i>	<i>Cost:</i>	<i>Price:</i>	<i>Water temperature variation</i>	

WAVEDRAGON		COMPANY DATA																				
  	<i>Name</i>	Wave Dragon ApS																				
	<i>Main investors/ Project partners</i>	SPOK ApS, Balslev A/S, Kössler Ges.m.b.H., Aalborg University, Dept. Civil Eng., Promecon A/S, Technical University of Munich, NIRAS A/S, Nöhrind Ltd, ESB International																				
	<i>Country</i>	 Denmark																				
	<i>Story</i>	The inventor is Erik Friis-Madsen																				
	<i>Founded</i>	2003																				
	<i>EU & Stat support</i>	Since 2003: €1.7M Danish Energy Authority, €1.5M EU, €0.25M Elkraft System's RTD 2006:EU FP6 €2.4M, Welsh Assembly Government €7.4M																				
<i>Technical referent</i>	Hans Sørensen																					
<i>Contact</i>	Web: www.wavedragon.net www.wavedragon.co.uk Phone: + 45 3536 0219 Fax: +45 3537 4537 Email: info@wavedragon.net																					
DEVICE TECHNOLOGY SPECIFICATION																						
<i>Category</i>	Overtopping - floating	<input checked="" type="checkbox"/> single device	<input type="checkbox"/> farm																			
<i>Position</i>	<input type="checkbox"/> shoreline	<input type="checkbox"/> nearshore	<input checked="" type="checkbox"/> offshore (>25-40m)																			
<i>Power Matrix (W)</i>																						
Wave Period - Tz (s)																						
	4.0	4.5	5.0	5.5	6.0	6.5	7.0	7.5	8.0	8.5	9.0	9.5	10.0	10.5	11.0	11.5	12.0	12.5	13.0	13.5	14.0	
0.5	0	0	0	0	0	0	0	0	0	0	0	0	0	0	0	0	0	0	0	0	0	0
1.0	203	276	348	432	516	608	699	798	896	925	953	958	962	941	919	870	820	742	663	555	448	337
1.5	412	448	485	617	750	899	1049	1212	1375	1433	1491	1509	1527	1502	1477	1404	1332	1209	1086	912	737	562
2.0	621	621	621	802	983	1191	1398	1626	1853	1941	2029	2061	2092	2063	2034	1939	1844	1677	1509	1269	1028	787
2.5	1123	1123	1123	1213	1304	1609	1914	2268	2602	2752	2903	2972	3041	3017	2993	2868	2743	2504	2266	1910	1555	1200
3.0	1624	1624	1624	1624	1624	2027	2430	2890	3350	3563	3776	3863	3949	3970	3951	3796	3641	3332	3022	2552	2082	1612
3.5	2581	2581	2581	2581	2581	2783	2984	3588	4191	4494	4796	4870	4945	4935	4926	4845	4755	4374	3983	3372	2761	2150
4.0	3538	3538	3538	3538	3538	3538	3538	4285	5032	5424	5816	5858	5900	5900	5900	5895	5889	5418	4943	4191	3439	2687
4.5	4719	4719	4719	4719	4719	4719	4719	5083	5456	5662	5858	5879	5900	5900	5900	5897	5895	5658	5422	4822	4222	3622
5.0	5900	5900	5900	5900	5900	5900	5900	5900	5900	5900	5900	5900	5900	5900	5900	5900	5900	5900	5900	5900	5900	5900
5.5	5900	5900	5900	5900	5900	5900	5900	5900	5900	5900	5900	5900	5900	5900	5900	5900	5900	5900	5900	5900	5900	5900
6.0	5900	5900	5900	5900	5900	5900	5900	5900	5900	5900	5900	5900	5900	5900	5900	5900	5900	5900	5900	5900	5900	5900
6.5	5900	5900	5900	5900	5900	5900	5900	5900	5900	5900	5900	5900	5900	5900	5900	5900	5900	5900	5900	5900	5900	5900
7.0	5900	5900	5900	5900	5900	5900	5900	5900	5900	5900	5900	5900	5900	5900	5900	5900	5900	5900	5900	5900	5900	5900
7.5	5900	5900	5900	5900	5900	5900	5900	5900	5900	5900	5900	5900	5900	5900	5900	5900	5900	5900	5900	5900	5900	5900
8.0	5900	5900	5900	5900	5900	5900	5900	5900	5900	5900	5900	5900	5900	5900	5900	5900	5900	5900	5900	5900	5900	5900
<i>Nominal Power</i>	20 kW		<i>Patent</i>	<input checked="" type="checkbox"/> yes (wave reflector) <input type="checkbox"/> no <input type="checkbox"/> no info																		
<i>PTO</i>	<input type="checkbox"/> linear generator	<input type="checkbox"/> hydraulic motor/generator	<input checked="" type="checkbox"/> water turbine	<input type="checkbox"/> air turbine																		
<i>Power transmission system</i>	<input type="checkbox"/> electrical energy		<input checked="" type="checkbox"/> AC/DC in converter																			
DEVICE DEVELOPMENT STRATEGY																						
<i>Phase</i>	<i>Scale</i>	<i>Facility</i>		<i>Rating</i>																		
1	1:50	HMRC, UCC, Ireland		-																		
1	1:45	Aalborg Uni., Denmark		-																		
2	1:4.5 (PTO)	Uni. of Munich, Germany		2.3kW																		
3	1:4.5	Nissum Bredning, Denmark		20kW																		
4	1.1	Celtic Sea, St Ann's Head in Pembrokeshire		7MW																		
				end 2010 [85]																		

4	1:1.5	Test centre DanWEC, Hanstholm	1.5MW	received founding 2011
5				
<i>Scientific Paper</i>	[84]			
ECONOMIC DATA		PREDICTABLE IMPACT		
<i>Joint stock composition</i>		<i>Noise</i>	no	
<i>R&D costs (€/kW)</i>		<i>Visual impact</i>	Low, height<7m	
<i>Commercial costs (€/kW)</i>	2700-4000 [85]	<i>Social impact</i>		
<i>Project costs</i>	€21M (Celtic project)	<i>Pollutant loss</i>	no	
<i>Device price</i>		<i>Seabed variation</i>		
<i>Selling energy (€/kWh)</i>	<i>Cost:</i> 0.06-0.11[86] <i>Price:</i>	<i>Water temp. Var.</i>		

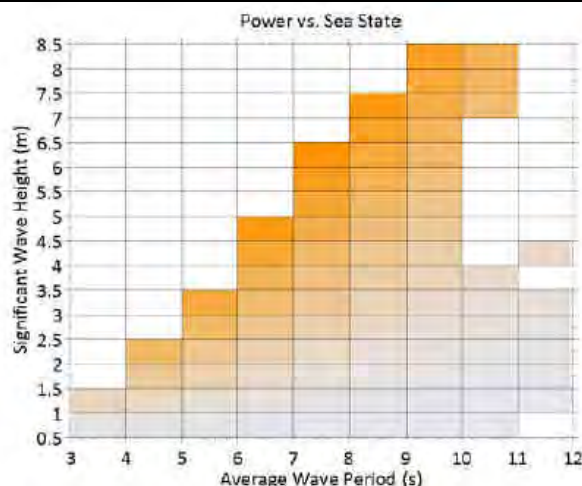
L10 Buoy		COMPANY DATA			
		<i>Name</i>	Columbia Power Technologies (CPT) and Oregon State University (OSU)		
		<i>Main investors/ Project partners</i>	Privately held/ Wallace Energy Systems and Renewables Facility (WESRF), Hatfield Marine Science Center (HMSC), O.H. Hinsdale.		
		<i>Country</i>	USA		
		<i>Story</i>	It was founded by Greenlight Energy Resources, Inc.		
		<i>Founded</i>	2005		
		<i>State support</i>	3.2M€		
		<i>Technical referent</i>	Ken Rhinefrank - VP of Research Reenst Lesemann - CEO		
<i>Contact</i>	Web: http://www.columbiapwr.com Email: info@columbiapwr.com Phone: (541)368-5033 Fax: 541 230 1498				
DEVICE TECHNOLOGY SPECIFICATION					
<i>Category</i>	Point absorber	X single device <input type="checkbox"/> farm			
<i>Position</i>	<input type="checkbox"/> shoreline	<input type="checkbox"/> nearshore	X offshore (>30-40m)		
<i>Power Matrix:</i>					
<i>Nominal Power</i>	10kW	<i>Patent</i>	X yes <input type="checkbox"/> no <input type="checkbox"/> no info		
<i>PTO</i>	X linear generator <input type="checkbox"/> hydraulic motor/generator <input type="checkbox"/> water turbine <input type="checkbox"/> air turbine				
<i>Power transmission system</i>	X electrical energy <input type="checkbox"/> AC/DC in converter				
DEVICE DEVELOPMENT STRATEGY					
<i>Phase</i>	<i>Scale</i>	<i>Facility</i>	<i>Rating</i>	<i>Date</i>	
1	-	Oregon State University	-	2006	
2	-	Oregon State University	-	2007	
3	-	2.5 miles off Newport Oregon	10kW	2008	
4					
5					
<i>Scientific Paper</i>	[87]				
ECONOMIC DATA			PREDICTABLE IMPACT		
<i>Joint stock composition</i>			<i>Noise</i>		
<i>R&D costs (€/kW)</i>			<i>Visual impact</i>		
<i>Commercial costs (€/kW)</i>			<i>Social impact</i>		
<i>Project costs</i>			<i>Pollutant loss</i>		
<i>Device price</i>			<i>Seabed variation</i>		
<i>Selling energy (€/kWh)</i>	<i>Cost:</i>	<i>Price:</i>	<i>Water temp. variation</i>		

POWER BUOY		COMPANY DATA	
		<i>Name</i>	Ocean Power Technology (OPT)
		<i>Main investors/ Project partners</i>	U.S. Navy, Mitsui Engineering & Shipbuilding Co. Ltd., U.S. Department of Energy, Oregon Department of Energy, Iberdrola S.A., PNGC Power, Lockheed Martin Corp, Leighton Contractors.
		<i>Country</i>	USA
		<i>Story</i>	OPT was listed on Nasdaq in April 2007.
		<i>Founded</i>	1994
		<i>State support</i>	2007: €1.5M, €0.9M Scottish Minister's Wave and Tidal Energy 2009: €50M Federal Government of Australia 2010: €2.2M EU (FP7), €290k, €1.1M and €3.7M US Department of Energy, €1.7M South West of England Regional Development Agency
		<i>Technical referent</i>	Dr. Philip R. Hart, CTO
<i>Contact</i>	Web: www.oceanpowertech.com Email: info@oceanpowertech.com Phone: +1 609 730 0400 Fax: +1 609 730 0404		

DEVICE TECHNOLOGY SPECIFICATION

<i>Category</i>	Point absorber	<input type="checkbox"/> single device	<input checked="" type="checkbox"/> farm
<i>Position</i>	<input type="checkbox"/> shoreline	<input type="checkbox"/> nearshore	<input checked="" type="checkbox"/> offshore (>30-50m)

Power Matrix





<i>Nominal Power</i>	150 kW	<i>Patent</i>	<input checked="" type="checkbox"/> yes (n=48)	<input type="checkbox"/> no	<input type="checkbox"/> no info
<i>PTO</i>	<input type="checkbox"/> linear generator	<input checked="" type="checkbox"/> hydraulic motor/generator	<input type="checkbox"/> water turbine	<input type="checkbox"/> air turbine	
<i>Power transmission system</i>	<input checked="" type="checkbox"/> electrical energy		<input type="checkbox"/> AC/DC in converter		





DEVICE DEVELOPMENT STRATEGY

<i>Phase</i>	<i>Scale</i>	<i>Facility</i>	<i>Rating</i>	<i>Date</i>
1				
2				
3	1:1.5	New Jersey, USA - Oahu, Hawaii	40kW	2004-2007
4	1:1 (h=14.6m, d=3.5m)	Santoña, Spain	(40kW) + 9 X 150kW	(2008) -




4	1:1	EMEC, Scotland	150kW	2011
4	1:1	Reedsport, Oregon, USA	10 x 150kW	2010 -
4	1.1	Coos Bay, Oregon, USA	20 x 500kW	Preliminary Application Document Submitted
5				
<i>Scientific Paper</i>				
ECONOMIC DATA			PREDICTABLE IMPACT	
<i>Joint stock composition</i>			<i>Noise</i>	
<i>R&D costs (€/kW)</i>			<i>Visual impact</i>	minimal
<i>Commercial costs (€/kW)</i>			<i>Social impact</i>	
<i>Project costs</i>			<i>Pollutant loss</i>	no
<i>Device price</i>			<i>Seabed variation</i>	minimal
<i>Selling energy (€/kWh)</i>		<i>Cost:</i> 0.11 ³	<i>Price:</i>	<i>Water temp. variation</i>

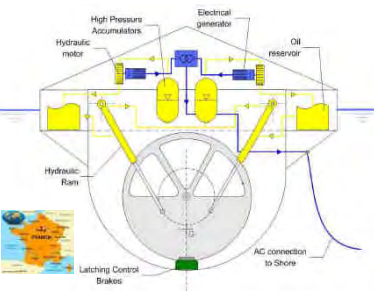

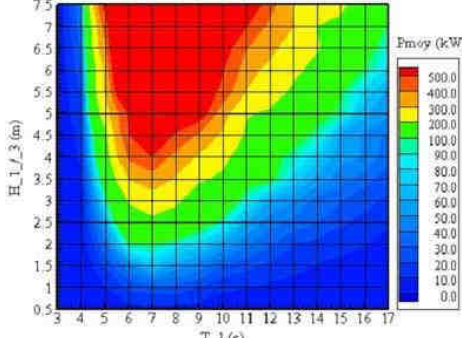
³ Company projected costs on production levels of 400 PowerBuoys per year

WaveEL-Buoy (IPS Buoy)		COMPANY DATA	
		<i>Name</i>	Waves4Power AB
		<i>Main investors/ Project partners</i>	Privately-held
		<i>Country</i>	 Sweden
		<i>Story</i>	Waves4Power is built on a foundation laid by its sister company InterProject Service AB (IPS) and the same group of experts that now have formed Waves4Power.
		<i>Founded</i>	2008
		<i>EU & State support</i>	
		<i>Technical referent</i>	Sven A. Noren (inventor)
		<i>Contact</i>	Web: www.Waves4Power.com Phone: +46 (0)31 706 09 00 Email: info@waves4power.com
DEVICE TECHNOLOGY SPECIFICATION			
<i>Category</i>	Point absorber	X single device <input type="checkbox"/> farm	
<i>Position</i>	<input type="checkbox"/> shoreline 50-100m)	<input type="checkbox"/> nearshore	X offshore (min 30m,
<i>Power Matrix</i>			
<i>Nominal Power</i>	150-250 kW (10 m IPS OWEC)	<i>Patent</i>	X yes <input type="checkbox"/> no <input type="checkbox"/> no info
<i>PTO</i>	<input type="checkbox"/> linear generator	X hydraulic motor/generator	<input type="checkbox"/> water turbine <input type="checkbox"/> air turbine
<i>Power transmission system</i>	X electrical energy <input type="checkbox"/> AC/DC in converter		
DEVICE DEVELOPMENT STRATEGY			
<i>Phase</i>	<i>Scale</i>	<i>Facility</i>	<i>Rating</i>
1	-		-
2			
3	1:2	Goteborg, Swedish west coast	17kW
4			
5			
<i>Scientific Paper</i>	[88] [89]		
ECONOMIC DATA		PREDICTABLE IMPACT	
<i>Joint stock composition</i>		<i>Noise</i>	
<i>R&D costs (€/kW)</i>		<i>Visual impact</i>	
<i>Commercial costs (€/kW)</i>		<i>Social impact</i>	
<i>Project costs</i>		<i>Pollutant loss</i>	
<i>Device price</i>		<i>Seabed variation</i>	
<i>Selling energy (€/kWh)</i>	<i>Cost:</i>	<i>Price:</i>	<i>Water temp. variation</i>

FO ³ /BOLT		COMPANY DATA			
  	<i>Name</i>	Fred. Olsen Renewables AS			
	<i>Main investors/ Project partners</i>	Owned subsidiary of Bonheur ASA and Ganger Rolf ASA/ AAB, Bosch-Rexroth, SINTEF Marintek			
	<i>Country</i>	 Norway			
	<i>Story</i>	The FO ³ project is terminated and the efforts are now focused on a single point absorber device called the Bolt.			
	<i>Founded</i>	2001			
	<i>EU & State support</i>	FP6: 2.3M€, 2011 2.3M€			
	<i>Technical referent</i>	Torre Guilli			
	<i>Contact</i>	Web: www.fredolsen-renewables.com Phone: +47-22 34 10 00 Email: renewables@fredolsen.no			
DEVICE TECHNOLOGY SPECIFICATION					
<i>Category</i>	Multi point absorber/point absorber		X single device		<input type="checkbox"/> farm
<i>Position</i>	<input type="checkbox"/> shoreline		X nearshore (30 m)		X offshore
<i>Power Matrix</i>					
<i>Nominal Power</i>	45kW (BOLT) – 225kW (BOLT2)		<i>Patent</i>	X yes <input type="checkbox"/> no <input type="checkbox"/> no info	
<i>PTO</i>	<input type="checkbox"/> linear generator		X hydraulic motor/generator		<input type="checkbox"/> water turbine <input type="checkbox"/> air turbine
<i>Power transmission system</i>			X electrical energy		<input type="checkbox"/> AC/DC in converter
DEVICE DEVELOPMENT STRATEGY					
<i>Phase</i>	<i>Scale</i>	<i>Facility</i>		<i>Rating</i>	<i>Date</i>
1					
2	1:20 (FO ³)	SINTEF, Trondheim , Norway		-	2004
3	1:3 (PTO) (FO ³)	SINTEF, Trondheim , Norway		-	2004
3	1:3 (FO ³)	Karmoy, Norway (12 x 12 x 8m)		40kW	2005-2008
4	1:1 (BOLT)	Risor , Norway (d=5.15m)		45kW	2009
4	1:1 (BOLT2)	Fabtest, UK (d=16m)		225kW	2011
4	1:1 (BOLT2)	WaveHub, UK		100kW	2012?
5					
<i>Scientific Paper</i>					
ECONOMIC DATA			PREDICTABLE IMPACT		
<i>Joint stock composition</i>			<i>Noise</i>		
<i>R&D costs (€/kW)</i>			<i>Visual impact</i>		
<i>Commercial costs (€/kW)</i>			<i>Social impact</i>		
<i>Project costs</i>	3-4M€ (FO ³) ⁴		<i>Pollutant loss</i>		
<i>Device price</i>			<i>Seabed variation</i>		
<i>Selling energy (€/kWh)</i>	Cost: 2.8 ⁴ (FO ³) Price:		<i>Water temperature variation</i>		



⁴ <http://www02.abb.com/global/gad/gad02077.nsf/lupLongContent/D74F5739AAE738F6C12571D800305007>

SSG		COMPANY DATA		
 		<i>Name</i>	Wave Energy AS	
		<i>Main investors/ Project partners</i>	Private Venture Capital	
		<i>Country</i>	 Norway	
		<i>Story</i>		
		<i>Founded</i>	2004	
		<i>EU & State support</i>	FP6: 1.0M€	
		<i>Technical referent</i>		
<i>Contact</i>		Web: www.waveenergy.no Phone: (+47) 51 61 09 30 Fax: (+47) 51 61 09 31 Email: espen.osaland@waveenergy.no		
DEVICE TECHNOLOGY SPECIFICATION				
<i>Category</i>	Overtopping - in breakwater		X single device <input type="checkbox"/> farm	
<i>Position</i>	X shoreline <input type="checkbox"/> nearshore		X offshore	
<i>Power Matrix</i>				
<i>Nominal Power</i>		<i>Patent</i>	X yes <input type="checkbox"/> no <input type="checkbox"/> no info	
<i>PTO</i>	<input type="checkbox"/> linear generator <input type="checkbox"/> hydraulic motor/generator		X water turbine <input type="checkbox"/> air turbine	
<i>Power transmission system</i>	X electrical energy		<input type="checkbox"/> AC/DC in converter	
DEVICE DEVELOPMENT STRATEGY				
<i>Phase</i>	<i>Scale</i>	<i>Facility</i>	<i>Rating</i>	<i>Date</i>
1	1:60 – 1:25	Aalborg University, Denmark	-	2003-2005
2	1:15	Aalborg University, Denmark	-	2003-2005
3	1:4 (PTO)	NTNU, Norway	-	2005-2006
4				
5				
<i>Scientific Paper</i>	[90]			
ECONOMIC DATA		PREDICTABLE IMPACT		
<i>Joint stock composition</i>		<i>Noise</i>		
<i>R&D costs (€/kW)</i>		<i>Visual impact</i>		
<i>Commercial costs (€/kW)</i>		<i>Social impact</i>		
<i>Project costs</i>		<i>Pollutant loss</i>		
<i>Device price</i>		<i>Seabed variation</i>		
<i>Selling energy (€/kWh)</i>	<i>Cost:</i>	<i>Price:</i>	<i>Water temperature variation</i>	


SEAREV		COMPANY DATA		
		<i>Name</i>	École centrale de Nantes	
		<i>Main investors/ Project partners</i>	CNRS	
		<i>Country</i>	 France	
		<i>Story</i>	-	
		<i>Founded</i>	-	
		<i>EU & State support</i>	FP6	
		<i>Technical referent</i>	M. Alain CLEMENT – Inventor	
		<i>Contact</i>	Web: www.ec-nantes.fr Email: Alain.Clement@ec-nantes.fr	
DEVICE TECHNOLOGY SPECIFICATION				
<i>Category</i>	Point absorber	<input checked="" type="checkbox"/> single device	<input type="checkbox"/> farm	
<i>Position</i>	<input type="checkbox"/> shoreline	<input type="checkbox"/> nearshore	<input checked="" type="checkbox"/> offshore (30-50m)	
<i>Power Matrix</i>				
				
<i>Nominal Power</i>	500 kW	<i>Patent</i>	<input checked="" type="checkbox"/> yes (2004) <input type="checkbox"/> no <input type="checkbox"/> no info	
<i>PTO</i>	<input type="checkbox"/> linear generator	<input checked="" type="checkbox"/> hydraulic motor/generator	<input type="checkbox"/> water turbine <input type="checkbox"/> air turbine	
<i>Power transmission system</i>	<input checked="" type="checkbox"/> electrical energy <input type="checkbox"/> AC/DC in converter			
DEVICE DEVELOPMENT STRATEGY				
<i>Phase</i>	<i>Scale</i>	<i>Facility</i>	<i>Rating</i>	<i>Date</i>
1				
2	1:12	École centrale de Nantes, France	-	2006
3				
4	1:1	Pays de la Loire, France	500kW	Planned 2012
5				
<i>Scientific Paper</i>				
ECONOMIC DATA		PREDICTABLE IMPACT		
<i>Joint stock composition</i>		<i>Noise</i>		
<i>R&D costs (€/kW)</i>		<i>Visual impact</i>		
<i>Commercial costs (€/kW)</i>		<i>Social impact</i>		
<i>Project costs</i>		<i>Pollutant loss</i>		
<i>Device price</i>		<i>Seabed variation</i>		
<i>Selling energy (€/kWh)</i>	<i>Cost:</i>	<i>Price:</i>	<i>Water temp. variation</i>	





GreenWAVE/BlueWAVE		COMPANY DATA		
		<i>Name</i>	Ocealinx	
		<i>Main investors/ Project partners</i>	Venture capital	
		<i>Country</i>	 Australia	
		<i>Story</i>	Ocealinx is founded by Dr. Tom Denniss (as Energetech Australia Pty Limited)	
		<i>Founded</i>	1997	
		<i>State support</i>	1999: 610k€, 2002: 3.4M€, 2003: 380k€, 2004: 1M€, 2005: 408k€, 2007: 14.2M€, 2011: 260k€	
		<i>Technical referent</i>	Ali Baghaei (CEO), Tom Denniss	
<i>Contact</i>	Web: www.oceanlinx.com Phone: + 61 (0) 2 9490 0100 Fax: + 61 (0) 2 9490 0199 Email: info@oceanlinx.com			
DEVICE TECHNOLOGY SPECIFICATION				
<i>Category</i>	OWC	<input checked="" type="checkbox"/> single device (greenWAVE)	<input checked="" type="checkbox"/> farm (blueWAVE)	
<i>Position</i>	<input type="checkbox"/> shoreline	<input checked="" type="checkbox"/> nearshore (greenWAVE in 10m)	<input checked="" type="checkbox"/> offshore (blueWAVE, in 40-80m)	
<i>Power Matrix</i>				
<i>Nominal Power</i>	2.5MW (blueWAVE, with 6 OWC), 500kW (MK1)		<i>Patent</i> <input checked="" type="checkbox"/> yes <input type="checkbox"/> no <input type="checkbox"/> no info	
<i>PTO</i>	<input type="checkbox"/> linear generator	<input type="checkbox"/> hydraulic motor/generator	<input type="checkbox"/> water turbine <input checked="" type="checkbox"/> air turbine	
<i>Power transmission system</i>	<input checked="" type="checkbox"/> electrical energy		<input type="checkbox"/> AC/DC in converter	
DEVICE DEVELOPMENT STRATEGY				
<i>Phase</i>	<i>Scale</i>	<i>Facility</i>	<i>Rating</i>	<i>Date</i>
1	1:40	Maritime College, Tasmania	-	1990-2000
1	1:40	HMRC, UCC, Ireland	-	2008
2	1:7 (PTO)	Uni. of Sydney, Australia	-	1990-2000
3	1:3	Port Kembla, Australia (MK2)	represented 1.5MW	2007-2008
3/4	1:3	Port Kembla, Australia (MK3PC, blueWAVE)	represented 2.5MW	2010
4	1:1	Port Kembla, Australia (MK1, greenWAVE)	500kW	2005-2009
5				
<i>Scientific Paper</i>				
ECONOMIC DATA		PREDICTABLE IMPACT		
<i>Joint stock composition</i>		<i>Noise</i>		
<i>R&D costs (€/kW)</i>		<i>Visual impact</i>	12m above MWL	
<i>Commercial costs (€/kW)</i>		<i>Social impact</i>		
<i>Project costs</i>		<i>Pollutant loss</i>	no	
<i>Device price</i>		<i>Seabed variation</i>		
<i>Selling energy (€/kWh)</i>	<i>Cost: 0.09⁵</i>	<i>Price:</i>	<i>Water temperature var.</i>	

⁵ <http://www2.hmc.edu/~evans/WPHPark.pdf>





MUTRIKU		COMPANY DATA		
		<i>Name</i>	Voith Hydro Wavegen Limited	
		<i>Main investors/ Project partners</i>	EVE, Fedarene, Cres	
		<i>Country</i>	 Scotland	
		<i>Story</i>	Power utility Ente Vasco de la Energia (EVE) in July 2011 has inaugurated the wave energy power plant at Mutriku, a Basque seaport. Construction of the Mutriku power plant began in 2006.	
		<i>Founded</i>	1990 by Allan Thomson (Wavegen)	
		<i>EU & State support</i>	EU FP6: 3.5M€	
		<i>Technical referent</i>	Yago Torre-Enciso (EVE) Matthew Seed (CEO-Wavegen)	
		<i>Contact</i>	Web: http://www.wavegen.co.uk http://www.eve.es Phone: +44 (0) 1463 238094 Fax: +44 (0) 1463 238096 Email: enquiries@wavegen.com	
DEVICE TECHNOLOGY SPECIFICATION				
<i>Category</i>	OWC – in breakwater		X single device <input type="checkbox"/> farm	
<i>Position</i>	X shoreline	<input type="checkbox"/> nearshore	<input type="checkbox"/> offshore	
<i>Power Matrix</i>				
<i>Nominal Power</i>	18.5kW	<i>Patent</i>	X yes <input type="checkbox"/> no <input type="checkbox"/> no info	
<i>PTO</i>	<input type="checkbox"/> linear generator <input type="checkbox"/> hydraulic motor/generator <input type="checkbox"/> water turbine X air turbine			
<i>Power transmission system</i>	X electrical energy <input type="checkbox"/> AC/DC in converter			
DEVICE DEVELOPMENT STRATEGY				
<i>Phase</i>	<i>Scale</i>	<i>Facility</i>	<i>Rating</i>	<i>Date</i>
1	-	Limpet, island of Islay, Scotland	-	2000
2				
3				
4				
5	1:1 (16 OWC)	Mutriku, Spain	296kW	2006-2011
<i>Scientific Paper</i>	[91]			
ECONOMIC DATA		PREDICTABLE IMPACT		
<i>Joint stock composition</i>		<i>Noise</i>		
<i>R&D costs (€/kW)</i>		<i>Visual impact</i>		
<i>Commercial costs (€/kW)</i>		<i>Social impact</i>		
<i>Project costs</i>	6.4 M€	<i>Pollutant loss</i>		
<i>Device price</i>		<i>Seabed variation</i>	-	
<i>Selling energy (€/kWh)</i>	<i>Cost:</i>	<i>Price:</i>	<i>Water temp. variation</i>	



CETO		COMPANY DATA		
		<i>Name</i>	Carnegie Wave Energy Limited	
		<i>Main investors/ Project partners</i>	Joint Venture License Agreement with EDF Energies Nouvelles/ EDF EN, DCNS	
		<i>Country</i>	Australia	
		<i>Story</i>	-	
		<i>Founded</i>	1999	
		<i>State support</i>	Western Australian Government : €10.1M French Government: €4.0M British Columbia Government: €1.6M	
		<i>Technical referent</i>	Jonathan Fievez, Technology Development Manager	
<i>Contact</i>	Web: www.carnegiwave.com Phone: +61 8 9486 4466 Email: enquiries@carnegiwave.com			
DEVICE TECHNOLOGY SPECIFICATION				
<i>Category</i>	Point absorber – submerged	<input checked="" type="checkbox"/> single device	<input type="checkbox"/> farm	
<i>Position</i>	<input type="checkbox"/> shoreline	<input checked="" type="checkbox"/> nearshore (20-50m)	<input type="checkbox"/> offshore	
<i>Power Matrix</i>				
<i>Nominal Power</i>	200kW	<i>Patent</i>	<input checked="" type="checkbox"/> yes <input type="checkbox"/> no <input type="checkbox"/> no info	
<i>PTO</i>	<input type="checkbox"/> linear generator <input type="checkbox"/> hydraulic motor/generator	<input checked="" type="checkbox"/> water turbine	<input type="checkbox"/> air turbine	
<i>Power transmission system</i>	<input checked="" type="checkbox"/> electrical energy <input type="checkbox"/> AC/DC in converter			
DEVICE DEVELOPMENT STRATEGY				
<i>Phase</i>	<i>Scale</i>	<i>Facility</i>	<i>Rating</i>	<i>Date</i>
1	-	Maritime College, Australia	-	1999-2003
2				
3	1:6	Fremantle, Australia (CETO I)	-	2003-2006
3/4	1:3	Fremantle, Australia (CETO II)	-	2006-2008
4	1:1	Garden Island, Australia (CETOIII)	200kW	2009-2011
4	1:1	Reunion Island, France (CETOIV)	-	in development
5				
<i>Scientific Paper</i>				
ECONOMIC DATA			PREDICTABLE IMPACT	
<i>Joint stock composition</i>			<i>Noise</i>	
<i>R&D costs (€/kW)</i>			<i>Visual impact</i>	no
<i>Commercial costs (€/kW)</i>			<i>Social impact</i>	
<i>Project costs</i>			<i>Pollutant loss</i>	no
<i>Device price</i>			<i>Seabed variation</i>	
<i>Selling energy (€/kWh)</i>		<i>Cost:</i>	<i>Price:</i>	<i>Water temp. variation</i>

MRC		COMPANY DATA			
		<i>Name</i>	Orecon Ltd		
		<i>Main investors/ Project partners</i>	Advent Ventures, Venrock, Wellington Partners, Northzone Ventures		
		<i>Country</i>	 UK		
		<i>Story</i>	University of Plymouth spin-off		
		<i>Founded</i>	2002		
		<i>EU & State support</i>	2006: €160k		
		<i>Technical referent</i>	Fraser Johnson		
		<i>Contact</i>	Web: www.orecon.com Phone: +44 (0) 1208 269 Email: fjohnson@orecon.com		
DEVICE TECHNOLOGY SPECIFICATION					
<i>Category</i>	Multiple resonant chamber OWC		X single device <input type="checkbox"/> farm		
<i>Position</i>	<input type="checkbox"/> shoreline <input type="checkbox"/> nearshore		X offshore (50-100m)		
<i>Power Matrix</i>					
<i>Nominal Power</i>	3x500kW (full scale)		<i>Patent</i>	X yes <input type="checkbox"/> no <input type="checkbox"/> no info	
<i>PTO</i>	<input type="checkbox"/> linear generator <input type="checkbox"/> hydraulic motor/generator <input type="checkbox"/> water turbine X air turbine				
<i>Power transmission system</i>	X electrical energy <input type="checkbox"/> AC/DC in converter				
DEVICE DEVELOPMENT STRATEGY					
<i>Phase</i>	<i>Scale</i>	<i>Facility</i>	<i>Rating</i>	<i>Date</i>	
1	1:100	University of Plymouth	-	2002	
2	1:20	IFREMER, Brest	-	2003	
2/3	1:12	Ocean	5kW	2004	
3					
4					
5					
<i>Scientific Paper</i>					
ECONOMIC DATA			PREDICTABLE IMPACT		
<i>Joint stock composition</i>			<i>Noise</i>		
<i>R&D costs (€/kW)</i>			<i>Visual impact</i>		
<i>Commercial costs (€/kW)</i>			<i>Social impact</i>		
<i>Project costs</i>			<i>Pollutant loss</i>		
<i>Device price</i>			<i>Seabed variation</i>		
<i>Selling energy (€/kWh)</i>	<i>Cost:</i>	<i>Price:</i>	<i>Water temp. variation</i>		


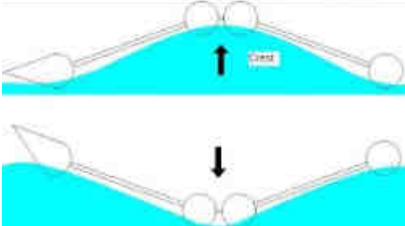

WAVEBERG		COMPANY DATA		
  		<i>Name</i>	Waveberg Development Limited (WDL)	
		<i>Main investors/ Project partners</i>	Venture capital/Wave Energy Centre, HMRC, OREC, Univ. New Hampshire	
		<i>Country</i>	 USA	
		<i>Story</i>	-	
		<i>Founded</i>	1992	
		<i>State support</i>	-	
		<i>Technical referent</i>	John Berg, Inventor of technology	
		<i>Contact</i>	Web: www.waveberg.com Email: info@waveberg.com Phone: 1 212 882 1788 Fax: 1 212 354 6412	
DEVICE TECHNOLOGY SPECIFICATION				
<i>Category</i>	OB - floating	X single device <input type="checkbox"/> farm		
<i>Position</i>	<input type="checkbox"/> shoreline	<input type="checkbox"/> nearshore	X offshore (20-40m)	
<i>Power Matrix</i>				
<i>Nominal Power</i>	100 kW (full scale)	<i>Patent</i>	X yes <input type="checkbox"/> no <input type="checkbox"/> no info	
<i>PTO</i>	<input type="checkbox"/> linear generator	<input type="checkbox"/> hydraulic motor/generator	X water turbine <input type="checkbox"/> air turbine	
<i>Power transmission system</i>	X electrical energy		<input type="checkbox"/> AC/DC in converter	
DEVICE DEVELOPMENT STRATEGY				
<i>Phase</i>	<i>Scale</i>	<i>Facility</i>	<i>Rating</i>	<i>Date</i>
1	1:50	HMRC, Ireland	-	2006
2	1:25	HMRC, Ireland	-	2007-2009
2	1:16	NRC Canada	-	1990-1991
2	1:10	Cape Canaveral, Florida	-	2000
3	1:5	San Francisco Bay, California	-	1988
3	1:4	Cape Canaveral, Florida	-	1996
4				
5				
<i>Scientific Paper</i>				
ECONOMIC DATA			PREDICTABLE IMPACT	
<i>Joint stock composition</i>		<i>Noise</i>		
<i>R&D costs (€/kW)</i>		<i>Visual impact</i>		
<i>Commercial costs</i>		<i>Social impact</i>		
<i>Project costs</i>		<i>Pollutant loss</i>		
<i>Device price</i>		<i>Seabed variation</i>		
<i>Selling energy (€/kWh)</i>		<i>Cost:</i> 0.05 ⁶	<i>Price:</i>	<i>Water temp. variation</i>


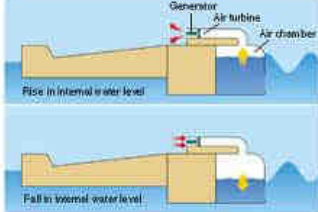



⁶ http://cnse.albany.edu/download/Waveberg_Development.pdf



WAVEPLANE		COMPANY DATA		
	<i>Name</i>	Waveplane A/S		
	<i>Main investors/ Project partners</i>	WPP A/S is shareholder in WavePlane		
	<i>Country</i>	 Denmark		
	<i>Story</i>	The WavePlane was invented by Erik Skaarup and first patented in October 1991. A revised patent application was submitted in 1998.		
	<i>Founded</i>	2006		
	<i>EU & State support</i>			
	<i>Technical referent</i>	Anders Vejby		
 	<i>Contact</i>	Web: www.waveplane.com Phone: +45 (0) 3975 1213 Fax: +45 (0) 3975 1214 Email: av@waveplane.dk		
DEVICE TECHNOLOGY SPECIFICATION				
<i>Category</i>	Overtopping - floating	X single device <input type="checkbox"/> farm		
<i>Position</i>	<input type="checkbox"/> shoreline	X nearshore (15m)	<input type="checkbox"/> offshore	
<i>Power Matrix</i>				
<i>Nominal Power</i>	100kW	<i>Patent</i>	X yes <input type="checkbox"/> no <input type="checkbox"/> no info	
<i>PTO</i>	<input type="checkbox"/> linear generator <input type="checkbox"/> hydraulic motor/generator	X water turbine	<input type="checkbox"/> air turbine	
<i>Power transmission system</i>	X electrical energy <input type="checkbox"/> AC/DC in converter			
DEVICE DEVELOPMENT STRATEGY				
<i>Phase</i>	<i>Scale</i>	<i>Facility</i>	<i>Rating</i>	<i>Date</i>
1	1:10	HMRC, UCC, Ireland	-	1996
2	1:18	HMRC, UCC, Ireland	-	1996
2	1:20	DTU – DMI, Denmark	-	1997-1998
3	1:7	DHI, Denmark	-	2001
3	1:2.5	Nissum Bredning-DMI, Denmark	4kW	1999
3	1:2.5	Copenhagen, Denmark	4kW	2000
4	1:1	Hanstholm, Denmark	100kW	2008
5				
<i>Scientific Paper</i>				
ECONOMIC DATA		PREDICTABLE IMPACT		
<i>Joint stock composition</i>		<i>Noise</i>		
<i>R&D costs (€/kW)</i>		<i>Visual impact</i>		
<i>Commercial costs (€/kW)</i>		<i>Social impact</i>		
<i>Project costs</i>		<i>Pollutant loss</i>		
<i>Device price</i>		<i>Seabed variation</i>		
<i>Selling energy (€/kWh)</i>	<i>Cost:</i>	<i>Price:</i>	<i>Water temp. variation</i>	


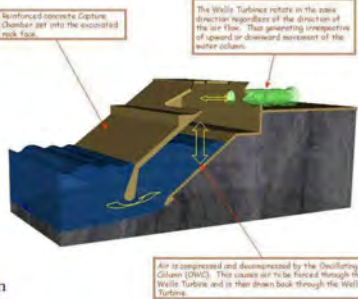

WET EnGen		COMPANY DATA		
		<i>Name</i>	Wave Energy Technologies Inc	
		<i>Main investors/ Project partners</i>	Private Investment/Dalhousie University of Halifax, Nova Scotia, the National Research Council of Canada	
		<i>Country</i>	 Canada	
		<i>Story</i>	-	
		<i>Founded</i>	2004	
		<i>State support</i>	-	
		<i>Technical referent</i>	Alan Vowles (CTO and inventor)	
<i>Contact</i>	Web: www.waveenergytech.com Email: info@waveenergytech.com Phone: 1 212 882 1788 Fax: 1 212 354 6412			
DEVICE TECHNOLOGY SPECIFICATION				
<i>Category</i>	Point Absorber	X single device <input type="checkbox"/> farm		
<i>Position</i>	<input type="checkbox"/> shoreline	<input type="checkbox"/> nearshore	X offshore (>50m)	
<i>Power Matrix</i>				
<i>Nominal Power</i>	200kW	<i>Patent</i>	X yes <input type="checkbox"/> no <input type="checkbox"/> no info	
<i>PTO</i>	<input type="checkbox"/> linear generator <input type="checkbox"/> hydraulic motor/generator	X water turbine	<input type="checkbox"/> air turbine	
<i>Power transmission system</i>	<input type="checkbox"/> electrical energy	X AC/DC in converter		
DEVICE DEVELOPMENT STRATEGY				
<i>Phase</i>	<i>Scale</i>	<i>Facility</i>	<i>Rating</i>	<i>Date</i>
1	-	-	-	2004-2005
2	-	NRC, Canada	-	2006
3	-	Sandy Cove, Nova Scotia	20kW	2006-2007
3	-	Sandy Cove, Nova Scotia	40kW	2008
4				
5				
<i>Scientific Paper</i>				
ECONOMIC DATA		PREDICTABLE IMPACT		
<i>Joint stock composition</i>		<i>Noise</i>		
<i>R&D costs (€/kW)</i>		<i>Visual impact</i>		
<i>Commercial costs (€/kW)</i>	1200 ⁷	<i>Social impact</i>		
<i>Project costs</i>		<i>Pollutant loss</i>		
<i>Device price</i>		<i>Seabed variation</i>		
<i>Selling energy (€/kWh)</i>	<i>Cost:</i> 0.06-0.12 <i>Price:</i>	<i>Water temp. variation</i>		

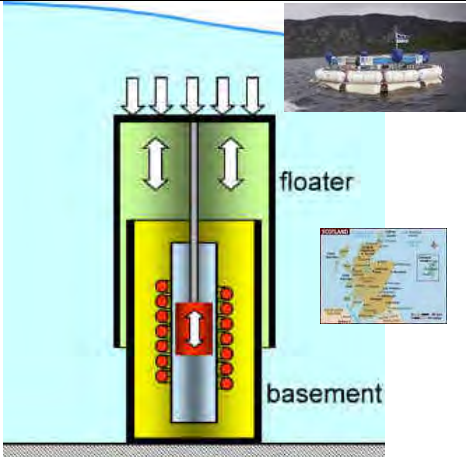

⁷http://canmetenergy.nrcan.gc.ca/sites/canmetenergy.nrcan.gc.ca/files/pdf/fichier/80634/NRCan_Marine_Energy_Technology.pdf

DEXA		COMPANY DATA			
 		<i>Name</i>	DEXAWAVE ApS		
		<i>Main investors/ Project partners</i>	Fjero A/S, Hanstholm Skibssmedie ApS, Uni El A/S, DIS A/S, A1 Consult ApS, Aalborg Universitet		
		<i>Country</i>	 Denmark		
		<i>Story</i>	-		
		<i>Founded</i>	-		
		<i>EU&State support</i>	FP7: € 195.463		
		<i>Technical referent</i>	Lars Clausen (inventor and CTO)		
<i>Contact</i>		Web: www.dexawave.com Phone: + 45 8651 8690 Email: info@dexawave.com			
DEVICE TECHNOLOGY SPECIFICATION					
<i>Category</i>	OB	X single device		<input type="checkbox"/> farm	
<i>Position</i>	<input type="checkbox"/> shoreline	X nearshore		<input type="checkbox"/> offshore	
<i>Power Matrix</i>					
<i>Nominal Power</i>	250 kW	<i>Patent</i>	X yes	<input type="checkbox"/> no <input type="checkbox"/> no info	
<i>PTO</i>	<input type="checkbox"/> linear generator	X hydraulic motor/generator		<input type="checkbox"/> water turbine <input type="checkbox"/> air turbine	
<i>Power transmission system</i>	X electrical energy		<input type="checkbox"/> AC/DC in converter		
DEVICE DEVELOPMENT STRATEGY					
<i>Phase</i>	<i>Scale</i>	<i>Facility</i>	<i>Rating</i>	<i>Date</i>	
1	1:60 – 1:30	Aalborg University, Denmark	-	-	
2	1:20	Aalborg University, Denmark	-	-	
2/3	1:10 (PTO)	Nissum Bredning, Denmark	160kW	2009	
3	1:5	DanWEC Hanstholm, Denmark	5kW	2010-2012	
4	1:1	Malta	3 X 250kW	agreement with the Gov.	
5					
<i>Scientific Paper</i>	[92] [93]				
ECONOMIC DATA			PREDICTABLE IMPACT		
<i>Joint stock composition</i>			<i>Noise</i>		
<i>R&D costs (€/kW)</i>			<i>Visual impact</i>		
<i>Commercial costs (€/kW)</i>			<i>Social impact</i>		
<i>Project costs</i>			<i>Pollutant loss</i>		
<i>Device price</i>			<i>Seabed variation</i>		
<i>Selling energy (€/kWh)</i>	<i>Cost:</i>	<i>Price:</i>	<i>Water temp. variation</i>		

MIGHTY WHALE		COMPANY DATA			
   		<i>Name</i>	Japan Agency for Marine-Earth Science and Technology (JAMSTEC)		
		<i>Main investors/Project partners</i>	-		
		<i>Country</i>	 Japan		
		<i>Story</i>	-		
		<i>Founded</i>	1971		
		<i>State support</i>	-		
		<i>Technical referent</i>	-		
		<i>Contact</i>	Web: www.jamstec.go.jp/e/ Email: www-admin@jamstec.go.jp Phone: +81-46-867-9070		
DEVICE TECHNOLOGY SPECIFICATION					
<i>Category</i>	OWC - floating		X single device <input type="checkbox"/> farm		
<i>Position</i>	<input type="checkbox"/> shoreline		<input type="checkbox"/> nearshore X offshore (40m)		
<i>Power Matrix</i>					
<i>Nominal Power</i>	120kW (60kW+2*30kW)		<i>Patent</i>	<input type="checkbox"/> yes <input type="checkbox"/> no X no info	
<i>PTO</i>	<input type="checkbox"/> linear generator <input type="checkbox"/> hydraulic motor/generator		<input type="checkbox"/> water turbine X air turbine		
<i>Power transmission system</i>	X electrical energy		<input type="checkbox"/> AC/DC in converter		
DEVICE DEVELOPMENT STRATEGY					
<i>Phase</i>	<i>Scale</i>	<i>Facility</i>	<i>Rating</i>	<i>Date</i>	
1	-	-	-	1987	
2					
3					
3					
4	1:1 (50m X 30m)	Gokasho Bay, Japan	120kW	1998-2002	
5					
<i>Scientific Paper</i>					
ECONOMIC DATA		PREDICTABLE IMPACT			
<i>Joint stock composition</i>		<i>Noise</i>			
<i>R&D costs (€/kW)</i>		<i>Visual impact</i>			
<i>Commercial costs (€/kW)</i>		<i>Social impact</i>			
<i>Project costs</i>		<i>Pollutant loss</i>			
<i>Device price</i>		<i>Seabed variation</i>			
<i>Selling energy (€/kWh)</i>	<i>Cost:</i>	<i>Price:</i>	<i>Water temperature variation</i>		


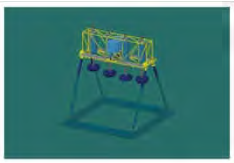


PICO		COMPANY DATA		
		<i>Name</i>	European Wave Energy Pilot Plan	
		<i>Main investors/ Project partners</i>	Portuguese Government, Electricidade de Portugal (EDP), Electricidade dos Açores (EDA)	
		<i>Country</i>	 Portugal	
		<i>Story</i>	The European Pico OWC plant was built from 1995 to 1998 within the framework of two EC JOULE projects and co-funding from EDP and EDA. Shortly after its creation in 2003, the Wave Energy Centre (WavEC) took over responsibility of the plant recovering the original layout with financial support of national funding and of some of its associates.	
		<i>Founded</i>	2003 (WavEC)	
		<i>EU & State support</i>	Portuguese public funds : 600k€	
		<i>Technical referent</i>	Frank Neumann (WavEC)	
		<i>Contact</i>	Phone.:(+351) 21 8482655 Fax:(+351) 21 8481630 Website: www.wavec.org Email: mail@wavec.org	
DEVICE TECHNOLOGY SPECIFICATION				
<i>Category</i>	OWC	X single device <input type="checkbox"/> farm		
<i>Position</i>	X shoreline	<input type="checkbox"/> nearshore <input type="checkbox"/> offshore		
<i>Power Matrix:</i>				
<i>Nominal Power</i>	400 kW	<i>Patent</i>	<input type="checkbox"/> yes <input type="checkbox"/> no X no info	
<i>PTO</i>	<input type="checkbox"/> linear generator <input type="checkbox"/> hydraulic motor/generator <input type="checkbox"/> water turbine X air turbine			
<i>Power transmission system</i>	X electrical energy <input type="checkbox"/> AC/DC in converter			
DEVICE DEVELOPMENT STRATEGY				
<i>Phase</i>	<i>Scale</i>	<i>Facility</i>	<i>Rating</i>	<i>Date</i>
1				
2				
3				
4	1:1	Pico Island, Azores, Portugal	400 kW	1995-1998
5				
<i>Scientific Paper</i>	[94] [95]			
ECONOMIC DATA		PREDICTABLE IMPACT		
<i>Joint stock composition</i>		<i>Noise</i>		
<i>R&D costs (€/kW)</i>		<i>Visual impact</i>		
<i>Commercial costs (€/kW)</i>		<i>Social impact</i>		
<i>Project costs</i>	€ 4M [96]	<i>Pollutant loss</i>		
<i>Device price</i>		<i>Seabed variation</i>		
<i>Selling energy (€/kWh)</i>	<i>Cost:</i>	<i>Price:</i>	<i>Water temp. variation</i>	

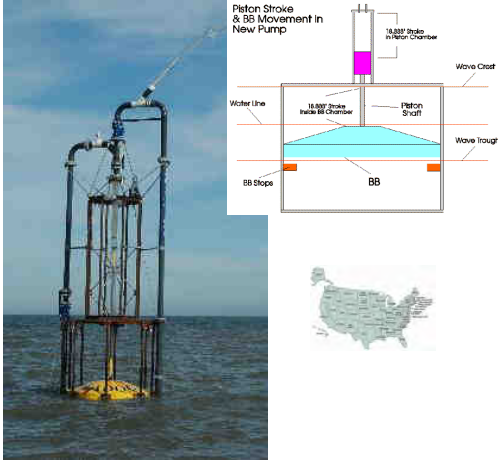

LIMPET		COMPANY DATA		
  <p>The Wells Turbine rotates in the same direction regardless of the direction of the air flow. This generating irrespective of upward or downward movement of the water column.</p> <p>Air is compressed and decompressed by the Oscillating Water Column (OWC). This causes air to be forced through the Wells Turbine and is then drawn back through the Wells Turbine.</p>		<i>Name</i>	Voith Hydro Wavegen Limited	
		<i>Main investors/ Project partners</i>	Wavegen, Queens University of Belfast (QUB)	
		<i>Country</i>	 Scotland	
		<i>Story</i>	The LIMPET (Land Installed Marine Powered Energy Transformer) shoreline OWC is a 500kW wave energy collector located on the South Western coast of the Hebridean island of Islay. It is situated close to the site of the now decommissioned 75kW prototype device that was installed by The Queens University of Belfast in 1991.	
		<i>Founded</i>	1990	
		<i>EU & State support</i>	-	
		<i>Technical referent</i>	David Langston	
<i>Contact</i>	Web: http://www.wavegen.co.uk Phone: +44 (0) 1463 238094 Fax: +44 (0) 1463 238096 Email: enquiries@wavegen.com			
DEVICE TECHNOLOGY SPECIFICATION				
<i>Category</i>	OWC	<input checked="" type="checkbox"/> single device	<input type="checkbox"/> farm	
<i>Position</i>	<input checked="" type="checkbox"/> shoreline	<input type="checkbox"/> nearshore	<input type="checkbox"/> offshore	
<i>Power Matrix</i>				
<i>Nominal Power</i>	500 kW	<i>Patent</i>	<input checked="" type="checkbox"/> yes <input type="checkbox"/> no <input type="checkbox"/> no info	
<i>PTO</i>	<input type="checkbox"/> linear generator <input type="checkbox"/> hydraulic motor/generator	<input type="checkbox"/> water turbine	<input checked="" type="checkbox"/> air turbine	
<i>Power transmission system</i>	<input checked="" type="checkbox"/> electrical energy	<input type="checkbox"/> AC/DC in converter		
DEVICE DEVELOPMENT STRATEGY				
<i>Phase</i>	<i>Scale</i>	<i>Facility</i>	<i>Rating</i>	<i>Date</i>
1				
2				
3	1:1.75	Islay, Scotland	75 kW	1988-1999
4	1:1	Islay, Scotland	500 kW	1998-2000
5				
<i>Scientific Paper</i>	[97]			
ECONOMIC DATA		PREDICTABLE IMPACT		
<i>Joint stock composition</i>		<i>Noise</i>		
<i>R&D costs (€/kW)</i>		<i>Visual impact</i>		
<i>Commercial costs (€/kW)</i>		<i>Social impact</i>		
<i>Project costs</i>		<i>Pollutant loss</i>		
<i>Device price</i>		<i>Seabed variation</i>		
<i>Selling energy (€/kWh)</i>	<i>Cost:</i>	<i>Price:</i>	<i>Water temp. variation</i>	



AWS (Archimede Wave Swing)		COMPANY DATA																										
		<i>Name</i>	AWS Ocean Energy Ltd.																									
		<i>Main investors/Project partners</i>	Shell Technology Ventures Fun, Alstom																									
		<i>Country</i>	 Scotland																									
		<i>Story</i>	Fred Gardner is the inventor																									
		<i>Founded</i>	2004																									
		<i>EU & State support</i>	2007:2.1M£ (≈2.5M€), Scottish Enterprise: 2M£ (≈2.4M€), Scottish Government: 1.39M£ (≈1.65M€)																									
		<i>Technical referent</i>	Ben Yeats (CTO)																									
<i>Contact</i>	Web: www.awsoccean.com Email: info@awsoccean.com Phone: +44 (0) 1463 725410																											
DEVICE TECHNOLOGY SPECIFICATION																												
<i>Category</i>	Point absorber – submerged (AWS), floating (AWS-III)	X single device <input type="checkbox"/> farm																										
<i>Position</i>	<input type="checkbox"/> shoreline <input type="checkbox"/> nearshore	X offshore (65-150m)																										
<i>Power Matrix (AWS)</i>																												
Wave Period – T _{10%} (s)																												
	5.0	5.5	6.0	6.5	7.0	7.5	8.0	8.5	9.0	9.5	10.0	10.5	11.0	11.5	12.0	12.5	13.0	13.5	14.0	14.5	15.0	15.5	16.0	16.5	17.0	17.5	18.0	
Significant Wave Height H _{sig} (m)	0.5	0	0	0	0	0	0	0	0	0	0	0	0	0	0	0	0	0	0	0	0	0	0	0	0	0	0	0
	1.0	2	7	13	19	26	34	41	48	58	68	81	93	105	118	131	144	153	163	183	203	213	223	223	223	225	227	
	1.5	4	15	28	41	56	72	85	99	121	143	173	203	225	248	265	285	309	334	357	380	389	398	398	398	398	403	409
	2.0	8	26	49	73	100	127	150	172	210	247	292	337	385	395	418	442	482	523	543	563	579	596	596	596	597	598	
	2.5	15	43	78	113	159	205	234	263	320	376	438	499	531	563	603	643	675	708	741	774	785	797	797	797	800	804	
	3.0	25	61	111	161	227	293	339	386	453	521	600	680	722	765	827	888	897	906	945	984	996	1009	1009	1009	1009	1003	998
	3.5	35	92	155	218	305	391	454	517	605	694	772	851	913	975	1036	1096	1110	1141	1163	1185	1198	1211	1211	1211	1211	1208	1206
	4.0	35	114	194	273	380	486	572	659	776	894	961	1027	1103	1179	1227	1275	1316	1357	1365	1374	1394	1414	1414	1414	1414	1415	1410
	4.5	0	0	235	332	479	626	722	819	957	1096	1168	1240	1320	1401	1449	1497	1547	1598	1590	1583	1610	1637	1637	1637	1637	1616	1595
	5.0	0	0	280	400	562	784	890	1014	1144	1274	1380	1487	1560	1651	1691	1731	1785	1838	1807	1777	1806	1836	1836	1836	1806	1777	
	5.5	0	0	320	432	641	849	1033	1216	1331	1445	1568	1690	1778	1857	1919	1970	1977	1984	1994	2005	2017	2030	2030	2030	2030	1990	1951
	6.0	0	0	0	0	680	944	1155	1367	1495	1623	1759	1895	1983	2072	2137	2202	2205	2207	2226	2245	2240	2234	2234	2234	2234	2194	2154
	6.5	0	0	0	0	720	1123	1335	1547	1678	1809	1963	2116	2206	2284	2332	2380	2425	2470	2452	2434	2403	2373	2373	2373	2373	2354	2336
<i>Nominal Power</i>	2.5MW (AWS-III)		<i>Patent</i>	X yes <input type="checkbox"/> no <input type="checkbox"/> no info																								
<i>PTO</i>	X linear generator <input type="checkbox"/> hydraulic motor/generator		<input type="checkbox"/> water turbine <input type="checkbox"/> air turbine																									
<i>Power transmission system</i>	X electrical energy		<input type="checkbox"/> AC/DC in converter																									
DEVICE DEVELOPMENT STRATEGY																												
<i>Phase</i>	<i>Scale</i>	<i>Facility</i>	<i>Rating</i>	<i>Date</i>																								
1	1:50	HMRC, UCC, Ireland (AWS)	-	1996-1998																								
1	1:60	HR Wallingford (AWS-III)	-	2007																								
2	1:20	Delft, The Netherlands (AWS)	-	1996																								
3	1:9	Loch Ness (AWS-III)	-	2010																								
4	1:1	Aguadoura, Portugal (AWS)	690kW	2004																								
4	1:1	EMEC, Scotland (AWS-III)	2.5MW	planned in 2014																								
5																												
<i>Scientific Paper</i>	[98]																											
ECONOMIC DATA		PREDICTABLE IMPACT																										
<i>Joint stock composition</i>		<i>Noise</i>																										
<i>R&D costs (€)</i>		<i>Visual impact</i>																										

<i>Commercial costs (€/kW)</i>		<i>Social impact</i>	
<i>Project costs (€/kW)</i>		<i>Pollutant loss</i>	
<i>Device price</i>		<i>Seabed variation</i>	
<i>Selling energy (€/kWh)</i>	<i>Cost:</i>	<i>Price:</i>	<i>Water temperature variation</i>






OCEANTEC		COMPANY DATA	
		<i>Name</i>	Oceantec Energías Marinas
		<i>Main investors/ Project partners</i>	Joint venture between Iberdrola and Tecnalia
		<i>Country</i>	Spain
		<i>Story</i>	Founded by Iberdrola and Tecnalia
		<i>Founded</i>	2008
		<i>EU & State support</i>	-
		<i>Technical referent</i>	Pablo Ruiz-Minguela
<i>Contact</i>	Web: www.oceantecenergy.com Phone: +34 946 575 609 Fax: +34 94 600 22 99 Email: info@oceantecenergy.com		
DEVICE TECHNOLOGY SPECIFICATION			
<i>Category</i>	OB	X single device <input type="checkbox"/> farm	
<i>Position</i>	<input type="checkbox"/> shoreline <input type="checkbox"/> nearshore X offshore (50-100m)		
<i>Power Matrix</i>			
<i>Nominal Power</i>	500kW (full scale)	<i>Patent</i>	X yes (PTO-2006) <input type="checkbox"/> no <input type="checkbox"/> no info
<i>PTO</i>	<input type="checkbox"/> linear generator X hydraulic motor/generator <input type="checkbox"/> water turbine <input type="checkbox"/> air turbine		
<i>Power transmission system</i>	X electrical energy <input type="checkbox"/> AC/DC in converter		
DEVICE DEVELOPMENT STRATEGY			
<i>Phase</i>	<i>Scale</i>	<i>Facility</i>	<i>Rating</i>
1	1:37.5	-	-
2	1:15	CEHIPAR, Spain	-
3	1:4	Cala Murgita, Spain (l=11.25m)	-
4			
5			
<i>Scientific Paper</i>	[99]		
ECONOMIC DATA		PREDICTABLE IMPACT	
<i>Joint stock composition</i>	Iberdrola (66.67%) ,Tecnalia (33.33%)	<i>Noise</i>	
<i>R&D costs</i>	€4.5M	<i>Visual impact</i>	
<i>Commercial costs (€/kW)</i>		<i>Social impact</i>	
<i>Project costs</i>		<i>Pollutant loss</i>	
<i>Device price</i>		<i>Seabed variation</i>	
<i>Selling energy (€/kWh)</i>	<i>Cost:</i>	<i>Price:</i>	<i>Water temp. variation</i>

DECM (Direct Energy Conversion Method)		COMPANY DATA		
  		<i>Name</i>	Trident Energy Ltd	
		<i>Main investors/ Project partners</i>		
		<i>Country</i>	 UK	
		<i>Story</i>	Hugh-Peter Kelly, Trident's founder	
		<i>Founded</i>	2003	
		<i>EU & State support</i>	Scottish Enterprise: 260k€	
		<i>Technical referent</i>	Malcolm van den Bergh	
<i>Contact</i>	Web: www.tridentenergy.co.uk Phone: +44 (0)20 7073 2963 Email: info@tridentenergy.co.uk			
DEVICE TECHNOLOGY SPECIFICATION				
<i>Category</i>	Point absorber	X single device <input type="checkbox"/> farm		
<i>Position</i>	<input type="checkbox"/> shoreline <input type="checkbox"/> nearshore	X offshore (50m)		
<i>Power Matrix</i>				
<i>Nominal Power</i>	1MW (full scale)	<i>Patent</i>	X yes <input type="checkbox"/> no <input type="checkbox"/> no info	
<i>PTO</i>	X linear generator <input type="checkbox"/> hydraulic motor/generator	<input type="checkbox"/> water turbine <input type="checkbox"/> air turbine		
<i>Power transmission system</i>	<input type="checkbox"/> electrical energy X AC/DC in converter			
DEVICE DEVELOPMENT STRATEGY				
<i>Phase</i>	<i>Scale</i>	<i>Facility</i>	<i>Rating</i>	<i>Date</i>
1	-	Devon	-	1999
2				
3	1:3 (PTO)	NaREC, UK	-	2005-2007
3	1:3	Suffolk coast, UK	20kW	2009
4				
5				
<i>Scientific Paper</i>	[100]			
ECONOMIC DATA		PREDICTABLE IMPACT		
<i>Joint stock composition</i>		<i>Noise</i>		
<i>R&D costs (€/kW)</i>		<i>Visual impact</i>		
<i>Commercial costs (€/kW)</i>		<i>Social impact</i>		
<i>Project costs</i>		<i>Pollutant loss</i>		
<i>Device price</i>		<i>Seabed variation</i>		
<i>Selling energy (€/kWh)</i>	<i>Cost:</i>	<i>Price:</i>	<i>Water temp. variation</i>	

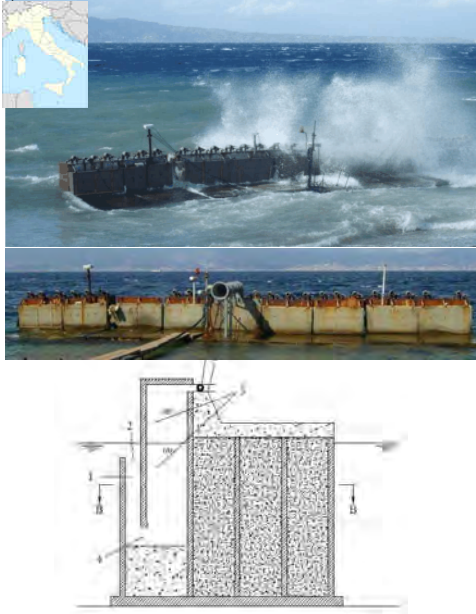

SEADOG Pump		COMPANY DATA		
	<i>Name</i>	Texas Natural Resources		
	<i>Main investors/ Project partners</i>	Venture capital/ Independent Natural Resources, Inc. (INRI)		
	<i>Country</i>	 USA		
	<i>Story</i>	TNR achieves the ownership of International Natural Resources, Inc. The Seadog Pump technology is invented by Kenneth W. Welch, Jr.		
	<i>Founded</i>	2008		
	<i>State support</i>	-		
	<i>Technical referent</i>	Mark Thomas (CEO INRI)		
	<i>Contact</i>	Web: www.inri.us www.txnaturalresources.com Email: info@txnaturalresources.com Phone: 832-623-7410		
DEVICE TECHNOLOGY SPECIFICATION				
<i>Category</i>	Point absorber	X single device <input type="checkbox"/> farm		
<i>Position</i>	<input type="checkbox"/> shoreline	X nearshore (25m)	<input type="checkbox"/> offshore	
<i>Power Matrix</i>				
<i>Nominal Power</i>	33kW	<i>Patent</i>	X yes <input type="checkbox"/> no <input type="checkbox"/> no info	
<i>PTO</i>	<input type="checkbox"/> linear generator	X hydraulic motor/generator	<input type="checkbox"/> water turbine <input type="checkbox"/> air turbine	
<i>Power transmission system</i>	X electrical energy <input type="checkbox"/> AC/DC in converter			
DEVICE DEVELOPMENT STRATEGY				
<i>Phase</i>	<i>Scale</i>	<i>Facility</i>	<i>Rating</i>	<i>Date</i>
1				
2	1:32	Texas University, USA	-	2003
3	1:4	Gulf of Mexico	12-18 g/min	2006-2007
4				
5				
<i>Scientific Paper</i>				
ECONOMIC DATA		PREDICTABLE IMPACT		
<i>Joint stock composition</i>		<i>Noise</i>		
<i>R&D costs (€/kW)</i>		<i>Visual impact</i>		
<i>Commercial costs (€/kW)</i>		<i>Social impact</i>		
<i>Project costs</i>		<i>Pollutant loss</i>		
<i>Device price</i>		<i>Seabed variation</i>		
<i>Selling energy (€/kWh)</i>	<i>Cost:</i>	<i>Price:</i>	<i>Water temp. variation</i>	

POSEIDON		COMPANY DATA		
		<i>Name</i>	Floating Power Plant A/S (FPP)	
		<i>Main investors/ Project partners</i>	Jotun, Dong Energy, HYDRAtch, Gaia, Tecinvest, Lolland Kommune	
		<i>Country</i>	 Denmark	
		<i>Story</i>	In 1980-1987 the inventor Hans Marius Pedersen developed wave energy concepts.	
		<i>Founded</i>	2004	
		<i>EU & Stat support</i>	-	
		<i>Technical referent</i>	Anders Køhler, CEO	
		<i>Contact</i>	Web:www.poseidonorgan.com/ Phone: +45 3391 9120 Email: info@floatingpowerplant.com	
DEVICE TECHNOLOGY SPECIFICATION				
<i>Category</i>	OB - floating	<input checked="" type="checkbox"/> single device	<input type="checkbox"/> farm	
<i>Position</i>	<input type="checkbox"/> shoreline	<input type="checkbox"/> nearshore	<input checked="" type="checkbox"/> offshore	
<i>Power Matrix</i>				
<i>Nominal Power</i>	140kW (wave) + 33kW (wind)	<i>Patent</i>	<input checked="" type="checkbox"/> yes <input type="checkbox"/> no <input type="checkbox"/> no info	
<i>PTO</i>	<input type="checkbox"/> linear generator	<input checked="" type="checkbox"/> hydraulic motor/generator	<input type="checkbox"/> water turbine <input type="checkbox"/> air turbine	
<i>Power transmission system</i>	<input checked="" type="checkbox"/> electrical energy <input type="checkbox"/> AC/DC in converter			
DEVICE DEVELOPMENT STRATEGY				
<i>Phase</i>	<i>Scale</i>	<i>Facility</i>	<i>Rating</i>	<i>Date</i>
1	1:30	Aalborg University, Denmark	-	1998
2/3	1:5	DHI, Denmark	-	1999-2000
2	1:10	DHI, Denmark	-	2001-2002
3/4	1:1 (37x25x6m)	Nakskov, Denmark (POSEIDON 37)	140kW	2008-2009
4				
5				
<i>Scientific Paper</i>				
ECONOMIC DATA		PREDICTABLE IMPACT		
<i>Joint stock composition</i>		<i>Noise</i>		
<i>R&D costs (€/kW)</i>		<i>Visual impact</i>		
<i>Commercial costs (€/kW)</i>		<i>Social impact</i>		
<i>Project costs</i>		<i>Pollutant loss</i>		
<i>Device price</i>		<i>Seabed variation</i>		
<i>Selling energy (€/kWb)</i>	<i>Cost:</i> 0.10-0.15 ⁸	<i>Price:</i>	<i>Water temp. Var.</i>	

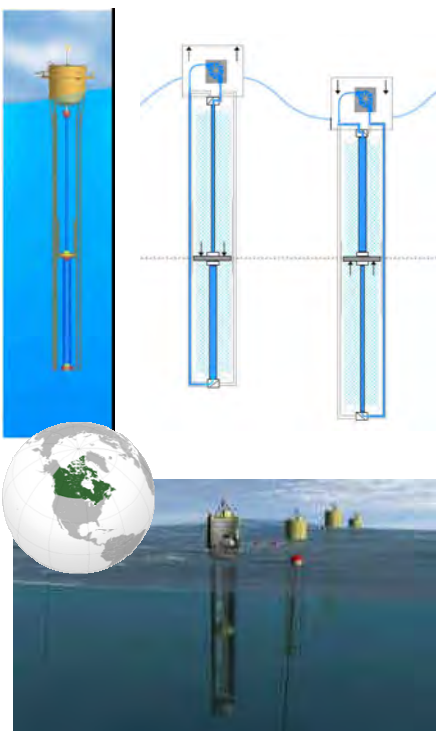

⁸ <http://www.greentechmedia.com/articles/read/a-power-plant-for-wind-and-waves>

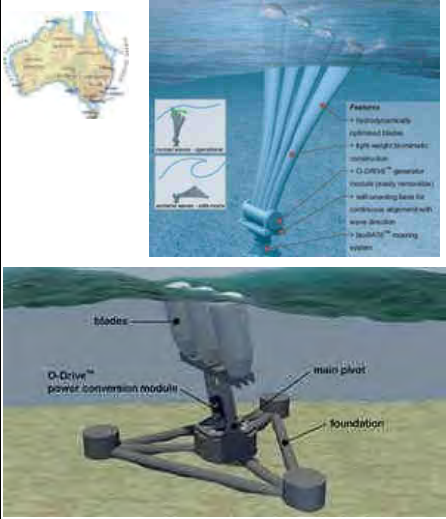

SPERBOY		COMPANY DATA		
   	<i>Name</i>	Embley Energy Ltd		
	<i>Main investors/Project partners</i>	Fully privately held company		
	<i>Country</i>	 UK		
	<i>Story</i>	The sperboy is developed and patented by Embley Energy		
	<i>Founded</i>	1998		
	<i>EU & State support</i>	2006: €180k (Carbon Trust)		
	<i>Technical referent</i>	Michael Burrett (CEO)		
	<i>Contact</i>	Web: www.sperboy.com Phone: 01454 617081 Email: info@sperboy.com		
DEVICE TECHNOLOGY SPECIFICATION				
<i>Category</i>	OWC – floating buoy	<input checked="" type="checkbox"/> single device <input type="checkbox"/> farm		
<i>Position</i>	<input type="checkbox"/> shoreline	<input type="checkbox"/> nearshore	<input checked="" type="checkbox"/> offshore (>30m)	
<i>Power Matrix</i>				
<i>Nominal Power</i>	1MW (full scale-expected)	<i>Patent</i>	<input checked="" type="checkbox"/> yes <input type="checkbox"/> no <input type="checkbox"/> no info	
<i>PTO</i>	<input type="checkbox"/> linear generator	<input type="checkbox"/> hydraulic motor/generator	<input type="checkbox"/> water turbine <input checked="" type="checkbox"/> air turbine	
<i>Power transmission system</i>	<input checked="" type="checkbox"/> electrical energy <input type="checkbox"/> AC/DC in converter			
DEVICE DEVELOPMENT STRATEGY				
<i>Phase</i>	<i>Scale</i>	<i>Facility</i>	<i>Rating</i>	<i>Date</i>
1	1:50	Uni Plymouth & HMRC	-	1999-2001
1	1:100	HMRC, Cork	-	2007
2				
3	1:5	Plymouth Sound	-	2001
4				
5				
<i>Scientific Paper</i>				
ECONOMIC DATA		PREDICTABLE IMPACT		
<i>Joint stock composition</i>		<i>Noise</i>		
<i>R&D costs (€/kW)</i>		<i>Visual impact</i>		
<i>Commercial costs (€/kW)</i>		<i>Social impact</i>		
<i>Project costs</i>	€5M ⁹	<i>Pollutant loss</i>		
<i>Device price</i>		<i>Seabed variation</i>	minimal	
<i>Selling energy (€/kWh)</i>	<i>Cost:</i> 0.06-0.17 <i>Price:</i>	<i>Water temp. variation</i>		

⁹ <http://www.traf-mar-tech.co.uk/documents/DTS100605WRECCONCRETEPAPER.pdf>

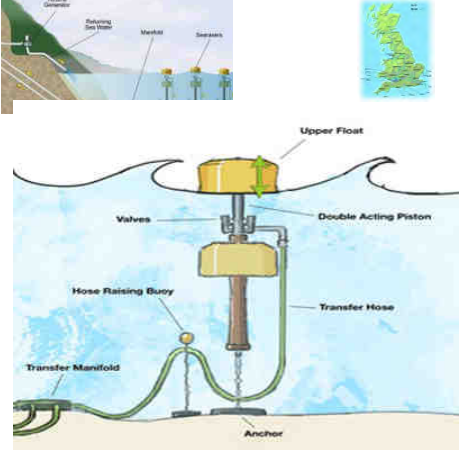

REWEC		COMPANY DATA	
		<i>Name</i>	Wavenergy.it s.r.l.
		<i>Main investors/ Project partners</i>	“Spin Off” of the Mediterranean University
		<i>Country</i>	 Italy
		<i>Story</i>	A new kind of OWC caisson (U-OWC or REWEC3/3, (REsonant Wave Energy Converter) has been patented by prof. Paolo Boccotti (Italy) in Europe (N. 1332519), which has the advantage to obtain an impressive natural resonance without any device for phase control.
		<i>Founded</i>	2010
		<i>EU & State support</i>	-
		<i>Technical referent</i>	Paolo Boccotti
<i>Contact</i>	Web: http://www.wavenergy.it/it Phone: +39 3497074760 Fax: +39 0965 28778 Email: info@wavenergy.it		
DEVICE TECHNOLOGY SPECIFICATION			
<i>Category</i>	OWC - in breakwater	<input checked="" type="checkbox"/> single device	<input type="checkbox"/> farm
<i>Position</i>	<input checked="" type="checkbox"/> shoreline	<input type="checkbox"/> nearshore	<input type="checkbox"/> offshore
<i>Power Matrix</i>			
<i>Nominal Power</i>		<i>Patent</i>	<input checked="" type="checkbox"/> yes <input type="checkbox"/> no <input type="checkbox"/> no info
<i>PTO</i>	<input type="checkbox"/> linear generator <input type="checkbox"/> hydraulic motor/generator	<input type="checkbox"/> water turbine	<input checked="" type="checkbox"/> air turbine
<i>Power transmission system</i>	<input checked="" type="checkbox"/> electrical energy	<input type="checkbox"/> AC/DC in converter	
DEVICE DEVELOPMENT STRATEGY			
<i>Phase</i>	<i>Scale</i>	<i>Facility</i>	<i>Rating</i>
1			
2			
3	1:10	Reggio Calabria, Italy	-
4	1:1	Marina di Cicerone – Formia, Italy	-
5			
<i>Scientific Paper</i>	[101] [102]		
ECONOMIC DATA		PREDICTABLE IMPACT	
<i>Joint stock composition</i>		<i>Noise</i>	
<i>R&D costs (€/kW)</i>		<i>Visual impact</i>	
<i>Commercial costs (€/kW)</i>		<i>Social impact</i>	
<i>Project costs</i>		<i>Pollutant loss</i>	
<i>Device price</i>		<i>Seabed variation</i>	
<i>Selling energy (€/kWh)</i>	<i>Cost:</i>	<i>Price:</i>	<i>Water temp. variation</i>

DWP		COMPANY DATA			
		<i>Name</i>	Danish Wave Power Aps.		
		<i>Main investors/ Project partners</i>	ELSAM, Hajgaard & Schultz A/S, NKT Cables A/S, IIT Flygt AIS, RAMBOLL		
		<i>Country</i>	Denmark		
		<i>Story</i>	The DWP was funded by the Danish Energy Agency and DW		
		<i>Founded</i>	1989		
		<i>EU & Stat support</i>	Danish Department of Energy: €3.5M		
		<i>Technical referent</i>	Kim Nielsen		
		<i>Contact</i>	-		
DEVICE TECHNOLOGY SPECIFICATION					
<i>Category</i>	Point absorber	X single device		<input type="checkbox"/> farm	
<i>Position</i>	<input type="checkbox"/> shoreline	<input type="checkbox"/> nearshore	X offshore (40-60m)		
<i>Power Matrix:</i>					
<i>Nominal Power</i>	-		<i>Patent</i>	<input type="checkbox"/> yes <input type="checkbox"/> no X no info	
<i>PTO</i>	<input type="checkbox"/> linear generator	X hydraulic motor/generator		<input type="checkbox"/> water turbine	<input type="checkbox"/> air turbine
<i>Power transmission system</i>	X electrical energy			<input type="checkbox"/> AC/DC in converter	
DEVICE DEVELOPMENT STRATEGY					
<i>Phase</i>	<i>Scale</i>	<i>Facility</i>		<i>Rating</i>	<i>Date</i>
1	-	Technical University in Denmark		-	1978-1986
2	1:10	Nissum Bredning, Denmark		-	-
3	- (d=6m)	Hansthalm, Denmark		45kW (broken)	1988-1890
3	1:4 (d=2.5m)	Hansthalm, Denmark		1kW	1994-1995
4					
5					
<i>Scientific Paper</i>	[103]				
ECONOMIC DATA			PREDICTABLE IMPACT		
<i>Joint stock composition</i>			<i>Noise</i>		
<i>R&D costs (€/kW)</i>			<i>Visual impact</i>		
<i>Commercial costs (€/kW)</i>			<i>Social impact</i>		
<i>Project costs</i>			<i>Pollutant loss</i>		
<i>Device price</i>			<i>Seabed variation</i>		
<i>Selling energy (€/kWh)</i>	<i>Cost:</i>	<i>Price:</i>	<i>Water temp. Var.</i>		

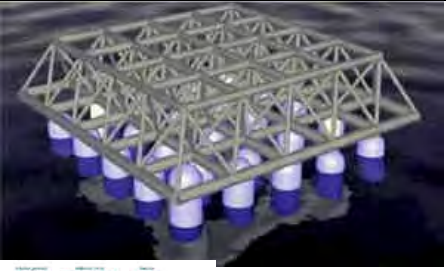



AquaBuOY		COMPANY DATA			
		<i>Name</i>	Finavera		
		<i>Main investors/ Project partners</i>	Privately-held/BC Hydro, GE Energy, SSE, Coillte, GENIVAR, TECO Natural Resource Group, Halfway River First Nation		
		<i>Country</i>	 Canada		
		<i>Story</i>	It is a point absorber that is the third generation of two Swedish designs that utilize wave energy to pressurize a fluid that is then used to drive a turbine generator. The predecessor technologies are the Swedish IPS Buoy (1980-1986) and Hose Pump (1983-1984). In December 2007 Finavera Renewables was granted an operating license for its Makah Bay, Washington pilot project to construct an offshore power plant which is expected to generate 1500MW/Year. Development program stalled at present.		
		<i>Founded</i>	2001		
		<i>State support</i>	FP6 TREN € 2M , SEI €100.000		
		<i>Technical referent</i>	Spyros P. Karellas (CEO)		
		<i>Contact</i>	Web: www.finavera.com Phone: +1.604.288.9051 Email: info@finavera.com		
DEVICE TECHNOLOGY SPECIFICATION					
<i>Category</i>	Point absorber	X single device <input type="checkbox"/> farm			
<i>Position</i>	<input type="checkbox"/> shoreline	<input type="checkbox"/> nearshore	X offshore		
<i>Power Matrix</i>					
<i>Nominal Power</i>	250 KW (full scale)	<i>Patent</i>	X yes <input type="checkbox"/> no <input type="checkbox"/> no info		
<i>PTO</i>	<input type="checkbox"/> linear generator	X hydraulic motor/generator	<input type="checkbox"/> water turbine	<input type="checkbox"/> air turbine	
<i>Power transmission system</i>	X electrical energy			<input type="checkbox"/> AC/DC in converter	
DEVICE DEVELOPMENT STRATEGY					
<i>Phase</i>	<i>Scale</i>	<i>Facility</i>	<i>Rating</i>	<i>Date</i>	
1	1:50	Aalborg Uni, Denmark	-	2005	
1	1:50	HMRC, UCC, Ireland	-	2007	
2	1:10	Nissum Bredning	-	2007	
3	1:2	Newport, Oregon, USA	20-50 KW	2007	
3	1:2	NEL, Glasgow, Scotland	-	2007	
4					
5					
<i>Scientific Paper</i>					
ECONOMIC DATA			PREDICTABLE IMPACT		
<i>Joint stock composition</i>			<i>Noise</i>		
<i>R&D costs (€/kW)</i>			<i>Visual impact</i>		
<i>Commercial costs (€/kW)</i>			<i>Social impact</i>		
<i>Project costs</i>			<i>Pollutant loss</i>		
<i>Device price</i>			<i>Seabed variation</i>		
<i>Selling energy (€/kWh)</i>		<i>Cost:</i>	<i>Price:</i>	<i>Water temp. variation</i>	



bioWAVE		COMPANY DATA		
		<i>Name</i>	BioPower Systems Pty. Ltd.	
		<i>Main investors/ Project partners</i>	AGL Energy, Bluescope Steel, Lend Lease, Swinburne University, University of Melbourne, University of Sydney	
		<i>Country</i>	 Australia	
		<i>Story</i>	Researchers at the University of Sydney have applied the concept of biomimicry in the development of new systems designed to convert power from ocean waves into electricity.	
		<i>Founded</i>	2006	
		<i>State support</i>	Victorian Government: \$5M(€4M)	
		<i>Technical referent</i>	Prof. Timothy Finnigan (CEO)	
		<i>Contact</i>	Web: www.biopowersystems.com Phone: +61 2 9146 4420 Email: t.finnigan@usyd.edu.au	
DEVICE TECHNOLOGY SPECIFICATION				
<i>Category</i>	OB - submerged	X single device	<input type="checkbox"/> farm	
<i>Position</i>	<input type="checkbox"/> shoreline	X nearshore (30m)	<input type="checkbox"/> offshore	
<i>Power Matrix</i>				
<i>Nominal Power</i>	250kW	<i>Patent</i>	X yes <input type="checkbox"/> no <input type="checkbox"/> no info	
<i>PTO</i>	<input type="checkbox"/> linear generator	X hydraulic motor/generator	<input type="checkbox"/> water turbine <input type="checkbox"/> air turbine	
<i>Power transmission system</i>	X electrical energy <input type="checkbox"/> AC/DC in converter			
DEVICE DEVELOPMENT STRATEGY				
<i>Phase</i>	<i>Scale</i>	<i>Facility</i>	<i>Rating</i>	<i>Date</i>
1				
2	-	Mascot NSW, Sydney	-	2007
3	-	Port Fairy, Victoria, Australia (test 21 months)	250kW	deployment in late 2013
3	-	Cantabria, Spain	-	under consideration
4				
5				
<i>Scientific Paper</i>				
ECONOMIC DATA		PREDICTABLE IMPACT		
<i>Joint stock composition</i>		<i>Noise</i>		
<i>R&D costs</i>		<i>Visual impact</i>	no	
<i>Commercial costs (€/ kW)</i>	2000 ¹⁰	<i>Social impact</i>		
<i>Project costs</i>	Port Fairy: \$14M(€11.4M)	<i>Pollutant loss</i>		
<i>Device price</i>		<i>Seabed variation</i>		
<i>Selling energy (€/ kWh)</i>	<i>Cost:</i> 0.10 ¹⁰ <i>Price:</i>	<i>Water temp. variation</i>		

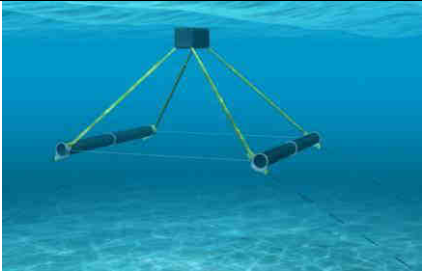



¹⁰ <http://www.science.org.au/events/publiclectures/re/finnigan.html>

SEARASER		COMPANY DATA		
		<i>Name</i>	Ecotricity	
		<i>Main investors/ Project partners</i>	WDM, The Ecologist, Tearfund, Soil Association, Sea Shepherd, RSPCA, Oxfam, Naked Wines, Lush, Green Party, Christian Aid, Café Direct	
		<i>Country</i>	 UK	
		<i>Story</i>		
		<i>Founded</i>	1995	
		<i>EU & State support</i>		
		<i>Technical referent</i>	Alvin Smith (inventor)	
		<i>Contact</i>	Web: www.ecotricity.co.uk Phone: (01453) 756 111 Email: home@ecotricity.co.uk	
DEVICE TECHNOLOGY SPECIFICATION				
<i>Category</i>	Point absorber	<input checked="" type="checkbox"/> single device	<input type="checkbox"/> farm	
<i>Position</i>	<input type="checkbox"/> shoreline	<input checked="" type="checkbox"/> nearshore (18-25m)	<input type="checkbox"/> offshore	
<i>Power Matrix</i>				
<i>Nominal Power</i>	1MW (full scale)	<i>Patent</i>	<input type="checkbox"/> yes <input type="checkbox"/> no <input checked="" type="checkbox"/> no info	
<i>PTO</i>	<input type="checkbox"/> linear generator	<input checked="" type="checkbox"/> hydraulic motor/generator	<input type="checkbox"/> water turbine <input type="checkbox"/> air turbine	
<i>Power transmission system</i>	<input checked="" type="checkbox"/> electrical energy <input type="checkbox"/> AC/DC in converter			
DEVICE DEVELOPMENT STRATEGY				
<i>Phase</i>	<i>Scale</i>	<i>Facility</i>	<i>Rating</i>	<i>Date</i>
1				
2				
3	1:4	Fabtest site-Falmouth, UK	-	2011
4				
5				
<i>Scientific Paper</i>				
ECONOMIC DATA		PREDICTABLE IMPACT		
<i>Joint stock composition</i>		<i>Noise</i>		
<i>R&D costs (€/kW)</i>		<i>Visual impact</i>	+1m a.s.l.	
<i>Commercial costs (€/kW)</i>		<i>Social impact</i>		
<i>Project costs</i>	\$385k (≈€290k) ¹¹	<i>Pollutant loss</i>		
<i>Device price</i>		<i>Seabed variation</i>		
<i>Selling energy (€/kWh)</i>	<i>Cost:</i>	<i>Price:</i>	<i>Water temp. variation</i>	



¹¹ <http://news.discovery.com/tech/aquatic-bike-pump-cranks-out-electricity-120123.html>

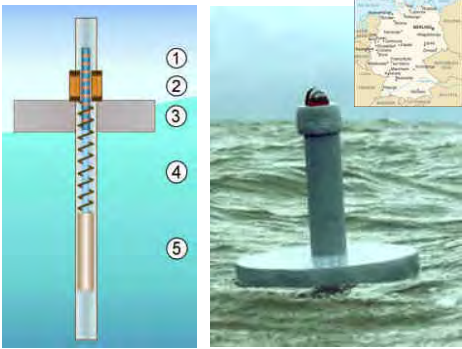

Manchester Bobber		COMPANY DATA		
  	<i>Name</i>	Bobber Company Ltd/UMIP Ltd		
	<i>Main investors/ Project partners</i>	ABB/ Mowlem plc, Royal Haskoning		
	<i>Country</i>	 UK		
	<i>Story</i>	-		
	<i>Founded</i>	2004		
	<i>EU & State support</i>	£1M (€1.2M)		
	<i>Technical referent</i>	John Loughhead, Executive Director		
<i>Contact</i>	Web:www.manchesterbobber.com Phone: +44 (0) 161 3068831 Email: frank.allison@umip.com			
DEVICE TECHNOLOGY SPECIFICATION				
<i>Category</i>	Point absorber – fixed/floating	<input type="checkbox"/> single device	<input checked="" type="checkbox"/> farm	
<i>Position</i>	<input type="checkbox"/> shoreline <input type="checkbox"/> nearshore	<input checked="" type="checkbox"/> offshore (fixed 20-60m, floating>60m)		
<i>Power Matrix</i>				
<i>Nominal Power</i>	500kW (each in full scale)	<i>Patent</i>	<input checked="" type="checkbox"/> yes <input type="checkbox"/> no <input type="checkbox"/> no info	
<i>PTO</i>	<input type="checkbox"/> linear generator	<input checked="" type="checkbox"/> hydraulic motor/generator	<input type="checkbox"/> water turbine <input type="checkbox"/> air turbine	
<i>Power transmission system</i>	<input checked="" type="checkbox"/> electrical energy <input type="checkbox"/> AC/DC in converter			
DEVICE DEVELOPMENT STRATEGY				
<i>Phase</i>	<i>Scale</i>	<i>Facility</i>	<i>Rating</i>	<i>Date</i>
1	1:100	Uni. Manchester, UK	-	2004
1	1:70 (Array)	Uni. Manchester, UK	-	2007-2008
2	1:10	NaREC, UK	-	2005
3				
4				
5				
<i>Scientific Paper</i>				
ECONOMIC DATA		PREDICTABLE IMPACT		
<i>Joint stock composition</i>		<i>Noise</i>		
<i>R&D costs (€/kW)</i>		<i>Visual impact</i>		
<i>Commercial costs (€/kW)</i>		<i>Social impact</i>		
<i>Project costs</i>		<i>Pollutant loss</i>		
<i>Device price</i>		<i>Seabed variation</i>		
<i>Selling energy (€/kW/h)</i>	<i>Cost:</i>	<i>Price:</i>	<i>Water temp. variation</i>	

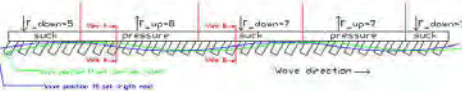

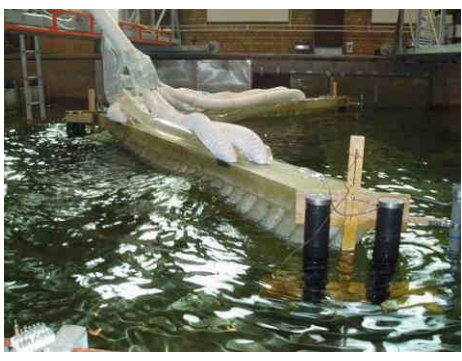

WAVE ROTOR		COMPANY DATA		
	<i>Name</i>	Ecofys		
	<i>Main investors/ Project partners</i>	Venture capital		
	<i>Country</i>	 Netherlands		
	<i>Story</i>			
	<i>Founded</i>	1984		
	<i>EU & State support</i>			
	<i>Technical referent</i>	Manon Janssen (CEO)		
	<i>Contact</i>	Web: www.ecofys.com Phone: +31 (0)30 662 3300 Email: info@ecofys.com		
DEVICE TECHNOLOGY SPECIFICATION				
<i>Category</i>	Point absorber	<input checked="" type="checkbox"/> single device	<input type="checkbox"/> farm	
<i>Position</i>	<input type="checkbox"/> shoreline	<input checked="" type="checkbox"/> nearshore (15-25m)	<input type="checkbox"/> offshore	
<i>Power Matrix</i>				
<i>Nominal Power</i>	500kW (full scale)	<i>Patent</i>	<input checked="" type="checkbox"/> yes <input type="checkbox"/> no <input type="checkbox"/> no info	
<i>PTO</i>	<input checked="" type="checkbox"/> linear generator	<input type="checkbox"/> hydraulic motor/generator	<input type="checkbox"/> water turbine <input type="checkbox"/> air turbine	
<i>Power transmission system</i>	<input checked="" type="checkbox"/> electrical energy <input type="checkbox"/> AC/DC in converter			
DEVICE DEVELOPMENT STRATEGY				
<i>Phase</i>	<i>Scale</i>	<i>Facility</i>	<i>Rating</i>	<i>Date</i>
1				
2	-	Nissum Bredning, Denmark	-	2002
2	1:10	NaREC, UK	-	2004
2	1:10	IFREMER, France	-	2007
3	1:2	Borssele, Netherlands	30kW	2008
4				
5				
<i>Scientific Paper</i>				
ECONOMIC DATA		PREDICTABLE IMPACT		
<i>Joint stock composition</i>		<i>Noise</i>		
<i>R&D costs (€/kW)</i>		<i>Visual impact</i>		
<i>Commercial costs (€/kW)</i>		<i>Social impact</i>		
<i>Project costs</i>		<i>Pollutant loss</i>		
<i>Device price</i>		<i>Seabed variation</i>		
<i>Selling energy (€/kWh)</i>	<i>Cost:</i>	<i>Price:</i>	<i>Water temp. variation</i>	




R38/R115		COMPANY DATA		
  	<i>Name</i>	40South Energy Srl		
	<i>Main investors/ Project partners</i>	Monte dei Paschi di Siena		
	<i>Country</i>	 Italy		
	<i>Story</i>	-		
	<i>Founded</i>	2008		
	<i>EU & State support</i>	-		
	<i>Technical referent</i>	Michele Grassi		
	<i>Contact</i>	Web: www. 40southenergy.com Phone: +39 0506160113 Email: info@40southenergy.com		
DEVICE TECHNOLOGY SPECIFICATION				
<i>Category</i>	OB		X single device <input type="checkbox"/> farm	
<i>Position</i>	<input type="checkbox"/> shoreline <input type="checkbox"/> nearshore		X offshore (>40m)	
<i>Power Matrix</i>				
<i>Nominal Power</i>	25-50kW/75-150kW		<i>Patent</i> X yes <input type="checkbox"/> no <input type="checkbox"/> no info	
<i>PTO</i>	<input type="checkbox"/> linear generator X hydraulic motor/generator		<input type="checkbox"/> water turbine <input type="checkbox"/> air turbine	
<i>Power transmission system</i>	<input type="checkbox"/> electrical energy		X AC/DC in converter	
DEVICE DEVELOPMENT STRATEGY				
<i>Phase</i>	<i>Scale</i>	<i>Facility</i>	<i>Rating</i>	<i>Date</i>
1	-	-	-	2007
2				
3	1:2	-	-	2009
4	1:1	Castiglioncello, Italy	100kW	2010
4	1.1	Maldives	-	Planned end 2012
5				
<i>Scientific Paper</i>				
ECONOMIC DATA		PREDICTABLE IMPACT		
<i>Joint stock composition</i>		<i>Noise</i>		
<i>R&D costs (€/kW)</i>		<i>Visual impact</i>		
<i>Commercial costs (€/kW)</i>		<i>Social impact</i>		
<i>Project costs</i>		<i>Pollutant loss</i>		
<i>Device price</i>	125.000€ (R38/25-50kW) 300.000€ (R115/75-150kW)	<i>Seabed variation</i>		
<i>Selling energy (€/kWh)</i>	<i>Cost:</i> <i>Price:</i>	<i>Water temp. variation</i>		



WEST		COMPANY DATA	
		<i>Name</i>	Atmocean
		<i>Main investors/ Project partners</i>	Private investors
		<i>Country</i>	USA
		<i>Story</i>	After Hurricane Katrina hit New Orleans in September 2005, Kithil conceived of a wave-driven ocean pump which would use the large waves produced by high winds to push deep cold water to the surface, reducing hurricane intensity.
		<i>Founded</i>	2006
		<i>State support</i>	-
		<i>Technical referent</i>	Philip W. Kithil, founder and CEO
<i>Contact</i>	Web: www.atmocean.com Phone: 505-310-2294 Email: atmocean.information@gmail.com		
DEVICE TECHNOLOGY SPECIFICATION			
<i>Category</i>	Point absorber	<input checked="" type="checkbox"/> single device	<input type="checkbox"/> farm
<i>Position</i>	<input type="checkbox"/> shoreline	<input checked="" type="checkbox"/> nearshore	<input type="checkbox"/> offshore
<i>Power Matrix</i>			
<i>Nominal Power</i>	-	<i>Patent</i>	<input checked="" type="checkbox"/> yes <input type="checkbox"/> no <input type="checkbox"/> no info
<i>PTO</i>	<input type="checkbox"/> linear generator	<input checked="" type="checkbox"/> hydraulic motor/generator	<input type="checkbox"/> water turbine <input type="checkbox"/> air turbine
<i>Power transmission system</i>	<input checked="" type="checkbox"/> electrical energy <input type="checkbox"/> AC/DC in converter		
DEVICE DEVELOPMENT STRATEGY			
<i>Phase</i>	<i>Scale</i>	<i>Facility</i>	<i>Rating</i>
1			
2			
3	-	California Polytechnic State University	-
4			
5			
<i>Scientific Paper</i>			
ECONOMIC DATA		PREDICTABLE IMPACT	
<i>Joint stock composition</i>		<i>Noise</i>	
<i>R&D costs (€/kW)</i>		<i>Visual impact</i>	
<i>Commercial costs (€/kW)</i>		<i>Social impact</i>	
<i>Project costs</i>		<i>Pollutant loss</i>	
<i>Device price</i>		<i>Seabed variation</i>	
<i>Selling energy (€/kWh)</i>	<i>Cost:</i>	<i>Price:</i>	<i>Water temp. variation</i>

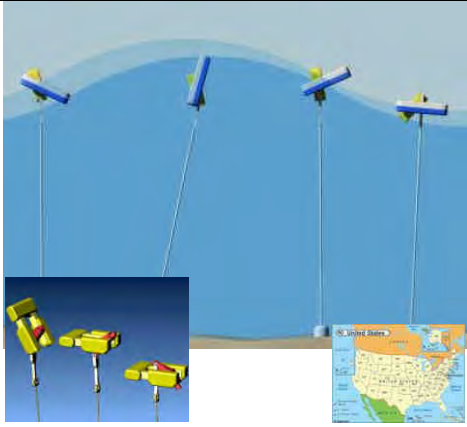

NAUTILUS		COMPANY DATA		
	<i>Name</i>	Advanced Wave Power		
	<i>Main investors/ Project partners</i>	-		
	<i>Country</i>	 RUSSIA		
	<i>Story</i>	-		
	<i>Founded</i>	-		
	<i>State support</i>	Bligh Government: €130k		
	<i>Technical referent</i>	Mr Vladimir Roudakov		
	<i>Contact</i>	Web:www.advancedwavepower.com		
DEVICE TECHNOLOGY SPECIFICATION				
<i>Category</i>	OWC - floating	X single device <input type="checkbox"/> farm		
<i>Position</i>	<input type="checkbox"/> shoreline <input type="checkbox"/> nearshore	X offshore		
<i>Power Matrix</i>				
<i>Nominal Power</i>	-	<i>Patent</i>	X yes <input type="checkbox"/> no <input type="checkbox"/> no info	
<i>PTO</i>	<input type="checkbox"/> linear generator <input type="checkbox"/> hydraulic motor/generator	<input type="checkbox"/> water turbine X air turbine		
<i>Power transmission system</i>	X electrical energy <input type="checkbox"/> AC/DC in converter			
DEVICE DEVELOPMENT STRATEGY				
<i>Phase</i>	<i>Scale</i>	<i>Facility</i>	<i>Rating</i>	<i>Date</i>
1				
2	-	University of Queensland	-	-
3	1:1	Morton Bay, Queensland	3kW	2009
4				
5				
<i>Scientific Paper</i>				
ECONOMIC DATA		PREDICTABLE IMPACT		
<i>Joint stock composition</i>		<i>Noise</i>		
<i>R&D costs (€/kW)</i>		<i>Visual impact</i>		
<i>Commercial costs (€/kW)</i>		<i>Social impact</i>		
<i>Project costs</i>		<i>Pollutant loss</i>		
<i>Device price</i>		<i>Seabed variation</i>		
<i>Selling energy (€/kWh)</i>	<i>Cost:</i>	<i>Price:</i>	<i>Water temp. variation</i>	



BRANDL GENERATOR		COMPANY DATA		
		<i>Name</i>	Brandl Motor	
		<i>Main investors/ Project partners</i>		
		<i>Country</i>	 Germany	
		<i>Story</i>		
		<i>Founded</i>		
		<i>EU & State support</i>	-	
		<i>Technical referent</i>	Gerhard Brandl (project manager)	
		<i>Contact</i>	Web: http://brandlmotor.de Phone: +49 30 39 48 06 38 Email: info@brandlmotor.com	
DEVICE TECHNOLOGY SPECIFICATION				
<i>Category</i>	Point absorber	X single device <input type="checkbox"/> farm		
<i>Position</i>	<input type="checkbox"/> shoreline <input type="checkbox"/> nearshore X offshore (40-200m)			
<i>Power Matrix</i>				
<i>Nominal Power</i>	1MW	<i>Patent</i>	X yes <input type="checkbox"/> no <input type="checkbox"/> no info	
<i>PTO</i>	X linear generator <input type="checkbox"/> hydraulic motor/generator <input type="checkbox"/> water turbine <input type="checkbox"/> air turbine			
<i>Power transmission system</i>	X electrical energy <input type="checkbox"/> AC/DC in converter			
DEVICE DEVELOPMENT STRATEGY				
<i>Phase</i>	<i>Scale</i>	<i>Facility</i>	<i>Rating</i>	<i>Date</i>
1				
2				
3	(D=15m)	North Sea	-	-
4				
5				
<i>Scientific Paper</i>				
ECONOMIC DATA			PREDICTABLE IMPACT	
<i>Joint stock composition</i>			<i>Noise</i>	
<i>R&D costs (€/kW)</i>			<i>Visual impact</i>	
<i>Commercial costs (€/kW)</i>			<i>Social impact</i>	
<i>Project costs</i>			<i>Pollutant loss</i>	
<i>Device price</i>			<i>Seabed variation</i>	
<i>Selling energy (€/kWh)</i>	<i>Cost:</i>	<i>Price:</i>	<i>Water temp. variation</i>	

MAWEC		COMPANY DATA	
  		<i>Name</i>	LEANCON Wave Energy
		<i>Main investors/ Project partners</i>	-
		<i>Country</i>	 Denmark
		<i>Story</i>	LEANCON Wave Energy has developed a Multi Absorbing Wave Energy Converter (MAWEC). The WEC is a offshore OWC type that preferably uses a special designed displacement turbine as power take off (PTO), but a traditional air turbine can also be used.
		<i>Founded</i>	2004
		<i>EU & State support</i>	-
		<i>Technical referent</i>	Kurt Due Rasmussen
		<i>Contact</i>	Web: http://www.leancon.com Phone: + 45 7550 5762 Email: kdr@leancon.dk
DEVICE TECHNOLOGY SPECIFICATION			
<i>Category</i>	Multi OWC - floating	<input checked="" type="checkbox"/> single device	<input type="checkbox"/> farm
<i>Position</i>	<input type="checkbox"/> shoreline	<input checked="" type="checkbox"/> nearshore	<input checked="" type="checkbox"/> offshore
<i>Power Matrix</i>			
<i>Nominal Power</i>	-	<i>Patent</i>	<input type="checkbox"/> yes <input type="checkbox"/> no <input checked="" type="checkbox"/> no info
<i>PTO</i>	<input type="checkbox"/> linear generator	<input type="checkbox"/> hydraulic motor/generator	<input type="checkbox"/> water turbine <input checked="" type="checkbox"/> air turbine
<i>Power transmission system</i>	<input checked="" type="checkbox"/> electrical energy <input type="checkbox"/> AC/DC in converter		
DEVICE DEVELOPMENT STRATEGY			
<i>Phase</i>	<i>Scale</i>	<i>Facility</i>	<i>Rating</i>
1	1:40	Aalborg University, Denmark	-
2			
3	1:10	Nissum Bredning, Denmark	-
4			
5			
<i>Scientific Paper</i>	[104]		
ECONOMIC DATA		PREDICTABLE IMPACT	
<i>Joint stock composition</i>		<i>Noise</i>	
<i>R&D costs (€/kW)</i>		<i>Visual impact</i>	
<i>Commercial costs (€/kW)</i>		<i>Social impact</i>	
<i>Project costs</i>		<i>Pollutant loss</i>	
<i>Device price</i>		<i>Seabed variation</i>	-
<i>Selling energy (€/kWh)</i>	<i>Cost: 0.06</i>	<i>Price:</i>	<i>Water temp. variation</i>



PROTEAN ECP		COMPANY DATA			
 	<i>Name</i>	Protean Energy Limited			
	<i>Main investors/ Project partners</i>	-			
	<i>Country</i>	 Australia			
	<i>Story</i>	The Protean technology is currently the only known independently verified wave energy system that uses all 6 degrees of freedom of movement .			
	<i>Founded</i>	2005			
	<i>State support</i>	-			
	<i>Technical referent</i>	Sean D. Moore, CTO			
	<i>Contact</i>	Web: http://proteanenergy.com Phone: (08) 6380 2555 Email: sean.moore@proteanenergy.com			
DEVICE TECHNOLOGY SPECIFICATION					
<i>Category</i>	Point absorber	<input checked="" type="checkbox"/> single device		<input type="checkbox"/> farm	
<i>Position</i>	<input type="checkbox"/> shoreline	<input checked="" type="checkbox"/> nearshore		<input checked="" type="checkbox"/> offshore	
<i>Power Matrix</i>					
<i>Nominal Power</i>	-		<i>Patent</i>	<input checked="" type="checkbox"/> yes <input type="checkbox"/> no <input type="checkbox"/> no info	
<i>PTO</i>	<input checked="" type="checkbox"/> linear generator <input type="checkbox"/> hydraulic motor/generator		<input type="checkbox"/> water turbine <input type="checkbox"/> air turbine		
<i>Power transmission system</i>	<input checked="" type="checkbox"/> electrical energy		<input type="checkbox"/> AC/DC in converter		
DEVICE DEVELOPMENT STRATEGY					
<i>Phase</i>	<i>Scale</i>	<i>Facility</i>		<i>Rating</i>	<i>Date</i>
1	-	-		-	2003
2	-	-		-	2006-2007
3	1:3	Fremantle Harbour, Western Australia.		-	2008
4					
5					
<i>Scientific Paper</i>					
ECONOMIC DATA			PREDICTABLE IMPACT		
<i>Joint stock composition</i>			<i>Noise</i>	no	
<i>R&D costs (€/kW)</i>			<i>Visual impact</i>	minimal	
<i>Commercial costs (€/kW)</i>			<i>Social impact</i>		
<i>Project costs</i>			<i>Pollutant loss</i>		
<i>Device price</i>			<i>Seabed variation</i>		
<i>Selling energy (€/kWh)</i>	<i>Cost:</i>	<i>Price:</i>	<i>Water temp. var.</i>		

RME		COMPANY DATA		
	<i>Name</i>	Resolute Marine Energy		
	<i>Main investors/ Project partners</i>	MIT, NREL, Duke University, Maine Marine Composites, Bureau of Ocean Energy		
	<i>Country</i>	 USA		
	<i>Story</i>	-		
	<i>Founded</i>	2007		
	<i>State support</i>	-		
	<i>Technical referent</i>	Bill Staby – Founder/CEO		
	<i>Contact</i>	Web: www.resolutemarine.com Phone: 617-600-3050 Email: contactus@resolutemarine.com		
DEVICE TECHNOLOGY SPECIFICATION				
<i>Category</i>	Point absorber - OB	X single device <input type="checkbox"/> farm		
<i>Position</i>	<input type="checkbox"/> shoreline	X nearshore	<input type="checkbox"/> offshore	
<i>Power Matrix</i>				
<i>Nominal Power</i>	-	<i>Patent</i>	X yes <input type="checkbox"/> no <input type="checkbox"/> no info	
<i>PTO</i>	<input type="checkbox"/> linear generator turbine	X hydraulic motor/generator	<input type="checkbox"/> water turbine <input type="checkbox"/> air	
<i>Power transmission system</i>	X electrical energy <input type="checkbox"/> AC/DC in converter			
DEVICE DEVELOPMENT STRATEGY				
<i>Phase</i>	<i>Scale</i>	<i>Facility</i>	<i>Rating</i>	<i>Date</i>
1	-	Alden Lab in Holden, MA	-	2009
2	-	BOEMRE's Ohmsett Facility (OB)	-	June 2011
3	-	- (point absorber)	-	2009
3	-	North Carolina (OB)	-	December 2011
4				
5				
<i>Scientific Paper</i>				
ECONOMIC DATA		PREDICTABLE IMPACT		
<i>Joint stock composition</i>		<i>Noise</i>		
<i>R&D costs (€/kW)</i>		<i>Visual impact</i>		
<i>Commercial costs (€/kW)</i>		<i>Social impact</i>		
<i>Project costs</i>		<i>Pollutant loss</i>		
<i>Device price</i>		<i>Seabed variation</i>		
<i>Selling energy (€/kWh)</i>	<i>Cost:</i>	<i>Price:</i>	<i>Water temp. variation</i>	

Lever Operated Pivoting Float (LOPF)		COMPANY DATA		
		<i>Name</i>	Swell Fuel	
		<i>Main investors/ Project partners</i>	Privately funded	
		<i>Country</i>	 USA	
		<i>Story</i>	-	
		<i>Founded</i>	-	
		<i>State support</i>	-	
		<i>Technical referent</i>	Christopher Olsen	
<i>Contact</i>	Web: http://www.resenwaves.com/ Phone: +45 4182 4696 Email: info@resenwaves.com			
DEVICE TECHNOLOGY SPECIFICATION				
<i>Category</i>	Point absorber	<input type="checkbox"/> single device <input checked="" type="checkbox"/> farm		
<i>Position</i>	<input type="checkbox"/> shoreline <input type="checkbox"/> nearshore <input checked="" type="checkbox"/> offshore			
<i>Power Matrix</i>				
<i>Nominal Power</i>	1kW – 5kW - 20kW - 50kW	<i>Patent</i>	<input checked="" type="checkbox"/> yes <input type="checkbox"/> no <input type="checkbox"/> no info	
<i>PTO</i>	<input type="checkbox"/> linear generator <input checked="" type="checkbox"/> hydraulic motor/generator <input type="checkbox"/> water turbine <input type="checkbox"/> air turbine			
<i>Power transmission system</i>	<input type="checkbox"/> electrical energy <input checked="" type="checkbox"/> AC/DC in converter			
DEVICE DEVELOPMENT STRATEGY				
<i>Phase</i>	<i>Scale</i>	<i>Facility</i>	<i>Rating</i>	<i>Date</i>
1				
2				
3	-	-	1kW-5kW	2009
4				
5				
<i>Scientific Paper</i>				
ECONOMIC DATA		PREDICTABLE IMPACT		
<i>Joint stock composition</i>		<i>Noise</i>	no	
<i>R&D costs (€/kW)</i>		<i>Visual impact</i>	minimal	
<i>Commercial costs (€/kW)</i>		<i>Social impact</i>		
<i>Project costs</i>		<i>Pollutant loss</i>		
<i>Device price</i>		<i>Seabed variation</i>		
<i>Selling energy (€/kWh)</i>	<i>Cost:</i>	<i>Price:</i>	<i>Water temp. variation</i>	

SDE		COMPANY DATA		
		<i>Name</i>	S.D.E. Energy Ltd	
		<i>Main investors/ Project partners</i>	-	
		<i>Country</i>	 Israel	
		<i>Story</i>	-	
		<i>Founded</i>	-	
		<i>State support</i>	Chief Scientist of Israel, Ministry of Industry and Trade: €1.5M	
		<i>Technical referent</i>	Shmuel Ovadia	
		<i>Contact</i>	Web: www.sde-energy.com Phone: 972-37397107 Email: info@sde-energy.com	
DEVICE TECHNOLOGY SPECIFICATION				
<i>Category</i>	OB in breakwater	X single device	<input type="checkbox"/> farm	
<i>Position</i>	X shoreline	<input type="checkbox"/> nearshore	<input type="checkbox"/> offshore	
<i>Power Matrix</i>				
<i>Nominal Power</i>	1MW (power station)	<i>Patent</i>	X yes <input type="checkbox"/> no <input type="checkbox"/> no info	
<i>PTO</i>	<input type="checkbox"/> linear generator	X hydraulic motor/generator	<input type="checkbox"/> water turbine <input type="checkbox"/> air turbine	
<i>Power transmission system</i>	X electrical energy <input type="checkbox"/> AC/DC in converter			
DEVICE DEVELOPMENT STRATEGY				
<i>Phase</i>	<i>Scale</i>	<i>Facility</i>	<i>Rating</i>	<i>Date</i>
1				
2				
3	1:1	Jaffa Port, Israel	40kW	2010
4				
5				
<i>Scientific Paper</i>				
ECONOMIC DATA		PREDICTABLE IMPACT		
<i>Joint stock composition</i>		<i>Noise</i>		
<i>R&D costs (€/kW)</i>		<i>Visual impact</i>		
<i>Commercial costs (€/kW)</i>		<i>Social impact</i>		
<i>Project costs</i>	€480k ¹²	<i>Pollutant loss</i>		
<i>Device price</i>		<i>Seabed variation</i>		
<i>Selling energy (€/kWh)</i>	<i>Cost:</i>	<i>Price:0.09</i>	<i>Water temp. variation</i>	

¹² http://www.energy-daily.com/reports/SDE_Has_Finalized_The_Construction_Of_The_First_Sea_Wave_Power_Plant_999.html

W2Power		COMPANY DATA			
		<i>Name</i>	Pelagic Power AS		
		<i>Main investors/ Project partners</i>	Fraunhofer, TWI		
		<i>Country</i>	 Norway		
		<i>Story</i>	-		
		<i>Founded</i>	-		
		<i>EU&State support</i>	-		
		<i>Technical referent</i>	Dr. Jan Erik Hanssen (CEO)		
		<i>Contact</i>	Web: www.pelagicpower.no Phone: +32 474 980 616 Email: post@pelagicpower.no		
DEVICE TECHNOLOGY SPECIFICATION					
<i>Category</i>	OB - floating		X single device <input type="checkbox"/> farm		
<i>Position</i>	<input type="checkbox"/> shoreline <input type="checkbox"/> nearshore		X offshore (>40m)		
<i>Power Matrix</i>					
<i>Nominal Power</i>	3MW + 6MW (wind) full scale		<i>Patent</i>	X yes <input type="checkbox"/> no <input type="checkbox"/> no info	
<i>PTO</i>	<input type="checkbox"/> linear generator X hydraulic motor/generator <input type="checkbox"/> water turbine <input type="checkbox"/> air turbine				
<i>Power transmission system</i>	X electrical energy <input type="checkbox"/> AC/DC in converter				
DEVICE DEVELOPMENT STRATEGY					
<i>Phase</i>	<i>Scale</i>	<i>Facility</i>		<i>Rating</i>	<i>Date</i>
1	-	Lycro, NTE, NTNU		-	2005
2	-	Sintef Marintek in Trondheim		-	2005
3	1:3	Flatanger in Nord-Trøndelag		-	2008
4					
5					
<i>Scientific Paper</i>					
ECONOMIC DATA			PREDICTABLE IMPACT		
<i>Joint stock composition</i>			<i>Noise</i>	no	
<i>R&D costs (€/kW)</i>			<i>Visual impact</i>	minimal	
<i>Commercial costs (€/kW)</i>			<i>Social impact</i>		
<i>Project costs</i>			<i>Pollutant loss</i>		
<i>Device price</i>			<i>Seabed variation</i>		
<i>Selling energy (€/kWh)</i>		<i>Cost:</i>	<i>Price:</i>	<i>Water temp. variation</i>	

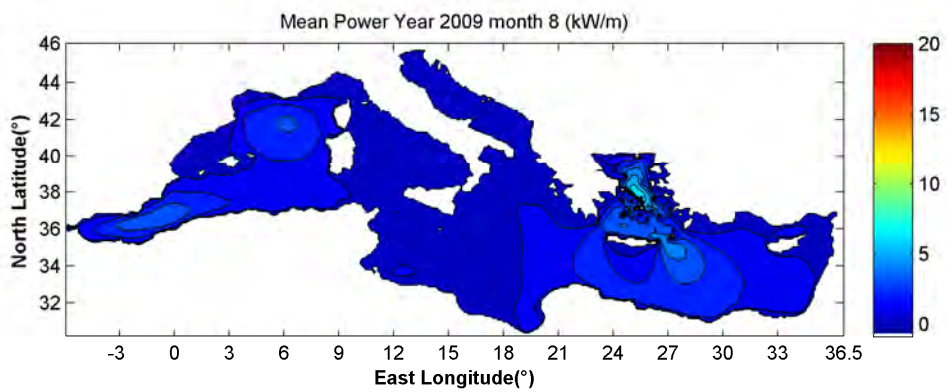
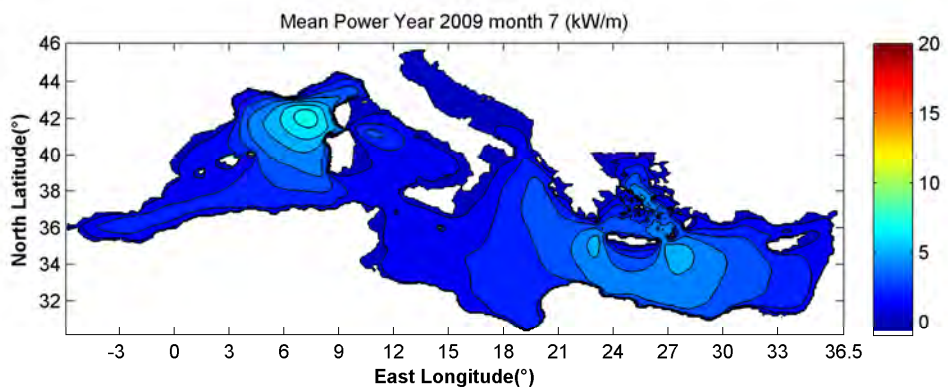
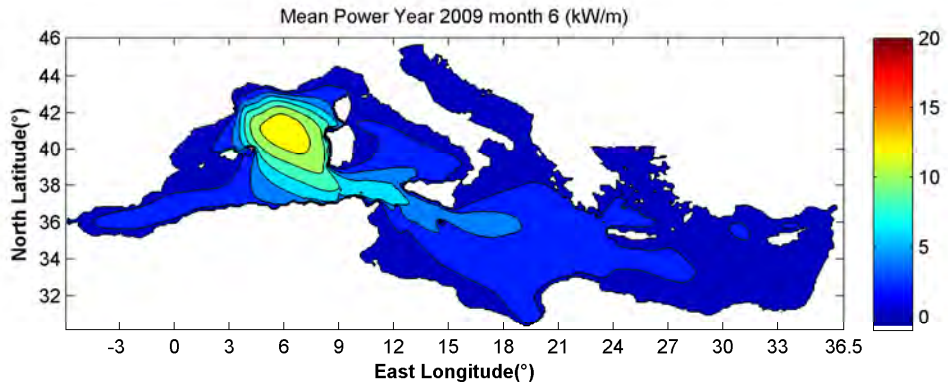
APPENDIX B

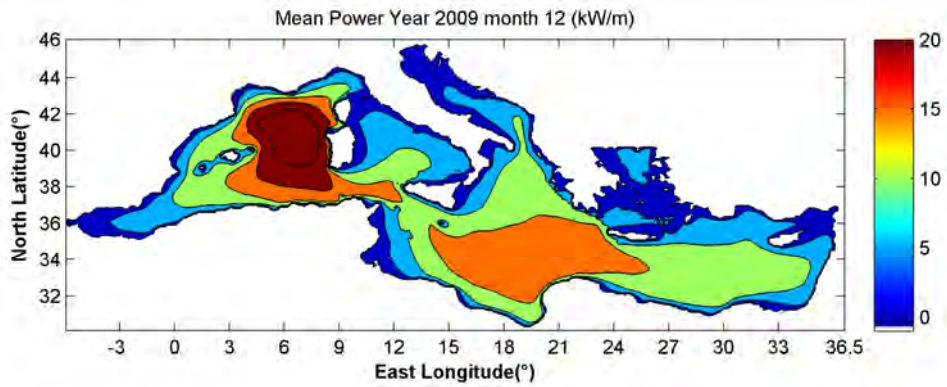
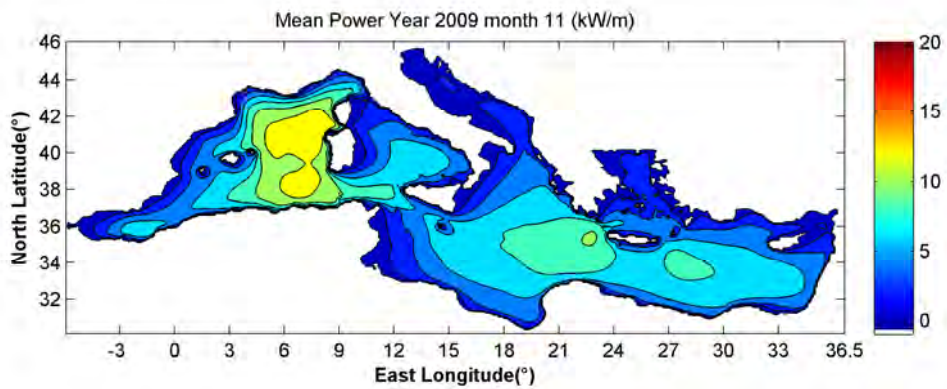
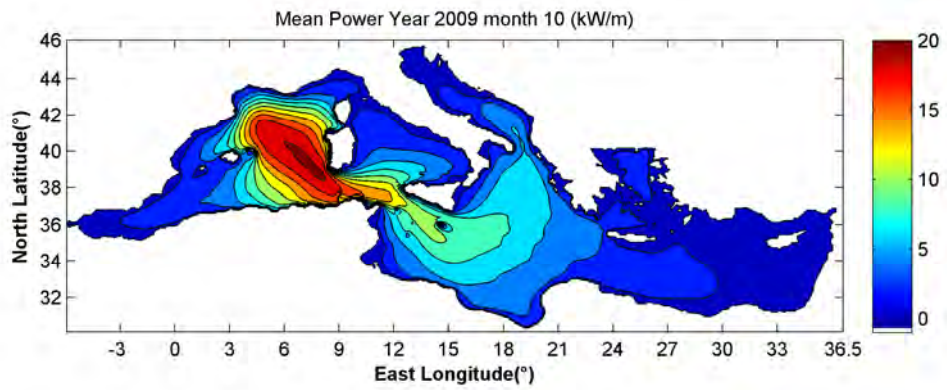
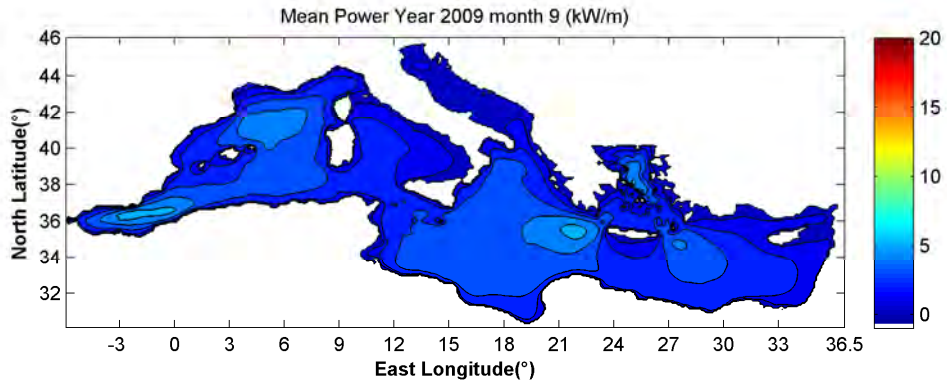
OFFSHORE CHARACTERIZATION

MEDITERRANEAN SEA

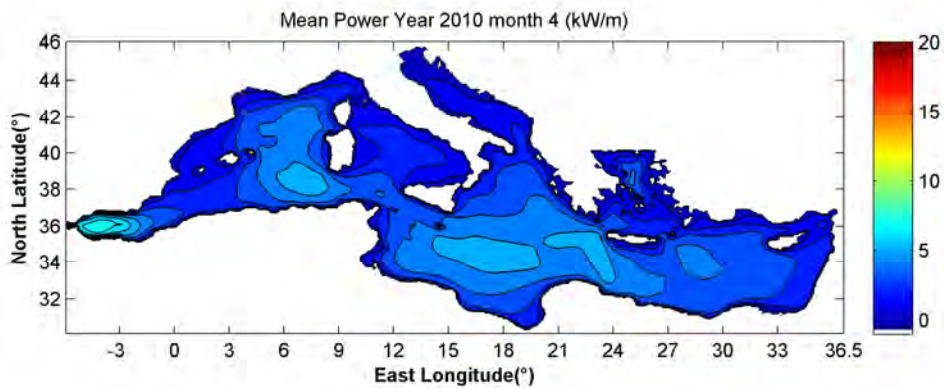
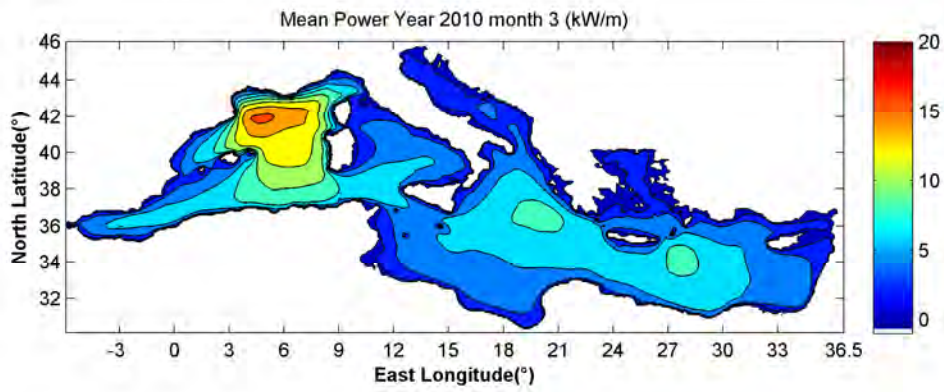
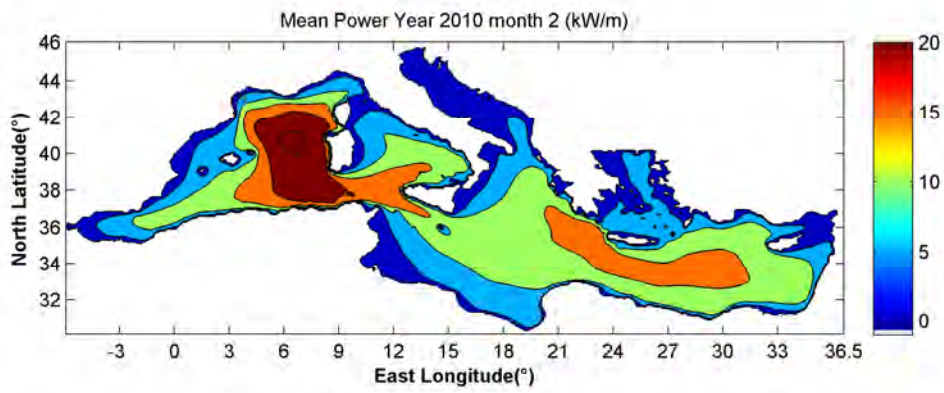
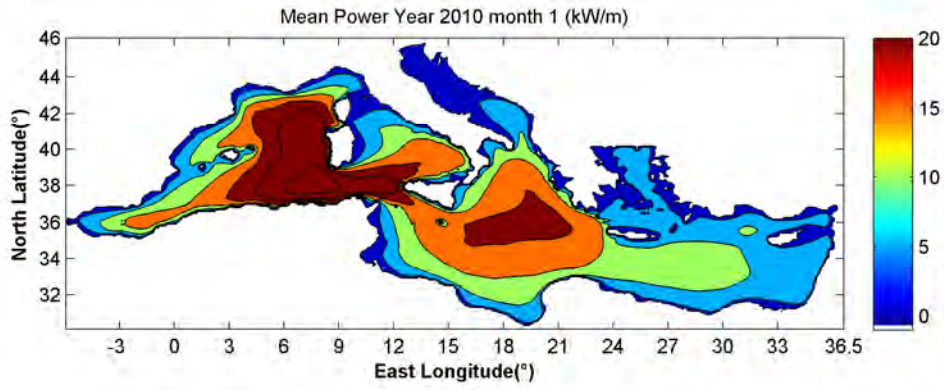
Previmer MED-6MIN model

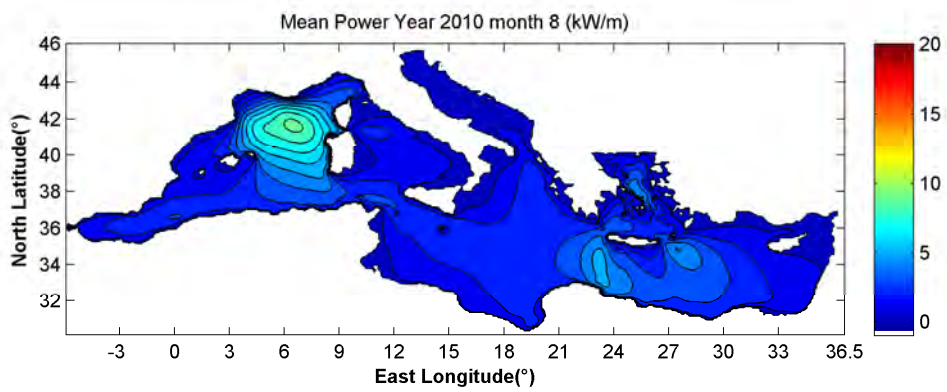
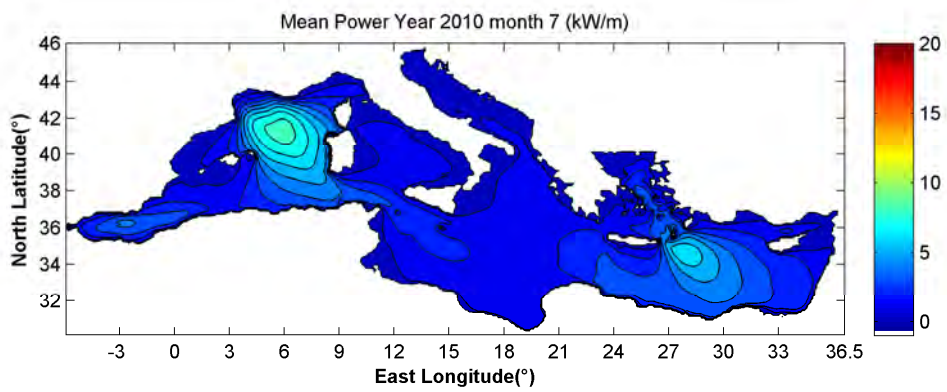
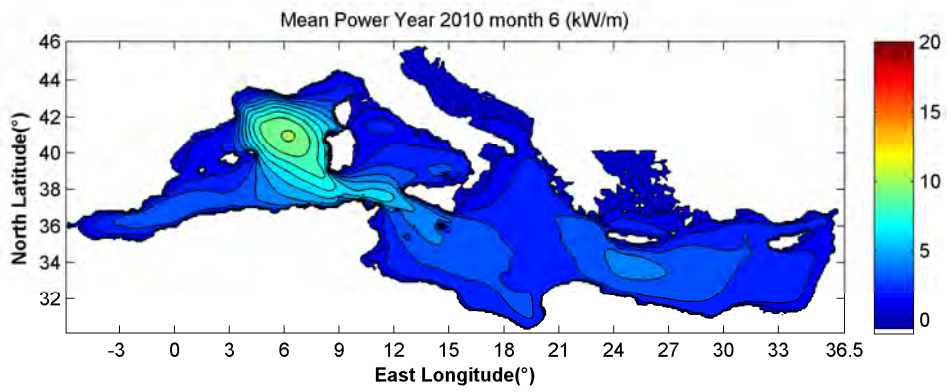
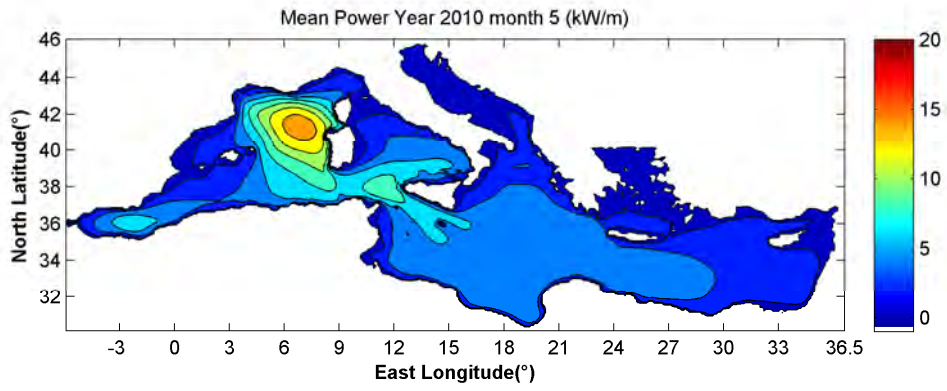
2009

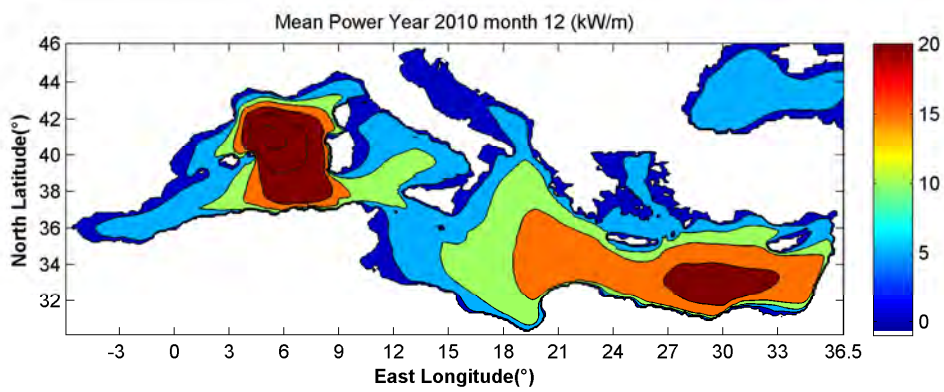
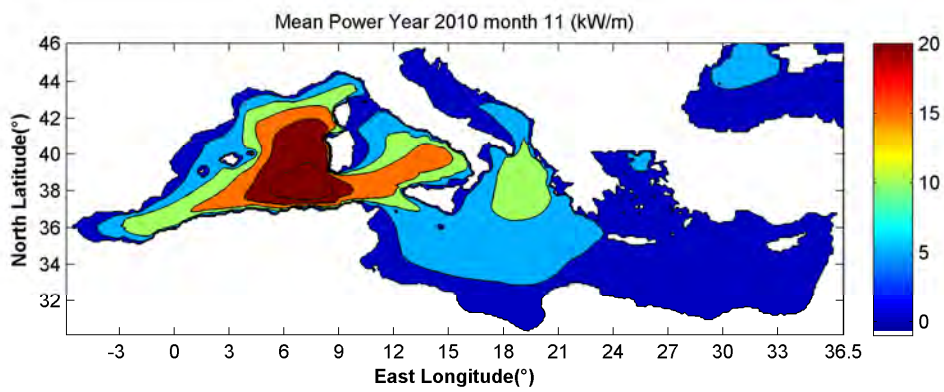
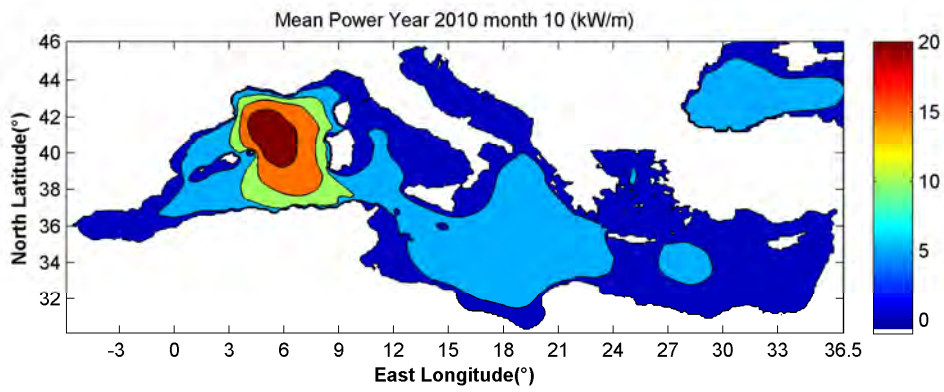
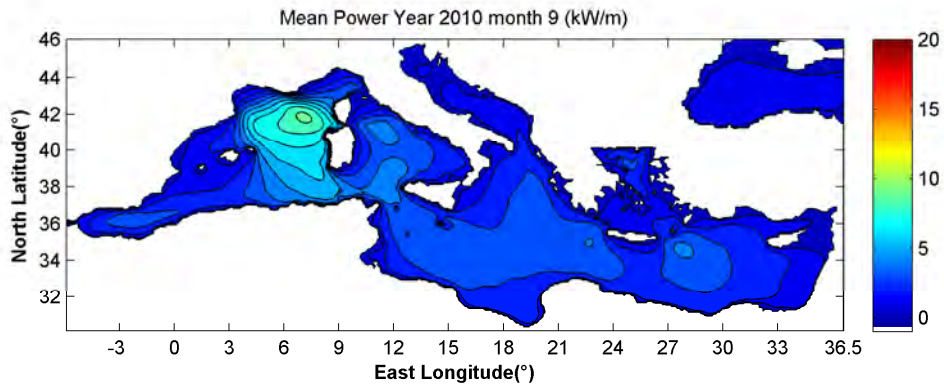




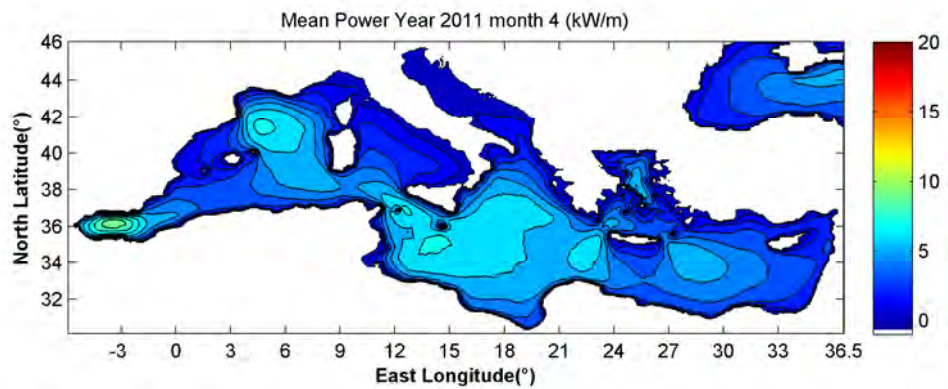
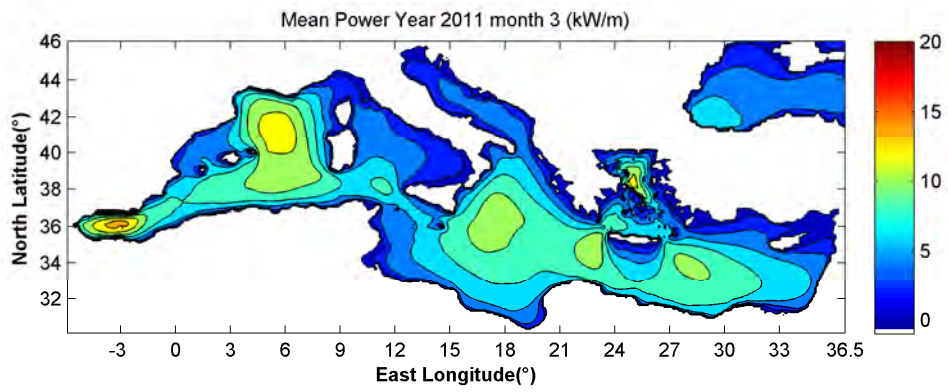
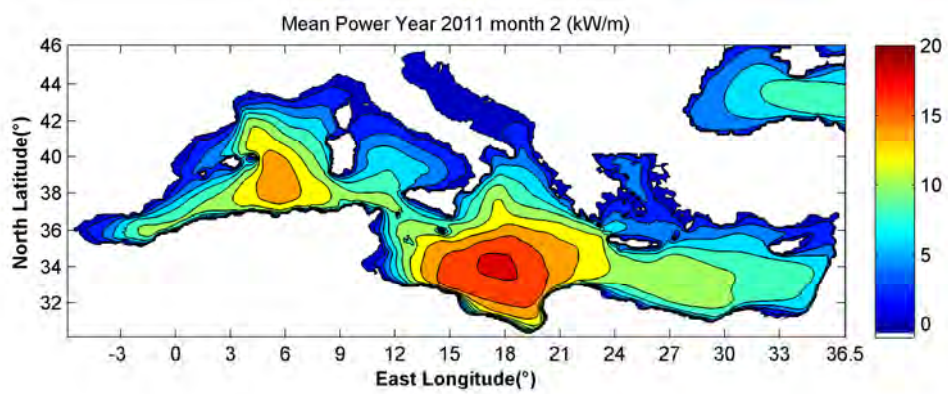
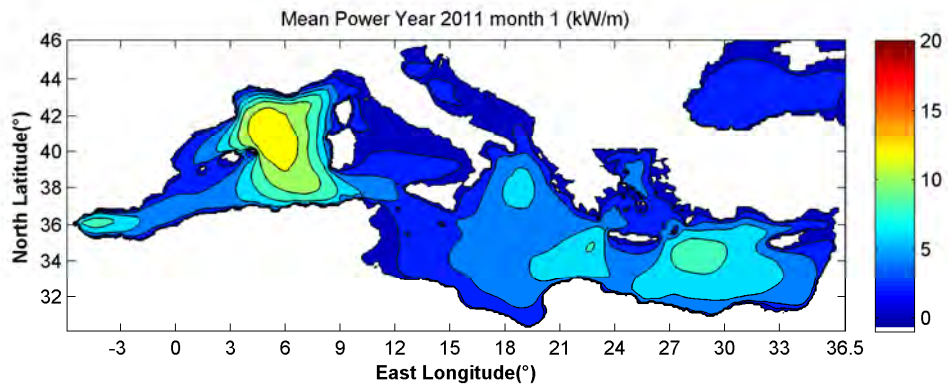
2010

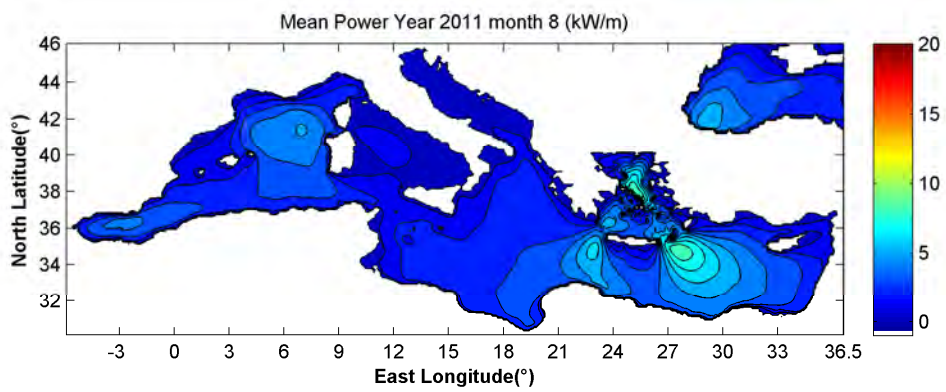
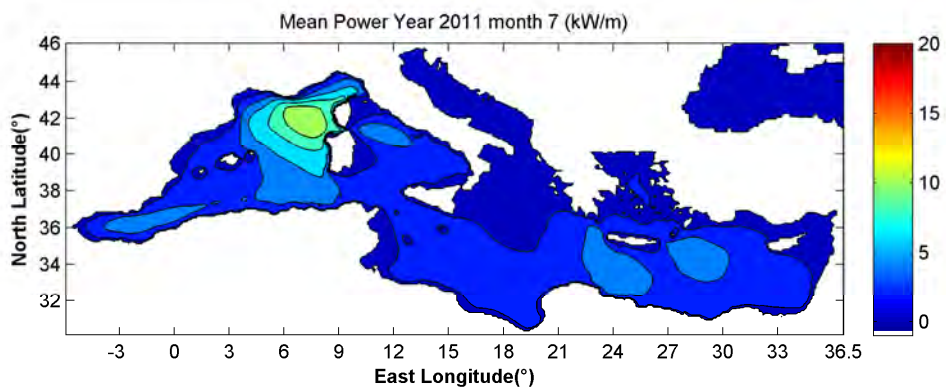
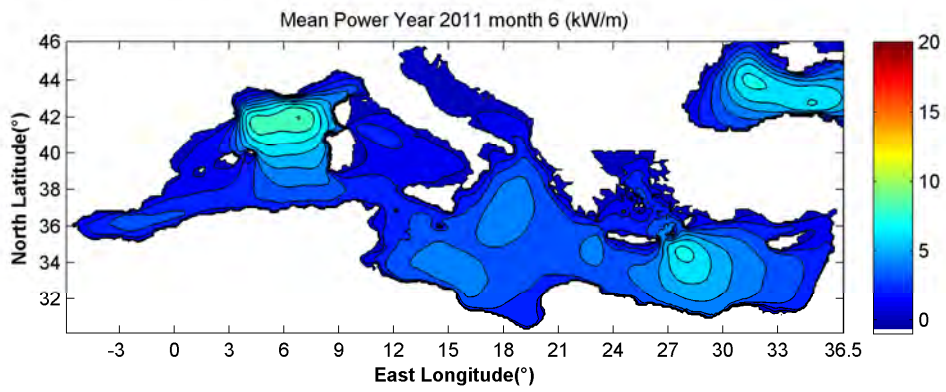
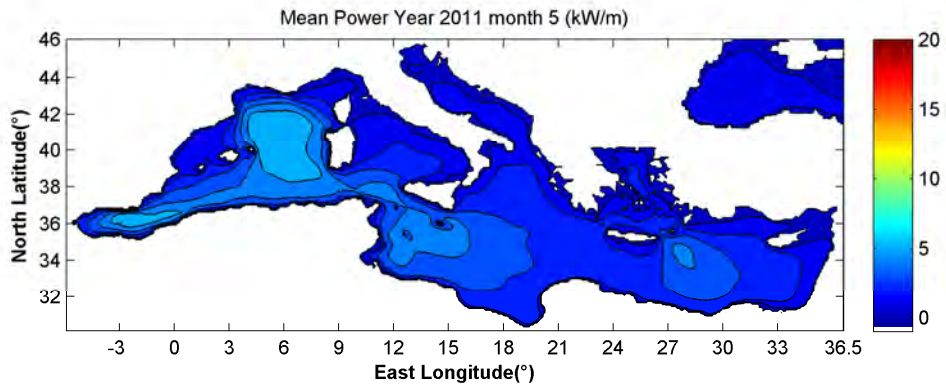


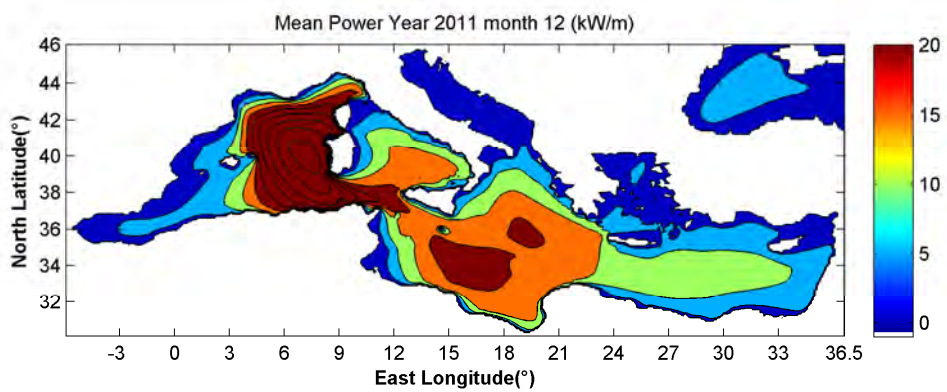
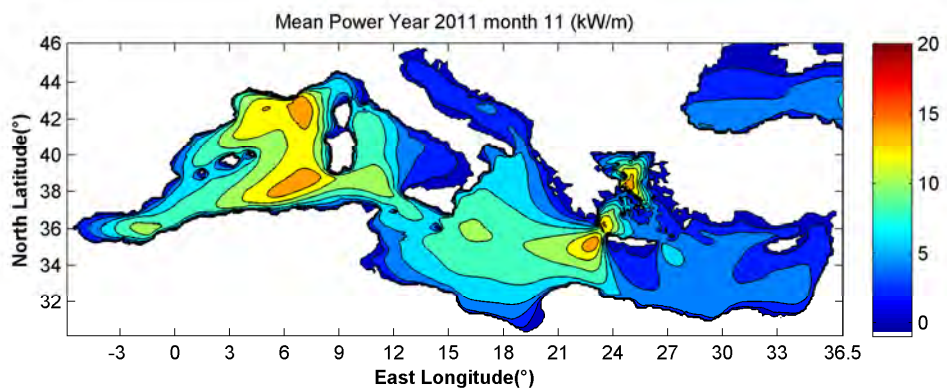
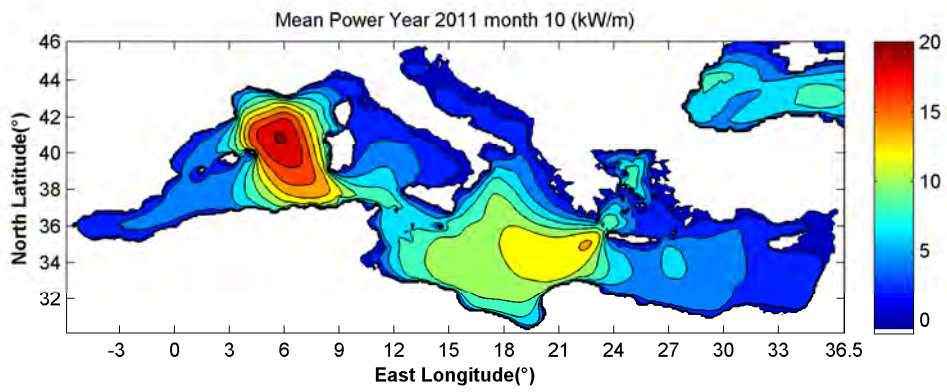
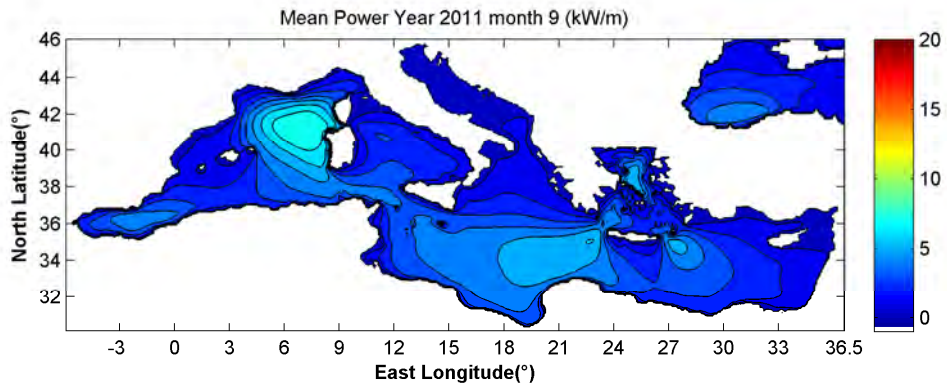


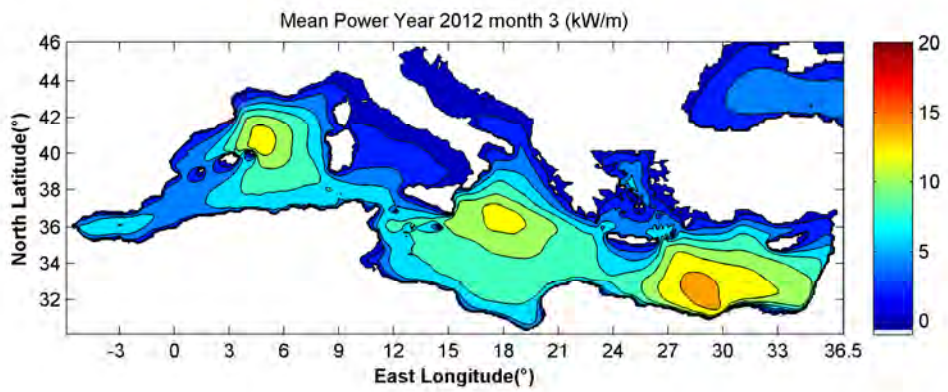
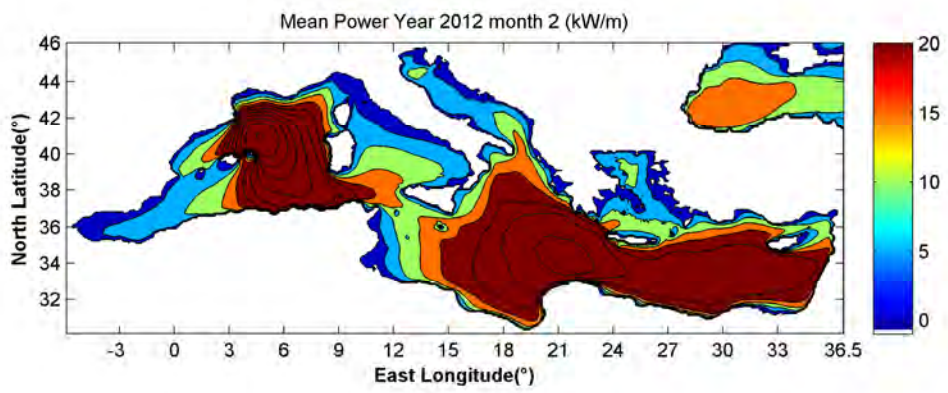
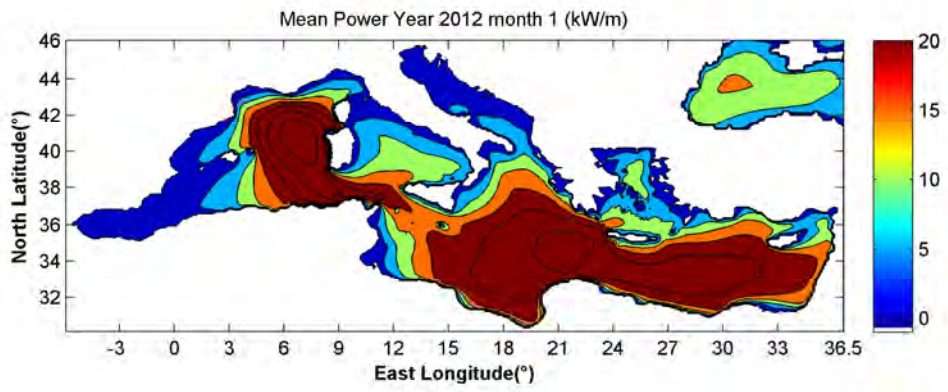


2011





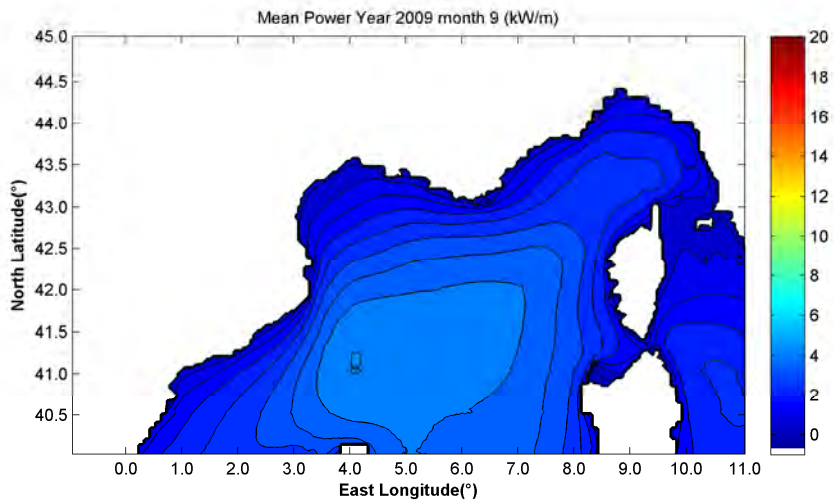
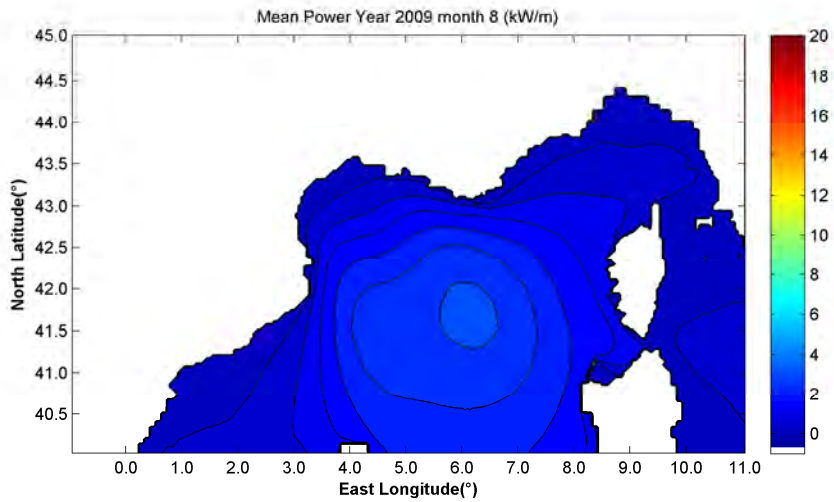
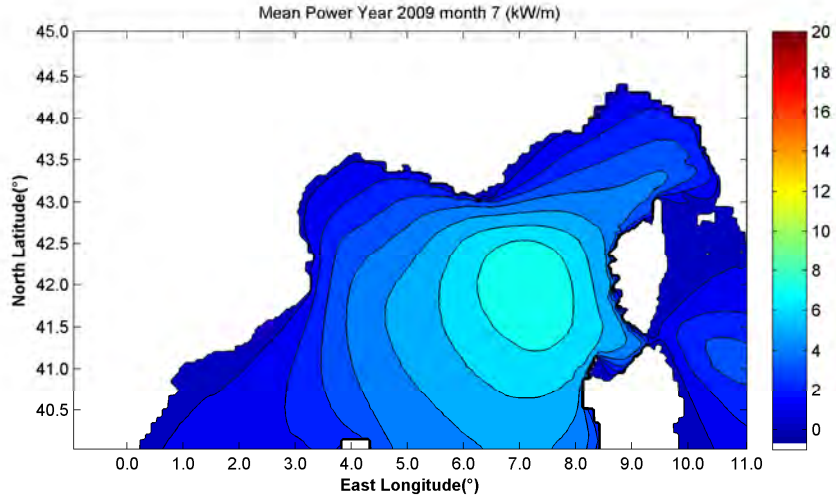


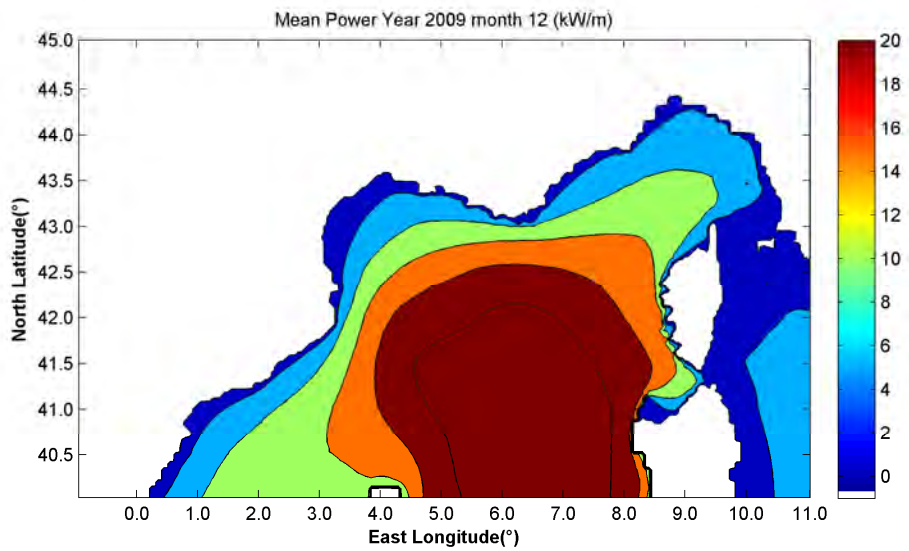
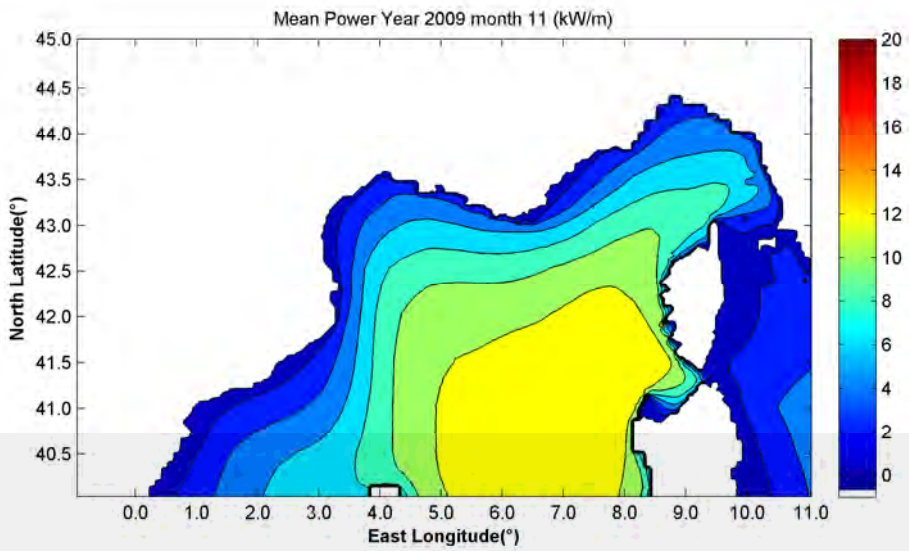
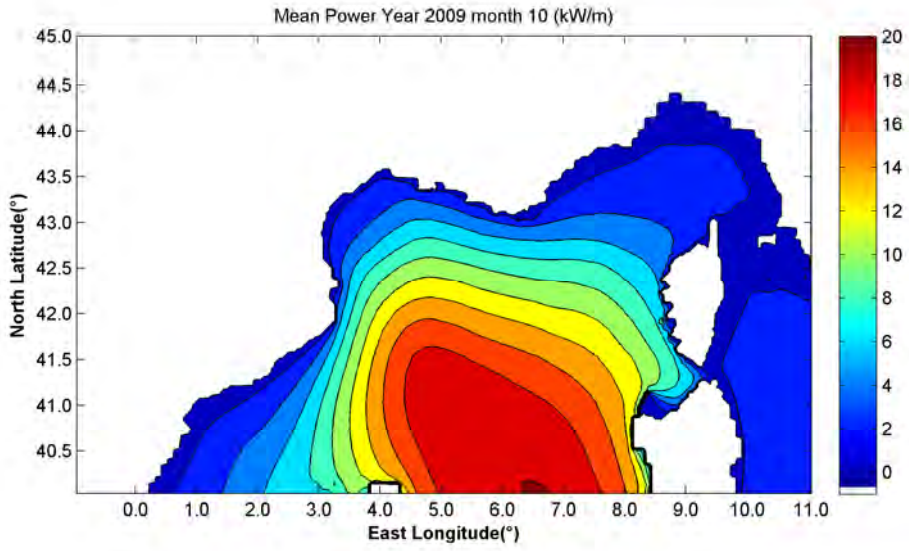


NORTH WESTERN MEDITERRANEAN SEA

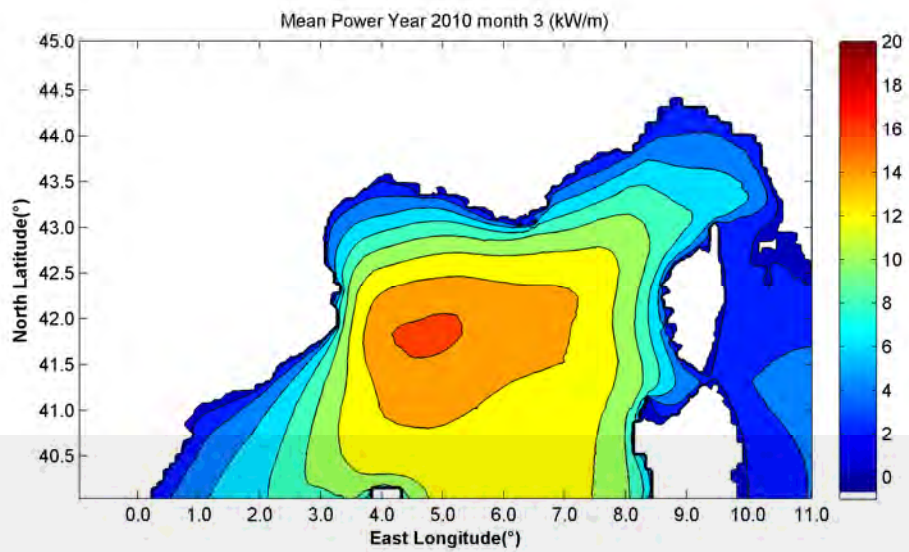
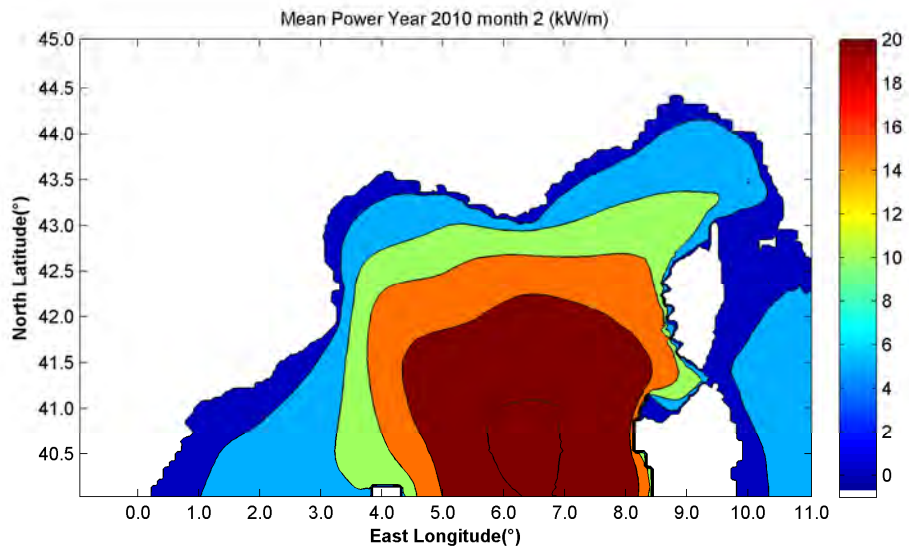
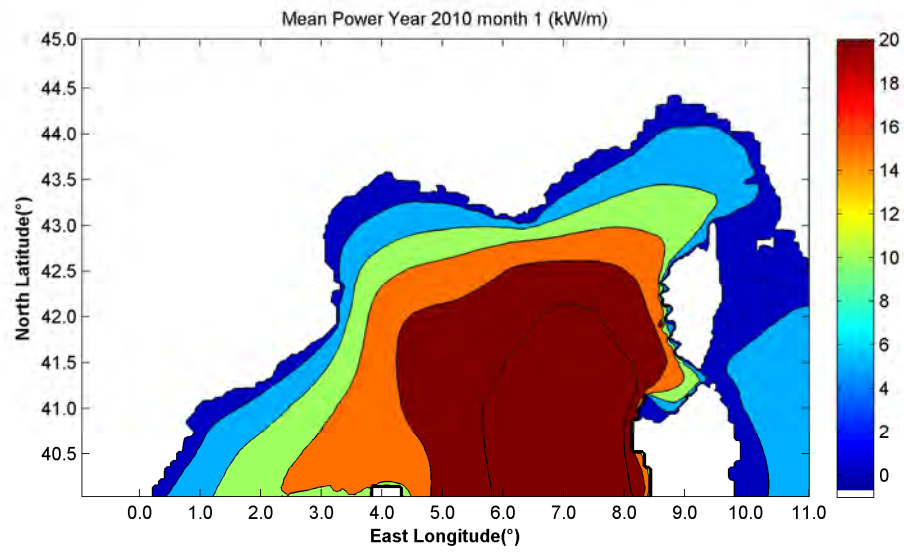
Previmer MENOR-4000M/MENOR-2MIN model

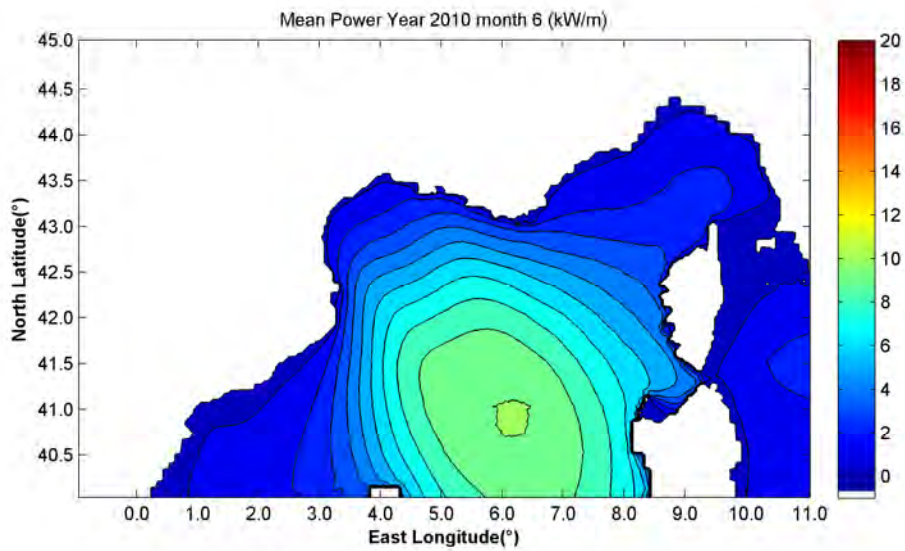
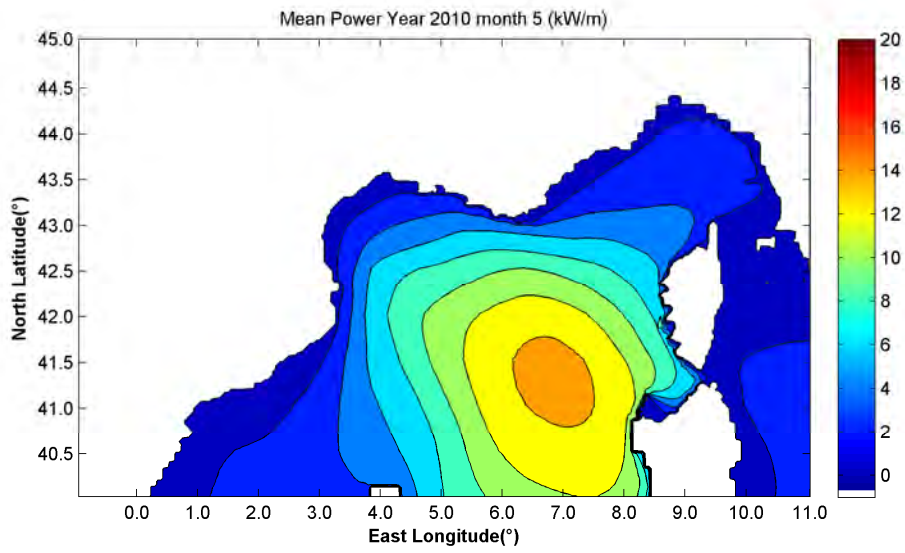
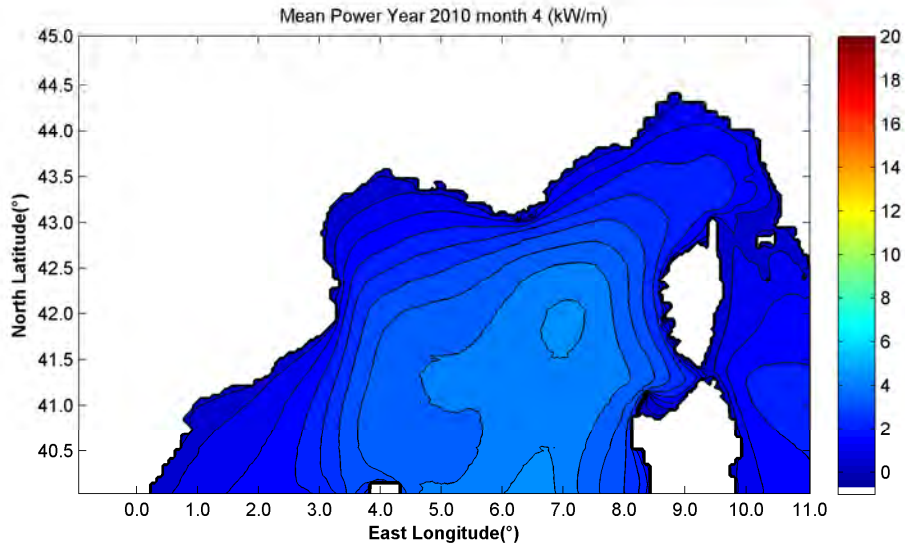
2009

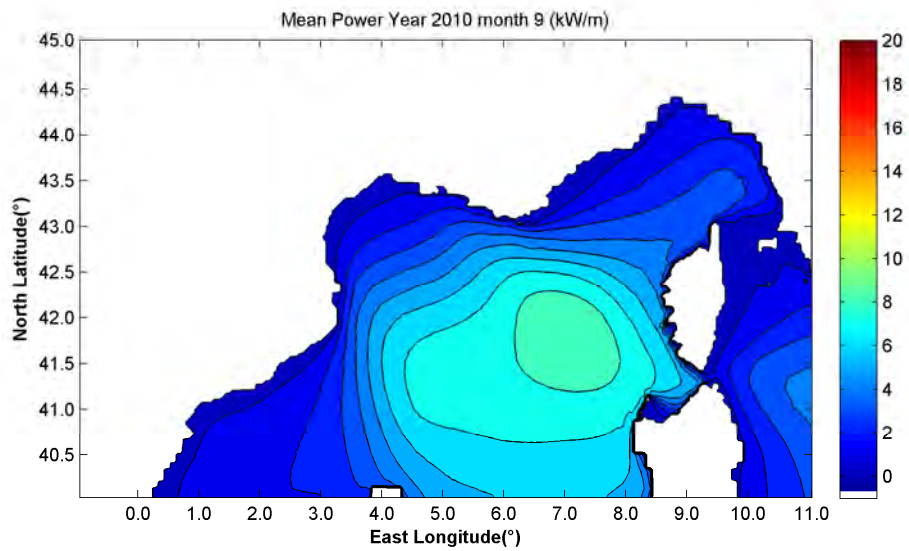
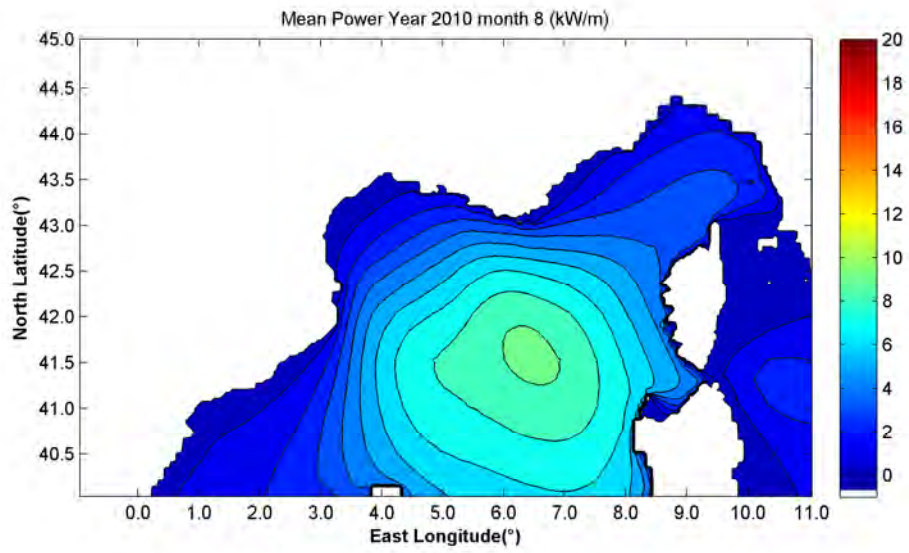
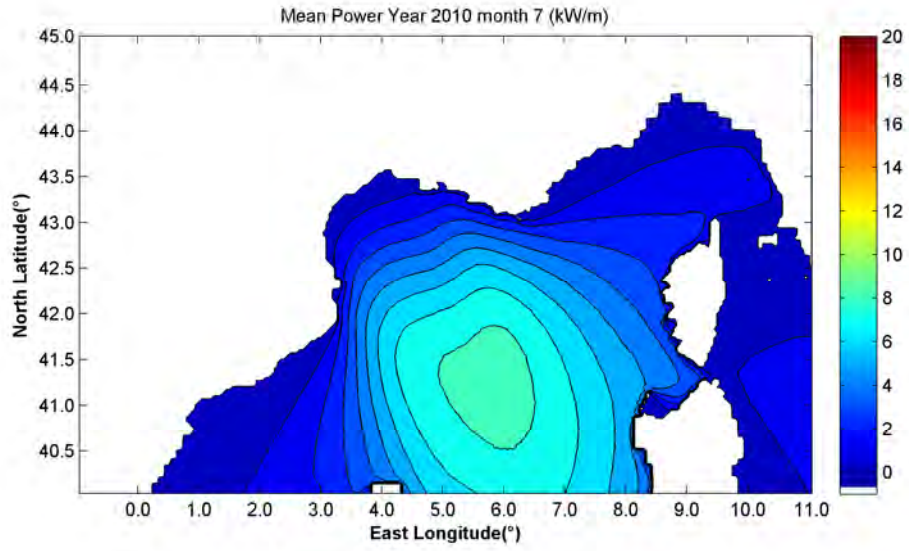


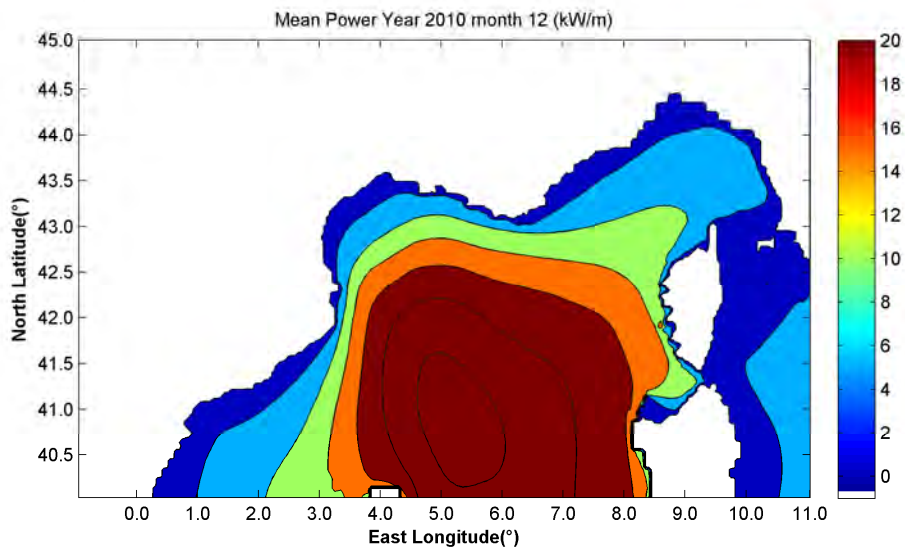
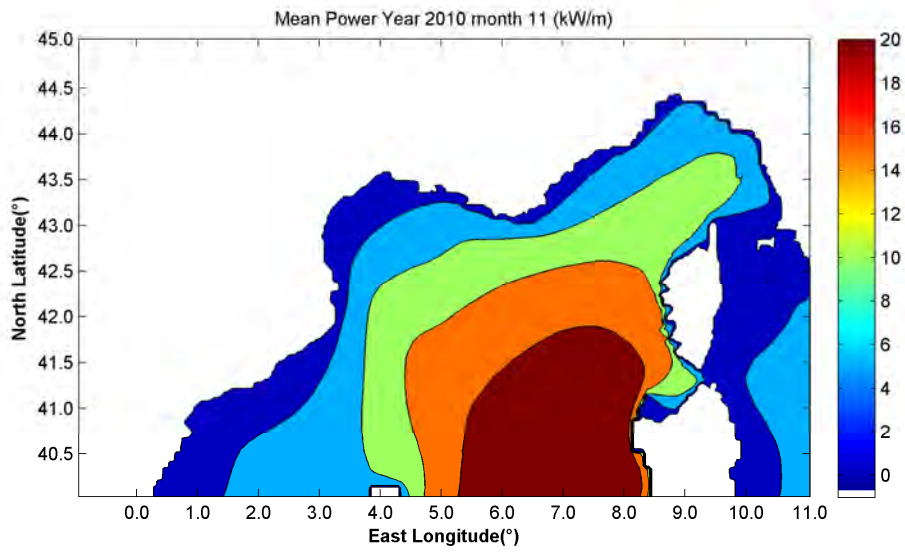
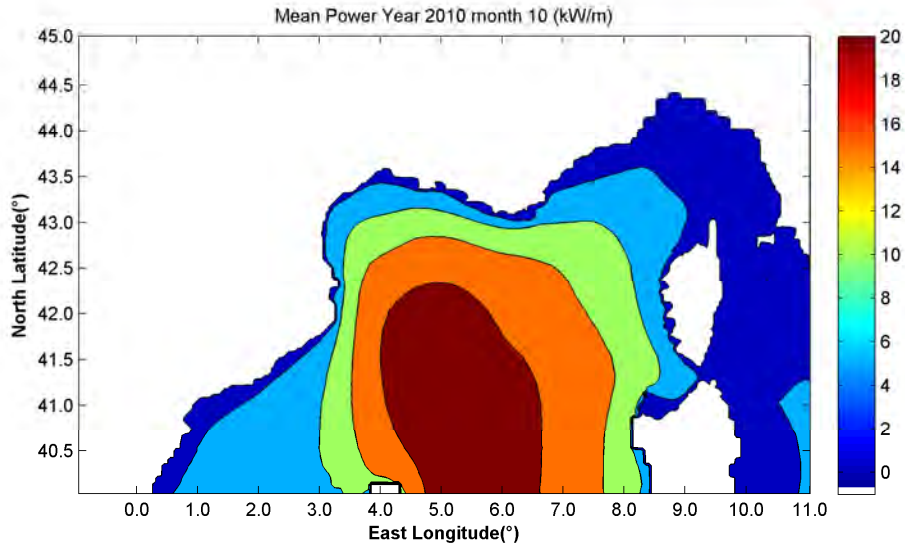


2010

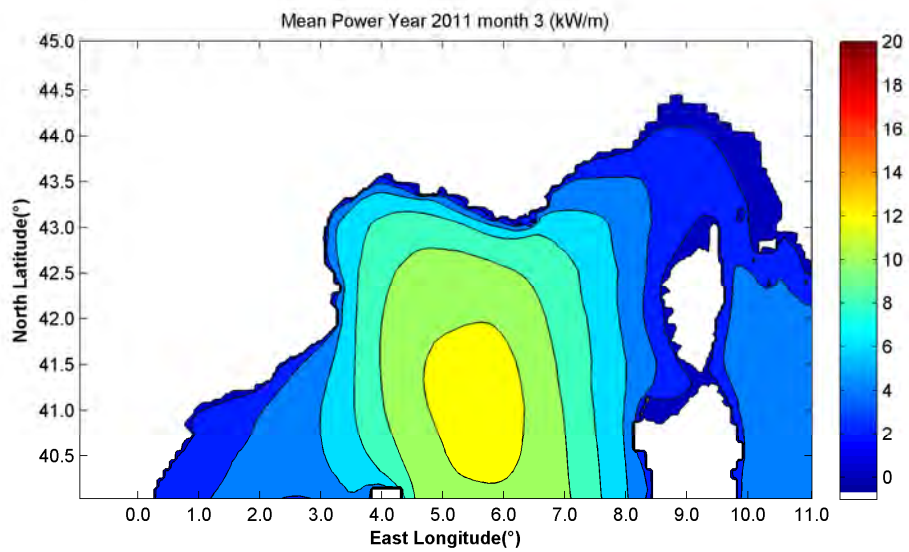
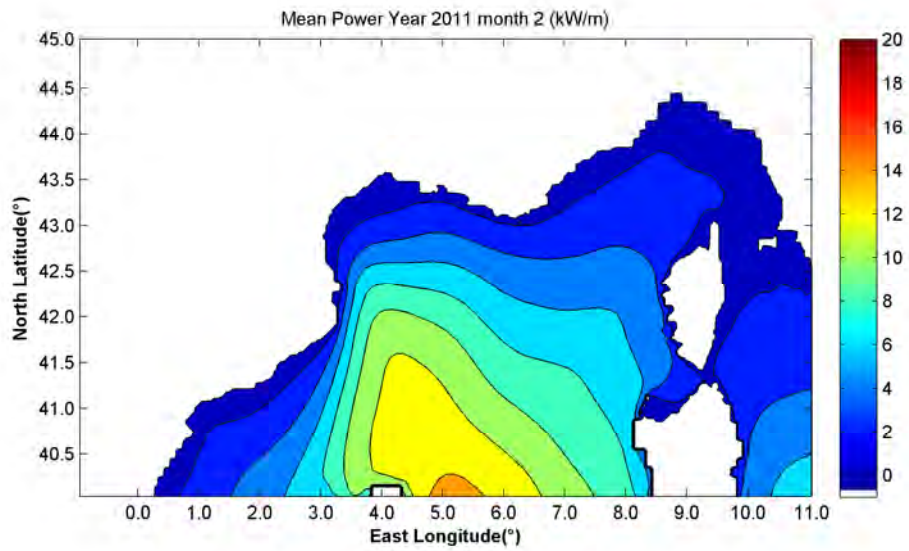
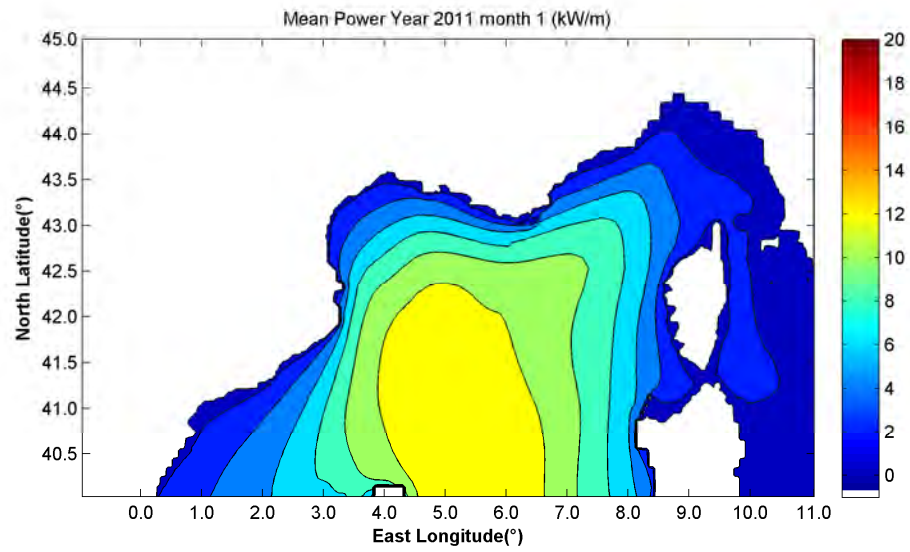


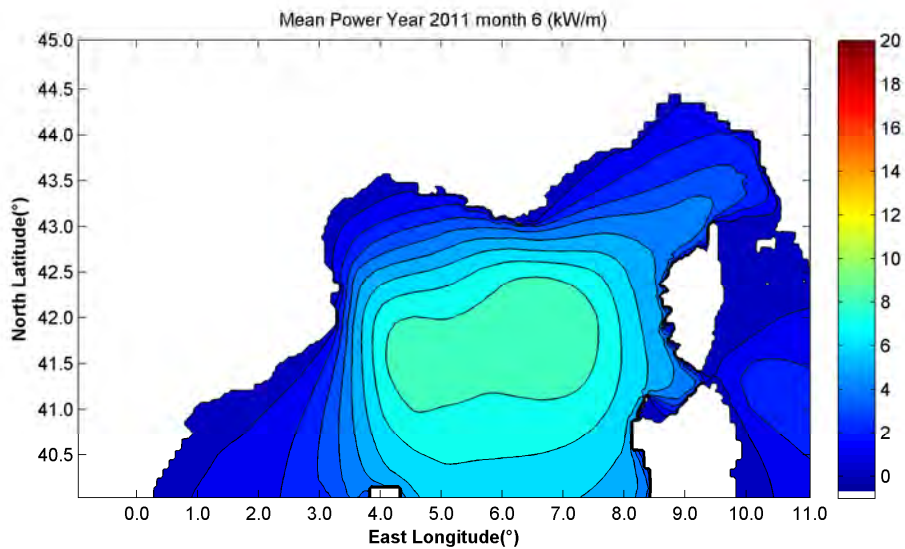
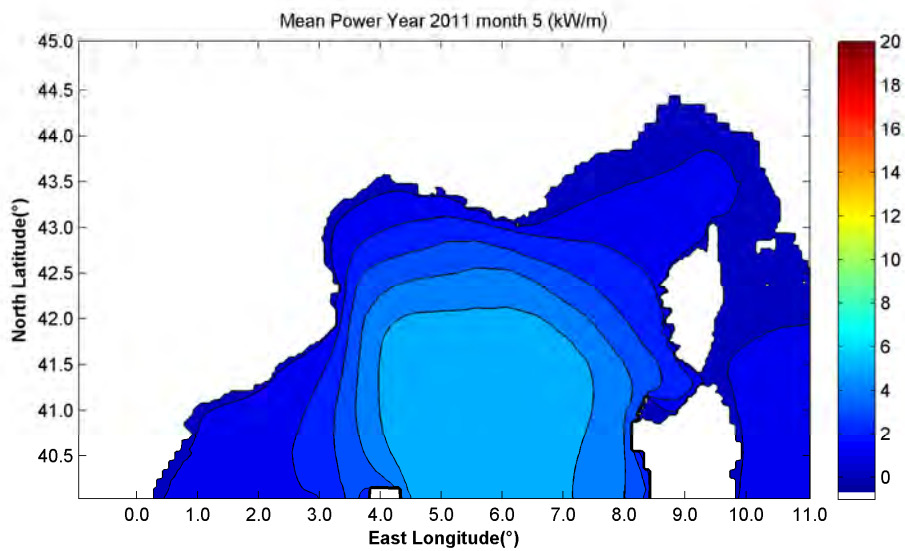
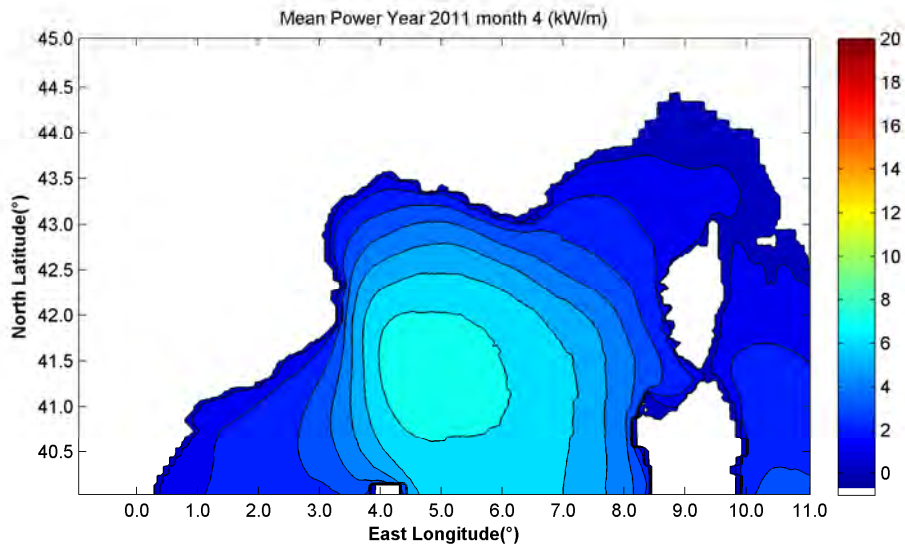


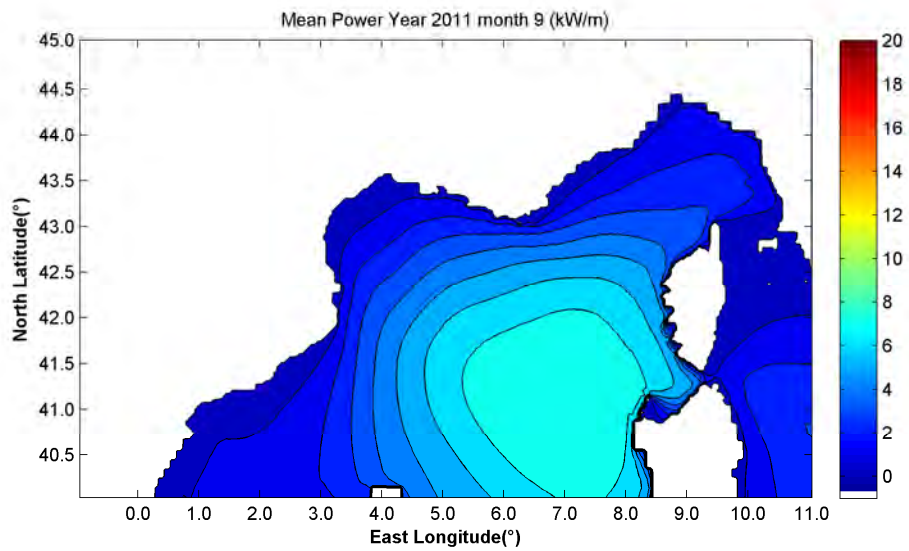
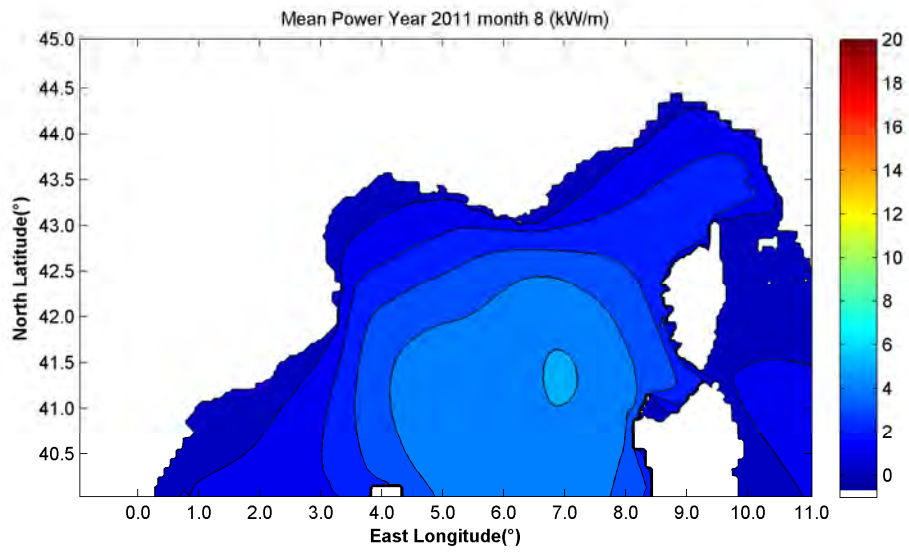
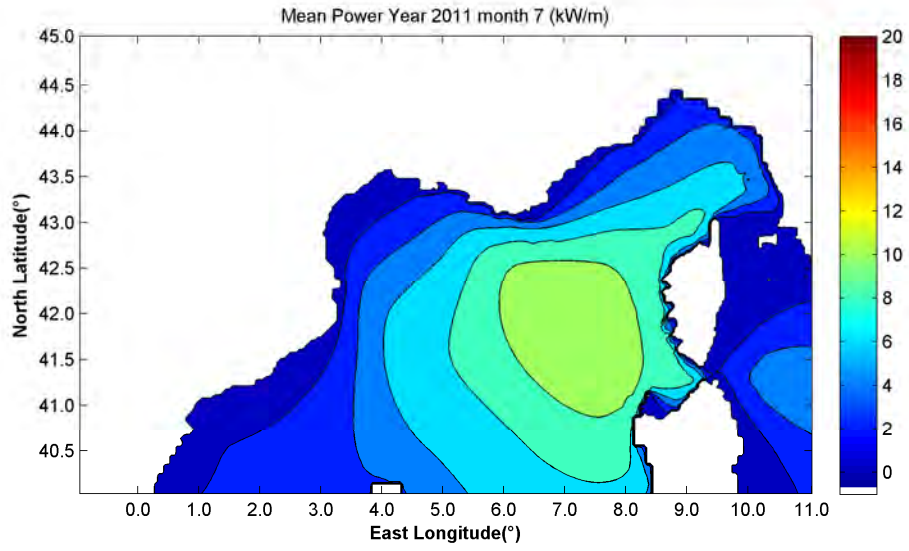


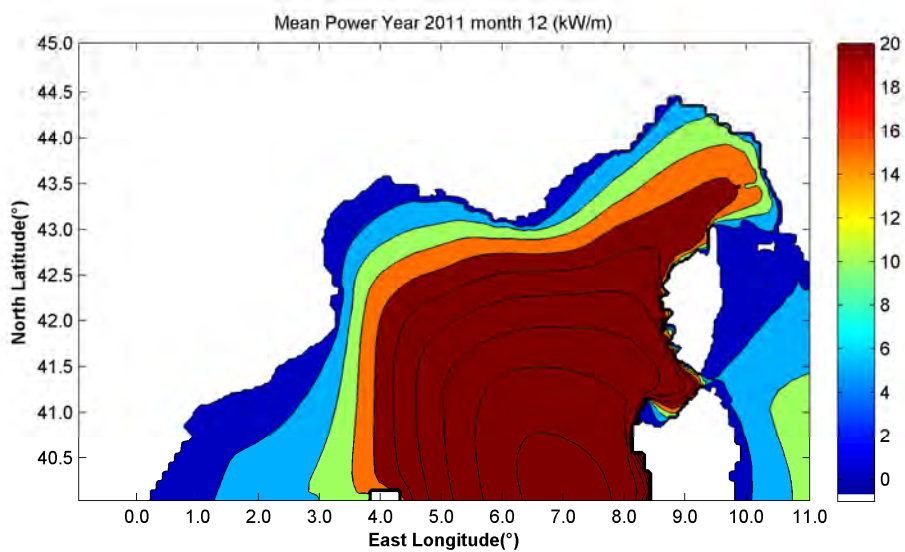
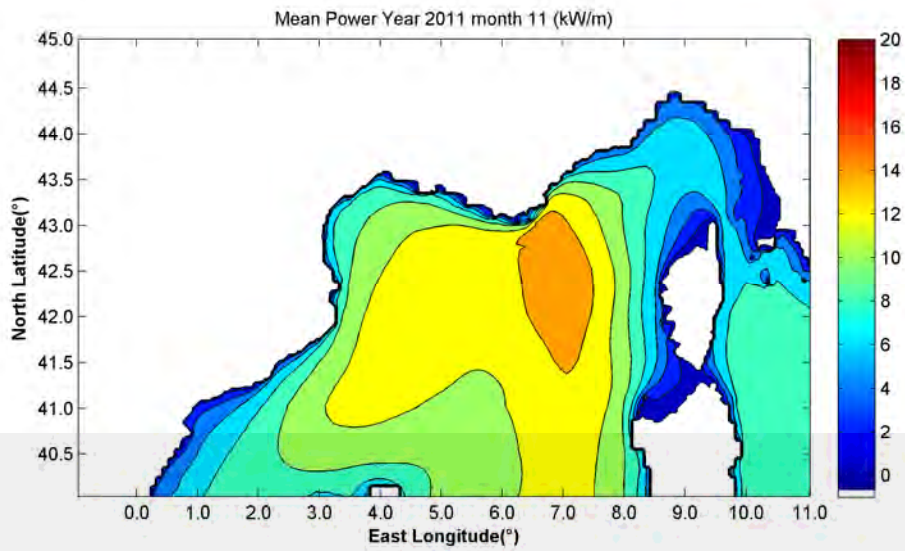
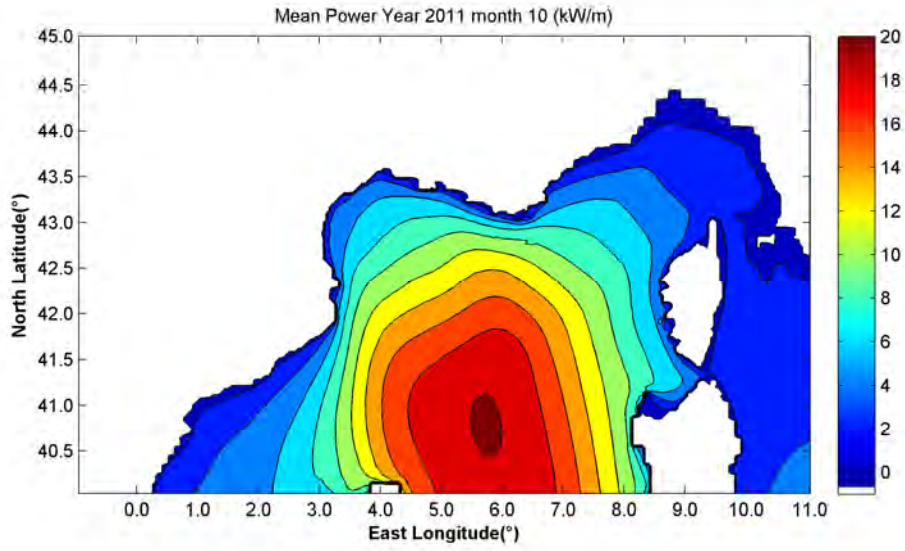


2011









2012

